UNIVERSITÀ DEGLI STUDI DI MILANO

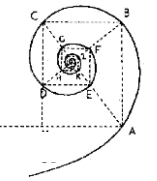

DOTTORATO IN MEDICINA MOLECOLARE E TRASLAZIONALE

CICLO XXIX

Anno Accademico 2015/2016

TESI DI DOTTORATO DI RICERCA

BIO/10

MULTI-AFFINITY NANOTRAPS THAT ENHANCE DETECTION OF LOW-ABUNDANT PROTEINS: A NOVEL AND HIGHLY SENSITIVE TEST FOR THE DIAGNOSIS OF LYME DISEASE

Dottorando: **Ruben MAGNI**

Matricola N° R10525

Tutore: Prof.ssa Cristina BATTAGLIA

Co-tutore: Dott.ssa Alessandra LUCHINI

Coordinatore del Dottorato: Prof. Mario CLERICI

SOMMARIO

L'identificazione di nuovi biomarcatori rilevanti dal punto di vista clinico risulta cruciale per la diagnosi precoce e miglioramanto terapeutico di diverse malattie con conseguentemente riduzione del tasso di mortalità. I fluidi biologici costituiscono circa il 60% della massa corporea e rappresentano una fonte significativa di biomarcatori. Sfortunatamente, molti biomarcatori sono difficilmente rilevabili nei fluidi biologici tramite spettrometria di massa o saggi immunologici a causa della loro ridotta concentrazione, della loro tendenza a degradarsi facilmente e della presenza di proteine molto abbondanti come albumina e immunoglobuline. Per superare tali barriere biologiche abbiamo sviluppato nanoparticelle composte da poly(N-isopropilacrilamide) (NIPAm) e funzionalizzate con "esche chimiche" in grado di catturare, concentrare e preservare i biomarcatori presenti in un fluido biologico (urina, sangue, sudore, fluido cerebrospinale) rapidamente attraverso pochi semplici passaggi. In questa tesi verranno descritte la composizione, la sintesi e l'applicazione delle nanoparticelle di idrogel (Nanotrap). La novità di questa tecnologia risiede nel fatto che mentre in passato le nanoparticelle di idrogel venivano studiate solo come mezzo di rilascio di molecole farmacologicamente attive, la loro applicazione nel nostro studio si focalizza invece sulle loro abilita' di riconoscere e catturare analiti in soluzione a scopi diagnostici. Le nanoparticelle vengono incubate con un fluido biologico e catturano i biomarcatori tramite ligandi ad alta affinità immobilizzati covalentemente al loro interno, allo stesso tempo escludendo proteine molto abbondanti come in cromatografia di esclusione molecolare. Una volta catturati, i biomarcatori potenzialmente significativi sono concentrati in volumi molto piccoli e poi analizzati con tecnologie di biologia molecolare. Il fattore di concentrazione (fino a 10000 volte a seconda del volume del campione di partenza) permette di migliorare l'effettiva sensibilità della spettrometria di massa e di saggi immunologici e identificare proteine precedentemente invisibili, quindi favorendo la scoperta di nuovi biomarcatori e lo sviluppo di nuovi test diagnostici.

La tesi si focalizza principalmente sullo sviluppo di un test antigenico in urina per la diagnosi della malattia di Lyme. Esiste una necessità clinica di migliorare la specificità di test diagnostici 1) per la diagnosi precoce della malattia di Lyme nel periodo precedente lo sviluppo di una robusta risposta sierologica e 2) per sorvegliare la terapia antibiotica. Borrelia burgdorferi è l'agente eziologico della malattia di Lyme. Grazie all'utilizzo delle Nanotraps abbiamo studiato la presenza della proteina di Borrelia Outer surface protein A (OspA) e nello specifico della sua regione C-terminale in pazienti nel primo stadio della malattia prima e dopo il trattamento antibiotico, e in pazienti nello stadio tardivo e disseminato dell'infezione. La cattura e concentrazione dell'OspA tramite Nanotraps unita all'utilizzo di un anticorpo monoclonale specifico contro il peptide C-terminale dell'OspA, ci ha consentito di ottenere un test ad alta sensibilita'(1.7pg/mL, limite di rilevazione analitico) e specificita'.

La regione C-terminale OspA236-239, riconosciuta dall'anticorpo, risulta conservata nelle specie infettive di Borrelia, e manca di omologia con proteine umane e cross-reattività con proteine di virus comuni e batteri non appartenenti al genus di Borrelia.

268 campioni di urina provenienti da pazienti in vari stadi della malattia sono stati raccolti in un'area endemica per la Borreliosi di Lyme (Virginia, Stati Uniti). I risultati di questo studio clinico indicano che, in assenza di terapia, 24 su 24 campioni appena diagnosticati con erythema migrans (EM) sono risultati positivi alla presenza di OspA in urina mentre nessun paziente asintomatico (0/117) e' risultato falsamente positivo ($p<10^{-6}$). 10 pazienti su 10 che hanno mostrato la persistenza di sintomi (EM rash) durante il corso della terapia antibiotica sono risultati positivi per la presenza di OspA in urina. 8 su 8 pazienti sono passati da un segnale positivo per l'OspA ad assenza di segnale dopo la risoluzione dei sintomi in seguito a trattamento. 40 su 40 campioni che mostravano sintomi clinici sono risultati positivi per l'OspA. La specificita' del nostro test antigenico in comparazione con il risultato serologico e' risultata essere del 87.5% (21 positivi per l'OspA in urina/24 positivi per serologia, $p=4.072e^{-15}$). 41 su 100 pazienti con sospetto di Borreliosi di Lyme in una zona endemica sono risultati positivi per l'OspA in urina. Il rilascio di OspA in urina è correlato con la presenza attiva di sintomi (EM rash e artrite), mentre la risoluzione di tali sintomi in seguito a terapia e' correlata alla conversione di OspA da positivo a negativo. La rilevazione dell'OspA e' stata inizialmente ottenuta tramite western blot, tuttavia maper ottenere risultati quantificabili, è stato successivamente sviluppato un saggio ELISA. Risultati preliminari hanno mostrato un limite di rilevazione analitico di 0.5 pg/mL3 pazienti su 3 con sintomatologia positiva che sono risultati positivi per il western blot sono risultati positivi anche in ELISA. Un altro formato promettente, attualmente in fase di sviluppo, consiste in un saggio che utilizza la spettrometria di massa (Multiple Reaction Monitoring) per l'identificazione di proteine di Borrelia nell'urina dopo processamento con Nanotraps. Di fondamentale importanza, infatti, e' la possibilità di misurare diversi antigeni in aggiunta a OspA, come OppA, e DbpA, cosi' da poter raccogliere informazioni più accurate sullo stadio della malattia e di raggiungere una migliore sensibilita' clinica. Risultati preliminari hanno mostrato una sensibilità di 5pg/ml e un'ottima riproducibilità utilizzando soluzioni modello di urina proveniente da individui sani e contenente quantità note di proteine di Borrelia. Per ultimo, abbiamo sviluppato una nuova generazione di nanoparticelle parzialmente degradabili che sono state utilizzate per produrre un prototipo di saggio immunologico a flusso. Questo saggio si basa sulla proprietà delle nanoparticelle di esporre l'antigene catturato al loro interno per un diretto riconoscimento da parte dell'anticorpo stampato sulla linea del dispositivo diagnostico. Dati preliminari supportano lo sviluppo di un saggio rapido per proteine di Borrelia nell'urina di pazienti caratterizzato da alta sensibilità e specificità.

In conclusione, questo lavoro di tesi raccoglie evidenze sperimentali dell'applicazione della tecnologia Nanotrap allo sviluppo di test antigenici per la malattia di Lyme. Le Nanotrap aumentano la sensibilità analitica di western blot, ELISA, spettrometria di massa e saggio immunologico a flusso rendendo possibile la misurazione di proteine batteriche, altrimenti invisibili, nell'urina di pazienti. Questi risultati dimostrano che l'uso di Nanotrap è indispensabile per saggi antigenici per la malattia di Lyme e in generale presentano un concetto valido per malattie trasmissibili causate da diversi agenti eziologici (tubercolosi, malattia di Chagas, toxoplasmosi etc...).

ABSTRACT

In the recent years a lot of emphasis has been placed on the discovery and better detection of clinically relevant biomarkers. Biomarkers are crucial for the early detection of several diseases, and they play an important role in the improvement of current treatments, thus reducing patient mortality rate. Biofluids account for 60% of the human body mass and can be a goldmine of significant biomarkers. Unfortunately, low abundance biomarkers are difficult to detect with mass-spectrometry or immunoassays because of their low concentration in body fluids, their lability, and the presence of high-abundance proteins (i.e. albumin and immunoglobulins). In order to overcome these physiological barriers, we developed nanoparticles made of poly(N-isopropylacrylamide) (NIPAm) and functionalized with affinity reactive baits that one single step capture, concentrate and preserve labile biomarkers in complex body fluids (i.e. urine, blood, sweat, CSF). The design, synthesis and application of the Nanotrap hydrogel particles are described in this thesis. The novelty of the technology relies in the fact that in the past hydrogel nanoparticles have been studied and used as a drug delivery tool, whereas our application focuses on their capturing abilities instead of the releasing of specific drug molecules. Once the functionalized nanoparticles are incubated with a biological fluid, low molecular weight biomarkers are captured by the affinity baits while unwanted high abundance analytes are excluded. The potentially relevant biomarkers are then concentrated into small volumes and analyzed. The concentration factor (up to 10000 fold depending on the initial volume) enhances the effective sensitivity of mass-spectrometry and immunoassays and permits to detect previously invisible proteins thus improving biomarker discovery and diagnostic testing. This thesis discusses the use of hydrogel nanoparticles to develop a urinary antigen test for the detection of Lyme Borreliosis. There is a clinical need to improve the diagnostic specificity of early stage Lyme assays in the period prior to the mounting of a robust serology response and to develop a diagnostic tool to monitor therapy success. Borrelia burgdorferi is the causative agent of Lyme disease. Using our hydrogel particles (Nanotraps) we evaluated the presence of urinary Borrelia Outer surface protein A (OspA) C-terminus peptide in early stage LB before and after treatment, and in patients suspected of late stage disseminated LB. We employed Nanotraps to concentrate urinary OspA and used a highly specific anti-OspA monoclonal antibody (mAb) as a detector of the C-terminus peptides. We mapped the mAb epitope to a narrow specific OspA C-terminal domain OspA236-239 conserved across infectious Borrelia species but with no homology to human proteins and no cross reactivity with relevant viral and non-Borrelia bacterial proteins. 268 urine samples from patients being evaluated for all categories of LB were collected in a LB endemic area. The urinary OspA assay, blinded to outcome, utilized Nanotrap particle pre-processing, western blotting to evaluate the OspA molecular size, and OspA peptide competition for confirmation. OspA test characteristics: sensitivity 1.7 pg/mL (lowest limit of detection), %coefficient of variation (CV)=8%, dynamic range 1.7-30 pg/mL. Pre-treatment, 24/24 newly diagnosed patients with an erythema migrans (EM) rash were positive for urinary OspA while false positives for asymptomatic patients were 0/117 (Chi squared $p<10^{-}$

[6]). For 10 patients who exhibited persistence of the EM rash during the course of antibiotic therapy, 10/10 were positive for urinary OspA. Urinary OspA of 8/8 patients switched from detectable to undetectable following symptom resolution post-treatment. Specificity of the urinary OspA test for the clinical symptoms was 40/40. Specificity of the urinary OspA antigen test for later serology outcome was 87.5% (21 urinary OspA positive/24 serology positive, Chi squared p=4.072e^{-15}). 41 of 100 patients under surveillance for persistent LB in an endemic area were positive for urinary OspA protein. OspA urinary shedding was strongly linked to concurrent active symptoms (e.g. EM rash and arthritis), while resolution of these symptoms after therapy correlated with urinary conversion to OspA negative. Detection of OspA was performed using Western blot analysis. In order to obtain a quantitative measurement of the antigen, an ELISA was developed. Preliminary results showed a lowest limit of detection of 0.5pg/ml and %coefficient of variation 2%, dynamic range 0.5pg-30 pg/ml. 3/3 of symptomatic patients that resulted positive with the western blot Lyme assay were also found positive when tested on ELISA. Another promising format under development uses Mass Spectrometry Multiple Reaction Monitoring (MRM) for the detection of multiple Borrelia proteins after Nanotrap processing. Developing a diagnostic test against a panel of analytes will improve clinical sensitivity and understanding of staging of disease. MRM is a prime technology that yield multiplex measurement of more than 100 peptides in a single sample. A sensitivity of 5pg/ml and high reproducibility in human urine spiked with OspA was observed. Lastly, partially degradable Nanotraps were employed to produce a prototype of Lateral Flow Immunoassay (LFI) which exploits the use of antigen displaying nanoparticles for a point of care test for Lyme disease. This technology will ensure high accuracy and sensitivity while allowing for rapid testing of Lyme disease antigens in the urine of patients in the doctor office.

In summary, this study presents data supporting the successful use of the Nanotrap technology to develop a more accurate and sensitive test for Lyme disease that can diagnose the disease before seroconversion and that can be used to monitor therapy success. Nanotraps increase the effective analytical sensitivity of western blot analysis, ELISA, mass spectrometry MRM and lateral flow immunoassay. This is a concept that can be extended to communicable diseases with different etiologic agents (e.g. Tuberculosis, Chagas disease, Toxoplasmosis, etc.).

TABLE OF CONTENTS

LIST OF FIGURES

Figure 36. Magni, R. *et al*. (2015). Peptides containing the narrow OspA236-239 region were successfully utilized for antibody competition and immunodepletion. In *Application of Nanotrap technology for high sensitivity measurement of urinary outer surface protein A carboxyl-terminus domain in early stage Lyme borreliosis*

Figure 37. Magni, R. *et al*. (2015). Remazol Brilliant Blue Nanotrap particles show the highest affinity for OspA among the tested dyes. In *Application of Nanotrap technology for high sensitivity measurement of urinary outer surface protein A carboxyl-terminus domain in early stage Lyme borreliosis*

Figure 38. Magni, R. *et al*. (2015). Relationship between dye content and capturing affinity. In *Application of Nanotrap technology for high sensitivity measurement of urinary outer surface protein A carboxyl-terminus domain in early stage Lyme borreliosis*

Figure 39. Magni, R. *et al*. (2015). Effect V/v ratio between Nanotraps and sample volume on capturing effciency. In *Application of Nanotrap technology for high sensitivity measurement of urinary outer surface protein A carboxyl-terminus domain in early stage Lyme borreliosis*

Figure 41. Magni, R. *et al*. (2015). Performance comparison of multiple batches of Nanotrap particles. In *Application of Nanotrap technology for high sensitivity measurement of urinary outer surface protein A carboxyl-terminus domain in early stage Lyme borreliosis*

Figure 42. Yield of Nanotrap particle pre-processing.

Figure 43. Yield of Nanotrap particle pre-processing using Sample Buffer 2X as elution buffer.

Figure 44. Magni, R. *et al*. (2015). Infection with common non-Lyme pathogens do not generate a false positive for *Borrelia* in the present Nanotrap test. In *Application of Nanotrap technology for high sensitivity measurement of urinary outer surface protein A carboxyl-terminus domain in early stage Lyme borreliosis*

Figure 45. Magni, R. *et al*. (2015). Interfering substances: the presence of a high amount of protein and blood in the urine does not interfere with Lyme antigen capture and detection. In *Application of Nanotrap technology for high sensitivity measurement of urinary outer surface protein A carboxyl-terminus domain in early stage Lyme borreliosis*

Figure 46. Magni, R. *et al*. (2015). Lower limit of detection/quantitation and reproducibility of the urinary OspA Lyme test. In *Application of Nanotrap technology for high sensitivity measurement of urinary outer surface protein A carboxyl-terminus domain in early stage Lyme borreliosis*

Figure 47. Nanotraps capture OspA in infected ticks.

Figure 48. Magni, R. *et al*. (2015). Nanotrap particle preprocessing step is necessary to detect an OspA specific band in the urine of a patient, clinically positive for Lyme disease. In *Application of Nanotrap technology for high sensitivity measurement of*

LIST OF TABLES

1. INTRODUCTION

1.1 BIOFLUID BIOMARKERS FOR EARLY DETECTION AND BETTER PROGNOSIS

Many diseases including cancer are currently detected only in later stages when enough damage has already been induced to the patient and the chance of a successful treatment is dramatically reduced[1]. The identification of novel biomarkers, as well as the improvement of the detection sensitivity of current analytical platforms, could have a great impact for the early diagnosis and the cure of many life-threatening diseases. On a cellular level, disease like cancer are characterized by several changes in the cellular networks that can be recognized by difference in mRNA, micro-RNA and protein profiles[2,3]. Generally an increase of abundance of specific biomarkers in body fluids (i.e. proteins/peptides or their prost-translational modifications) is often associated to the presence of an active disease. The reason is that many classes of proteins or fragments of proteins are shed into the body fluids that surround the organ and transported to different parts of the body by diffusion or convection. As a consequence, changes in protein expression profiles that can be found in body fluids can be considered 'disease fingerprints' of altered cellular networks[2]. The peptidome, or low-molecular-weight (LMW) proteome, is of particular interest because it may contain a high number of clinically relevant markers yet to be discovered. It is in fact important to note that LMW proteins are able to passively diffuse through the endothelial cell barrier of blood vessels, a barrier that effectively prevents the passive perfusion of molecules above 60 kDa[4]. Because biofluids account for 60% of the body mass[5], they represent a goldmine of significant biomarkers whose discovery could greatly increase the possibility of early

diagnosis, better monitoring of disease progression and development of more successful treatments.

As a consequence there is a particular focus in developing and improving analytical techniques for the analysis of biofluids that could allow the discovery of new biomarkers or could increase the sensitivity of detection of biomarkers that are currently used in clinical tests[6–8].

Body fluids are divided in intracellular and extracellular which include fluids that are excreted or secreted as a consequence of physiological and pathological body functions as shown in Figure 1 (Ahn, S. *et al*, 2007). Different body fluids and their distribution. In Proteomics of Human Body Fluids p.30. The extracellular fluid include the tissue interstitial fluid (TIF) (around 75%), the blood plasma (around 25%), the fluid of bone and dense connective tissue and, the smallest component, named trans-cellular fluid. Trans-cellular fluids are separated from plasma and interstitial fluid by cellular barriers. Examples of these fluids are cerebrospinal fluid, ocular fluid, joint fluid, peritoneal fluid, pleural fluid, breast ductal fluids and bladder urine[9]. The TIF sorrounds tissues and exchange molecules with the intracellular fluid, while plasma is in constant communication with all the microenviroments throughout the body and constantly exchanges signals and nutrients directly or via lymphatic system. Although plasma and serum are the richest source of potential biomarkers and reflect the state of all tissues, other biological fluids (such as CSF, urine, sweat, saliva…) can be significant in the description or a particular pathological state.

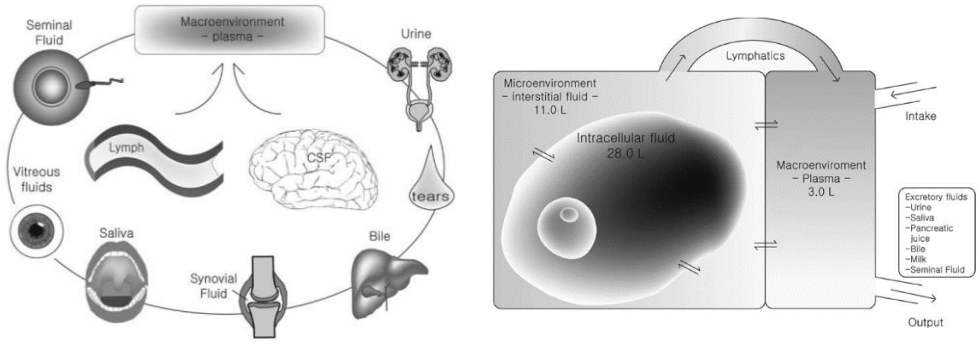

Figure 1. Different body fluids and their distribution. (Source: Ahn, S. et al.,2007)

Each body fluid has a peculiar composition which depends on the specific functions and includes proteins, salts, and variables amounts of glucose, urea, and other substances. Proteins from tissues are found in biological fluids, and their concentration varies depending on the fluids. In the tissues, proteins secreted or shed from cells, reach the lymphatic system from the TIF. Then lymph fluids from various regions of the body, drain into the circulatory system, where the tissue protein will result diluted several folds. Approximately 2.5 L of lymph drains into the systemic circulation per day, whereas about 3 L of plasma, approximately 5 L of blood, is ejected from the heart every minute. The concentration of a biomarker thus decreases from TIF to blood. Sedlaczek *et al*. observed a differential enrichment of CA125, an ovarian cancer marker, in different body fluids from patients with ovarian carcinoma. According to this study, the median value of CA125 is approximately 64-fold higher in cyst fluid than in serum[10].

1.1.1 Proteomic approaches to the analysis of body fluids

Mass spectrometry is considered the gold standard technology for discovering new biomarkers in bodily fluids. Five are the main steps involved in the analysis of body fluids: 1) sample collection and storage; 2) sample enrichment (removal of high abundance proteins); 3) protein separation; 4) protein analysis; 5) protein identification and quantitation.

Sample collection and storage

Sample preparation plays a fundamental role in the proteomic analysis pipeline. Standardized procedures regarding sample collection, processing and storage are crucial in order to guarantee precision and reproducibility of the results. A number of phenomena can occur after collection such as degradation, modification, and precipitation[3,11,12]. Different anti-coagulants, protease inhibitors are often added depending on the biological fluid and the analytical method that will be used. Freezing and thawing procedures are also crucial in preserving the original characteristics of the bio-sample.

Removal of the high abundant proteins and sample enrichment

Protein concentration in biological fluids can span for 12 orders of magnitude while on the other hand the dynamic range of mass spectrometers covers only 5 orders of magnitude. For this reason high abundant proteins such as albumin can mask less-abundant proteins, thus decreasing the chance of detecting them. In order to overcome this issue, several depletion methods have been developed. Immunoaffinity depletion columns, for example, have been previously employed in order to deplete the samples from high abundant proteins before analysis. Depletion of high abundant proteins is usually performed by affinity columns based on dye ligands or antibodies for albumin removal[13] and protein A or G for the removal of immunoglobulins. Ammonium sulfate precipitation (ASP) has also been utilized as a method for removal of highly abundant proteins from blood plasma with good

reproducibility[14]. Another approach that significantly reduces the dynamic concentration range of proteins present in a complex sample is based on peptide libraries or selective capture. A large peptide library is created through the use of combinatorial chemistry and immobilized on a solid surface. Because the library contains 20^6 hexapeptide ligands, each protein or peptide should be able to bind at least one of the ligand. Because of their high concentration, high-abundance proteins saturate their specific ligands and the excess will be washed away. As a consequence a greater fraction of the LMW analytes will be bound to the library compared to the HMW abundant proteins and their relative concentration will be increased[15].

An alternative method used to reduce the dynamic range is selective capturing. This method exploits the unique properties of a selected group of proteins for the enrichment. Immunoprecipation for example employs the affinity of an antibody to its target proteins to selectively bind and enrich proteins and proteins isoforms, phosphorylated proteins and protein-protein complexes[15]. Protein glycosylation is an abundant and biologically significant posttranslational modification - commercially available lectin affinity chromatography columns and, immobilization methods based on hydrazide chemistry are widely used for the purification of glycoproteins[16,17]. Phosphorylation plays a pivotal role in the regulation of many biological processes, such as cell growth, division, and signaling. Dysregulation of these phosphorylation-mediated signaling pathways has been found to be the underlying basis of many human diseases such as cancers and heart diseases[18–20]. Commonly used phosphopeptide enrichment methods can be grouped into chemical and affinity based methods. The three major methods to capture phosphopeptides include immobilized metal affinity chromatography (IMAC), reversible covalent binding, and metal oxide affinity chromatography (MOAC). Oxides that have been applied towards selective phosphopeptide enrichment include titanium dioxide (TiO_2), zirconium

dioxide (ZrO_2), aluminum oxide (Al_2O_3), and niobium oxide (N_2O_5). Aluminum hydroxide has also been used[21].

Another recent technique called activity based protein profiling (ABPP) uses protease inhibitors to act as affinity ligands in order to enrich selective classes of proteins based on their activity[22].

Protein separation

After performing an enrichment of LMW proteins depleting the HMW high-abundance protein from the sample, additional separation processes are required. While several methods for sample fractionation such as ultrafiltration, combination of ultrafiltration and chromatography are used on body fluids, the most universally applicable method for separating proteins is 2D polyacrylamide gel electrophoresis (2D-PAGE). 2D electrophoresis is a technique that combines a protein separation along a first dimension based on the isoelectric point of the proteins in the sample (Isoelectric Focusing IEF), and a second separation on a second dimension as a function of the protein molecular weight (gel filtration). 2-DE can be used to separate more than 5000 proteins at the same time and those can be also identified through Coomassie brilliant blue or silver staining[23]. Unfortunately 2-DE is not sensitive enough for biomarker detection (1-10ng) and suffers from issues related to lack of reproducibility and resolution, and low sensitivity.

Liquid chromatography is another very common separation technique used in analytical chemistry, the separation is based on the partition coefficient of analyte between a stationary phase (Solid or Liquid) and a mobile phase (Liquid). The solid phase is placed in a column and the mobile phase where the analytes are dissolved flows through the column. The mobile phase speed is dependent on its own chemo-physical properties as well as the one of the stationary phase, and the analyte. Different stationary phases are available and allow to perform different types of separation. Examples are normal phase (NP), reverse phase (RP), Size-exclusion chromatography

(SEC), ion-exchange chromatography (IEC), immunoaffinity chromatography (IAC), or hydrophilic interaction chromatography (HIC) columns. Reverse phase high pressure liquid chromatography (RP-HPLC) is the most widely used technique used for sample fractionation in proteomic analysis. In this particular technique the stationary phase is often a hydrophobic material, Octadecysilyl (C_{18}Si-)(ODS) column, and the mobile phase is often water combined with organic solvents such as methanol or acetonitrile. Analytes are separated through the increasing of the organic component in the liquid phase because of their hydrophobicity. Reverse phase chromatography is often coupled with mass-spectrometry.

Another approach to protein fractionation is called shotgun method. In this method all the proteins are digested to peptides that are then separated with 2D high performance liquid chromatography 2D-HPLC[24,25].

Protein analysis and quantification

MS is considered a go-to method for the identification of proteins and peptides in complex biological samples. MS measures the mass-to-charge ration, m/z) of the molecules (ref T) permitting their identification, sequencing and characterization of post-traslational modifications. The mass spectrometer is composed by an ion source, a mass analyzer, and a detector.

The ion source allows for the ionization of the analytes; two of the most common techniques used to ionize proteins and peptides are Electrospray ionization (ESI) and matrix-assisted laser desorption (MALDI). In ESI the ionization happens at atmospheric pressure, and the ions are transferred into the mass spectrometer. One of the advantage of this technique is that high molecular weight compounds can be observed at low m/z values because multi-charged analyte ions are produced during the process. In MALDI the analytes are ionized through laser pulses and it is best suited for the analysis of relatively simple protein mixtures and proteins with high molecular weight.

Ionized proteins and peptides are then analyzed by a mass analyzer according to their m/z. Different kind of analyzers are: Quadrupole (Q), Ion Trap (IT), Fourier Transform ion cyclotron resonance (FT-ICR) and Time of Flight (TOF).

Each of these technologies, exploit a different physics principles and separate ions based on their behaviors in electric fields and/or in vacuum. Once the ions are produced and analyzed, they are registered by an ion detector. The Ion detector generates a signal from incidents ions by either generate secondary electrons or by inducing a current generated by a moving charge. The ion signal is amplified, and based on the method applied, the detector is called Electron Multiplier or Photomultiplier. All advanced modern mass spectrometers use photomultiplier ion detectors.

Protein identification follows two paradigms: top-down and bottom-up (REF T). A top-down approach involves the direct ionization of undigested intact proteins. An ion source which is normally ESI or MALDI is often used. Using an ESI source, the ions generated have multiple charges, thus the resulting spectra are very complex. Because proteins do not have a stable mass value but a mass distribution due to the presence of stable isotopes the resulting spectrum appear complicated and the identification requires higher resolution and accuracy. As of today, only Fourier Transform Ion Cyclotron resonance (FT-ICR) analyzers reach the required level of accuracy. Furthermore a top-down approach requires the use of an efficient method of fragmentation of whole proteins. A top-down approach allows to achieve higher total sequence coverage of proteins than a bottom-up approach, however expensive instruments and sophisticated data processing software are required.

Bottom-up approaches are normally used for proteomic analysis. In these methods, both the mass and the sequence of peptides are used to identify a particular protein. Proteins are first digested with proteases, the masses are

then measured and a mass profile is created, then they are compared to a database that contains sequences of predicted proteins belonging to a particular species that is examined. The comparison between the experimental and theoretical mass is called peptide mass fingerprinting. Because many peptides can have a very similar molecular weight within the methods error limit, it is necessary to know the sequence of the peptides as well as their masses. Information about the sequence are obtained by performing sequential mass analysis using MS-MS instruments. In the first MS analysis peptide ions that fall into a specific m/z interval are selected, a fragmentation step then produces a number of fragment per selected ion. The m/z of those fragments is then measured with a second MS analysis. MS-MS analysis allow the identification of a single precursor with a high level of confidence because even though analytes can have the same mass, it is very unlikely that they will also have the same fragments.

With this approach only 20-40% coverage of a particular protein is obtained. Not all the peptides are detected because they can be too small or too large, or not all the proteins are ionized. Because a MS-MS analysis produces several thousands of peptides they can exceed the analytical capacity of the mass spectrometers. Protein quantification based on mass spectrometry is becoming increasingly popular. Protein quantification is particularly important in order to know which proteins are up or down regulated during particular stages of a disease and quantification based on 2D gels is often not accurate or sensitive. MS-based quantitation is often performed using calibrator proteins or peptides that are isotopically enriched with ^{13}C, ^{15}N or ^{18}O that are then mixed with the samples and analyzed together. A comparison between the reference peak and the analyte peak is used for quantification[26].

1.2 HYDROGEL NANOTRAPS

The identification of novel biomarkers as well as the improvement of the detection sensitivity of current analytical platforms could have a great impact for the early diagnosis and the cure of several diseases including cancer. Unfortunately, while studies focusing on the discovery of low abundance biomarkers are increasing, the results are not very encouraging considering that very few candidates have been clinically validated in the recent years[27,28]. Primary physiological and technical roadblocks thwarting biomarker discovery can be summarized as follows:

1- Several relevant biomarkers exist in body fluids in extremely low concentrations (attomolar) that fall below the detection limits of mass-spectrometry and conventional immunoassays. In its early stage, a diseased tissue releases only a small amount of biomarkers. Furthermore only a small sample volume, usually few µl, containing a very low number of the relevant molecules can be loaded for analysis on MS and immunoassays[29].
2- Biomarkers are often masked by high-abundance proteins that are several orders of magnitude more concentrated[3,30]. Proteins like albumin and immunoglobulins in fact account for more than 90% of the plasma proteins and exist in a billion fold excess compared to several biomarkers which are often non-covalently and endogenously associated with these resident proteins.
3- Biomarker stability poses a challenge due to the presence of endogenous or exogenous proteases which make candidate biomarkers subject to degradation immediately after sample collection[31]. Therefore an important question relates to how biological fluids can be successfully transported and stored without incurring into the loss of clinically relevant

proteins. This becomes even a more important issue when we consider the large repository of serum and body fluids collected from several different hospitals or institutions where samples are collected and shipped at different temperatures or without freezing.

Hydrogel Nanotraps have been proposed as a novel and successful tool that allows to overcome the previous technical and physiological challenges regarding the biomarker purification and preservation[29,32–34]. Hydrogel Nanotraps are a technology with a large applicability in biology and medicine and they have been often described as good candidates for drug delivery[35–37] and in-vivo imaging[38]. In contrast to their common application as a drug delivery tool, we employed hydrogel Nanotraps in order to capture, instead of releasing target analytes.

Our hydrogel Nanotraps are polymers that contain a large fraction of water in their structure, and are formed by hydrophilic organic monomers that are cross-linked into a network by covalent interactions. This open-meshwork core can be functionalized with several organic dyes that act as high affinity ($Kd<10^{-11}$) baits for different macromolecules such as proteins and peptides. Hydrogel Nanotraps are in fact able in one single step, in solution, to concentrate target analyes improving the sensitivity of detection of analytical instruments as well as preserving the biomarkers from proteases. Nanotrap chemistry can be tailored in order to specifically attract and sequester relevant and low abundant proteins and peptides while excluding high abundance proteins like immunoglobulins and albumin[29].

As shown in Figure 2 (Magni, R. *et al*., 2014) virtually all the target proteins present in a body fluid sample are sequestered by the Nanotraps and are then eluted in small volumes, usually few µl, with the use of specific elution buffers that have a composition compatible with the assay that will be used for the following analysis. As a results of their increased concentration, many

previously invisible proteins can be successfully detected by mass-spectrometry, western blotting and other immunoassays[32,34,39,40]. Although hydrogel Nanotraps have been widely applied to capture proteins and peptides, their physical and chemical properties can be modified in order to target all the major categories of body fluid bioanalytes including such as nucleic acids and metabolites as well as entire viruses[41]. Nanotraps are a very versatile technology that can allow with a simple pre-processing step to increase the sensitivity of current diagnostic test[34,39], as well as allowing the discovery of new and clinically relevant biomarkers[29,32,42].

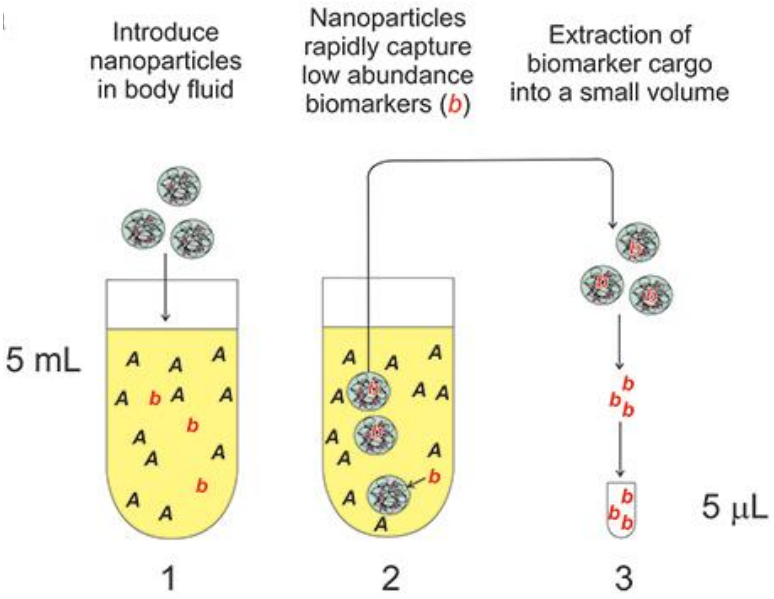

Figure 2: Nanotraps harvest and concentrate low abundance proteins from complex biological fluids. a) Workflow for harvesting proteins. Total processing time is approximately 1.5 hr. Proteins in solution are concentrated from blood, serum, plasma, urine, sweat, saliva, or other body fluids (1000-fold concentration depicted). (Source: Magni, R. et al., 2014).

1.2.1 ARCHITECTURE OF HYDROGEL NANOTRAPS

Hydrogel Nanotraps are characterized by high homogeneity in size distribution (diameter of 300 - 1000nm) and form a stable suspension in aqueous solution. They have a spherical physical structure, they are formed by the free radical polymerization of monomers and cross-linking agents[43,44] and they show specific physicochemical properties that are different from simple polymer solutions. Their dimension is dependent on several condition such as temperature, pH, electric field strength, light, ionic strength and solvent. Because 99% of the Nanotrap is composed by water, protein and peptides can freely penetrate. For our applications we synthesized hydrogel Nanotraps that are made by the co-polymerization of N-isopropylacrylamide (NIPAm) and co-monomers like Acrylic Acid (AAc) and Allylammine (AA),

vinil sulfonic acid (VSA) but other monomers such as boronic acid, and N-Allylannine can be included in the structure (Figure 3).

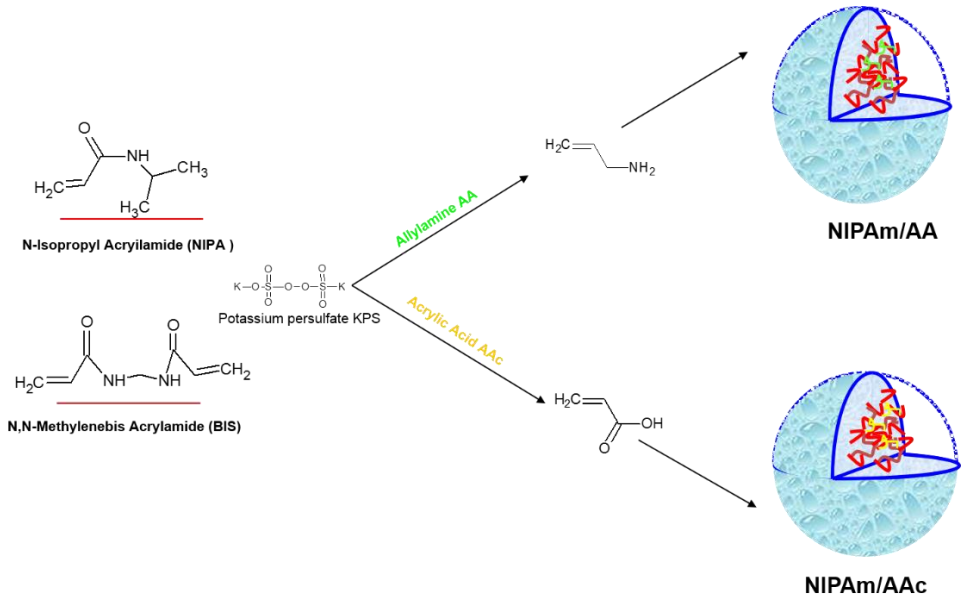

Figure 3. Hydrogel Nanotrap synthesis. Hydrogel Nanotraps are formed by the co-polimerization of N-Isopropyacrylamide (NIPA) and monomers like Acrylic Acid or Allylamine in the presence of a cross-linking agent such as N, N-Methylenbis Acrylamide.

The presence of co-monomers is used to tailor Nanotraps to provide unique chemo-physical characteristic such as pH sensitive size variation, affinity or repulsion of particular proteins or analytes, and ability to chemically bind several functional groups post-polymerization. The structure of the Nanotrap can be modified in order to provide a different permeability and porosity. The porosity determines a molecular weight cut-off size that excludes high MW proteins from entering the Nanotrap and it is obtained by changing the molar ratio between the monomer and the cross-linker. When added to a body fluid the Nanotraps behave as a molecular sieve, physically excluding high molecular weight proteins (i.e. albumin and immunoglobulin) (Figure 4). Each

class of particle will sequester and concentrate a class of analytes below the molecular cut-off recognizable by the bait.

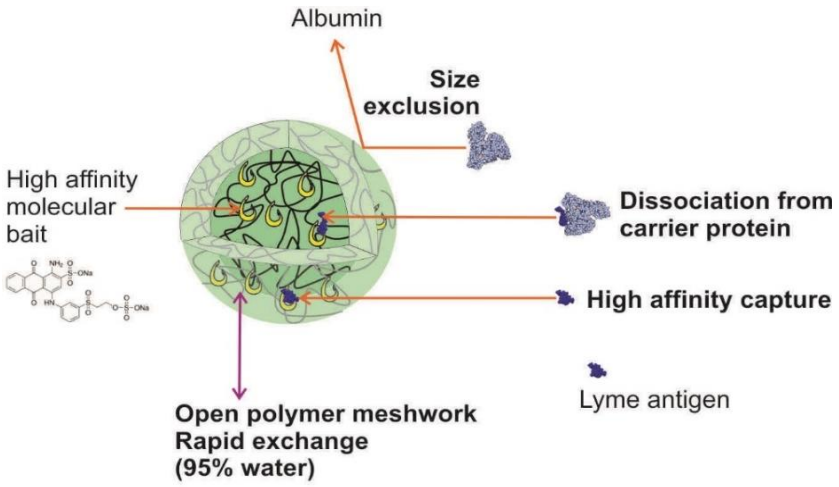

Figure 4. Structure of core-shell hydrogel Nanotrap. The porous structure allows LMW proteins to enter while excludes HMW proteins. The presence of an outer shell actively excludes unwanted protein such as albumin and albumin fragments. The core is functionalized with chemical affinity bait that are able to attract and immobilize target biomarkers.

1.2.2 Use of commercial dyes as high affinity baits for proteins

Organic dyes have been used widely in the textile industry and their chemistry has been extensively studied. Several dyes show strong affinity for protein fibers such as cotton, wool or other fibers, depending on the class of the dye. The binding mechanism can differ, but often a strong affinity is established between the dye and the fiber (Figure 5). These dyes usually contain reactive groups such as hydroxyl (-OH), chloride (-Cl), amine ($-NH_2$), sulfonate (SO_3H), and aromatic rings. These groups often play important roles in their binding to proteins and peptides, which is typically achieved by a combination of ionic, hydrophobic, and electrostatic interactions, along with stabilizing Van der Waals interactions which are maximized when the 3-D structure of the dye matches with the one of the target protein.

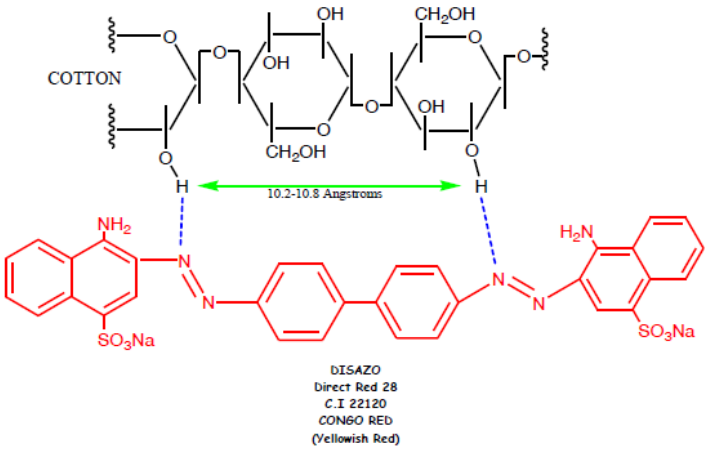

Figure 5. Dye interaction with fibers. Example of a dye (Direct Red 28) and mechanism of interaction with cellulose (cotton). Hydrogen bonds are formed when the two azo likages are separated by ~10.2-10.8 Angstroms

Different classes of organic dyes have been previously used in proteomics and analytical chemistry to bind proteins, as inhibitors of protein-protein interactions[45], and to remove some specific proteins like albumin from complex matrices. In affinity chromatography, ligands are particular molecules that possess the ability to bind specific analytes or classes of analytes. Normally ligands are immobilized on an insoluble support made of polymeric material and they are often very specific, but because they require several steps of preparation and purification, they are also very expensive. Dye ligands on the contrary represent an inexpensive alternative to conventional ligands used in affinity chromatography and show a high affinity toward many different proteins. Several studies focusing on the affinity of dyes and proteins have been performed. For example Dextran blue was shown to have affinity for kinases and Cibacron blue was immobilized on Sephadex in order to purify pyruvate kinase[46,47]. The dye-ligands commonly used in affinity chromatography are often formed by a chromophore groups linked to a functional group such as sulfonic acid, carboxylic, ammonium

chloride, or metal-complexing groups. Many dyes employed for purification purposes have triazine moieties, $C_3H_3N_3$, in which the three carbon atoms are highly positively charged. Dye ligands can also be chemically modified adding particular functional groups in order to target specific proteins. Cibacron blue specificity towards certain classes of proteins is due to mainly hydrophobic interactions and the binding is stabilized by electrostatic forces[45,48,49]. Most of the dyes available have never been tested in affinity chromatography or for protein capture.

It has been shown that the affinity of the dye for carrier bound biomarkers is higher than the affinity of the biomarker for the carrier protein and it is dependent on the isoelectric point of the proteins and the dissociation constant of the Nanotraps[50]. Acrylic acid is negatively charged at pH higher than 3.5 and so able to attract proteins and peptides positively charged. Allylammine on the other hand act as a bait for carrier proteins that have a negative charge.

Triazine derived textile dyes (Cibacron blue F3G-A, Procion red H8BN) represent a class of dyes that have shown strong affinity for proteins[51]. The mechanisms used to bind proteins is still unclear. In the case of Cibacron and related dyes blue hypotheses include: a) the interaction between the dinucleotide fold structural domains of proteins with the dye, which can assume a conformation that mimics the orientation and the anionic group characteristic of NAD[52]; b) non-polar pockets surrounded by hydrophilic amino acids residues that can interact with the aromatic rings of the dyes or positively charged groups which binds the sulfonate residue[53]; c) a mixture of ionic and hydrophobic forces.

A menu of baits (Figure 6) has been selected and successfully immobilized onto the Nanotraps in order to selectively bind and concentrate a diverse classes of biomarkers, such as proteins, peptides, glycolipids, nucleic acid and lipids.

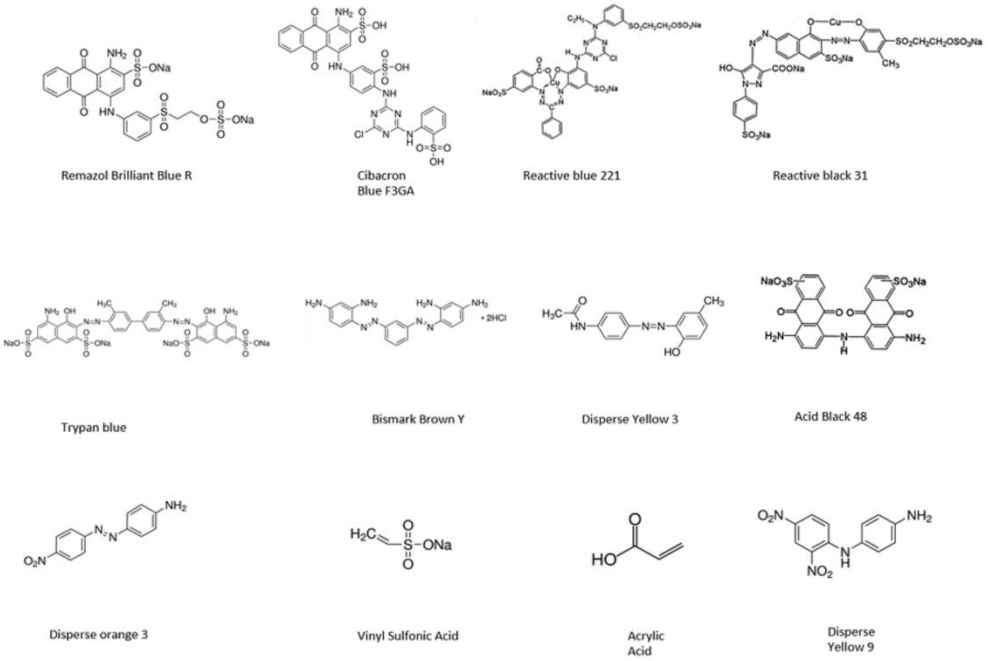

Figure 6. List of dye baits. Representation of few examples of chemical dyes that can be incorporated into the hydrogel Nanotraps.

Because of the bait chemistries that selectively interact with the 3-D conformation of target proteins with very high affinity, dye-functionalized Nanotraps are able to virtually deplete the entire content of the target biomarker from the solution in only few minutes[32,50,54].

Each bait shows a different affinity for different classes of proteins, and if the Nanotraps are used to sequester a wide spectrum of analytes, a mixture of differently functionalized Nanotraps can be used[29] (Figure 7).

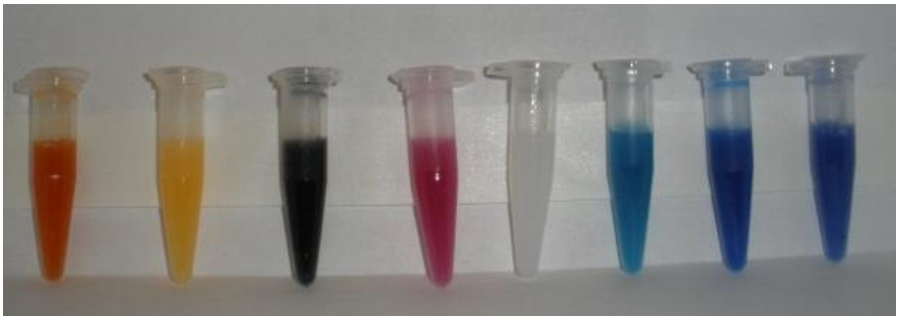

Figure 7. Different batches Nanotraps functionalized with several commercial dyes.

When a high affinity binding is established between a dye and a protein, the equilibrium is shifted towards the bound state and the dissociation constant is low (K_D<10^{-12} M) (Figure 8).

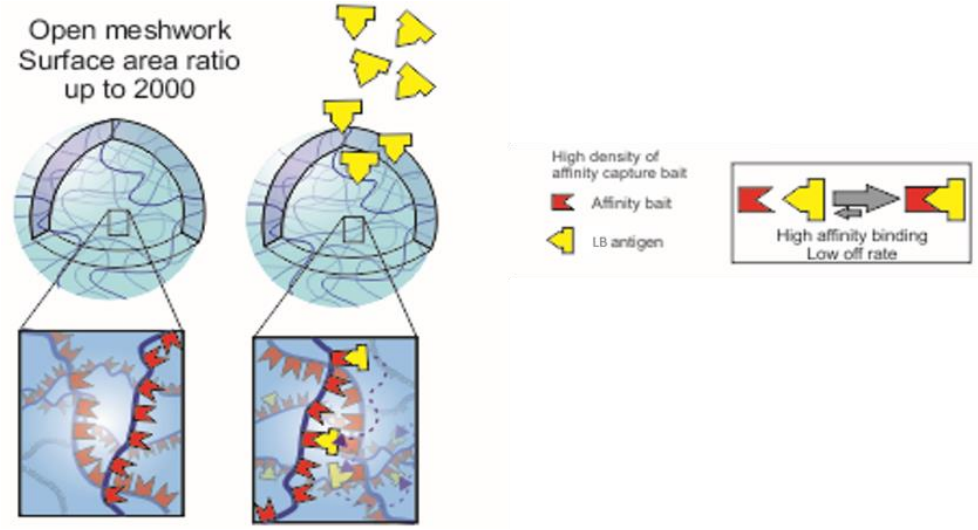

Figure 8. Nanotrap particles are characterized by a very high surface area ratio and high binding capacity. Dye baits are covalently immobilized in the core of the Nanotrap and are able to form high affinity non-covalent interaction with different classes of proteins. In the binding equilibrium between ligands and proteins, high binding affinity and high density of ligands ensure high on rate and very low off rate.

Hydrogel Nanotraps that do that do not contain any chemical bait have inefficient capture equilibrium because many target proteins are not “free” in

the bloodstream, but they are instead associated with high-abundance resident proteins such as albumin via non-covalent interactions. The efficiency with which these proteins are captured is therefore affected by the rate at which this equilibrium is reached. On the other hand, chemical baits that have been incorporated into the Nanotrap compete with high-abundance resident carrier proteins for the binding of the target biomarker.

1.2.3 Nanotrap characterization

To assess the quality of a Nanotrap batch, a strict quality control needs to be performed; particle size variation with temperature, uniformity of their size distribution, as well as dye incorporation need to be evaluated.

The volume phase transition temperature (VPTT) is a property of the hydrogel which consist of a change in volume at a particular temperature[55]. NIPAm Nanotraps swell at temperature below 32°C and shrink when the temperature increases. The VPTT is dependent upon different conditions such as the amount of cross-linker, the solvent, the ionic strength of the surrounding medium and the type of co-monomer used. For example if AAc (pKa=4.35) is present, the size changes when the pH>4.35 because of the charge repulsion that is created.

In this thesis particle size was determined by photon correlation spectroscopy (PCS) using a light scattering detector (LSD) (submicron particle size analyzer, Beckam Coulter)(Figure 9). PCS is based on “Rayleigh scattering” which is the scattering of a light or electromagnetic radiation by a particle much smaller than its wavelength. The fluctuation in the intensity of the laser beam is function of the particle size. Particles diameters are measured in water (refractive index=1.333, diluent viscosity=0.890 cP) and a test angle of 90° is used. Values are then converted to particle size via the Stokes-Einstein relationship. Change regarding the molar ratio of reagents used in the Nanotrap synthesis allow to

produce Nanotraps of different sizes. For our study the average dimension ranges between 300nm and 1µm.

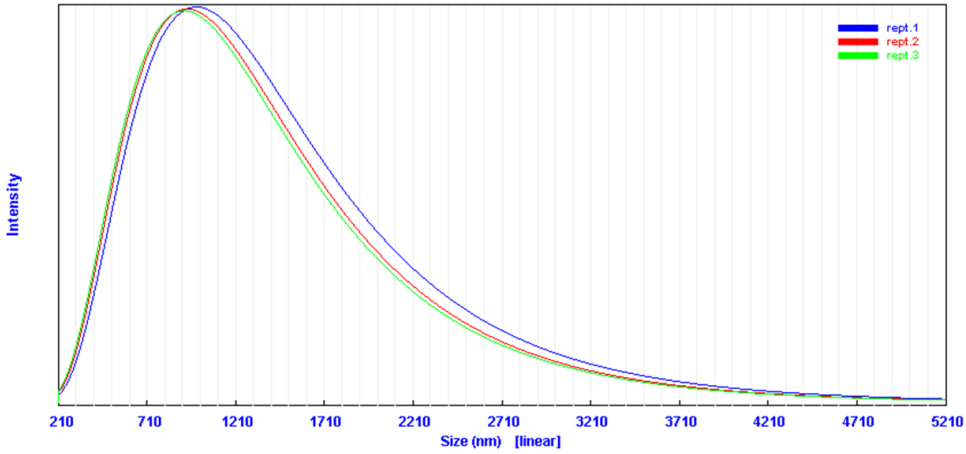

Rept#	Mean [nm]	P.I.	Diff.Coef [m^2/s]	Counts/s	Baseline error
1	1097.4	-1.065	4.47e-13	1.02e+5	4.50%
2	1042.8	-1.230	4.70e-13	1.01e+5	1.21%
3	1024.0	-1.422	4.79e-13	9.95+4	0.33%
Average	1054.7 ± 31.11	-1.239 ± 0.146			

Figure 9. Example of Nanotrap size measurement through light scattering. Hydrodynamic diameter of a batch of Remazol brilliant blue functionalized Nanotrap particles was 1054.7 +/- 31.11 nm.

1.2.4 Measuring uniformity of size distribution through Atomic Force Microscopy

The uniformity of Nanotrap size distribution was measured with atomic force microscopy as shown in Figure 10 (Luchini, A. *et al.*, 2010). AFM is a microscope that measure a sample surface "feeling" it with the use of a very sharp probe. This sharp tip is mounted on the end of a cantilever that moves

on the surface of the sample. When the tip approaches the sample surface a combination of forces, including Van der Waals, electrostatic, capillary and double layer interactions are generated and cause a deflection of the cantilever. A laser beam is directed to the upper surface of the cantilever and reflected onto an array of photodiodes. Once the tip moves over the sample surface the deflection of the cantilever changes the reflection of the laser and the intensity of the beam striking the photodiodes varies in relation to the roughness of the sample surface. Modern AFM can operate in two modes: contact mode and dynamic mode. In the first one the tip is in contact with the sample surface, while in the second the tip does not make contact with the sample surface but the cantilever oscillates at a resonant frequency that is perturbed by the forces acting between the tip and the sample surface. While contact mode is preferred for characterizing the roughness of metal and other material surfaces that cannot contaminate the tip, the dynamic mode is preferred when cells, or biological molecules that could contaminate the tip need to be visualized.

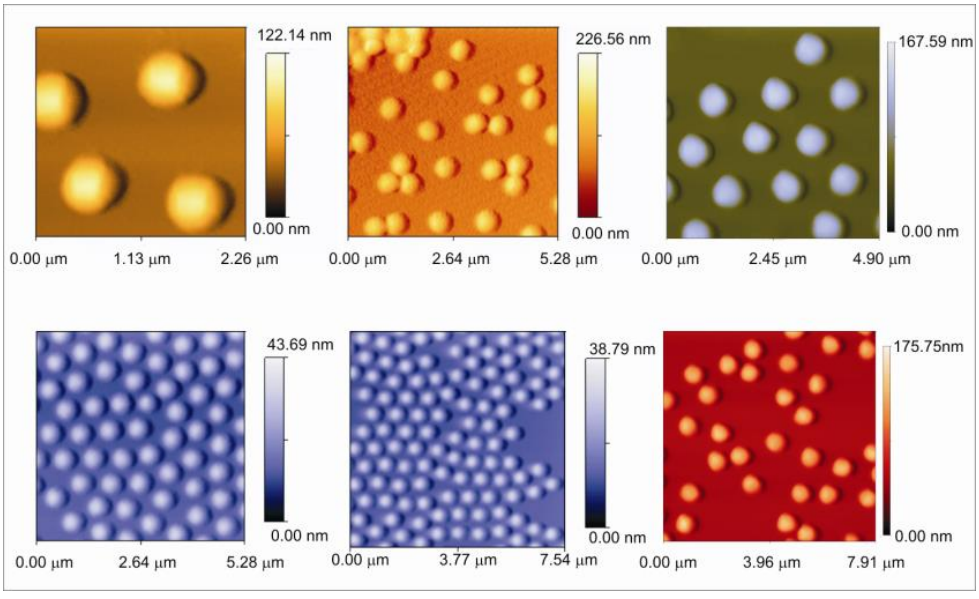

Figure 10. Atomic force microscopy (AFM) of hydrogel Nanotraps. The scale bar (visible on the right-hand side of each picture) shows Nanotrap heights, which range between 76 and 270 nm. The variability of the measured values is probably due to the fact that the picture was acquired under dry status so the particles are distorted from their normal spherical shapes. (Source: Luchini, A. et al., 2010)

1.2.5 Size sieving and exclusion of high-abundance proteins

The pore size of the Nanotraps can be tuned in order to selectively capture low molecular weight proteins by adjusting the degree of cross-linker used. That is very useful in analytical chemistry because the LMW peptidome is regarded as a rich source of potential biomarkers. Proteins with a molecular weight lower than the pore size cut-off will be able to enter the core of the Nanotraps and interact with the affinity bait. Since albumin is present in million fold excess relative to the proteins and peptides of interest, it is crucial to design a Nanotrap that can actively exclude albumin and albumin fragments from entering.

VSA was used as a co-monomer in the preparation of hydrogel Nanotraps to assess its influence in actively exclude albumin. The incorporation of sulfonate groups into the substrate reduces proteins adsorption to the surface due to the negative charge they carry in aqueous media[56].

VSA shelled Cibacron Functionalized Nanotraps were synthesized in order to determine if the BSA repelling properties could be exploited in a biological fluid using a core-shell architecture. In an experiment conducted by Tamburro *et al.*[29], it was shown how CB core/VSA shell Nanotraps were able to exclude albumin while retaining high affinity for other proteins, CB-core particles, VSA-core particles and CB-core/VSA-shell particles were incubated with serum samples. Eluates from the Nanotraps were then loaded on a gel and silver stained as well as run on mass-spectrometry. As shown in Figure 11 (Tamburro, D. *et al*., 2011), the use of VSA shelled Nanotraps decreased the number of unwanted human serum albumin (HAS) fragments

and did not affect the sequestration of target proteins by the CB bait in the core.

Number of peptide hits of HAS as well as the low abundant marker Apo-CIB were measured through mass-spectrometry in unprocessed serum sample as well as in the eluated from the three Nanotrap batches. The eluate from CB functionalize Nanotraps showed 131 HAS peptide hits, more than 10 times less than in crude serum. VSA and CB-VSA showed only 9 and 5 peptide hits for HAS. Interestingly the number of target proteins such as Apo-CIB that were undetected in human serum because of the presence of high abundance proteins, were detected in all the three batches of Nanotraps reaching the highest peptide hits in the CB-VSA Nanotraps.

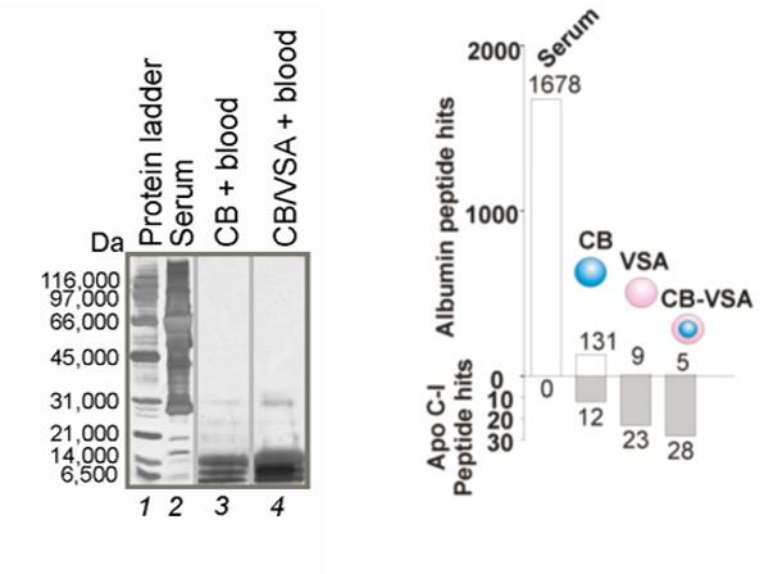

Figure 11. Core-shell hydrogel Nanotrap enrich LMW proteome while excluding abundant HMW proteins. and exclude On the left: Cibacron blue F3GA (CB) core- Vinylsulfonic acid (VSA) shell particles greatly enhance the low molecular weight protein concentration in whole blood (lane 2) with respect to serum (lane 1) while fully excludes abundant albumin, albumin peptides and immunoglobulins. On the right: the number of peptide hits for Albumin and Apo-CIB proteins measure in eluates from serum incubated with CB-core particlse, VSA-core particles and CB-core/VSA-shell particles. The presence of VSA shell excluded unwanted peptides such as albumin without reducing the particles' affinity for a wide range of interesting peptides and proteins. (Source: Tamburro, D. et al., 2011)[29]

1.2.6 Protection of biomarkers from degradation

One of the major problem associate to biomarker discovery and measurement is represented by the degradation by exogenous and endogenous proteases. As shown in Figure 12 (Tamburro *et al.*, 2009), several chemokines (MEC/CCL28, SDF-1B/XCL12b, CCL24) were incubated with trypsin at 37°C in the presence or absence of Nanotraps. Results showed that once captured in the Nanotraps, because immobilized to the affinity bait, labile biomarkers such as chemokines are immune to protease recognition and cleavage. Once the proteins are captured inside the Nanotraps they become immune to degradation by exogenous and endogenous proteases[33].

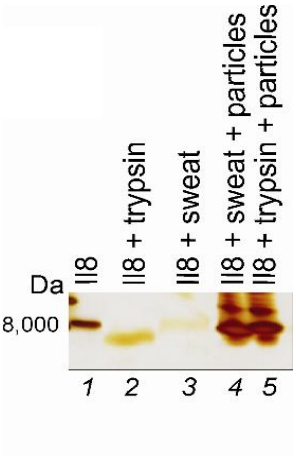

Figure 12. Proteins sequestered in the Nanotraps are protected from enzymatic degradation. Interleukin 8 (IL8) diluted in artificial sweat was incubated with excess trypsin at 37 °C in presence or absence of disperse yellow 9 (DY9) functionalized particles. SDS PAGE analysis revealed that in absence of DY9 particles, the IL8 band disappeared and a fainter band at lower molecular weight appeared indicating the presence of a degradation product (lane 2). In presence of DY9 particles, IL8 is fully protected from trypsin degradation (lane 5). Incubation of IL8 with sweat at 37 C alone caused the intact IL8 band to disappear (lane 3) while the DY9 particles yielded a full density band for the intact protein (lane 4), suggesting that IL8 was protected from degradation at 37 °C. (Source: Tamburro, D. et al., 2011).

1.2.7 Nanotrap processing increases biomarker concentration

Bait-functionalized hydrogel Nanotraps are a very versatile tool for the pre-processing of several biological fluids such as blood, serum, cerebrospinal fluid, saliva, sweat, tears, urine[32–34]. Before processing relevant clinical samples it is mandatory to optimize each Nanotrap parameters in order to obtain ideal results. Some important parameters are: selection of the dye, Nanotrap ratio to sample volume, elution buffer composition. It is advisable

for this reason to create before sample processing a dose-response curve that could provide useful information regarding the reproducibility of the results and the limit of detection. Because the different dyes act as molecular baits thanks to a combination of hydrophobic and electrostatic forces [29], their affinity towards specific proteins cannot be predicted. For this reason a panel of different dyes should be tested and the capturing and elution efficiency measured as a preliminary step. Also, depending on the nature and the strength of the interaction between the capture protein and the chemical baits, different elution buffers should be selected case by case, in order to obtain the maximum recovery of the interest analyte. Tamburro *et al.*[29] describe the screening of Nanotraps functionalized with a panel of 15 different baits in their ability to capture a list of 13 known low abundance biomarkers in order to determine whether the uptake of proteins by the particles was dependent on the specific chemical structure of the dye. Each chemical bait exhibited a unique pattern of captured proteins with different efficiency (Figure 13).

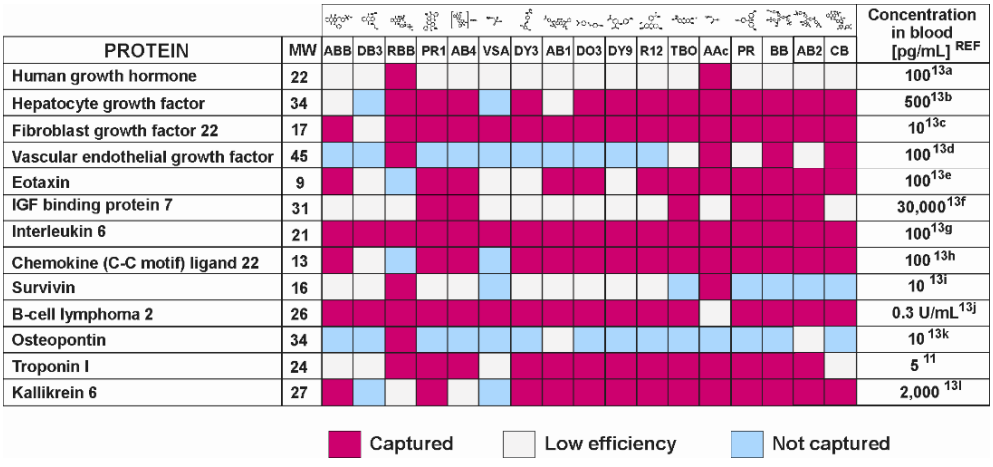

Figure 13. Differently functionalized Nanotraps have affinity for biomarkers. Nanotraps functionalized with 17 different molecular baits show preferential high affinities for 13 specific low abundance biomarkers among which interleukin 6 (Tamburro, D. et al., 2011)[29].

In addition it is important to mention that the elution buffer, especially if detergents are present, needs to be chosen to ensure to the compatibility with the downstream assay.
The concentration factor obtained using hydrogel Nanotraps is a function of the starting volume of the sample. The following formula shows how the detection limit of an assay directed toward a particular analyte can be enhanced by the use of hydrogel Nanotraps.

$$C_{min}=L/(V_i/V_f)=L/c$$

Where Cmin represents the lowest amount of analyte that can be normally detected by that specific assay, L is the lowest limit of sensitivity of the assay, Vi is the initial volume of the sample before processing, Vf is the final volume of the sample after the elution and c is the concentration factor obtained by the ration between the initial and the final volume. Let's assume that we are targeting a particular protein in urine[33]. If our urine sample has an initial volume 50 mL, and the captured proteins are finally eluted into 50 µL, we obtain a concentration factor of 1000. Assuming that the assay we are using has a detection limit of 100 pg/mL, then the Cmin of the assay after Nanotrap processing becomes 0.1pg/ml. This is a hypothetical example and shows how hydrogel Nanotraps can dramatically increase the effective sensititvity of any analytical platforms.

1.2.8 Antigen-displaying Nanotraps

The use of Nanotraps containing degradable cross-linker is a novel concept that permits to combine the concentration ability of the Nanotraps to lateral flow immunoassay (LFA) and ELISA. Partially or fully degradable Nanotraps can be synthesized and could serve for different purposes. In regular Nanotraps, because of their small pore size, high molecular weight proteins

are prevented to enter the core structure. Because immunoglobulins are too big to enter the particles, an elution step to extract proteins from the Nanotraps is required before performing an immunoassay[4,32,40,54]. Partially degradable Nanotraps offer the advantage to increase the Nanotrap pore-size, allowing the antibodies to directly access the target analyte, while still keeping some of the characteristics of the Nanotraps, such as capability of being centrifuged at relatively low speed and re-suspended in smaller volumes. Also, because of an intrinsic affinity of the Nanotraps to functionalized high-binding ELISA plates, they can be deposited on a multi-well plate and directly analyzed. Fully degradable Nanotraps on the other hand are optimal when centrifugation steps are no longer required and the absence of a Nanotrap sterical hindrance could actually negatively affect the assay.

Partially degradable Nanotraps are mixed with the bio-fluid of interest and in minutes capture the target analytes. A degradable cross-linker such as Dihydroxyethylenebis-acrylamide (DHEA) can be degraded through an oxidizing reagent, $NaIO_4$ (sodium periodate), causing an increase in the particle pore size that allows the antibody used in the ELISA or LFA to directly access the antigen captured by the particles (Figure 14). Several other strategies can be used in order to synthesize Nanotraps that can be degraded under different chemical conditions.

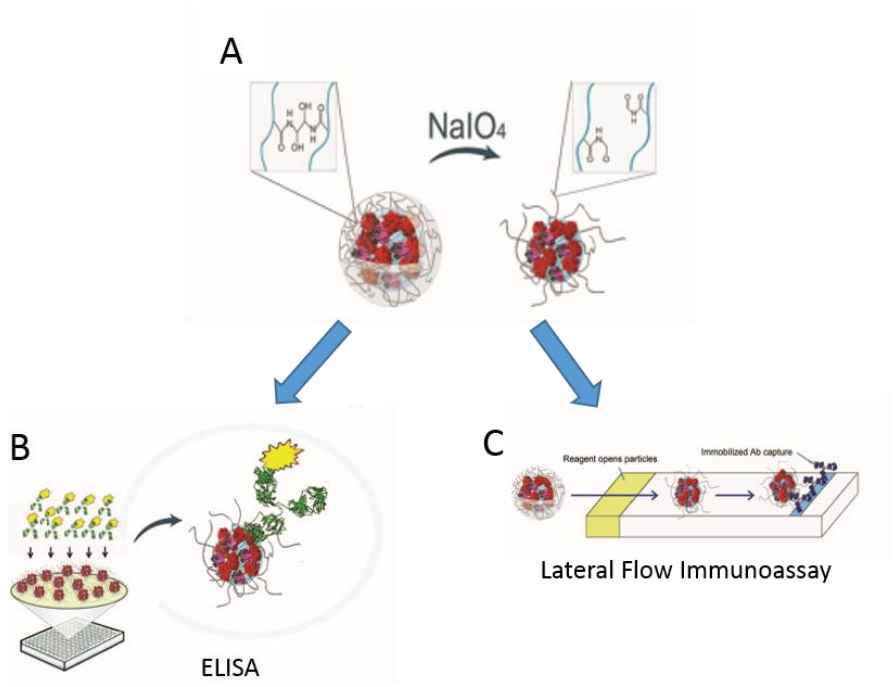

Figure 14. Partially degradable nanotraps are able to expose the captured antigens for direct antibody binding in several types of immunoassays. a) In presence of oxidizing conditions (i.e. $NaIO_4$) Nanotraps can be partially dissolved. b) scheme of an ELISA through immobilization of partially degradable nanotraps. c) scheme of a lateral flow immunoassay using degradable nanotraps. Nanotraps can flow thorough the membrane, once the antigen displaying nanotraps reach the antibody line, they are immobilized and allow for colorimetric detection.

Another degradable crosslinker is bis(acryloyl)cystamine (BAC). Previous studies have already shown the possibility to incorporate BAC as a cross-linker in the synthesis of NIPAm based hydrogels[57]. Because of the presence of the disulfide bond in the BAC structure, the Nanotrap can be degraded in the presence of reducing conditions (Figure 15). The use of a disulfide containing cross-linker was employed to enable erosion of drug carriers in a triggered fashion, while also offering thiol groups within the hydrogel for bioconjugation and controlled assembly[58,59]. Disulfide bond incorporation during Nanotrap synthesis can be challenging, because numerous side reactions that disrupt the sulfur−sulfur bond can occur. The disulfide bond may be homolytically cleaved at high temperatures, resulting in sulfur radical

formation during the synthesis. Additionally, the disulfide bond may enable a chaintransfer reaction, wherein a radical attack at the disulfide leads to the formation of a thioether, with a second sulfur radical released as a result.

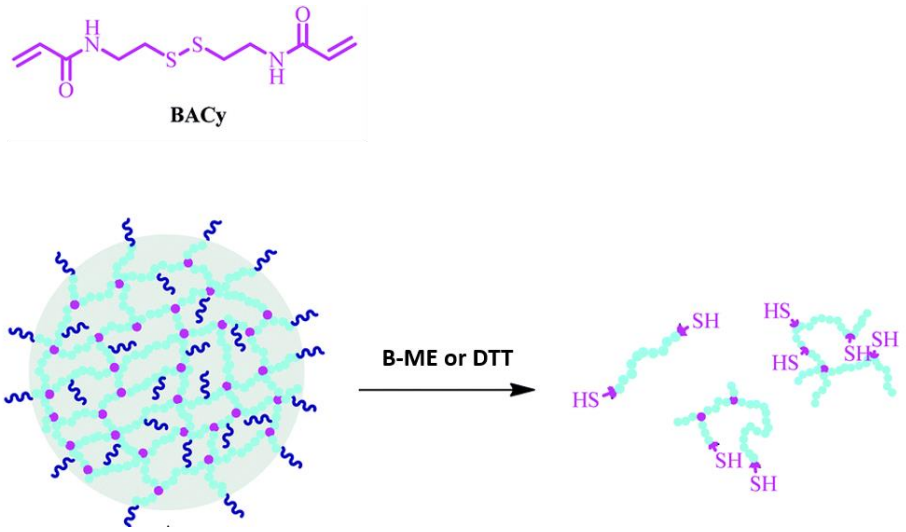

Figure 15. Schematic representation of a partially degradable Nanotrap using BAC as a crosslinker. The disulfide bond of the BAC is cleaved using reducing reagents such as β-Mercaptoethanol or Dithiothreitol.

Pyrazolone containing dyes, characterized by the presence of two acidic groups, can also be used to cross-link allylammine containing polymers. 1-4-Sulfophenyl)-3-methyl-5-pyrazolone was conjugated with vanillin in order to obtain an orange dye that possesses a carboxylic group on one end and a sulfonic group on the other. In basic/neutral condition both groups are negatively charged and can create strong ionic bonds with allylammine groups thus acting as a cross-linker between polymeric strands of NIPAm. By reducing the pH of the particle containing solution the carboxylic end will become protonated, inducing a partial degradation of the Nanotrap. A further drop in pH will induce also the sulfonic group to detach, leading the particle to complete erosion (Figure 16).

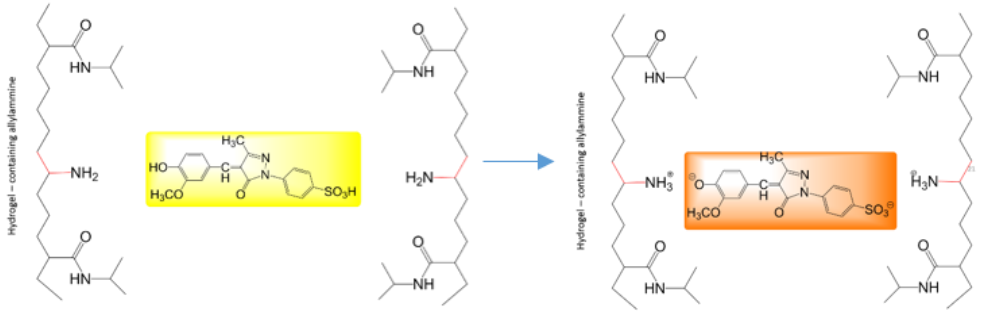

Figure 16. Pyrazolone containing dyes as degradable crosslinkers. The primary ammines of the two parallel poly(Nipam) strands react with the carboxylic and the sulfonic group of the pyrazolone dye at neutral/basic pH. The strong ionic bond formed allow to act as a crosslinker and the reaction can be easily visualized by a change in color of the solution from yellow to orange.

Fast blue B is a dye that can be easily incorporated into previously synthesized hydrogel Nanotraps and shows affinity with different classes of proteins. Its chemical structure also makes it a suitable candidate as a cleavable cross-linker. Fast blue B forms an azo-compound with NIPAm and once the polymeric strands of NIPAm are cross-linked, the azo-bond can be cleaved by the use of sodium dithionite as a reducing agent (Figure 17).

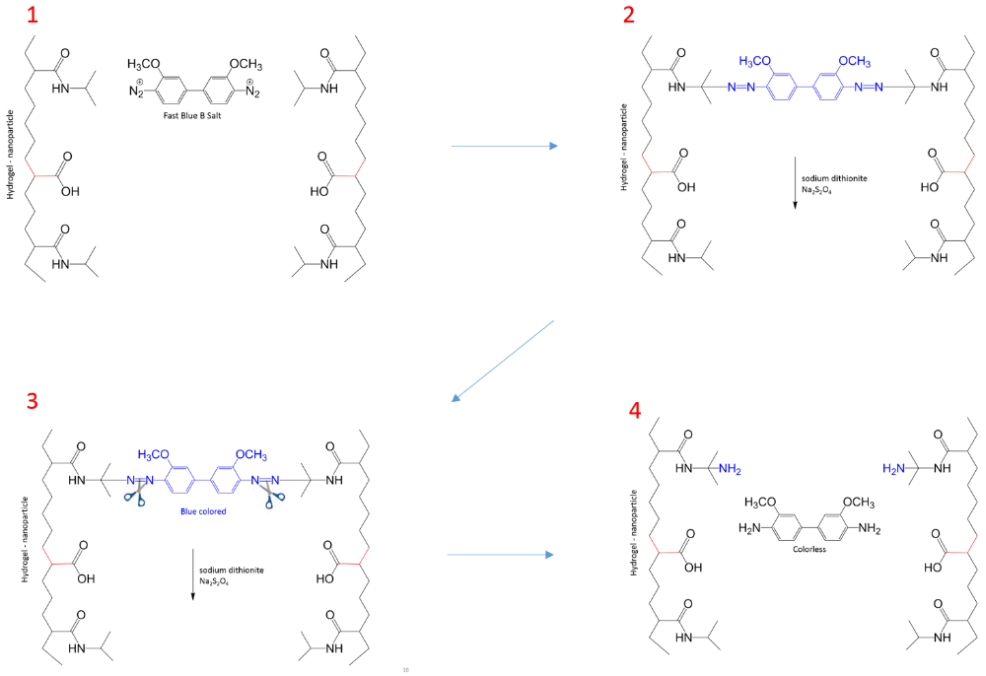

Figure 17. Schematic representation of incorporation and cleavage of Fast Blue B. Fast Blue B is used not only as a high affinity dye but also as a cleavable crosslinker. Once the complex is formed, degradation occurs through incubation of the Nanotraps with sodium dithionite.

1.2.9 Application of hydrogel Nanotraps for biomarker discovery

Nanotraps have been successfully employed for the identification of specific biomarkers related to different cancers; previous studies conducted in our laboratory focused on the investigation of prostate, ovarian[4], soft tissue sarcoma[60], melanoma[32] and pediatric brain tumors. The following paragraph illustrate an example of how a biomarker discovery study could be performed by using hydrogel Nanotraps.

1.2.10 Exploring the CSF proteome in children affected by brain tumors

Central Nervous System (CNS) tumors are the second most common pediatric malignancies, accounting for approximately 25% of all childhood neoplasms. They comprise several groups of tumors, with different histology, arising in different sites of the Central Nervous System[61]. Several studies have shown that pediatric brain tumors often have a very distinct pathogenesis and biology compared to the adult counterpart, even in the presence of an indistinguishable histopathology[62]. Cerebrospinal fluid (CSF) is a very valuable source of biomarkers for brain tumors and represents a potential indicator of pathological processes that happen in the CNS. CSF biomarker discovery poses some physiological and technical challenges: low protein levels (total protein concentration 1.5 to 6 mg/mL), dynamic range (up to approximately 12 order of magnitude), and the presence of highly abundant proteins masking the less abundant ones. Core-shell capturing hydrogel Nanotraps can overcome these challenges capturing, preserving and concentrating candidate low molecular weight, low abundance proteins in solution, in one step, improving the effective sensitivity of mass-spectrometry by several orders of magnitude. Cerebrospinal fluid from 27 pediatric brain cancer patients at initial diagnosis and 13 pediatric oncology controls (extra-CNS non Hodgkin lymphoma) were processed with core-shell hydrogel Nanotraps and then analyzed with reverse-phase liquid chromatography/electrospray tandem mass spectrometry (MS/MS). The MS data was searched against a human protein database NCBI (National Center for Biotechnology) with Mascot software. Spectral counting analysis was accomplished using Scaffold software (Proteome Software Inc.). Protein identification was performed with SEQUEST. The data were searched against a fully tryptic indexed, human protein database maintained by the National Center for Biotechnology Information. Gene ontological annotations for selected proteins was performed using the Database for Annotation,

Visualization and Integrated Discovery (DAVID) as well as IPA Ingenuity System. After label free spectral counting (scaffold analysis) of the LC-MS/MS results, a total of 559 NCBI annotated proteins were identified in both case and control groups. This first list of proteins was searched against the public CSF proteome database www.biosino.org/bodyfluid in order to identify proteins that were not known to exist in CSF. Of the 559 unique proteins that were identified in both cases and controls, 147 (26%) were previously not known to exist in CSF.

Starting from the 559 non redundant proteins indentified by the LC-MS/MS analysis 486 were eventually considered in the statistical analysis as the remaining 91 were not expressed or were always expressed in all the 40 subjects. The designed statistical selection procedure allowed the identification of 47 proteins with a significantly statistical result (alpha level=0.05)[63]. Then, by taking into consideration both the biological function and the statistical relevance, a final list of 26 top-proteins was eventually selected (Supplementary table 1).

Fourteen of the 26 selected top-proteins were chosen for validation by WB, RPPA and ELISA methods, on the base of antibody availability and reliability. Six proteins (PCOLCE, COL1A1, GFRalpha2, ITIH4, NPDC1, IGFBP4) were eventually validated. All of them reported a good capability to discriminating metastatic cases from controls (AUC values from 0.76 to 0.99). Some of the proteins we found associated with the status of the subject (cases or only metastatic vs controls) were known to be involved in the process of extracellular matrix (ECM) remodeling, including collagen XVIII and procollagen C-endopeptidase, and have previously been associated with tumor progression and worse prognosis[64,65]. Statistical analysis between non-metastatic and metastatic patient samples also highlighted potentially relevant proteins such as GDNF family receptor α-2 (GFRα2); GFRα1 and GFRα3 were previously reported to have a role in tumor growth and

invasiveness[66]. Among the candidate biomarkers were also identified Dickkopf homolog 3 related to *Wnt/β-catenin pathway* and involved in tumorigenesis[67], prosaposin previously found over-expressed in breast and prostate cancer and melanoma inhibitory activity expressed in a variety of malignant tumors of mainly neuroectodermal origin[68].

In conclusion, combining a unique dataset of CSF from pediatric cancer patients with a novel enabling nanotechnology allowed us to identify candidate biomarkers that could generate important insights for diagnosis, prognosis and molecular stratification of CNS pediatric tumors. These finding will be first confirmed by using more standard methods such as Western Blot analysis and then validated in independent series of subject.

1.2.11 Hydrogel Nanotraps for the development of diagnostic tests

Hydrogel Nanotraps can be successfully applied to a plethora or biofluids including urine. Urine is an ideal biological fluid for clinical analysis because can be collected easily and in large amounts without performing any invasive procedure. Although urine analysis is often proposed as an alternative to blood collection, the very low concentration of analytes of interest, and the presence of interfering substances, has challenged the development of urine-based diagnostic tests as well the discovery of clinically relevant biomarkers. Through the application of recent proteomic technologies, several hundreds of proteins have been lately identified in urine as potential disease biomarkers[63,69]. The discovery of several new urine biomarkers brought to light some of the weaknesses of this biological fluid, such as the total protein variability due to hydration state and kidney function, low concentration of biomarkers that may be present one hundred to one thousand times less than in blood (which because of glomerular filtration are not proportional to the blood concentration), and the rapid degradation of biomarkers. Our group applied hydrogel Nanotraps to amplify the sensitivity

of diagnostic tests in urine. In a paper published by Luchini *et al.*[40] urine was used as a viable biofluid for noninvasive measurement of Human Growth Hormone (hGH) secretion. Because of the very low concentration of hGH in urine (1pg/ml range), current commercially available immunoassay are not suitable for the detection in this biofluid. Hydrogel Nanotraps were used to concentrate hGH in urine so that its levels could be measured with a clinical grade standard immunoassay designed for serum (Immulite 1000, Siemens). A population of healthy young adults (age 18–30, N=33, median 21, M: F=39%:61%, with no reported medical therapies) was used to determine the hGH baseline using the Nanotrap enhanced immunoassay was applied to evaluate the baseline value of urinary hGH. Results showed that Nanotrap sample preprocessing effectively improved the lower limit of detection of the Immulite hGH assay by more than 50 fold, shifting the linear range of the assay to encompass the expected value of urinary hGH. The full process between run and within run CV% was 7.9 and 9.0%, respectively.

Nanotrap preprocessing constitutes a reliable mean of measuring urinary hGH with a clinical grade immunoassay, now establishing a normal baseline value for hGH in urine. An important question can now be addressed as to whether the excretion of hGH in the urine has a longer time course than the spike of hGH in serum following exogenous administration. Moreover it will now be possible to study factors that affect urinary hGH doping that would otherwise be missed with serum testing.

1.3 APPLICATION OF HYDROGEL NANOTRAPS FOR HIGH SENSITIVITY MEASUREMENT OF URINARY OUTER SURFACE PROTEIN A IN EARLY STAGE LYME BORRELIOSIS

Lyme disease (also known as Lyme Borreliosis) is a bacterial infection caused by the bacteria belonging to the genus *Borrelia*, that is transmitted by Ixodes sp. ticks to humans[70]. *B. burgdorferi sensu stricto* (*s.s.*) is particularly predominant in the Americas, and *B. afzelii* and *B. garinii*, in addition to *B. burgdorferi s.s.*, in Europe and Asia. Other two *Borrelia* species are known to be pathogenic, *B. baverensis* and *B. spielmanii* and three are suspected *B. valaisiana*, *B. bissettii* and *B. lusitaniae*[71]. *B. afzelii* and *B garinii* account for most Lyme Borreliosis infections in Europe, while *B. garinii* is the most diffused in Asia. Whereas *B. afzelii* is mostly associated with skin manifestations, *B. garinii* seems to be the most neurotropic, and *B. burgdorferi* seems to be the most arthritogenic[72]. *B burgdorferi* genome was the first to be sequenced[73]. Because of an almost complete absence of biosynthetic pathways, the microorganism is suggested to be fully dependent on its environment for nutritional requirements. Nonetheless, Lyme *Borrelia* can be grown in vitro in highly enriched culture media[74,75].

1.3.1 Ecology of the spirochete and the tick vector

The tick *Ixodes ricinus* is the main vector in Europe, *Ixodes persulcatus* in Asia, *Ixodes scapularis* in northeastern and upper midwestern USA and *Ixodes pacificus* is the vector in western USA[76]. Their life cycle is made of four-stages—egg, larva, nymph, and adult (Figure 18, Stanek, G. *et al.*, 2012) —feeding only once during every active stage.

Figure 18. Developmental stages of Ixodes ricinus tick. From left to right: larva, nymph, adult female, adult male. (Source: Stanek, G. et al., 2012).

Male ticks rarely feed and never engorge. While a host animal passes through the vegetation, unfed ticks use their mouthparts to attach to the animal skin. The feeding process takes few days (about 3 days for larvae, 5 for nymphs, and 7 days for adult females), then the ticks drop off their host and live on the soil requiring humidity of 80% for survival. The ticks take several months to develop into their next developmental stage, or, in the case of adult females, lay about 2000 eggs. The tick's life cycle varies between 2 years and 6 years depending on climate[77]. *Borrelia* is passed to the host through the tick saliva during feeding. A feeding period of more than 36 h is usually needed for transmission of *B. burgdorferi* by *I. scapularis* or *I. pacificus* ticks[78–80] while the transmission of .*B afzelii* by *I. ricinus*, however, can be faster.

In endemic areas, Lyme disease can be transmitted in either peri-urban areas or rural areas used for forestry and recreational activities[81]. The lifecycle of the different tick species have distinct seasonality. *I. ricinus* and *I. persulcatus*, nymphs and adults become active in early spring and continue to seek hosts until mid-summer, or even later in favourable environments. *I. ricinus* has also a second peak of activity in the autumn. *I .scapularis* nymphs are active from early summer to early autumn, but the adults do not become active until autumn and remain so through winter until early spring, apart from

periods when temperatures are too low for activity (<3°C). *I. pacificus* seem to have a cycle similar to *I. ricinus*[80]. The main host for Lyme *Borrelia* are small mammals, such as mice and voles, and some species of birds. Deer are essential for the maintenance of tick populations but as well as cattle are incompetent hosts for *Borrelia*. Once a small populations of deer is present in a tick habitat Lyme borreliosis risk increases because of the presence of other hosts, including reservoir competent animals. However, if most animals in a habitat are not competent the likelihood of Lyme disease decreases because the ticks will feed mostly on those animals and not become infected. Risk of infections for humans is high from late May to late September, coinciding with the tick's life cycle and the increasing recreational use of tick habitats by the public. A typical habitat for the transmission of Lyme *Borrelia* often consists of areas of deciduous or mixed woodland, occasionally coniferous, with a layer of decaying vegetation on the ground, providing enough humidity for the development and survival of ticks, and supporting a range of potential vertebrate reservoir hosts. . Unlike other spirochete-borne infections where vertical transmission of the bacteria from the mother to the fetus through the placenta is well documented[82], data regarding transplacental transmission rate through the placenta remain controversial. According to CDC, Lyme disease infection during pregnancy may potentially lead to infection of the placenta and possible stillbirth; however, no negative effects on the fetus have been documented if proper antibiotic treatment is administered to the mother.[83]

1.3.2 Geographic distribution

In the United States about 30,000 new Lyme disease cases are reported annually, but a number almost 10 times higher is estimated to be unreported by the CDC[84]. The spreading of the disease beyond its endemic foci is predicted to accelerate with climate change. Climatic variables and climate

change are found to be associated with tick survival and their geographic distribution[85]. Cases occur primarily in the northeast and upper midwest regions of the US; however, ecologic and environmental changes have catalyzed a gradual geographic expansion[86]. In the US, most cases of Lyme disease have been recorded in coastal and riparian regions of southern New England, southeastern New York, New Jersey, eastern Pennsylvania, eastern Maryland, Delaware, Virginia and parts of Minnesota and Wisconsin[87]. The incidence in the ten states with the highest numbers of cases averaged 302 cases per 100,000 persons between years of 1991 and 2006[88]. In Canada, Lyme disease became nationally notifiable in 2009 and since then the number of cases more than doubled in four years, from 144 in 2009 to 338 in 2012, which means an increase in incidence from 0.4 to 1.0 cases per 100,000 population. Endemic LD occurs in British Columbia and in the eastern and central Canadian provinces of Nova Scotia, New Brunswick, Quebec, Ontario and Manitoba where it is continuing to emerge[89]. In Europe, 85,000 cases of LB are estimated each year; however, the reporting in Europe is inconsistent and many infections go undiagnosed[90]. The highest incidence has been recorded in the Scandinavian countries and in central and eastern Europe, especially in Germany, Belgium, Austria, Slovenia, and Czech republic between the years of 2009 and 2012[91]. The highest annual incidence is 80 cases per 100,000 persons or higher reported for Slovenia (155/100,000), Austria, Southern Sweden, Netherlands and Switzerland. Incidence lower than 20 cases per 100,000 persons have been reported in France and Poland[92]. The lowest incidences are in UK (0.7/100,000) and Ireland (0.6/100,000). Cases have been reported in over 60 countries and endemic foci in North America, Europe, and Asia[93] (Figure 19, Stanek, G., et al., 2012).

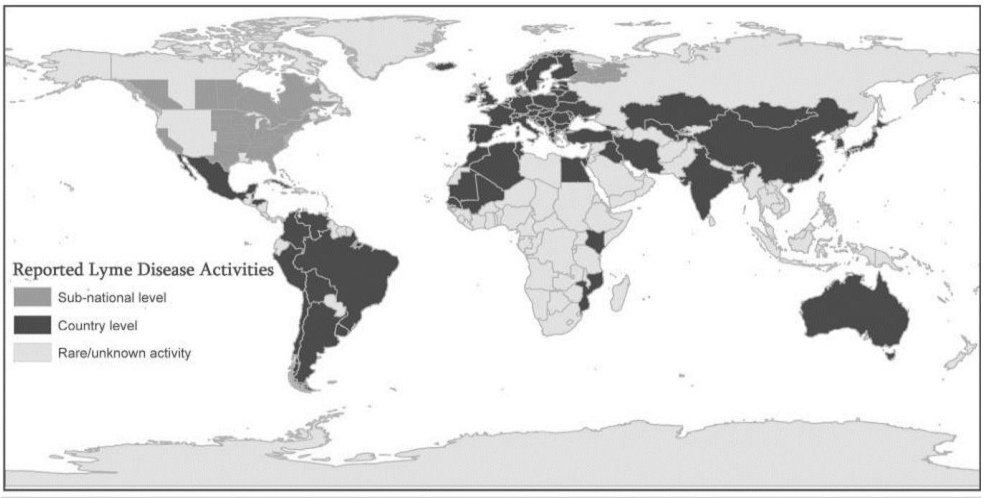

Figure 19. Global distribution of Lyme disease. The distribution shows that LD has extended to many countries around the world beyond the endemic foci. Reported LD activities that were mapped include diagnosed cases as well as infected ticks, infected animals, and seropositive human samples. The dark gray shading signifies countries with (at least) some reported LD activity, and the presence of activity is known only at the country level. The lighter gray shading represents areas in which Lyme disease has been reported at the sub-national level in particular regions of some countries. The lightest gray represents counties with rare or unknown activity. (Source: Stanek, G et al., 2012).

Lyme disease is also endemic in several areas of Italy[90]. Several species *B. afzelii*, B. garinii, and *B. burgdorferi s.s.* and *B. valaisiana* were identified in several provinces of the Northeast of Italy. Even though mountain regions are the more at risk for the incidence of Lyme disease, evidence of *I. ricinus* harboring *Borrelia* have been identified in the Po river region of Italy showing that its distribution extends to the plains such as the Po river valley and potentially to suburban areas[94].

1.3.3 Pathogenesis

Borrelia burgdorferi is carried in the midgut of unfed *Ixodes* ticks. During feeding, of the mammal host's blood, the spirochaetes increase in number and incur phenotypic changes, such as the expression of outer surface protein C (OspC), that allows the invasion of the tick's salivary glands. This

process takes days and it's the reason why the transmission can occur only after a delay. Expression of OspC plays an essential role in the infection of a mammalian host, but the mechanisms is still unknown[95,96]. The infected tick then deposits spirochaetes into the skin of a host animal and later *Borrelia* disseminate from that site through blood to other body sites. Once the infection is established a humoral and cellular immunological response is triggered in the human or animal host. Unfortunately, because of the bacteria's ability to down-regulate the expression of specific immunogenic surface exposed proteins, such as OspA and to alter rapidly through recombination of a surface lipoprotein known as variable major protein-like sequence expressed (VIsE) the *Borrelia* can escape the immune system and infection can persist. *Borrelia*'s abitlity to bind to various components of the extracellular matrix also contribute to its persistence[97–99]. Because *Borrelia* does not produce any toxins the tissue damage in patients derives from host inflammatory reactions and the intensity of the inflammatory response is depends on the different *Borrelia* genospecies[100]. Host genetic factors have an important role in the expression and severity of infection in animals, the only role established in man is in the development of antibiotic refractory Lyme arthritis, which is seen most often in patients with specific *HLA-DR* alleles[98].

The immunopathology of Lyme disease is still a major challenge. Although it induces strong immune activation, e.g., in phases of arthritis, the spirochete can persists in the organism and lead to a chronic pathology in the immunocompetent host. The inflammatory episodes suggest the presence of anti-inflammatory mechanisms and the long phases of latency suggest immune-evasion. Several studies proposed that *Borrelia* modulates the host's immune system in order to evade immune clearance. Evidence that *Borrelia* could indeed render human PBMC tolerant, i.e., was shown by Diterich *et al*.[101]. They in fact demonstrated that *Borrelia* render PBMC

hyporesponsive to subsequent stimulation with heterologous stimuli such as the TLR2 agonist LTA or the TLR4 agonist LPS. The OspA C-terminus domain plays an important role in *Bb* induced immune tolerance, induction of the inflammatory response through TLR2[101,102], and host immunologic recognition[103].

1.3.4 Clinical Symptoms

Borrelia infection and can lead to serious complications including chronic joint inflammation[104], cognitive defects[105], heart irregularities[106], and memory loss[107]. The most common and earliest clinical evidence of Lyme disease is a skin lesion called erythema migrans (EM), which appears to be present in approximately 70-80% of patients[108]. EM normally occurs in the first 2 weeks after the tick bite. It manifest as an expanding red or bluish-red patch (≥5 cm in diameter), with or without central clearing. The advancing edge is very distinct, often intensely colored. Diagnosis is made on the basis of history and visual inspection of the skin lesion. Culture or PCR of skin biopsy can be done but it is not needed for routine clinical practice. Relatively common symptoms are early complications (neurologic Lyme disease; 10-15% of patients) which manifests as facial nerve palsy, lymphocytic meningitis, and radiculopathy[109], myopericarditis that typically occurs in form of heart block (1-2%)[110] and Lyme arthritis (approximately 30%). Cardiac and neurologic symptoms normally occur within weeks to a couple of months after the tick bite[111]. Cardiac symptoms manifest through an acute onset of atrioventricular (I–III) conduction disturbances, rhythm disturbances, and sometimes myocarditis or pericarditis. Lyme arthritis manifests through recurrent attacks or persisting objective joint swelling in one or more large joints. Migratory monoarticular or pauciarticular arthritis affecting large joints normally appears after 6 months after the tick bite[112]. Other less frequent symptoms are: *Borrelia*l lymphocytoma manifesting as a painless bluish-red nodule or

plaque, usually on ear lobe, ear helix, nipple, or scrotum and it's more frequent in children (especially on ear) than in adults; ocular manifestations such as conjunctivitis, uveitis, papillitis, episcleritis, keratitis. Diagnosis of Lyme disease is tipically made by recognition of erythema migrans coupled with serological testing based on a two-tier approach (an immunoenzymatic test followed by a Western blot confirmatory test).

1.3.5 Treatment

In-vitro studies showed that *Borrelia* are susceptible to tetracyclines, most penicillins, many second-generation and third-generation cephalosporins, and macrolides while show resistance to specific fluoroquinolones, rifampicin, and first-generation cephalosporins[113–115].

Erythema migrans will resolve naturally without antibiotics, but antibiotic treatment is recommended to prevent later stages of dissemination. Doxycycline, amoxicillin, phenoxymethylpenicillin, and cefuroxime axetil are highly effective and are the first line of treatment while macrolides such as azithromycin are less effective and only administered as second-line treatment[113]. Doxycycline is the only antibiotic that showed in several study its efficacy with only 10 days of treatment[116]. Doxycycline, is contraindicated in children younger than 8 years and in women who are pregnant or breastfeeding[113]. Erythema migrans can manifest as an increase in the size or intensity within 24 h from the beginning of the treatment. Fever, when present, often resolve within 48 h and the skin lesion usually disappears within one or two weeks. Fatigue or arthralgia could take longer to resolve even up to three months[116]. Parenteral antibiotic treatment is recommended when patients are admitted to the hospital for Lyme neuroborreliosis and as an initial treatment for those with cardiac Lyme borreliosis. Ceftriaxone is the first choice because of its efficacy against *Borrelia in vitro*, and also because it crosses the blood–brain barrier well, and has a long serum half-life.

Alternative choices are cefotaxime and intravenous penicillin. Studies showed that oral doxycycline is as effective as ceftriaxone for any of the primary manifestations of early Lyme neuroborreliosis[117,118].

Symptomatic patients with cardiac Lyme borreliosis and those with high-grade first-degree atrioventricular block (PR interval of ≥300 ms), and second-degree or third-degree atrioventricular block, should be admitted to hospital and closely monitored. Complete heart block generally resolves within 1 week and less after treatment and conduction disturbances within 6 weeks[113]. Studies showed that patients whose arthritis is not improved after the first cycle of antibiotics can be re-treated with a second course of oral antibiotics, and parenteral antibiotic treatment in case of absence of any substantial clinical response[113].

1.3.6 Chronic Lyme disease

Persistent symptoms related to patients infected by *Bb* are often referred as chronic Lyme disease syndrome. The Infectious Diseases Society of America (IDSA) and the International Lyme and Associated Diseases Society (ILADS) differ in their recommendations for the clinical assessment and treatment of persistent Lyme Borreliosis. IDSA recognizes that Lyme disease can be painful and that the disease is not always properly identified or treated. They recognize that some patients may continue to experience prolonged Lyme disease symptoms even after a course of antibiotic therapy has killed the Lyme disease bacterium. They remain concerned that a diagnosis of so-called “chronic Lyme disease,” suggesting that active infection is ongoing, is not supported by scientific evidence and the treatment of long-term antibiotic therapy will be harmful for patients. They advocate that standard courses of antibiotics (between 10-28 days depending on the manifestation of Lyme disease) are effective to clear the infection in the vast majority of cases but they recognize that some patients continue to

experience Lyme symptoms, such as arthritis, after the infection has been cleared by standard antibiotic therapy. According to peer-reviewed studies, these stubborn symptoms may be due to persisting inflammatory responses, by genetically predisposed individuals, to bacterial debris left in the body after the infection is cleared as well as joint damage caused by the initial infection. One study focusing on patients with antibiotic-refractory late Lyme arthritis found that these symptoms may persist for nine years, but the incidence and severity of these symptoms do decrease over time and eventually stop. During the first year following the first onset of illness, 90% of patients had bouts of arthritis, and the number of individuals who continued to have recurrences decreased by 10–20% each year[119].

On the contrary ILADS members believe in the existence of chronic Lyme disease. They sustain that persistent infection has been demonstrated in a mouse model by Hodzic *et al*, in which the *Bb* could survive an exposure of 30 days of ceftriazone and still remain infectious. The microbiology of *Borrelia* needs to be considered when discussing the bacterial survival potential. *Borrelia* can evade the immune system not only by antigenic variation, immune suppression and "cloaking"[120] in host derived proteins but also by residing in intracellular locations, body sites such as brain and eyes. By residing in endothelial cells, neurons and glial cells[121,122] the bacteria would be unaffected by penicillins and cephalosporins and higher doses of intracellular antibiotics might be needed.

1.3.7 Clinical Diagnosis

Diagnosis of the erythema migrans is performed by visual inspection. EM presents as a erythemaotous skin lesion that develops at the site of a tick bite (Figure 20)[111]. These lesions can be homogenous in color or have a central clearing bull's eye-like.

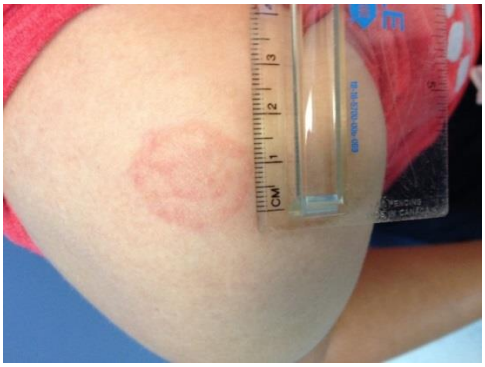

Figure 20. EM Rash. Example EM rash from the cohort of patients that participated in this study (Courtesy of SS).

Lyme diagnosis based on symptomatology is often coupled with serological testing. Unfortunately serological detection of antibodies in presence of erythema migrans is characterized by a low sensitivity, usually less than 40%[112]. A Lyme disease test can fall into three categories: serum antibody tests, antigen tests, PCR for bacterial nucleic acid.

1.3.8 Serological testing

The discovery of *B. burgdorferi* as the cause of Lyme disease in 1982 was followed by the development of several tests both by clinical and private laboratories. Because of the low number of bacteria that enter the bloodstream the development of a PCR based test has been particularly challenging[123,124]. For this reason most of the test development entailed the indirect detection of the infection by measuring the antibody response of the patient. Because the first tests lack of standardization and concordance of results, it became very clear that no test was sufficient on its own. In order to obtain a better reproducibility and specificity a 2-tiered algorithm was developed as shown in Figure 21 (Elitza ST, 2016).

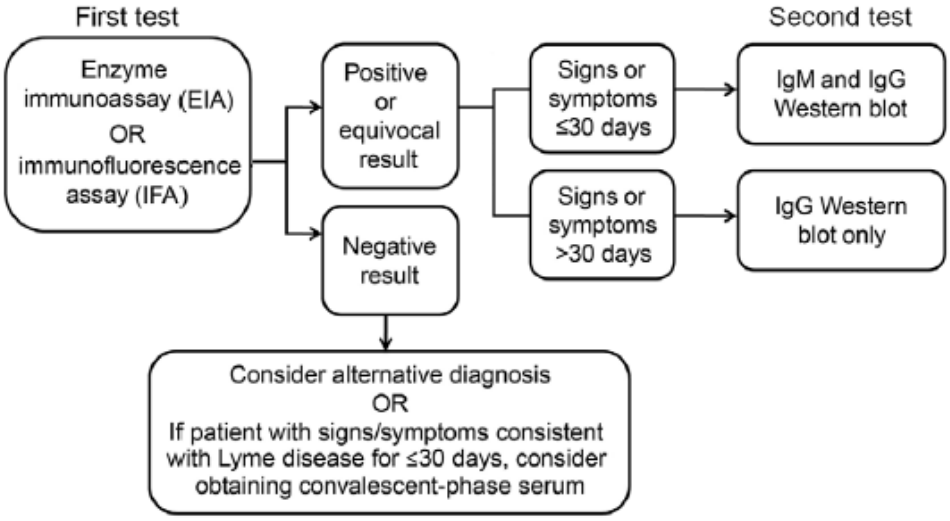

Figure 21. CDC guidelines for a serological detection of Lyme Disease. The two-tier approach uses a sensitive enzyme immunoassay (EIA) or immunofluorescent assay (IFA) followed by a Western immunoblot. Positive or equivocal samples by EIA or IFA should be tested with western immunoblot. Specimens negative by a sensitive EIA or IFA don't need to be tested further. When western immunoblot is used during the first 4 weeks of disease onset (early LD), both immuno- globulin M (IgM) and immunoglobulin G (IgG) procedures should be performed. A positive IgM test result alone is not recommended for use in determining active disease in people with illness greater than 1 month's duration because the likelihood of a false-positive test result for a current infection is high for these people. If a patient with suspected early LD has a negative serology, serologic evidence of infection is best obtained by testing of paired acute- and convalescent-phase serum samples. (Source: Elitza ST, 2016)

The first tier consist of an enzyme immunoassay EIA or IFA that if results positive or equivocal is followed by western blot as the second tier[125]. The first-tier consist of measuring the overall antibody response of a patient (both IgM and IgG)[126]. Even though both EIA and IFA are approved by FDA, EIA is usually performed because it can be easily automated and it provides a quantitative value which translates in objective cut-off values[123]. The majority of EIAs use a whole-cell sonicate of *B. burgdorferi* as antigen. Unfortunately, because of cross-reactivity with antigen from the host and or other pathogens, the specificity is far from being optimal[123]. New EIA that use fewer antigens instead of whole-cell lysate have recently become commercially available, one example is the variable-major protein-like sequence

expressed (VIsE) lipoprotein and its sixth invariable region, the C6 peptide[127]. In patients within the 4 weeks from suspected infection that result positive for EIA, separate IgM and IgG western blot are recommended as a second step testing[125]. The second tier consist in performing a western blot to test the patient antibodies against a preselected bacterial antigens. The type of western blot performed is dependent upon the time course of the illness. Because IgM response appears first and it is generally directed at the most immunogenic antigens, IgM along with IgG response is run in patients that have been manifesting symptoms for less than 30 days. If the symptoms have been manifesting for more than 4 weeks, IgG western blot alone is recommended. IgM WB testing should not be performed or, if performed, the result should not be considered, because IgM seroreactivity can remain detectable for months to years following disease resolution. According to CDC guidelines, a positive IgM western immunoblot result is indicated by the scored presence of $\geq$2 of 3 bands (21–24, 39, and 41 kDa), and a positive IgG result is indicated by the scored presence of $\geq$5 of 10 bands (18, 21–24, 28, 30, 39, 41, 45, 58, 66, and 93 kDa). If initial test is negative but early neurologic and cardiac symptoms remain, serologic testing might be repeated after 2-4 weeks. Because a 2-step test is time and cost inefficient, various improvement have been attempted. One approach consists in the use of fewer cross-reactive antigens to develop EIA. For example the use of the C6 peptide EIA which uses a highly invariant region of ViSE (variable major protein-like sequence expressed), showed higher specificity compared to whole cell lysate based EIA[127,128]. Still C6 based EIA alone doesn't reach the specificity of the two tier test and for this reason is not recommended in most cases except for the detection of Lyme disease in patients that were exposed to European tick strains[129,130] (*Borrelia garinii* and *Borrelia afzelii*). Another antigen that shows an increased sensitivity in diagnosing Lyme disease is PepC10, an invariant epitope of Outer Surface Protein C[131]. Other

strategies to improve the specificity are currently under development. The diagnostic accuracy of serologic assays is dependent on multiple factors such as the timing of the specimen collection in respect to the disease state, the kinetics of antibody expansion to the particular infectious agent, the selection of immunodominant target peptides and the assay methodology. In the Early localized stage of Lyme disease normally characterized by the presence of EM rash, only 10 to 50% of patients with culture-confirmed early LD show a detectable antibody response[123,132]. Other studies show that sensitivity of 2-tiered testing is low (30%–40%) during early infection while the antibody response is developing (window period) and sensitivity increases to 70% for disseminated Lyme disease. For this reason a serologic test performed soon after the tick bite or the detection of the EM rash is not recommended because results are often negative. Also the testing after treatment can in many case result negative because of the short exposure of the humoral immune system to the bacteria. Both ELISA and western blotting don't have an adequate sensitivity. Serological testing alone has been found to only be 77% specific when coupled with symptomatic analysis[133].

A possible method for diagnosis could entail the screening of ticks found on a patient for the presence of *B. burgdorferi* performing PCR for total *B. burgdorferi* genes (e.g., OspA and Ly1 Chromosomal gene). Nonetheless even the presence of a positive tick does not necessarily mean that the infection is established in the patient.

Beyond the low specificity, a serological test has other limitations. Since humoral response is long-lasting the treated patients who have resolved the infection can remain seropositive for several months or years, and a serological test following a previous infection would not be meaningful. Also, a serological test has limited utility for monitoring therapy success. In patients who are known to be seropositive, another kind of test is necessary to

ascertain if persisting Lyme disease or deranged immunological response to an original. symptoms are due to the presence of active Lyme disease. Likewise an alternative test would be helpful for the diagnosis of patients that previously contracted Lyme disease.

1.3.9 Laboratory testing: other approaches

Attempts to use CSF for intrathecal antibody production against *Borrelia* or detection of bacterial DNA have been performed but resulted in a very poor sensitivity[134,135]. CXCL13 has been proposed as a marker of neurologic Lyme disease in CSF but the sensitivity and specificity achieved are still too low to use it as a routine test[136–138], furthermore to be relevant the CSF should be obtained before administering any antibiotics. Testing the intrathecal antibody production is particularly important in Europe where multiple *Borrelia* species and high background seroprevalence reduce even further the success of a serologic analysis[139]. However negative results for intrathecal antibodies don't necessarily rule out the possibility of an active disease.

Other approaches aimed at improving sensitivity for the early detection of Lyme disease consist in the identification of proteins, nucleic acids and metabolites in serum of patients affected with Lyme disease. PCR could be used to determine the presence of nucleic acid of *B. burgdorferi* in different biological tissues such as synovial fluid, blood, serum CSF, skin biopsy. Synovial fluid PCR reaches a sensitivity of 75% in case of Lyme arthritis[123], while PCR on CSF samples is much less sensitive, studies show a sensitivity of only 38% in patients with early neuroborreliosis and even lower for late neuroborreliosis[140]. Researchers have reported also the possibility to use an immune-PCR, which combines the sensitivity of PCR with EIA-based antibody detection[141]. PCR in blood showed very high specificity but very low

sensitivity[123,142]. Because of these issues, PCR has not been standardized for Lyme disease, although some clinical laboratory offer PCR testing.

Another approach to improve the detection of early stage Lyme disease involves the identification of diagnostic proteins and metabolites in serum of patients with Lyme disease. These proteomic and metabolomics approaches, are particularly appealing because they also have the potential to identify biomarkers indicative of cure[143,144]. Bacterial culture are also not recommended for clinical purposes considering that *B. burgdorferi* is a slow-growing organism and current culturing methods are labor-intensive and have poor sensitivity.

Presence of background seropositivity is a major concern when testing for Lyme disease. Seropositivity due to previous exposure can be the result of the presence of IgG and IgM in the patient even after several years after the infection or due to a false positive result.

1.3.10 Development of a urinary Lyme antigen test

For the reasons mentioned above there is a strong clinical need to improve the specificity of diagnosis for the early stage of Lyme disease, particularly in the period preceding the mounting of a serologic response. It would be also very important to understand with higher certainty if the first round of therapy has been successful or a second round should be required because of *Borrelia* persistence. Ideally the Lyme disease test would utilize a non-invasive body fluid such as urine or saliva and would have a sufficient sensitivity to detect the infection in its early stage (before seroconversion). Previous studies investigated the possibility to develop an antigen assay tests but failed to reach adequate sensitivity and specificity.

In order to address these needs we evaluated the presence of Outer surface protein A (OspA) from *B. burgdorferi* in urine, using harvesting hydrogel Nanotraps in combination with a highly specific antibody which recognize a

very narrow epitope of present in the C-terminal region Osp236-239. This particular OspA sequence is conserved among several pathogenic species of *Borrelia*. Moreover this particular epitope does not show sequence homology with human proteins or other tick-borne pathogens.

OspA was shown to have a central role in the early stage of pathogenesis[103]; evidence of antibodies against OspA was found in patients in the early stage of the disease. Another study shows the presence of OspA in the urine of mice as early as 72 hours after the infection with *Borrelia burgdorferi*[145]. OspA is produced as *Borreliae* enters the tick vector and is the major surface protein during midgut colonization. OspA mutant bacteria showed a reduced survival rate in immunocompetent mice, while in naïve mice it was able to proliferate. OspA was in fact suggested to have a critical antibody shielding role once the infection of the host occurs. OspA sequence is also conserved among different species of *Borrelia*[146,147]. Sequencing of different strains showed that although some sequence variability is present in the middle region, the N-terminus and C-terminus are highly conserved. As shown in Figure 22 (Benjamin J. *et al*., 2002), OspA is a 273 amino acid protein that folds in an elongated conformation spanning 80 Å from end to end. OspA binds to the surface of the spirochete at the N-terminus via a lipid anchor. The structure consists of 21 consecutive antiparallel β-strands followed by a short α-helix in the C-terminus and can be divided into two discrete domains: a sandwich domain at the N-terminus and a barrel domain at the C-terminus connected by a long central b-sheet. The presence of an extended surface close to the lipid anchor suggest the presence of a contact point to a different protein on or in the *B. burgdorferi* membrane. The long cleft on the C-terminus suggests the possible binding with a ligand.

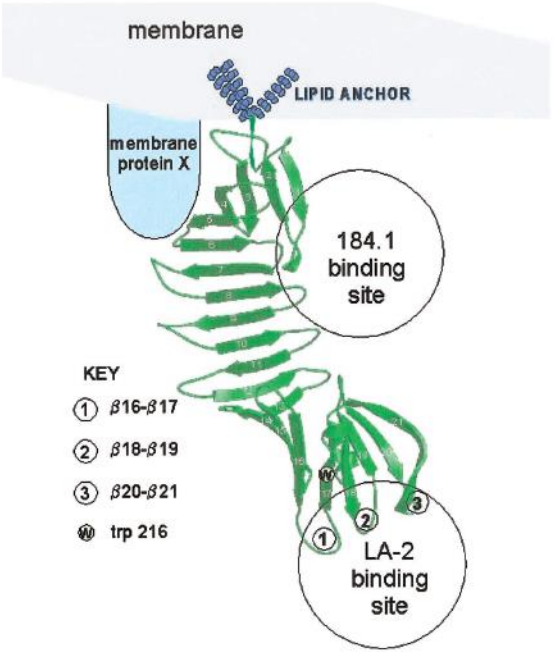

Figure 22. 3D structure of OspA. OspA is characterized by and elongated shape, spanning 80A ° from end to end, consisting of 21 antiparallel b-strands that fold hairpin style into 4 antiparallel b-sheets plus a single COOH-terminal a-helix. (Source: Benjamin, J., 2002)

1.3.11 Detection of OspA peptides in urine using multi-affinity capturing hydrogel Nanotraps

The focus of this study is to detect OspA peptides containing the C-terminus domain in urine of patients affected by Lyme disease. Because of low specificity and sensitivity, previous attempts of developing an antigen test remain controversial. Previous immunoassays may have employed polyclonal antibodies[148] raised against *Borrelia* lysate that may have not been directed towards a specific and highly conserved epitope of OspA that lack homology with other human or bacterial proteins belonging to different spirochetes. PCR and attempts to culture the bacteria from blood failed due to the low titer of *Borrelia* in the host[149]. Also, it has been suggested that *Borrelia* can be sequestered and persist in joint tissue[150]. The amount of

Borrelia antigen in urine is estimated to be very low and previous studies did not address the importance epitope selection in order to overcome low sensitivity and specificity issues. In order to overcome the previous physiologic and immunologic barriers and achieve high sensitivity and specificity, we combined our nanotechnology that capture and concentrate low abundance analytes allowing to reach high detection sensitivity with a monoclonal antibody highly specific for a narrow epitope in the C-terminus region of the OspA. Our Nanotrap particles consist of hydrogel Nanotraps containing high affinity chemical baits for the capturing of OspA. Once immersed in urine, Nanotraps are able to rapidly capture and concentrate virtually all the bacterial antigen present in the solution (Figure 23b, 23c). The sequestered OspA can be eluted from the Nanotrap and measured by immunoassay or mass spectrometry (Figure 23d).

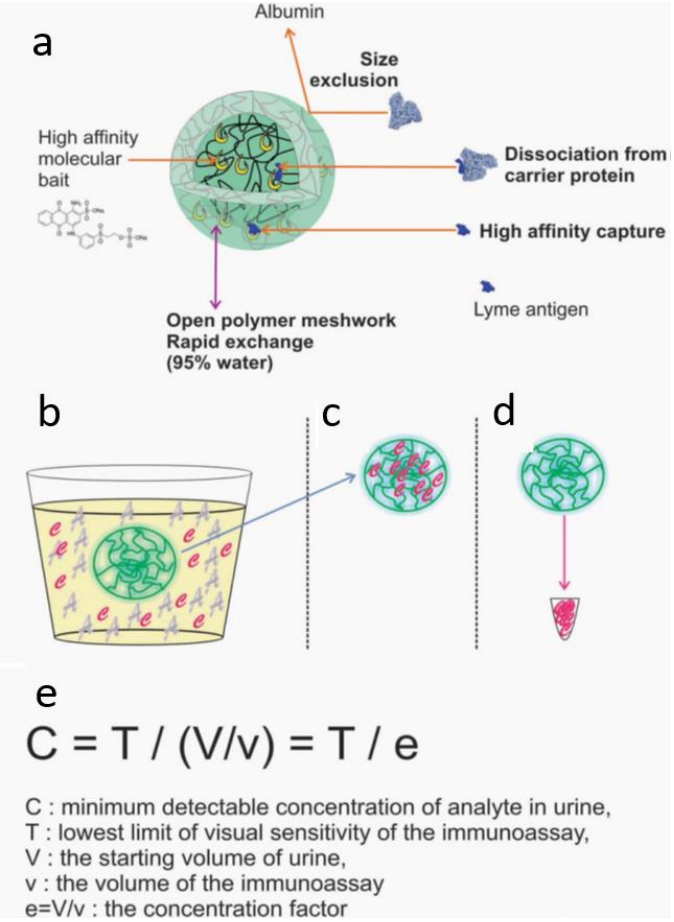

Figure 23. Application of Nanotrap particles to capture, concentrate and preserve OspA in urine and increase the sensitivity of immunoassay. A) Nanotrap are functionalized with a baits that has high affinity for low abundance and low molecular weight antigens such as OspA. B) Nanotrap particles are incubated with urine of patients containing Lyme disease antigens (yellow "c"). C) Nanotrap are separate from urine through centrifugation. D Lyme antigens captured in the Nanotrap are then eluted into a small volume (0.015 mL). D) Nanotrap pre-processing increases the sensitivity of any analytical technology by a concentration factor e. Assume that the initial volume is V = 40 mL and the final elution volume is v = 0.015 mL, the concentration factor e = V/v = 40/0.015 = 2,667.

The amount of OspA captured is function of the sample volume, the concentration factor is dependent on the initial volume of the solution and the final volume used to elute the antigen from the Nanotraps. In previous studies we proved how our Nanotraps can sequester, preserve and concentrate

antigen, enhancing immunoassay sensitivity of several hundred fold without increasing the background[50]. For this study we selected the anti-OspA mAb clone 0551, verified the specificity, and assessed the lack of cross-reactivity with human and other bacterial species. After assay validation we were able to apply our enhanced immunoassay for the detection of OspA in 151 patients suspected of Lyme disease and 117 healthy controls (Supplementary 2).

2. AIMS OF THE PROJECT

Discovery and improved measurements of clinically relevant biomarkers is crucial for understanding the pathophysiology of several diseases as well as for improving their detection and prognosis. Biofluids account to 60% of the body mass, and contain a plethora of low abundant biomarkers that often fall below the detection limit of mass spectrometry and standard immunoassays. Beyond their low concentration, biomarkers are often masked by high abundance proteins and are subject to the rapid degradation by exogenous and endogenous proteases.

Nanotraps functionalized with high affinity chemical baits have been proposed as a solution for these physiological roadblocks, and in few seconds, in solution, are able to capture, concentrate and preserve low abundance biomarkers in complex biological fluids. Nanotraps have been successfully employed by our group for the processing of different biofluids.

2.1 Aim 1. Synthesis, characterization and performance evaluation of Nanotraps

The first aim of this thesis consists in the synthesis and characterization of Nanotraps and their functionalization with novel classes of dyes that have never been employed for protein chemistry. Nanotraps are agnostic to the downstream assay and require an elution step that helps release the protein cargo for further analysis. The synthesis of hydrogel Nanotraps using a degradable cross-linker may display the antigen to an antibody directly without the need of an elution step. For these reason we incorporated during Nanotrap synthesis several cross-linking reagents that could undergo degradation following certain chemical conditions.

2.2 Aim 2. Development of a Nanotrap-based urinary antigen test for Lyme disease

Lyme disease is a tick-borne disease of endemic proportions in several areas of the United States and Europe. Serological tests for Lyme disease lack sensititvity and specificity particularly in the early stage of the disease. Also, attemps to create an antigen test for Lyme disease failed in the past because of the low concentrations of *Borrelia* biomarkers in body fluids. For this reason the second aim of the thesis consists in the application of harvesting Nanotraps for the development of a novel highly sensitive, precise, and specific urinary antigen test for Lyme disease. Differently engineered Nanotraps, different immunoassay formats, as well as mass-spectrometry are used to detect OspA, a clinically relevant protein that is highly expressed during the early stage of the infection. Experiments are first performed in model solution consisting of urine of healthy volunteers spiked with OspA. In parallel, clinical urine samples of patients suspected of different stages of Lyme disease were collected in several clinical practices in Virginia and sent to George Mason University for Nanotrap processing. Clinical samples are processed and results of serological testing, treatment modalities and outcome are correlated with the presence of OspA detected in urine.

3. MATERIALS AND METHODS

3.1 NANOTRAP SYNTHESIS AND DYE COUPLING

Hydrogel Nanotraps, poly(N-isopropylacrylamide-co-acrylic acid) and poly(NIPAm-co-AA), are synthesized by precipitation polymerization[151]. (poly(NIPAmco-AAc)) are covalently functionalized with amino-containing dyes using amidation chemistry, while amine-containing hydrogel Nanotraps, poly(NIPAm-co-AA), are covalently functionalized by nucleophilic substitution of the amine groups in the Nanotraps and the leaving group od the dye. An outer shell containing vinylsulfonic acid (VSA) copolymer can also be synthesized on the dye-functionalized particles by a second polymerization reaction.

3.1.1 Synthesis of poly(N-isopropylacrylamide-co-acrylic acid)

4.750 g of N-isopropylacrylamide (NIPAm) and 0.400 g of N, N′-methylenebisacrylamide (BIS) were dissolved in 500 mL of MilliQ water and filtered under vacuum into a three neck round bottom flask. 0.525 g of Acrylic Acid (AAc) were added, and the solution was purged with nitrogen for 30 min under medium stirring and then heated up to 70 °C. 0.276 g of Potassium Persulfate (Sigma Aldrich) was dissolved in 5 mL of H_2O and added to the reaction in order to initiate the polymerization. The reaction was kept for 6 h at 70 °C. Particles were washed 5 times by centrifugation (19,000 rcf, 50 min, room temperature) with MilliQ H_2O in order to eliminate unreacted monomer. Particles were resuspended in a total volume of 600 mL of water.

3.1.2 Dye coupling of AAc Nanotraps

Particles functionalization is performed by condensation of the primary amine contained in the dye to the carboxylic group of the AAc present in the Nanotraps. The reaction can be conducted in a water-based solvent for the following dyes: Acid Blue 22 (AB2, Sigma), Remazol Brilliant Blue R (RBB, Sigma), Acid Black 1 (AB1, Sigma), Brilliant Blue R250 (BB, Fisher), Toluidine Blue O (TBO, J.T. Baker), Rhodamine 123 (R12, Sigma), Disperse Yellow 3 (DY3, Fluka), and Disperse Blue 3 (DB3, Sigma). The protocol is the same for the incorporation of each dye, although the amount of dye used should be adjusted to maintain the molarity. Briefly, 40 mL of particles were centrifuged and the pellet was re-suspendend in 40 mL of 0.2M NaH_2PO_4 pH 5. The particles were transferred into a round bottom flask and 2 mL of 1% sodium dodecyl sulfate (SDS, Sigma) 1648 mg of N-(3 Dimethylaminopropyl) N′ ethyl carbodiimide hydrochloride (EDC; Fluka Analytical) and 1224 mg of solid N-Hydroxysuccinimide (NHS; Sigma-ALBrich) were added. The reaction was kept for 15 minutes at room temperature under medium stirring, then the particles were centrifuged, and the pellet resuspended in 0.2 M Na_2HPO_4 pH 8. In parallel, 2 g of Remazol Brilliant Blue were dissolved in 100 mL of Na_2HPO_4 pH 8 and filtered twice with 0.2 µm nitrocellulose membrane disk filter (Millipore). Particles were then transferred to the dye containing solution and the reaction was held overnight at room temperature under medium stirring rate. The Nanotrap particles were washed by centrifugation (19,000 rcf, 50 minutes, room temperature) 6 times in order to eliminate the unreacted dye and then resuspended in a final volume of 40 mL with MilliQ H_2O.

3.1.3 Synthesis of poly(N-isopropylacrylamide-co-allylammine)

9g of N-isopropylacrylamide (NIPAm) and 0.400g of N,N′-methylenebisacrylamide (BIS) were dissolved in 250 mL of MilliQ water and filtered under vacuum into a three neck round bottom flask. The filter was then washed with an additional 100 ml of Milli-Q water and collected in the same flask. The solution was purged with nitrogen for 30 min under medium stirring. 676 µl of Allylammine were added, and the solution was purged for another 15 min under medium stirring and then heated up to 70 °C. 0.100 g of Potassium Persulfate (Sigma Aldrich) was dissolved in 5 mL of H_2O and added to the reaction in order to initiate the polymerization. The reaction was kept for 6 h at 70 °C. Particles were washed 5 times by centrifugation (19,000 rcf, 50 min, room temperature) with MilliQ H_2O in order to eliminate unreacted monomer. Particles were resuspendend in a total volume of 300 mL of water.

3.1.4 Dye Coupling of AA Nanotraps

In order to incorporate the dye Cibacron Blue F3GA (CB) dye, CB (0.76 g, 0.90 mmol) was dissolved in 10 mL of 0.1 M aqueous sodium carbonate. The poly(NIPAm-co-AA) particle suspension (10 mL volume) was purged with nitrogen for 15 min with a medium stirring rate in a three-neck round-bottom flask. Solid sodium carbonate (0.106 g, 1.0 mmol) was added to the suspension. The suspension was then stirred at room temperature under nitrogen for about 1 min. The CB solution was then added to the poly(NIPAm-co-AA) particle suspension, and the combined reaction mixture was then stirred at room temperature under nitrogen for 48 h. The resulting poly(NIPAm/CB) particles were harvested and washed using centrifugation (19,000 rpm, 50 min, 25 C).

3.1.5 Synthesis of DHEA hydrogel Nanotraps

N-Isopropylacrylamide(NIPAm,210mg), N,N'Methylenbisacrylamide(BIS,32.7mg),1,2-Dihydroxyethylenebis-acrylamide(DHEA,42.4mg), and Allylamine (AA,158µl) were dissolved in 65mL of water and filtered into a three-neck round bottom flask using a nitrocellulose membrane disk filter. The system was purged with nitrogen for 1 hour at room temperature and medium stirring rate and then heated to 70°C before potassium persulfate (KPS,46mg) was added. The system was held at 70°C under nitrogen for 4 hours. The Nanotraps were washed five times by centrifugation (19000 rpm, 50 min, 25°C). Remazol Brilliant Blue R Dye (3.5g) and Na_2CO_3 (371mg) were dissolved in 28mL of water and filtered twice. The dye solution and 35mL of poly(NIPAm-co-AA) particles were transferred to a three-neck round bottom flask and held overnight at room temperature and medium stirring rate.

3.1.6 Synthesis of bis(acryloyl)cystamine (BAC) hydrogel Nanotraps

Synthesis was performed as follows: N-Isopropylacrylamide (NIPAm,210mg), N,N'Methylenbisacrylamide(BIS,32.7mg),1,2-bis(acryloyl)cystamine (BAC,42.4mg), and Allylamine (AA,336µl) were dissolved in 100mL of water and filtered into a three-neck round bottom flask using a nitrocellulose membrane disk filter. The system was purged with nitrogen for 30 minutes at room temperature and medium stirring rate and then heated to 50°C before potassium persulfate (TEMED,1mM) was added. The system was held at 50°C under nitrogen for 4 hours. Nanotraps were the washed five times to eliminate the unreacted reagents. After the particles were washed, B-mercaptoethanol was added 1:1 to the Nanotraps. An incubation of 30 minutes is sufficient to degrade BAC changing the physical properties of the Nanotraps.

3.1.7 Synthesis of pyrazolone Nanotraps

N-Isopropylacrylamide (NIPAm, Sigma-Aldrich, 4.5 g), was dissolved in 105 mL of H2O, filtered using a nitrocellulose membrane disk filter (0.45 μm pore size, Millipore), and transferred in a three-neck round-bottom flask. The solution was purged with nitrogen for 30 min at room temperature, at medium stirring rate, and then heated to 70°C. In parallel pyrazolone dye (0.305g) was added to 20 ml of Milliq H_20 and 136ul of allylammine was added to the solution and purged under nitrogen for 10 minutes. Potassium persulfate (KPS, Sigma-Aldrich, 138mg) was dissolved in 2.5 mL of H2O and was added to the solution to initiate the polymerization. At the same time pyrazolone solution was added to the reaction. The reaction was allowed to continue for 6 hours. Particles were washed five times by centrifugation (19,000 rpm, 50 min, 25 C) to eliminate the unreacted reagents.

3.1.8 Syntesis of Fast Blue B Nanotraps

N-Isopropylacrylamide (NIPAm, Sigma-Aldrich, 2.375 g), and N,N'Methylenbisacrylamide (BIS, 0.1g) were dissolved in 150 mL of H2O, filtered using a nitrocellulose membrane disk filter (0.45 μm pore size, Millipore), and transferred in a 500ml three-neck round-bottom flask. The solution was purged with nitrogen for 30 min at room temperature, at medium stirring rate. In parallel fast blue B (0.308g) was dissolved in 400ml of water and the solution was purged for 30 min. Acrylic acid (88ul) was added to the solution and stirred for other 15 min. The solution containing NIPAm and BIS was added using a 60ml syringe to the dye soliutuion and purged for 5 minutes under nitrogen. Acrylic acid was added (262ul) and the solution was allowed to purge for other 10 minutes. The reaction was then brought to 70C. Potassium persulfate (KPS, Sigma-Aldrich, 138mg) was dissolved in 2.5 mL of H2O and was added to the solution to initiate the polymerization. The

reaction was hold under medium stirring for 6 hours. Particles were washed five times by centrifugation (19,000 rpm, 50 min, 25 C) to eliminate the unreacted reagents.

3.1.9 Nanotrap characterization

The temperature dependence of particle size was determined via photon correlation spectroscopy (Submicrometer Particle Size Analyzer, Beckman Coulter). The measurement of particle diameter was performed using water as a diluent (refractive index (RI) = 1.333, diluent viscosity = 0.890 cP). The test angle was 90°. Average values were calculated for three measurements using a 200 s integration time, and the solutions were allowed to thermally equilibrate for 10 min before each set of measurements. Measured values were then converted to particle sizes via the Stokes–Einstein relationship[152]. Further characterization of the Nanotraps was performed through atomic force microscopy (AFM) using an NSCRIPTOR™ DPN® System (NanoInk). Particles solution (1 µg/ml) was deposited on freshly cleaved mica under humid atmosphere for 15 minutes and dried under nitrogen before measurement. Images were acquired under AC mode using a silicon tip with a typical resonance frequency of 300 kHz and a radius smaller than 10 nm. Incorporation of dye in the particles was assessed by weighing the dry particles before and after dye coupling (supplementary data).

3.2 DEVELOPMENT OF A NANOTRAP-BASED LYME DISEASE TEST

3.2.1 Ethics statement

Urine samples were collected under informed consent from patients suspected of having Lyme disease at any stage from four different community physician practices in Northern Virginia, a high risk geographic region for LB. This study met the requirements for IRB approval (Pro00008518, Chesapeake IRB). Matched coded clinical records and LB serology results were also provided under patient consent. Immunoassay testing for urinary OspA utilized Nanotrap particle pre-processing and western blotting to evaluate the OspA analyte molecular size, and OspA peptide competition was applied to fully confirm a positive test.

3.2.2 Study design and human sample collection

Subjects with all stages of documented or suspected Lyme disease were considered eligible for the study. Mid-stream urine specimens were self-collected by 268 participants Urine samples were stored at the collection sites (Care-ID, VA; Frekko Primary Care, MD; Internal medicine of Northern Virginia, VA; Novant Health Virginia Internal Medicine & Primary Care, VA) at - 20^{o}C. Samples were frozen within two hours of collection. Sample were then transferred to George Mason University and stored at -80^{o}C. Whole blood from each subject was drawn on the same day as urine collection. Each participant donated blood only once. The blood drawing procedure was performed at the physician's office by a registered nurse. Six mL of whole blood was drawn into a red top tube. Blood samples were sent to Quest Diagnostics for Total Lyme Disease Antibody (EIA) and Lyme IgG and IgM

Western Blot tests. Results of serological testing were recorded as well as treatment modalities and outcome, and used to correlate serology outcome with the presence of OspA detected in urine (Figure 24). Age matched, non-symptomatic patients with no history of Lyme disease as well as patients being evaluated for other non-Lyme infectious diseases were included in the control group. In addition, the study set contains Lyme borreliosis patients before and after antibiotic treatment.

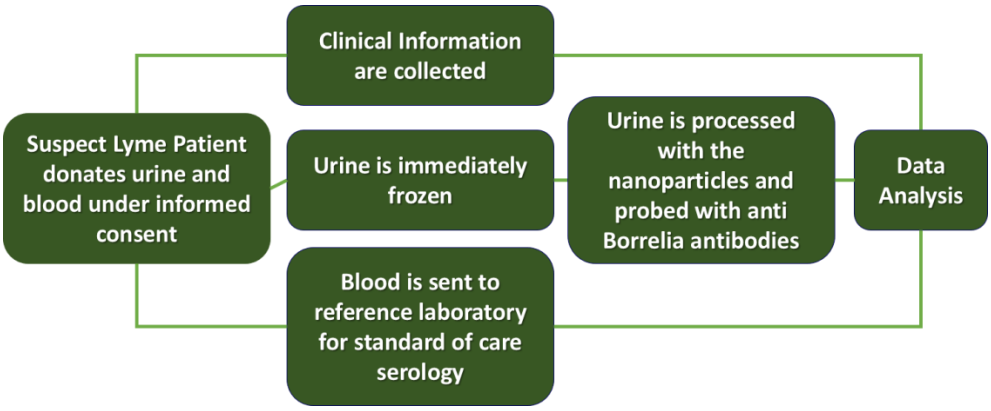

Figure 24. Clinical study design.

3.2.3 Mass spectrometry analysis of B. burgdorferi lysate

Mass spectrometry analysis was performed using *Borrelia burgdorferi* Lyme, Grade 2 Antigen (ARP American Research Products. 5µg of Lyme antigen were reduced through incubation with a 10mM dithiothreitol in 8M urea for 30 minutes and alkylated with 50mM iodacetamide at room temperature in the dark for 20 minutes. The enzymatic digestion ran overnight with 0.5µg sequencing grade trypsin (Promega) in 50mM ammonium bicarbonate pH 8 at 37°C. Digestion was then stopped by adding 5µl of glacial acetic acid. Digested samples were then desalted with C-18 Zip Tips (Millipore). Final eluates from Zip Tips were then dried with a nitrogen evaporator. Samples

were reconstituted in 6 µl of 0.1% Formic Acid and analyzed with a Thermo LTQ Orbitrab Mass spectrometer. After sample injection by autosampler, the C18 column (0.2 mm × 50 mm, NanoLCMS Solutions) was washed for 2 min with mobile phase A (0.1% formic acid), and peptides were eluted using a linear gradient of 0% mobile phase B (0.1% formic acid, 80% acetonitrile) to 50% mobile phase B in 90 min at 500 nL/min, then to 100% mobile phase B for an additional 5 min. The LTQ mass spectrometer was operated in a data-dependent mode in which each full MS scan was followed by five MS/MS scans where the five most abundant molecular ions were dynamically selected for collision induced dissociation (CID) using a normalized collision energy of 35%. Tandem mass spectra were searched against the NCBI *Borrelia burgdorferi* database with SEQUEST software using tryptic cleavage constraints. High-confidence peptide identifications were obtained by applying the following filter criteria to the search results: Xcorr versus charge 1.9, 2.2, 3.5 for 1+, 2+, 3+ ions; ΔCn > 0.1; probability of randomized identification e0.01.

3.2.4 Epitope mapping of the anti-OspA Monoclonal Antibody

In order to identify the epitope of the anti-OspA mAb, partial enzymatic digestion, western blotting and mass spectrometry analysis were performed using *Borrelia burgdorferi* Lyme, Grade 2 Antigen (ARP American Research Products) and anti-OspA mAb clone 0551 (Santa Cruz). Bb (Lyme), Grade 2 Antigen was derived from Bb Strain B31 cultured in BSK II Medium. Microorganisms were harvested from growth medium and washed in PBS using low speed centrifugation. The pellet was resuspended in PBS and gently sonicated. The antigen preparation was evaluated by gel electrophoresis followed by silver staining and in gel trypsin digestion followed by mass spectrometry. In this study, partial enzymatic digestion was carried out as follows: 80 µL of Bb Lyme antigen Grade 2 (0.2 µg/ml) was

acidified with 80 µL of 10 mM HCl (Fisher Scientific). 10 µL of 4 mg/mL pepsin solution (Sigma) was added to the sample and incubated for 1 hour at RT. After the incubation, the sample was immediately purified with ZipTip (Millipore) according to manufacturer instructions and dried with Nitrogen evaporator. The dried pepsinized sample was resuspended in 22.5 µL of water by repeated pipetting. An aliquot of 2.5 µL was subjected to western blot analysis with the anti OspA mAb used above in order to determine the smallest OspA pepsin fragment that retains antigenicity toward the antibody. The remaining amount of pepsinized Lyme antigen (20 µL) was subjected to SDS PAGE fractionation and silver staining. Bands on the low molecular weight region of the gel that mirrored the signal on the western blot were cut using a razor blade and subjected to in gel digestion. Samples were reduced with 500 µL of 10 mM dithiothreitol (DTT, Fisher Scientific) in 50 mM ammonium bicarbonate (Fluka) and then alkylated with 500 µL of 50mM iodoacetamide (Acros Organic) in 50 mM ammonium bicarbonate at room temperature in the dark for 20 minutes. Overnight enzymatic digestion was carried out with 0.5 µg sequencing grade trypsin (Promega) dissolved in 60 µL of 50 mM ammonium bicarbonate pH 8 at 37°C. Solutions were separated from the gel pieces and saved in clean Eppendorf tubes. Aliquots of 60 µL of extraction buffer (50% acetonitrile, 2% acetic acid (Acros Organic)) were added to the gel pieces and incubated at room temperature for 15 minutes. Solutions were separated from the gel pieces and combined with the previous ones. Samples were then dried using a nitrogen evaporator. Samples were reconstituted in 6 µl of 0.1%. Mass-Spectrometry was performed with Thermo LTQ Orbitrab Mass spectrometer as described in the previous paragraph.

3.2.5 Urine sample handling prior to analysis

All urine used in this study was processed as follows. Urine samples were thawed in a water bath at room temperature. Urinalysis was performed on urine samples using Siemens Multistix 10SG. Specific gravity was measured with digital refractometer (Atago). Urine samples were then centrifuged at 3,700 rcf for 10 minutes at 25 °C to remove cellular debris. Supernatant was transferred in a new tube. Urine pH was measured and adjusted to 5.5 with 1M HCl when necessary.

3.2.6 Nanotrap particle performance assessment with model solutions

Bb Lyme antigen Grade 2 (American Research Products) spiked in human urine was used as model solution to test Nanotrap particle performance. OspA Lyme antigen (1.2 ng) was spiked in 40 mL of human urine collected from healthy volunteers and processed as described above and incubated with 1:10 Nanotrap particle suspension (5 mg/mL dry weight concentration) / urine solution volume. After 30 minutes incubation, Nanotrap particles were separated by centrifugation (16.1 rcf, 10 minutes, 25 °C). Two washes were performed by re-suspending the Nanotrap particles in 1mL of MilliQ H_2O and centrifuged at 16.1 rcf for 10 minutes at 25 °C. Nanotrap particles were incubated with 600 µL of elution buffer (70% acetonitrile (Fisher Scientific), 10% ammonium hydroxide (Sigma)) for 30 minutes at 25 °C. Samples were then centrifuged at 16,100 rcf for 15 minutes at 25 °C; the eluates were transferred to new tubes and 50 µL of a 50 mg/mL D-(+)-Trehalose dihydrate (Sigma) water solution was added. Eluates were then dried under nitrogen flow (Microvap 118, Organomation Associates, Inc) and analyzed by western blot. Alternatively 2X Sample Buffer Solution (475 µl 2X Laemli Sample Buffer, 25 µl TCEP) in lieu of acetonitrile-ammonium hydroxide elution buffer. Nanotrap pellet is vigorously resuspend particle pellet in 30 µl 2X sample

buffer solution and heated at 100°C for 10 minutes. Nanotrap are centrifuged, supernatant is recovered and analyzed by western blot.

3.3 NANOTRAP-ENHANCED WESTERN BLOT FOR DETECTION OF URINARY OSPA

3.3.1 Patient urine processing with Nanotrap particles for Western Blot

In order to analyze patient urine samples, urine samples (40 mL) were transferred in Nalgene™ Oak Ridge High-Speed Polycarbonate Centrifuge Tubes and incubated with 4 mL of Nanotrap particles (5 mg/mL) for 30 min on a rocker at room temperature. Samples were then centrifuged at 19,000 rcf for 30 minutes at 25 °C. Two washes were performed by re-suspending the Nanotraps in 2 mL of MilliQ H_2O and centrifuging at 16,100 rcf for 15 minutes at 25 °C. Nanotrap particles were incubated with 600 µL of elution buffer (70% acetonitrile, 10% ammonium hydroxide) for 30 minutes at room temperature. Samples were then centrifuged at 16,100 rcf for 15 minutes at 25 °C; the eluate was transferred to new tubes and 50 µL of D-(+)-Trehalose dihydrate solution (50 mg/mL in water) were added. Eluates were then dried under nitrogen flow and analyzed with western blot.

3.3.2 OspA detection with western blot

Dried particle eluates were resuspended in 15 µL of MilliQ water by repeated pipetting. 5 µL of 4X sample buffer: 50 mM Tris HCl (Biorad) pH 6.8, 2% SDS, 144 mM 2-mercaptoethanol (Fisher Scientific), 10% glycerol (Sigma) and 0.01% bromophenol blue (Fisher Scientific) was added and samples were heated at 100°C for 10 minutes. Samples were loaded on 4-20% Tris-Glycine gel (Invitrogen Corporation) and separated by SDS-PAGE gel

electrophoresis. Gel was run in Tris-Glycine SDS running buffer using Novex X-Cell IITM Mini-Cell (Invitrogen Corporation) at 120 V for 90 minutes. Proteins were transferred onto a PVDF membrane (Millipore), blocked with a solution of 0.2% I-Block (Applied Biosciences) and 0.1% Tween 20 (Fisher) in PBS (Life Technologies). The membrane was incubated overnight with a mouse anti-OspA mAb (Santa Cruz, sc-58093, Clone ID 0551). This mouse mAb was purified from ascites fluid by protein A chromatography. The final preparation was formulated to a protein concentration of 100 µg/ml in 0.01 M phosphate buffered saline, pH 7.2 and contained 0.1% sodium azide. The mAb was used at a 1:100 dilution in PBS supplemented with I-Block and Tween 20. After mAb incubation, the membrane was washed three times for 10 minutes with 0.2% I-Block, 0.1% Tween 20 in PBS. The membrane was incubated with a peroxidase conjugated goat anti-mouse IgG adsorbed against bovine, equine and human serum proteins (Life Technologies, #A16090) diluted 1:5,000 in 0.2% I-Block, 0.1% Tween 20 in PBS. Three washes of 10 minutes in 0.2% I-Block, 0.1% Tween 20 in PBS were performed. Proteins were detected with an enhanced chemiluminescence system (West Dura, Thermo Fischer Scientific) on a Kodak MM4000 Imager.

3.3.3 OspA dot blot analysis

Proteins and peptides (2 µL) were spotted with a capillary tube on a PVDF membrane previously wetted in methanol. The membrane was blocked with a solution of 0.2% I-Block and 0.1% Tween 20 in PBS. The membrane was incubated overnight with anti-OspA mAb clone 0551 diluted 1:100 in 0.2% I-Block, 0.1% Tween 20 in PBS (4 °C) and then washed three times for 10 minutes with 0.2% I-Block, 0.1% Tween 20 in PBS. The membrane was incubated with a peroxidase conjugated goat anti-mouse IgG adsorbed against bovine, equine and human serum proteins diluted 1:5,000 in 0.2% I-Block, 0.1% Tween 20 in PBS. Three washes of 10 minutes in 0.2% I-Block,

0.1% Tween 20 in PBS were performed. Proteins were detected with an enhanced chemiluminescence system (West Dura, Thermo Fischer Scientific) on a Kodak MM4000 Imager.

3.3.4 In solution competition assay and solid phase immunodepletion

In order to verify the specificity of band reactivity of the anti-OspA mAb clone 0551, a competition assay was developed. Prior to staining, the mAb was neutralized by incubation with a solution containing excess OspA or synthetic peptides containing partial OspA sequences. The mAb that was bound to the neutralizing protein or peptide was no longer available to bind to the epitope transferred on the western blot membrane. The blocked mAb and the mAb alone were used to probe duplicate western blots. All other parameters of the western blotting remained the same. The comparison of neutralized mAb to mAb alone showed which staining was specific: the specific staining was absent from the western blot membrane probed with the neutralized mAb. More in detail, 100 µL of anti-OspA antibody (0.1 mg/mL) was added to 900 µL of 0.2% I-Block, 0.1% Tween 20 in PBS and incubated overnight with 400 µL (0.1 mg/mL) of a custom made recombinant OspA (Genecopoeia). In parallel, Bb Lyme antigen Grade 2 (0.5 ng) was separated by 1-D gel electrophoresis and then transferred onto Immobilon PVDF membranes as previously described. OspA-saturated and un-modified antibodies were used to probe the PVDF membranes. Competition assays were also performed neutralizing the anti OspA mAb with Bb Lyme antigen Grade 2 (37 µg), 80 kDa OspA chimera recombinant protein (12 µg, Genway), and peptide fragments mimicking the antibody epitope (60 µg, Supplementary Table 3, Peptide 2.0).

The peptide OspA219-235 (Peptide 2.0) was utilized for solid phase affinity depletion of the mAb clone 0551. The peptide (300 µg) was deposited on ELISA plate wells. The wells were washed with PBS supplemented with 0.1%

Tween 20 and the excess peptide removed. The wells were then blocked with PBS supplemented with 0.2% I-Block, 0.1% Tween 20. The mAb clone 0551 (3 µg) was incubated with the solid phase adsorbed peptides overnight at 4 °C under rotation. After incubation, the supernatant was recovered and brought to a volume of 3 mL in PBS supplemented with 0.2% I-Block and 0.1% Tween 20. In parallel, 600 pg of Bb Lyme antigen Grade 2 were spiked in urine and processed through the Nanotrap particles. The immunodepleted mAb and the mAb alone were used side by side to stain membranes containing the Nanotrap particle eluates.

3.3.5 Reproducibility and sensitivity of the urinary OspA Lyme assay

In order to assess intra-assay reproducibility of the urinary OspA Lyme assay, nine experimental replicates were performed in one day as follows. Bb Lyme antigen Grade 2 (1.2 ng) was spiked in 40 mL of urine collected from healthy volunteers and incubated with 4 mL of Nanotrap particle suspension (5 mg/mL). Samples were processed as described above and the Nanotrap particle eluates were analyzed by western blot using anti-OspA mAb clone 0551.

In order to determine the lower limit of detection and the lower limit of quantitation of the urinary OspA assay, different quantities of Lyme antigen (1.2, 0.6, 0.3, 0.15, 0.075, 0.038, 0.019, and 0.009 ng) were spiked in 40 mL of human urine. Aliquots of 4 mL of Nanotrap particle suspension (5 mg/mL) were mixed with the urine samples and processed as described above. Nanotrap particle eluates were analyzed by Western blot. The experiment was repeated three times in three different days. Multiple batches of Nanotrap particles were used in this study. Batch validation and batch to batch reproducibility experiments were performed following the same protocol described above.

3.3.6 Interfering substances and cross-reactivity with relevant non Bb infections

In order to exclude possible cross-reactivity of the mAb clone 0551 with interfering substances, a series of Nanotrap experiments were performed and analyzed using western blotting. Increasing amount of the following antigens were spiked in 40 mL of human urine in presence or absence of OspA Lyme antigen: bovine serum albumin, human healthy volunteer whole blood, Bartonella henselae lysate (ATCC 49793), Babesia microti (ATCC PRA-399), Epstein-Barr virus (EBV) Inactivated P3HR1 Cell Extract (Advanced Biotechnologies Inc.; 10-501-001), Herpes Simplex virus-1 (HSV-1) Inactivated Vero Cell Extract (Advanced Biotechnologies Inc; 10-515-001), Cytomegalovirus (CMV) HEK293 Cell Lysate (Sino Biological Inc.; 10202-VCCH1L), Hepatitis C Virus HEK293 Cell Lysate (Sino Biological Inc.; 10202-VCCH1L). These samples were processed following the protocol described above.

3.3.7 Data analysis

Statistical Chi squared test for equality of proportions was applied in order to correlate urinary OspA outcome (detectable or non-detectable) to clinical LB diagnosis and serology. Power calculations were performed in order to estimate the power of the test, given the number of samples in each group, the proportions of urinary OspA outcome, and a significance level of 0.05. Calculations were performed using R software (www.r-project.com).

Western blotting band intensity was quantified with ImageJ software (http://imagej.nih.gov/ij/index.html) by selecting the area of interest and calculating area, mean and standard deviation of selection per software instructions. Blast analysis and protein alignment was performed using pBLAST [31]. Search parameters were as follows: query sequence:

KTSTLTISVNSKKTTQLVFTKQDTITVQKYDSAGT, Database Name: non redundant, Program: BLASTP 2.2.31+.

3.4 NANOTRAP ENHANCED ELISA FOR THE DETECTION OF URINARY OSPA

3.4.1 Nanotrap processing of urine samples for ELISA

Urinalysis was performed on the urine sample and pH was adjusted to 5.5. Urine samples (40 mL) were transferred in Nalgene™ Oak Ridge High-Speed Polycarbonate Centrifuge Tubes and incubated with 200 µL of Nanotrap® particles (5 mg/mL) for 30 min at room temperature. Samples were then centrifuged at 19,000 rcf for 30 min at 25 °C. One wash was performed by re-suspending the Nanotraps in 1 mL of MilliQ H_2O and centrifuging at 16,100 rcf for 15 min at 25 °C. Nanotrap® particles were incubated with 100 µL of elution buffer (Octylthioglucoside 2%+0.5% n-Dodecyl β-D-maltoside in PBS) for 20 min at room temperature. Samples were then centrifuged at 16,100 rcf for 15 min at 25 °C; the eluate was saved at -80°C overnight.

3.4.2 Elution Buffers

Performance of different elution buffers at different concentrations were tested in 40 ml of urine spiked with Lyme antigen following the protocol listed above.

Elution buffers evaluated were:

- n-Octyl-β-D-thioglucopyranoside (OTG) at 2%, 5%, and 10% in PBS
- Sodium Lauroyl Sarcosinate (Sarkosyl) at 2% in PBS

- Sodium Lauryl Sulfate (SLS) 2% in PBS
- Dithionite at 0.1M, 1%, 0.5%, 0.1%, and 0.01% in water
- N-octyl-β-D-glucoside (OBG) at 5%, 2%, 1%, and 0.5% in PBS
- Chaps at 5%, 2%, 1% in PBS
- 15% Methanol in water
- 30% Isopropanol in water
- 0.1M Ammonium Carbonate
- 0.1M Ammonium Acetate
- 0.1M Dithiothreitol (DTT)
- 0.5M Imidazole
- Tissue Protein Extraction Reagent (T-PER)

3.4.3 HRP-labelling of Anti-OspA monoclonal antibody

100 µl of monoclonal antibody Virostat 0551 (1mg/ml) were HRP-labelled using the Lightning-link HRP conjugation kit (Innova Biosciences Cat#701-0000). 10µl of LL-modifier reagent were added to 100µl of the antibody and mixed gently. The antibody sample (with added LL-modifier) was pipetted directly onto the lyophilized material and resuspended gently by withdrawing and redispensing the liquid once or twice using a pipette. The vial was left in incubation for 3 hours at room temperature (20-25^{0}C). After incubating for 3 hours, add 10µl of LL quencher were added to the solution and the conjugated antibody was stored at 4°C.

3.4.4 OspA detection with ELISA

200µL of Virostat capture antibody 1:100 in PBS was deposited on the ELISA plate and incubated at 37^{o}C for 30 minutes. The plate was washed for 5X with 300µl of wash buffer (PBS, 0.05% tween). 200µl of I-Block was pipetted

into each well and incubated at room temperature for 1.5 hours. The plate was washed 5X with 300µl of wash buffer. Lyme antigen was diluted to prepare control samples. Standards, controls, and samples were pipetted into the appropriate wells and incubated at room temperature for 2 hours. Detection antibody (Thermo Scientific, PA173006) was diluted 1:200 in I-Block and the plate was washed 5X with 300µl of wash buffer. 200µl of detection antibody was pipetted into each well and incubate at room temperature for 1.5 hours. Plate was washed 7X with 300µl of wash buffer. 100µl of TMB substrate was pipetted into each well and incubate in the dark at room temperature for 12-16 minutes. 50µl of stop buffer was pipetted into each well and absorbance was read at 450nm with on the plate reader.
Other detection antibodies were evaluated: abcam, ab156277; abcam, ab20757; thermo Scientific. PA1-27289.

3.4.5 Reproducibility and sensitivity of ELISA

40 ml urine in duplicate were spiked with Lyme antigen in three different concentrations (5, 1, 0.5, 0 pg/ml). Elution was performed with OTG 2%. A dilution curve of the Bb antigen was produced in parallel spiking 2ng/ml, 0.4ng/ml, 0.2ng/ml in OTG 2%. Linearity was observed in the spike-ins samples with and without Nanotrap processing. To test the reproducibility of the urinary OspA Lyme ELISA assay, two experimental replicates of urine samples spiked with Lyme antigen in four different concentrations (2.5, 1.25, 0.62, 0 pg/ml) were processed in different days by two different operators. Samples were processed as described above and the Nanotrap particle eluates were analyzed by ELISA. In order to determine the lower limit of detection and the lower limit of quantitation, different concentration of urine controls spiked with Lyme antigen (0-500 pg/ml) and loaded on the ELISA plate. In parallel, different amount of Lyme antigen (0-2.5 pg/ml) were spiked

in human urine and processed through Nanotraps and measured with the ELISA.

3.5 NANOTRAP-ENHANCED LFA FOR THE DETECTION OF URINARY OSPA

3.5.1 Testing antigen-displaying Nanotraps with dot blot

Remazol functionalized Nanotraps (100 µL) were added to 1 mL urine spiked with OspA (10 ng/mL) and incubated for 30 minutes. Samples were centrifuged and washed twice. DHEA oxidation was performed adding 100 µL of solution of $NaIO_4$ (27 mg of $NaIO_4$ in 1mL 0.05M citrate) to 100 µL of Nanotraps and incubating for 10 minutes. Samples were centrifuged, resuspended in 50 µL water, and diluted (1:1, 1:2, and 1:4 dilutions) before being immobilized on the nitrocellulose membrane and incubated for one hour at room temperature in I-Block. The membrane was incubated in primary antibody (*Borrelia burgdorferi* OspA, Virostat 1:100) and secondary antibody (Life Technologies, Catalog #A16090, 1:5000). The membrane was then developed with ECL SuperSignal and the image was captured using Kodak imager.

3.5.2 Testing antigen-displaying Nanotraps with western blot

1ml of urine was then spiked with OspA (10 ng/ml). 200 µL of michea Brilliant Blue Nanotraps were then added to the urine, incubated for 30 minutes at room temperature and centrifuged (16.1 rcf, 15 min, 25°C). Samples were washed twice with water and then centrifuged (16.1 rcf, 15 min, 25°C). DHEA oxidation was performed by adding 200 µL of solution of $NaIO_4$

(27 mg of $NaIO_4$ in 1mL 0.05M citrate) to 200 µL of Nanotraps and incubating for 10 minutes. Particles were centrifuged (16.1 rcf, 15 min, 25°C), resuspended in 20 µl sample buffer, and heated at 100°C for 10 minutes. Gel electrophoresis was performed and proteins were transferred onto an Immobilon PVDF membrane. The membrane was incubated for 60 minutes in 5% milk, and subsequently in primary antibody (*Borrelia burgdorferi* OspA, 1:100) and secondary antibody (Life Technologies, Catalog #A16090, 1:5000). The membrane was drained and coated with 2mL Chemiluminescent ECL SuperSignal and developed with Kodak imager.

3.5.3 Lateral flow immunoassay development and optimization

DHEA Remazol Brilliant Blue R Nanotraps (200µl) were oxidized adding 200 µL of solution of $NaIO_4$ (54 mg of $NaIO_4$ in 1mL 0.05M citrate) and incubated for 10 minutes. Nanotraps were centrifuged (16.1 rcf, 15 min, 25°C) and washed twice with 200 µl of water. Nanotraps were then incubated with OspA (0.5, 1, 1.5, 2 and 4 ng) for 30 minutes. The solution was centrifuged (16.1 rcf, 15 min, 25°C) and washed twice with water. Nanotraps were resuspended in 200µl of water. Nitrocellulose membranes were spotted with 4µl primary antibody 0551 creating a thin antibody line and dried at 37°C for 10 minutes. The membranes were then incubated in PEG blocking solution (50mg/mL in water) for 30 minutes before being washed twice with PBS Tween 0.1%). The membranes were dried again at 37°C for 10 minutes, and then placed in the lateral flow device with filter pads overlapping it at either end (Figure 25). A solution of 100µl of particles and 400µl water was placed directly on the sample pad and allowed to run through the nitrocellulose membrane. Different membrane materials tested: nitrocellulose, glass fiber filter without binder resin, polyethersulfone, MF-Millipore Filter, and Isopore filter. Different blocking agents were tested: PBS

supplemented with 0.2% (w/v) I-Block and 0.1% Tween 20, polyethylene glycol (PEG), and acrylic acid Nanotraps.

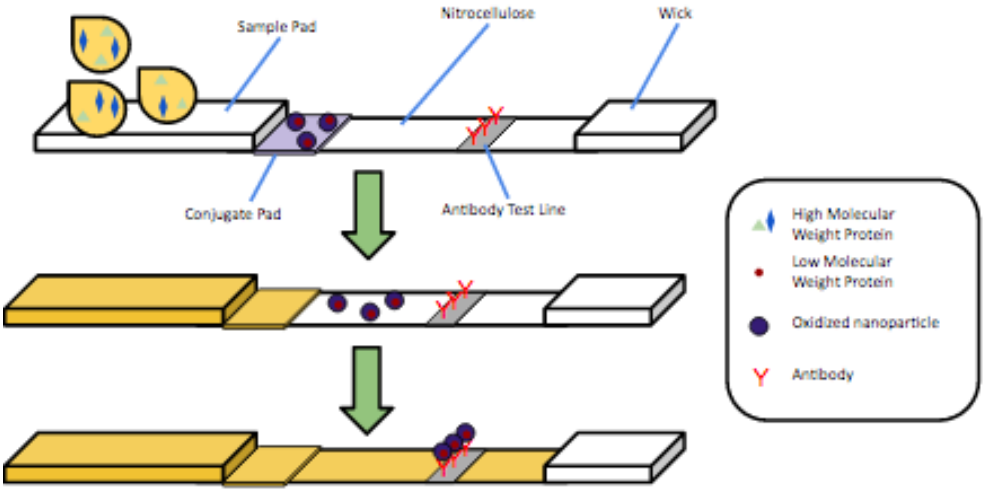

Figure 25. Schematic representation of a Nanotrap-based lateral flow. The urine sample is placed on the sample bad and allowed to flow through the nitrocellulose. The oxidized Nanotraps on the conjugate pad capture the antigen present in the fluid and flow to the membrane. Once the Nanotrap reaches the antibody line, the exposed OspA cargo will be bound by the antibody and it will result in the formation of a colored line.

3.6 NANOTRAP-ENHANCED MULTIPLE REACTION MONITORING FOR THE DETECTION OF URINARY OSPA

3.6.1 Selection of Elution Buffer for mass spectrometry analysis

In order to select the best elution conditions compatible with mass-spectrometry 10 replicates of 40 ml of urine spiked with 320 pg of Lyme antigen were processed as described above until the elution step. Elution was then performed resuspending the Nanotrap pellet using 20µL of the three different elution buffers: sample buffer, Protease Max (Promega, 1% in

ammonium bicarbonate) and Rapigest (Waters, 1% in ammonium bicarbonate). Incubation was either performed for 20 minutes at room temperature or for 10 minutes at 100°C. Each condition was performed in duplicate except for the samples eluted with sample buffer. One duplicate of sample eluted with Rapigest and ProteaseMax were processed for mass spec (see sample preparation for mass spectrometry below), while the other duplicates as well as the samples eluted with sample buffer were used for western blot and efficiency was assessed as densitometric analysis.

3.6.2 Sample preparation for mass spectrometry

40 mL of urine were spiked with 2.5, 5, 10, 25, 50 and 100 pg/mL of *Borrelia* antigen grade 2 in duplicate. Samples were incubated with the Nanotrap particles, washed according to the patient processing sample (p. 85), one set was then eluted with 20ul of sample buffer and the other was eluted 20ul of 1% Rapigest SF surfactant (Waters)in 50 mM ammonium bicarbonate and 5% TCEP. The first set was loaded on an electrophoresis gel and western blot was performed. In the second set of samples the elutions were acidified with 0.1% TFA for 30 minutes in order to degrade the surfactant and the resuspended with 180 ul of 50mM ammonium bicarbonate. Samples were alkylated with 50mM iodacetamide at room temperature in the dark for 20 minutes. The enzymatic digestion ran overnight with 0.5µg sequencing grade trypsin (Promega) in 50mM ammonium bicarbonate pH 8 at 37°C. Digestion was then stopped by adding 5µl of trifluoracetic acid (TFA). Digested samples were then desalted with C-18 Zip Tips (Millipore). Final eluates from Zip Tips were then dried with a nitrogen evaporator. Samples were reconstituted in 6µl of 0.1% Formic Acid added with 100fmol angiotensin 1.

3.6.3 MRM analysis

OspA was monitored for peptide GYVLEGTLTAEK using precursor 640.84 $^{2+}$ and transitions 719.40, 848.43, and 961.52. OspB was monitored for peptide ATIDQVELK using precursor 508.78 $^{2+}$ and transitions 422.74, 731.40, and 844.48 (Figure 2). Results were analyzed using Skyline (Univ. of Washington) and reported as the area under the curve for transition 961.52 from peptide GYVLEGTLTAEK and transition 844.48 from peptide ATIDQVELK. After desalting with Pierce C18 spin columns, all samples were analyzed by LC-MRM on a Thermo Quantum Ultra triple quadrupole and Orbitrap Fusion Tribrid mass spectrometers. Samples were loaded onto a 1mm x 150mm Hypersil Gold 3µm particle C-18 reversed phase column with an Accela autosampler (Thermofisher Scientific) fitted with a 10 µL sample loop. The LC pump was an Accela operated at 160 µL/min, and effluent will be directed into the mass spectrometer using an IonMax source. After sample injection, the column was washed for 5 min with 98% mobile phase A (0.1% formic acid), and peptides were eluted using a linear gradient of 2% mobile phase B (0.1% formic acid in acetonitrile) to 50% mobile phase B in 40 min. The instrument divert valve was switched to waste before and after the peptides eluted in order to keep the source free of excess salts and debris. Both Q1 and Q3 resolution were set to 0.7 FWHM. Q2 contained 1.5mTorr of argon. Phosphorylated Angiotensin II (DRV(pY)IHP, Protea Biosciences) was measured in urine for analytical verification. Results were analyzed using the program Skyline (University of Washington) and reported as the area under the curve for optimized transitions.

4. RESULTS

4.1 HYDROGEL NANOTRAP SYNTHESIS AND CHARACTERIZATION

Allylammine and Acrylic Acid core Nanotraps were synthesized. N-isopropylacrylamide-co-allylammine Nanotraps were then functionalized with Cibacron Blue, and Remazol Brilliant Blue. N-isopropylacrylamide-co-acrylic acid Nanotraps were functionalized with Trypan Blue, Remazol Brilliant blue, Reactive Blue 221, Bismark Brown, Diamine Green. Partially degradable Nanotraps using 1,2-Dihydroxyethylenebis-acrylamide (DHEA), bis(acryloyl)cystamine (BAC) hydrogel Nanotraps, pyrazolone and Fast Blue 221 (as crosslinker) were also synthesized. Nanotraps were characterized and dynamic diameter was measured with light scattering. Allylammine hydrogel Nanotraps size measured 253.2 ± 3.13 nm in diameter (Figure 26). Because dyes are small organic compounds after functionalization of Allylammine-core Nanotraps with Remazol Brilliant Blue dye, no significant increase in size can be noted (Figure 26).

90.0° Unimodal Distribution

Unimodal Results Summary

Rept#.	Mean (nm)	P.I.	Diff.Coef (m^2/s)	Counts/s	Baseline Error	Overflow
Rept.1	257.1	-0.130	1.91e-12	1.66e+06	-0.01%	0
Rept.2	253.0	-0.139	1.94e-12	1.69e+06	-0.01%	0
Rept.3	249.5	-0.179	1.97e-12	1.71e+06	0.02%	0
Average	253.2 ± 3.13	-0.149 ± 0.021				

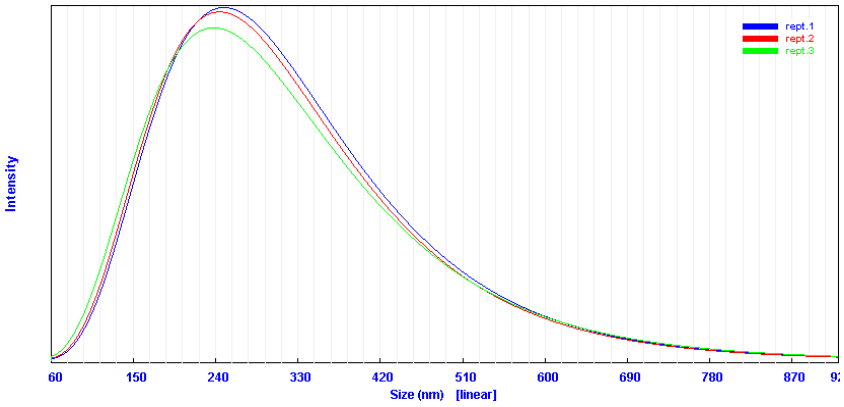

90.0° Unimodal Distribution

Unimodal Results Summary

Rept#.	Mean (nm)	P.I.	Diff.Coef (m^2/s)	Counts/s	Baseline Error	Overflow
Rept.1	262.0	-0.147	1.87e-12	1.03e+06	0.01%	0
Rept.2	259.0	-0.157	1.89e-12	1.05e+06	-0.01%	0
Rept.3	257.1	-0.142	1.91e-12	1.05e+06	0.01%	0
Average	259.4 ± 2.02	-0.149 ± 0.006				

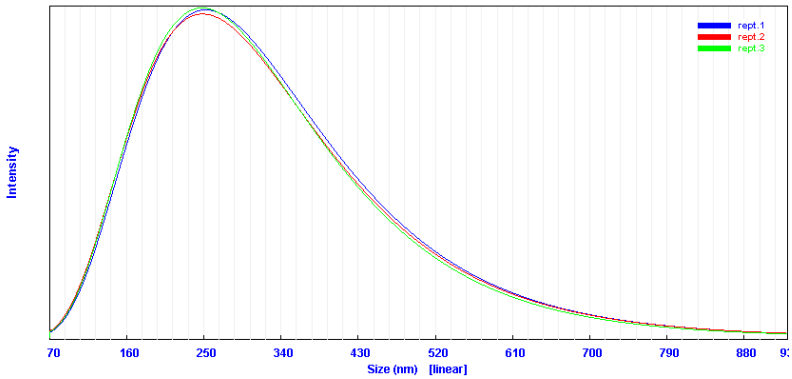

Figure 26. Light scattering measurements of Allylammine-core Nanotraps. Average diameter was 253.2 ± 3.13 nm (upper panel). Light scattering measurements of Allylammine-core Nanotraps functionalized with Remazol Brilliant Blue dye. Average diameter was 259.4 ± 2.02 nm. The functionalization does not significantly increase the Nanotrap size (lower panel).

4.1.1 Size variation of partially degradable Nanotrap

When exposed to the environmental condition that allows the cleavage of the crosslinker, Nanotraps undergo a partial degradation. Their structure becomes loose and the pore size increases allowing antibodies to directly access the target antigen *in situ* obviating the need of an elution step. The change in the physical structure of the Nanotraps can be observed visually as a color/opacity change of the Nanotraps solution and as well as a change in their hydrodynamic diameter.

DHEA cross-linked Nanotraps

N-isopropylacrylamide (NIPAm) Nanotraps were synthesized via dual cross-linking (degradable N,N'-(1,2-Dihydroxethylene)-bisacrylamide [DHEA] and nondegradable N,N'-methylenebis(acrylamide) [BIS] crosslinkers), and then functionalized with Remazol Brilliant Blue dye. DHEA can be degraded through an oxidizing reagent, $NaIO_4$ which causes an increase in Nanotrap diameter and pore size (Figure 27).

Rept#.	Mean (nm)	P.I.	Diff.Coef (m^2/s)	Counts/s	Baseline Error	Overflow
Rept.1	990.9	0.157	4.95e-13	8.70e+04	1.09%	0
Rept.2	1005.1	0.196	4.88e-13	8.48e+04	1.32%	0
Rept.3	966.4	0.033	5.08e-13	8.02e+04	0.13%	0
Average	987.5 ± 16.01	0.129 ± 0.069				

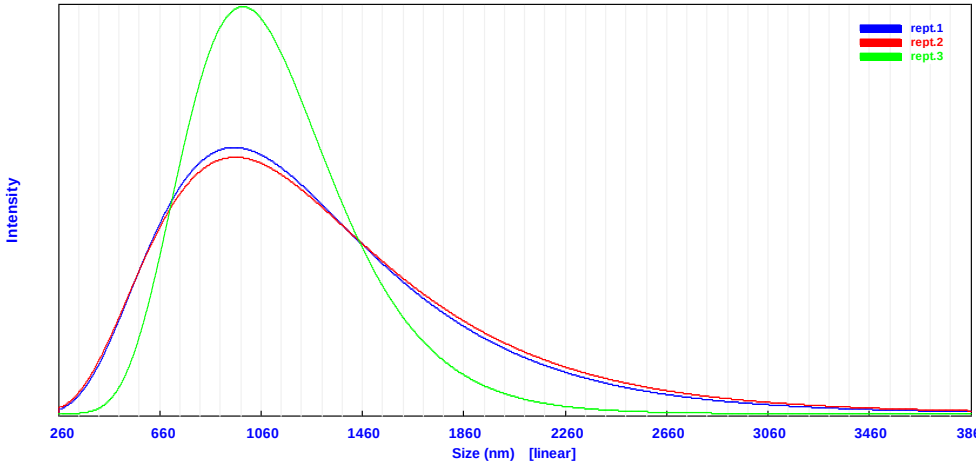

Rept#.	Mean (nm)	P.I.	Diff.Coef (m^2/s)	Counts/s	Baseline Error	Overflow
Rept.1	1168.4	0.397	4.20e-13	6.47e+04	1.62%	0
Rept.2	1117.9	0.109	4.39e-13	6.26e+04	-0.01%	0
Rept.3	1068.3	0.439	4.59e-13	6.30e+04	0.38%	0
Average	1118.2 ± 40.87	0.315 ± 0.147				

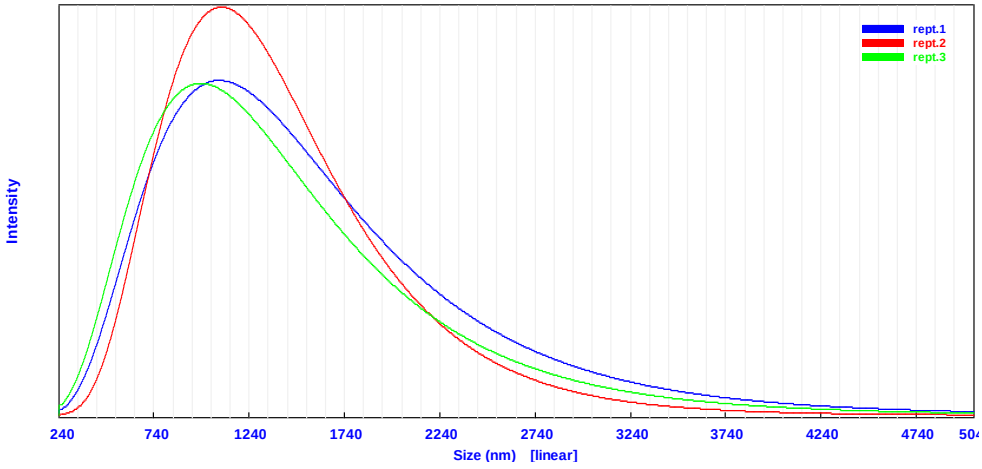

Figure 27. Light scattering measurements of DHEA containing Nanotraps. DHEA Nanotraps functionalized with Remazol brilliant blue show an average diameter of 987±16.01 nm before oxidation via sodium periodate (upper panel). After DHEA oxidation the diameter increases to 1119.2±40.87 nm (lower panel).

Light scattering results show an increase in the hydrodynamic diameter of the particles after oxidation of ~10-15%, with an increase in effective sieving cut off from 50,000 to 300,000 Da which can easily allow the access of an antibody.

BAC cross-linked Nanotraps

BAC cross-linked Nanotrap undergo partial degradation in presence of reducing conditions. 100 µL of β-mercaptoethanol was added to 100 µL of the Nanotraps and incubated for 30 minutes. Light scattering results show an increase in the hydrodynamic diameter of the particles after reduction of ~20-25% (Figure 28).

90.0° Unimodal Distribution

Unimodal Results Summary

Rept#.	Mean (nm)	P.I.	Diff.Coef (m^2/s)	Counts/s	Baseline Error	Overflow
Rept.1	498.4	0.424	9.84e-13	5.48e+05	1.17%	0
Rept.2	520.4	0.637	9.43e-13	5.80e+05	3.57%	0
Rept.3	514.6	0.495	9.53e-13	5.34e+05	1.81%	0
Average	511.1 ± 9.29	0.519 ± 0.089				

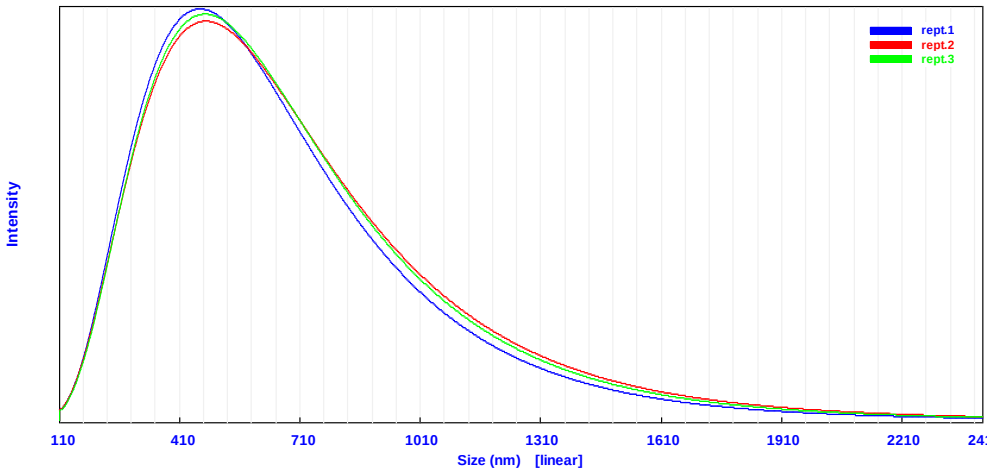

90.0° Unimodal Distribution

Unimodal Results Summary

Rept#.	Mean (nm)	P.I.	Diff.Coef (m^2/s)	Counts/s	Baseline Error	Overflow
Rept.1	654.0	-0.253	7.50e-13	3.89e+05	0.12%	0
Rept.2	639.5	-0.063	7.67e-13	4.27e+05	0.06%	0
Rept.3	644.2	-0.050	7.61e-13	4.29e+05	0.26%	0
Average	645.9 ± 6.02	-0.122 ± 0.093				

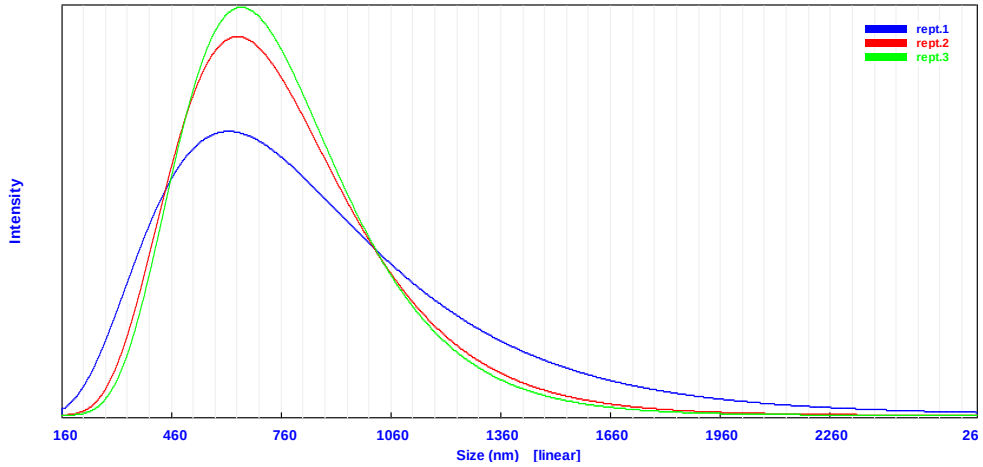

Figure 28. Light scattering measurements of BAC containing Nanotraps. BAC Nanotraps functionalized with Remazol brilliant blue show an average diameter of 511.1±9.29 nm before oxidation via sodium periodate (upper panel). After BAC oxidation the diameter increases to 645.9±6.02 nm (lower panel).

Pyrazolone Nanotraps

Pyrazolone was successfully incorporated into the Nanotraps as a cross-linker. Light scattering results show an increase in the hydrodynamic diameter under acid condition of ~15-20%. Hydrodynamic diameter resulted 703 ± 2.42 nm and 841.4±38.54 nm before and after acid treatment respectively (Figure 29).

90.0° Unimodal Distribution

Unimodal Results Summary

Rept#.	Mean (nm)	P.I.	Diff.Coef (m^2/s)	Counts/s	Baseline Error	Overflow
Rept.1	701.3	-0.010	6.11e-13	4.70e+05	0.25%	0
Rept.2	706.7	0.074	6.06e-13	4.56e+05	0.37%	0
Rept.3	702.0	-0.053	6.10e-13	4.54e+05	0.24%	0
Average	703.3 ± 2.42	0.004 ± 0.053				

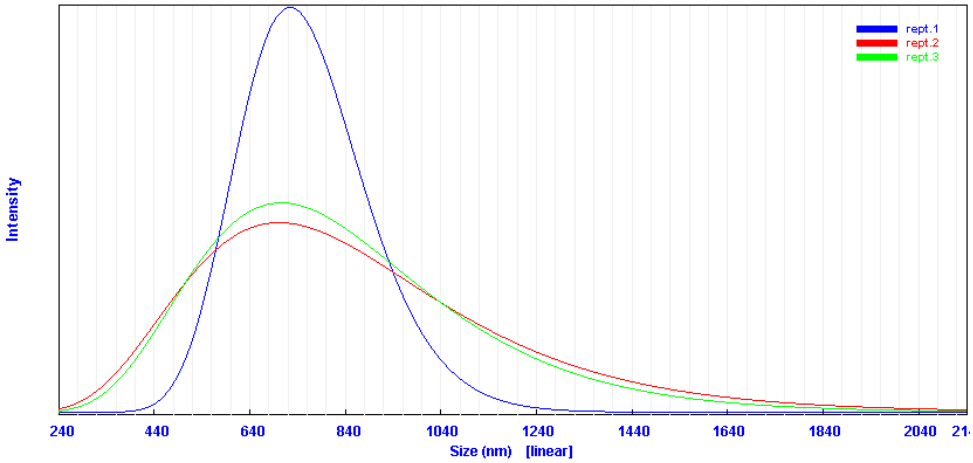

90.0° Unimodal Distribution

Unimodal Results Summary

Rept#.	Mean (nm)	P.I.	Diff.Coef (m^2/s)	Counts/s	Baseline Error	Overflow
Rept.1	895.4	0.368	5.48e-13	5.83e+05	5.90%	0
Rept.2	808.3	0.281	6.07e-13	5.80e+05	2.91%	0
Rept.3	820.5	0.462	5.98e-13	5.82e+05	3.52%	0
Average	841.4 ± 38.54	0.370 ± 0.074				

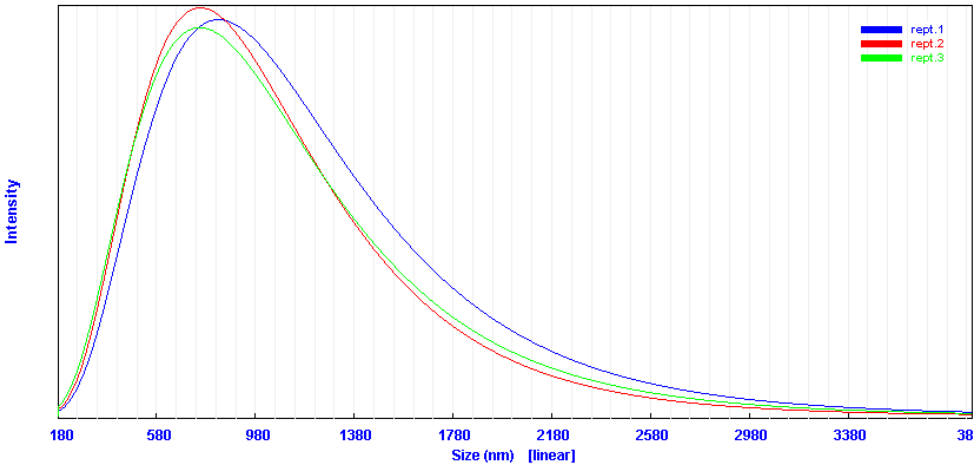

Figure 29. Light scattering measurements of pyrazolone containing Nanotraps. Nanotraps have been synthesized with pyrazolone as a cross-linker. Reducing the pH of the solution promotes the degradation of the Nanotraps. Hydrodynamic diameter was 703 ± 2.42 nm before treatment (upper panel) and 841.4±38.54 nm after treatment (lower panel).

Fast Blue B Nanotraps

Fast Blue 221 can act not only as a high affinity dye but also as a degradable cross-linker was successfully incorporated into the Nanotraps as a cross-linker. Once NIPAm strands are cross-linked by the Fast Blue B, the azo-bond can be cleaved by the use of sodium dithionite as a reducing agent. Hydrodynamic diameter resulted 590.9 ± 6.80 nm and 727.8.4 ± 2.49 before and after reducing treatment respectively thus showing an increase under reducing conditions of ~20-25% (Figure 30).

90.0° Unimodal Distribution
Unimodal Results Summary

Rept#.	Mean (nm)	P.I.	Diff.Coef (m^2/s)	Counts/s	Baseline Error	Overflow
Rept.1	585.9	0.160	8.37e-13	3.36e+05	1.19%	0
Rept.2	600.5	0.272	8.17e-13	3.53e+05	2.24%	0
Rept.3	586.3	0.282	8.37e-13	3.53e+05	1.70%	0
Average	590.9 ± 6.80	0.238 ± 0.056				

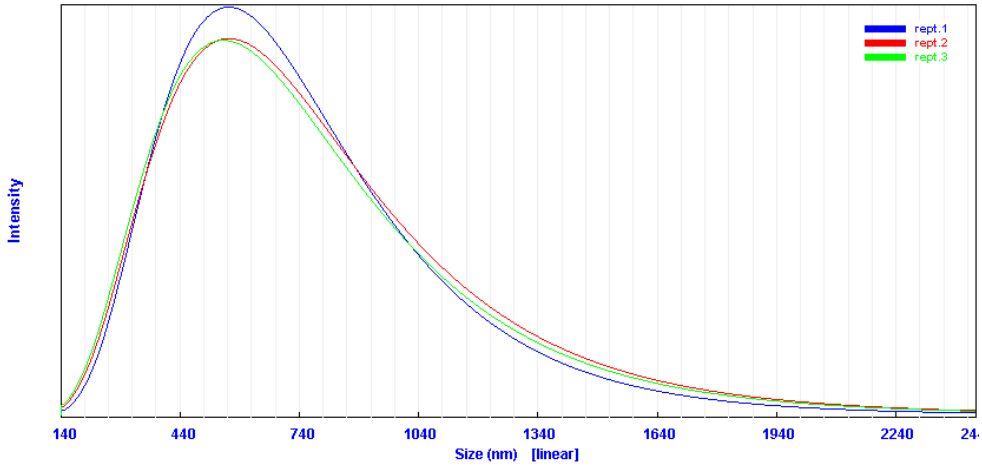

90.0° Unimodal Distribution

Unimodal Results Summary

Rept#.	Mean (nm)	P.I.	Diff.Coef (m^2/s)	Counts/s	Baseline Error	Overflow
Rept.1	726.7	-0.247	6.75e-13	4.64e+05	0.11%	0
Rept.2	725.4	-0.015	6.76e-13	4.56e+05	0.18%	0
Rept.3	731.2	-0.041	6.71e-13	4.49e+05	0.16%	0
Average	727.8 ± 2.49	-0.101 ± 0.104				

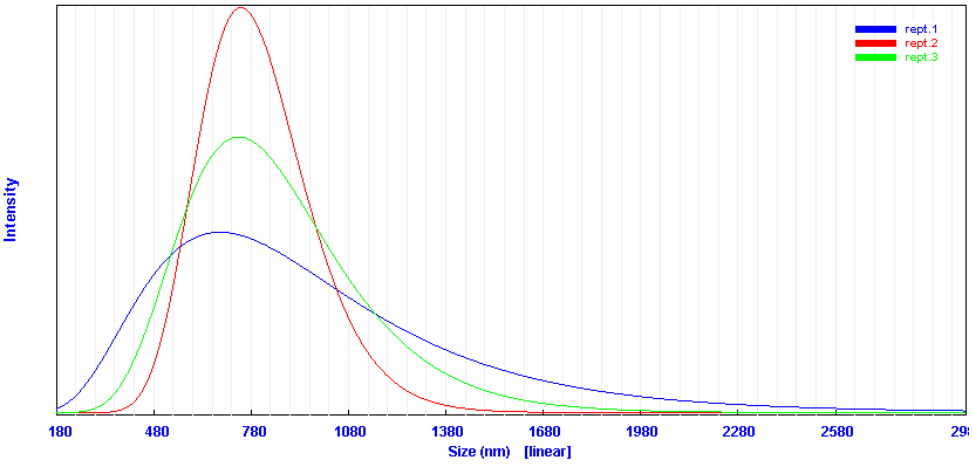

Figure 30. Light scattering measurements of Fast Blue B Nanotraps. Nanotraps containing Fast Blue B as a cross-linker show an average diameter of 590.9 ± 6.80 nm before reduction via sodium dithionite (upper panel). After treatment with sodium dithionite the diameter increases to 727.8.4 ± 2.49 (lower panel).

4.2 NANOTRAP ENHANCED WESTERN BLOT FOR THE DETECTION OF LYME DISEASE

4.2.1 Mass spectrometry sequencing of *Borrelia burgdorferi* Outer Surface Protein A

In this study we used Bb Lyme antigen Grade 2 as our primary source of OspA. A dilution (ranging from 100ng to 100ong) of a recombinant purified OspA protein (Genecopoeia) was analyzed by SDS-PAGE and silver staining (Figure 31). The band intensities were quantified using ImageJ software and a calibration curve was built. A linear regression curve was

fitted (y=5.39x+12281, R^2 = 0.9873). 500 ng of Bb Lyme antigen Grade 2 were loaded on the gel (Lane 2) and compared to the recombinant OspA calibration curve (Lanes 3-7). From this procedure we estimated that 81% of Bb Lyme antigen Grade 2 total protein content is OspA. In gel protein digestion and mass spectrometry (MS) analysis verified the predominant presence of tryptic peptides belonging to OspA in the bands at ~30 kDa and ~60kDa present both in the Bb Lyme antigen Grade 2 and in the recombinant OspA. In particular, tryptic peptides containing the epitope for mAb clone 0551 OspA236-239 were present in both bands (MS-MS spectra are reported in the insert).

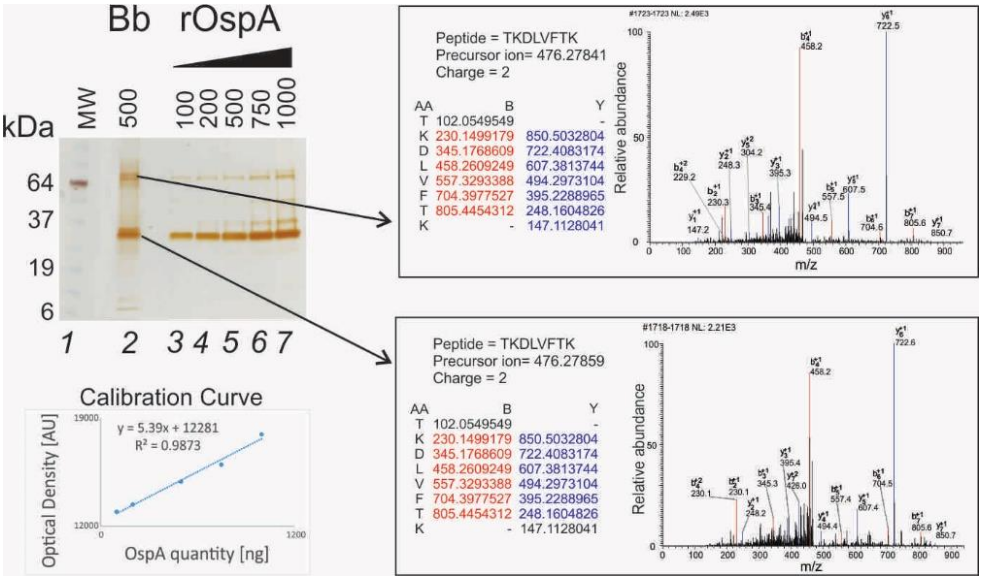

Figure 31. Mass Spectrometry analysis of Bb Lyme antigen Grade 2 (American Research Products). 81% of the total protein of the Bb Lyme antigen Grade 2 is constituted by OspA. A calibration curve was performed using OspA recombinant protein and band intensity of 500ng of Bb Lyme antigen Grade 2 was compared to the calibration curve obtained. Highest intensity bands at approximately 30 and 60 kDa were digested and analyzed by mass-spectrometry. Both resulted to be OspA as a single protein as well as a dimer. (Source: Magni, R. et al., 2015)

4.2.2 Mass spectrometry sequencing and peptide competition reveals the OspA C-terminal epitope recognized by the anti-OspA mAb

Bb Lyme antigen Grade 2 was partially digested with different proteolytic enzymes such as trypsin, pepsin and GluC. Protease derived fragments were split in different aliquots. One aliquot was analyzed by western blotting using the anti-OspA monoclonal antibody 0551. In parallel the other aliquots were run on a SDS gel and silver stained. The band in the SDS-page mirroring the smallest peptide fragments were cut out of the gel and processed for mass spectrometry analysis (Figure 32). In presence of trypsin digestion the lysate did not produce clear and detectable bands that could be cut out of the gel and analyzed. Although clear bands were produced at lower molecular weight using GluC, after analyzing them with mass spectrometry, no proteins were identified probably due to the poor ionization efficiency. On the contrary pepsin digestion produced visible fragments that could be identified by mass-spectrometry.

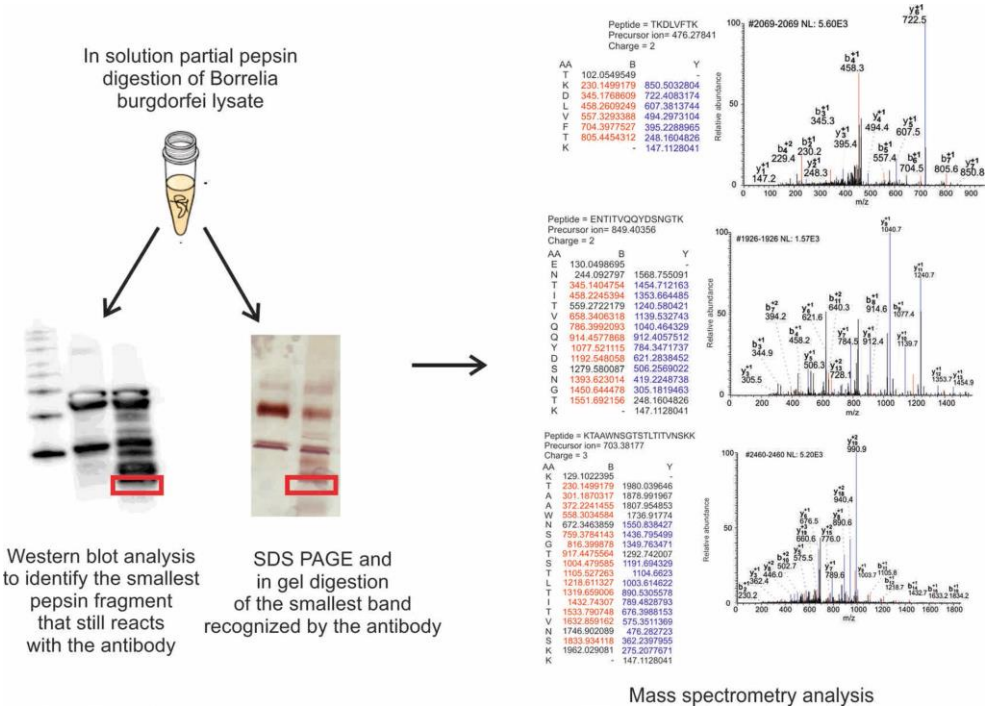

Figure 32. Proteolytic digestion for mapping the OspA epitope. Bb Lyme antigen was partially digested with pepsin and the loaded on two SDS-gel. One was used for western blot and incubated with mAb 0551, the other was silver stained. The smallest band mirroring the WB was cut out of the gel and analyzed by mass spectrometry. (Source: Magni, R. et al., 2015)

The fragment KTSTLTISVNSKKTTQLVFTKQDTITVQKYDSAGT (OspA219-253, Figure 33 and Supplementary Table 3) was the smallest sequence that reacted with the mAb clone 0551. This sequence is located on the C-terminal region of the protein.

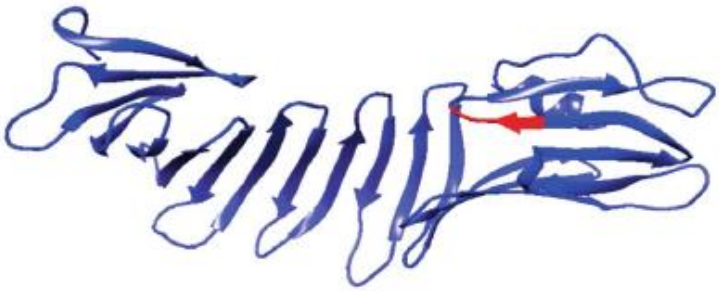

Figure 33. Cristallography structure of the OspA. The identified epitope is highlighted in red. (Source: Magni, R. et al., 2015)

Two overlapping peptides, Peptide 5 (OspA219-239) = KTSTLTISVNSKKTTQLVFTK and peptide 6 (OspA234-253) = QLVFTKQDTITVQKYDSAGT were synthesized and evaluated against control peptides from other regions of the molecule for their reactivity with the mAb (Figure 34 C). Whereas no detectable signal was obtained for different peptides of the OspA, both peptide 5 and 6 showed a detectable signal on dot blot (Figure 34 A, B)

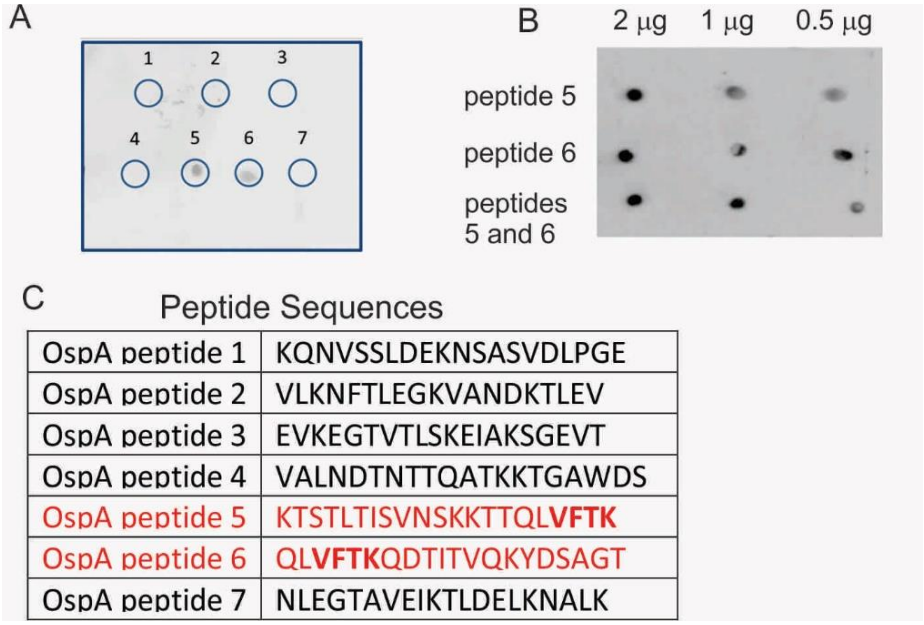

Figure 34. High specificity of a narrow OspA epitope. a) Dot blot analysis revealed that only 2 out of 7 synthetic peptides with sequence highlighted in red (c) show reactivity with the anti OspA monoclonal antibody used in this study. b) dot blot analysis of a dilution curve of peptides 5 and 6. (Source: Magni, R. et al., 2015)

The overlapping region of these peptides (OspA236-239 = VFTK) was found to be necessary and sufficient for antibody recognition via dot blot (Figure 35). The flanking regions, highly variable in the *Borrelia burgdorferi* sensu strictu and across different *Borrelia* species were devoid of immunoreactivity with the mAb clone 0551 (Figure 35).

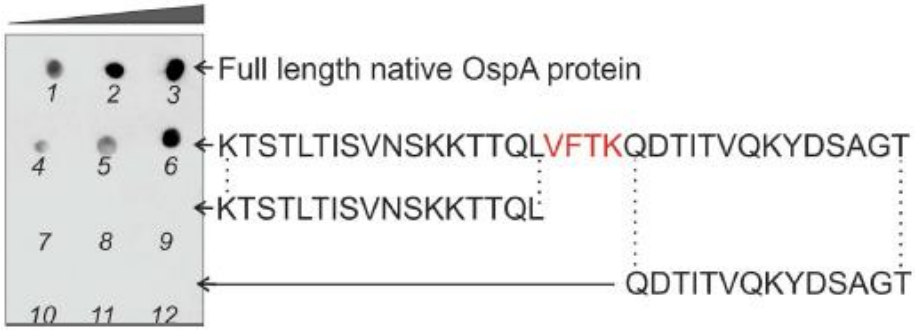

Figure 35. Reactivity of mAb against synthetic OspA peptides. Synthetic peptides mimicking the OspA236-239 region interact with the mAb in a dose dependent manner (dot blot analysis, 1, 2, 3 = Bb Lyme antigen 0.5, 5, and 10 ng, respectively; 4, 5, and 6 = OspA219-253 0.5, 1, and 2 µg, respectively; 7, 8, and 9 = OspA219-235 0.5, 1, and 2 µg, respectively; 10, 11, and 12 = OspA240-253 0.5, 1, and 2 µg, respectively). Negative control peptides (OspA219-235 and OspA240-253) containing flanking regions but lacking the OspA236-239 sequence were devoid of immunoreactivity with the mAb clone 0551. (Source: Magni, R. et al., 2015)

4.2.3 Competition assay shows high affinity between epitope containing peptide and mAb

In order to further prove the specificity of the mAb towards the antigenic epitope OspA236-239, peptide solution phase competition and solid phase affinity depletion were performed. Peptide containing the putative epitope region were able to compete the antibody, while peptides lacking of the epitope regions failed to compete the antibody (Figure 36 A). Another proof of the specificity of the antibody for the epitope containing peptide was obtained through peptide solid phase affinity depletion. Antibody was incubated on an ELISA plate coated with the peptide OspA219-253 containing the epitope recognized by the antibody. After incubation the antibody supernatant was recovered and its ability to react with the OspA was tested on a western blot. No immunoreactivity in the mAb preparation after immunodepletion was observed. This is a further confirmation of the absence of non-specific signal in the mAb clone (Figure 36 B).

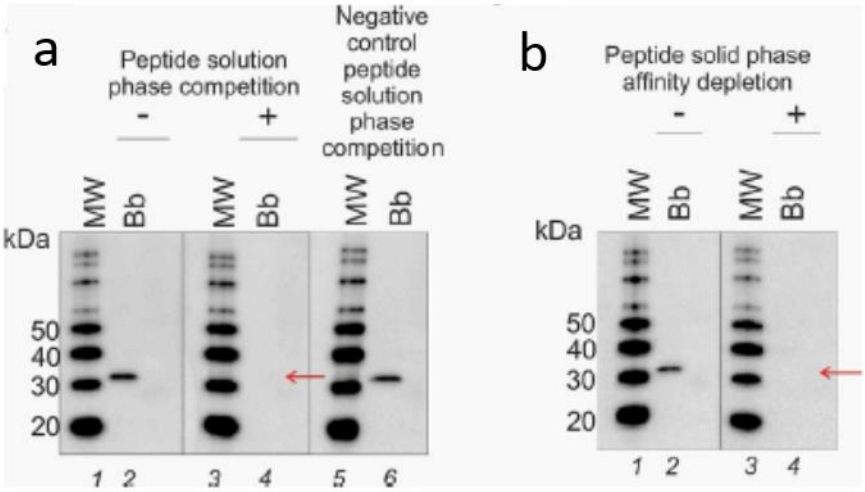

Figure 36. Peptides containing the narrow OspA236-239 region were successfully utilized for antibody competition and immunodepletion. A) 600 pg of Bb Lyme antigen Grade 2 were spiked in human urine. Samples were processed through the Nanotrap particles and analyzed by western blot. Lane 2, 4 and 6 were obtained staining the western blot membranes with the mAb clone 0551 alone, the mAb neutralized with OspA219-253 peptide, and the mAb neutralized with a combination of OspA219-235 and OspA240-253, respectively. The peptide containing the OspA236-239 region successfully competed the mAb, whereas peptide missing the OspA236-239 region failed to compete the mAb clone ID 0551. B) Peptide OspA219-235 was utilized for solid phase affinity depletion of the mAb clone 0551. The peptide (30 µg) was deposited on ELISA plate wells. The wells were washed and the excess peptide removed. The mAb clone 0551 (3 µg) was incubated with the solid phase adsorbed peptides overnight. After incubation, the supernatant was recovered and brought to a volume of 3 mL in PBS supplemented with 0.2 % I-Block and 0.1 % Tween 20. In parallel, 600 pg of Bb Lyme antigen Grade 2 were spiked in urine and processed through the Nanotrap particles (lane 2 and 4). Lane 2 and 4 were obtained staining the western blot membranes with the mAb alone (3 µg) and the mAb after immunodepletion, respectively. There is no immunoreactivity in the mAb preparation after immunodepletion (lane 4). This is a further confirmation of the absence of non-specific signal in the mAb clone 0551 preparation. (Source: Magni, R. et al., 2015)

4.2.4 The anti-OspA mAb epitope is conserved in common pathogenic species of *Borrelia*

The antigenic epitope OspA236-239 is highly conserved among major pathogenic *Borrelia* strains, these includes: *Borrelia burgdorferi sensu stricto*, several *Borrelia burgdorferi sensu lato* (*Borrelia garinii, Borrelia valaisiana, Borrelia bissettii, Borrelia afzelii,* and *Borrelia spielmanii*) and additional more recently characterized candidate pathogenic species (Table

2, Supplementary Table 4). BLAST analysis[153] performed on the sequence of the fragment OspA219-253 TSTLTISVNSKKTTQLVFTKQDTITVQKYDSAGT identified by mass spectrometry showed that it was not homologous to any human protein and not homologous to any other non-*Borrelia* spirochetes.

Borrelia Burgdorferi B31	1OSP	TSTLTITVNSKKTKDLVFTKENTITVQQYDSNGT
Borrelia burgdorferi ss	CAA46549	TSTLTISVNSKKTKNIVFTKEDTITVQKYDSAGT
Borrelia burgdorferi ss	CAA45010	TSTLTISVNSQKTKNLVFTKEDTITVQRYDSAGT
Borrelia burgdorferi ss	CAA46551	TSTLTISKNRQKTKQLVFTKEDTITVQNYDSAGT
Borrelia burgdorferi ss	CAA56544	TSTLTISKNRTKTKQLVFTKEDTITVQNYDSAGT
Borrelia burgdorferi ss	CAB64756	TSTLTITVNSKKTKALVFTKEGTITQQSYDTNG
Borrelia burgdorferi ss	CAB64755	TSTLTITVNSKKTKDLVFTKEGTITQQSYNTNG
Borrelia burgdorferi ss	CAB64754	TSTLTITVNSKKTKALVFTKEGTITQQSYDTNG
Borrelia burgdorferi ss	CAB64757	NSTLTIIVDSKNKTKLVFTKQDTITVQSYNPAG
Borrelia Burgdorferi ss	OSPA6	TSTLTISVNSKKTTQLVFTKQDTITVQKYDSAGT
Borrelia afzelii	ADG01987	TSTLTISVNSKKTTQLVFTKQDTITVQKYDSAGT
Borrelia bissettii	WP_014023199	TSTLTISVNSKKTKNLVFTKQDTITVQKYDSAGT
Borrelia bissettii	AAB21761	TSTLTITVNNKKTKALVFTKQDTITSQKYDSAGT
Borrelia garinii	WP_014695383	TSTLTISVNSKKTTQLVFTKQDTITVQKYDSAGT
Borrelia japonica	CAB64759	STLTISVNSKKTTQLVFTKQDTITMQKYNTNG
Borrelia valaisiana	ACA13517	TSTLTIAVNNKNTKSLVFTKEDTITVQNYDSAGT
Borrelia americana	ABX51936	TSTLTITVNSKKTKDLVFTKENT
Borrelia spielmanii	ADG02097	TSTLTITVNSKKTKDLVFTKQDTITVQKYDSAGT

Table 2. Blast search against different species of Borrelia. The identified epitope is highly conserved in different species of Borrelia while flanking regions are variable. (Source: Magni, R. et al., 2015)

4.2.5 Selection of high affinity bait loaded Nanotraps for capturing Bb antigen

Nanotrap particles were functionalized with a series of chemical baits[29,50] that bind solution phase analytes with high affinity. 1 ng of Bb Lyme antigen was spiked in 500ul of human urine from healthy volunteers and incubated with differently functionalized nanotrap: Remazol Brilliant Blue, Reactive Blue 221, Diamine Green, vinyl phenyl boronic acid, allylamine. The recovered amount of protein after Nanotrap processing as well as the initial solution and supernatant after Nanotrap protein capturing step were loaded on a gel and western blot was performed. Results (Figure 37) show that Lyme antigen

was successfully depleted from supernatants and detectable in each elution. The eluate from Remazol Brilliant Blue Nanotrap particles show the highest intensity suggesting a higher yield of the overall process. Interestingly to be noted is that Nanotrap particles with no bait are also able to sequester some of the antigen but not concentrate the analyte from the surrounding solvent volume, because there is no affinity gradient without the dye bait.

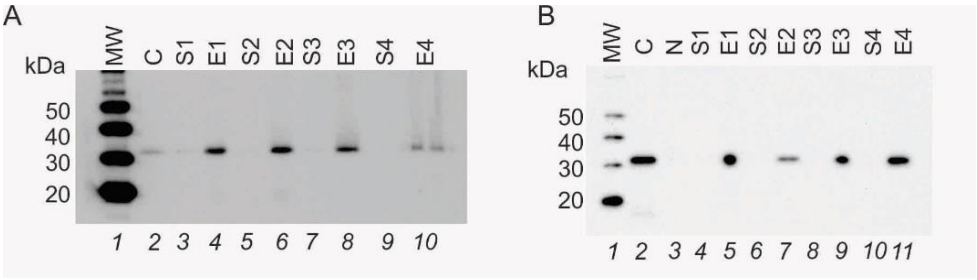

Figure 37. Remazol Brilliant Blue Nanotrap particles show the highest affinity for OspA among the tested dyes. (A) Nanotrap particles Lyme antigen (1 ng) was spiked in 500 µL of human urine and incubated with Nanotrap particles functionalized with different dyes. After Nanotrap particles processing, Lyme antigen is successfully depleted from supernatants (S) and easily detectable in the eluate (E). The A) Lanes 1) ladder; 2) Lyme antigen 0.1 ng; 3) Supernatant Remazol Brilliant Blue Nanotrap 1; 4) Eluate Remazol Brilliant Blue Nanotrap 1; 5) Supernatant Remazol Brilliant Blue Nanotrap 2; 6) Eluate Remazol Brilliant Blue Nanotrap 2; 7) Supernatant Reactive Blue Nanotrap; 8) Eluate Reactive Blue Nanotrap; 9) Supernatant Diamine Green Nanotrap; 10) Eluate Diamine Green Nanotrap.(B) Nanotrap particles without dye bait can volume sequester some antigen but not concentrate the analyte from the surrounding solvent volume, because there is no affinity gradient without the dye bait. Lanes 1) ladder; 2) Lyme antigen 1 ng; 3) Negative control = urine without Bb antigen 4) Supernatant vinyl phenyl boronic acid Nanotrap 1; 5) Eluate vinyl phenyl boronic acid Nanotrap 2; 6) Supernatant acrylic acid Nanotrap; 7) Eluate acrylic acid Nanotrap; 8) Supernatant allylamine Nanotrap; 9) Eluate allylamine Nanotrap; 10) Supernatant Remazol Brilliant Blue Nanotrap; and 11) Eluate Remazol Brilliant Blue Nanotrap. (Source: Magni, R. et al., 2015)

4.2.6 Determining the optimal amount of Dye for sample processing

Remazol Brilliant Blue nanotrap particles were able to efficiently capture and concentrate the Lyme antigen. Different amount of Nanotraps which correspond to a different amount of nanomoles of dye were incubated in 500µl of urine spiked with 0.6 ng of Bb antigen. We measured the relationship

between the amount of Remazol Brilliant Blue and the % of antigen depletion from the solution phase. Among the concentration tested 34, 68, 171, 343, 686 nmoles of Remazol Brilliant Blue, 686 nmoles showed the highest efficiency fully depleting the solution of Lyme antigen and providing clear evidence of 100% antigen depletion from the solution phase and saturation of binding (Figure 38).

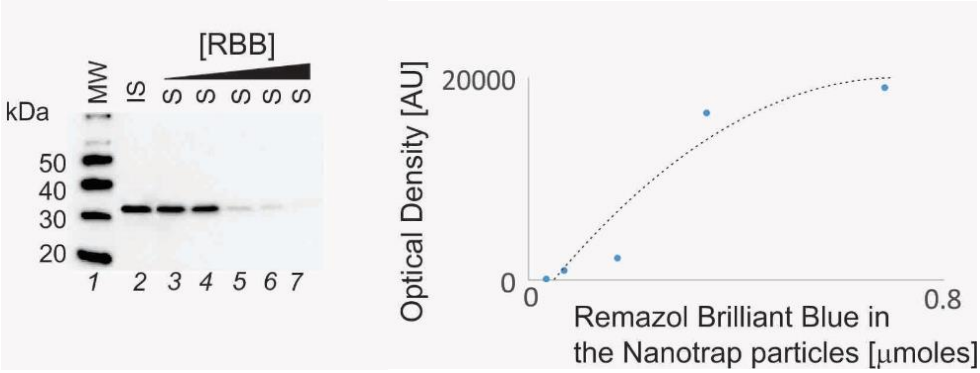

Figure 38. Relationship between dye content and capturing affinity. Left panel; Western blot showing the relationship between the Remazol Brilliant Blue in the particles and depletion of the antigen in the supernatant: 100% antigen depletion from the solution phase and saturation of binding. Lane 1: ladder, lane 2: initial solution, lanes 3-7: supernatants after incubation of containing increasing amounts of dye containing Nanotrap particles with a urine solution containing 0.6 ng of Bb antigen: 34, 68, 171, 343, 686 n moles of Remazol Brilliant Blue dye, respectively. Right panel; ImageJ quantification of the optical density in the western blot. Y axis: Antigen sequestered in the Nanotrap particles obtained as difference between the initial solution (lane 2) and the supernatants (lanes 3–7) of the western blot. X axis: μmoles of Remazol Brilliant blue in the Nanotrap particles. (Source: Magni, R. et al., 2015)

4.2.7 Determination of optimal amount of Nanotrap to sample volume ratio to optimize OspA capturing

The volume of Remazol Brilliant blue Nanotrap used to capture OspA can be adjusted to the sample volume in order to sequester virtually 100% of the target antigen. Different amount of Nanotraps were incubated in aliquots of 500ul of urine. A volume of 1/10 (V/v ration of Nanotrap suspension volume (V) and sample volume (v) (Figure 39).

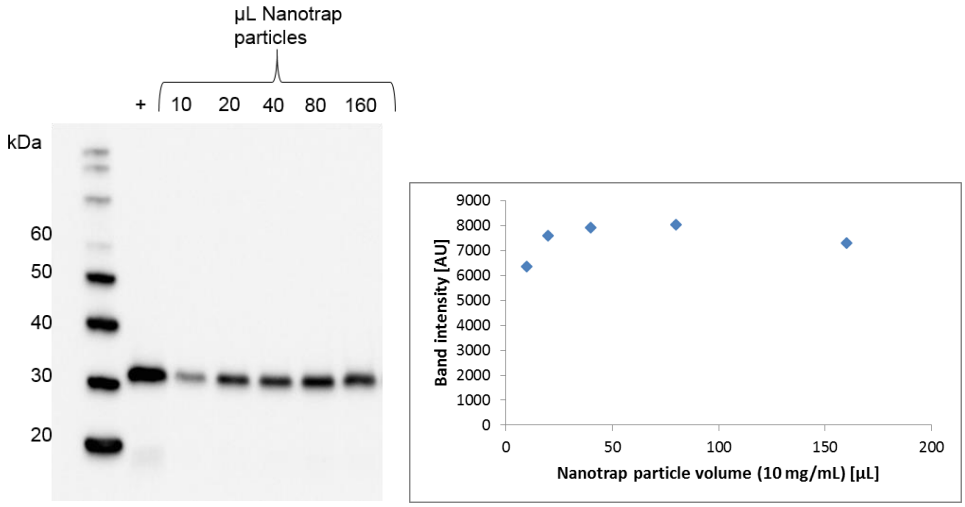

Figure 39. Effect V/v ratio between Nanotraps and sample volume on capturing effciency. a) V/v ratio (V=Nanotrap suspension volume, v=sample volume) of 1/10 was optimized in order to maximize Lyme antigen capturing. 2 ng of Lyme antigen was spiked in 500 µL urine aliquots. Urine samples were incubated with increasing amount of Nanotrap particle suspension (10-160 µL of Nanotrap at 5 mg/mL concentration). Lanes 1) ladder; 2) Positive control (OspA 1ng); 3) 10µL of Nanotrap particles; 4) 20 µL Nanotrap particles; 5) 40µL Nanotrap particles; 6) 80 µL Nanotrap particles; 7) 160µL Nanotrap particles; b) Band intensity was measured with ImageJ, plateau is reached with > 40µL of Nanotrap particles. (Source: Magni, R. et al., 2015)

4.2.8 Reproducibility of Nanotrap particles performance

Several Nanotrap batches were used for our study and strict validation criteria for each batch have been applied according to CAP CLIA guidelines. A criteria for batch to batch validation was CV<10%. Batch validation was performed incubating 200µl of Nanotraps in 40 ml of urine spiked with decreasing concentration (30pg/ml – 1.7 pg/mL) of Bb Lyme antigen Grade 2 (Figure 40 A). For a validated batch of Nanotraps a band should be visible for each concentration. Comparison between batches is performed spiking a dilution curve of the new batch (range is 32pg/mL to 0pg/mL) and two concentrations of the previous batch, 1pg/ml and 16 pg/ml (Figure 40 B).

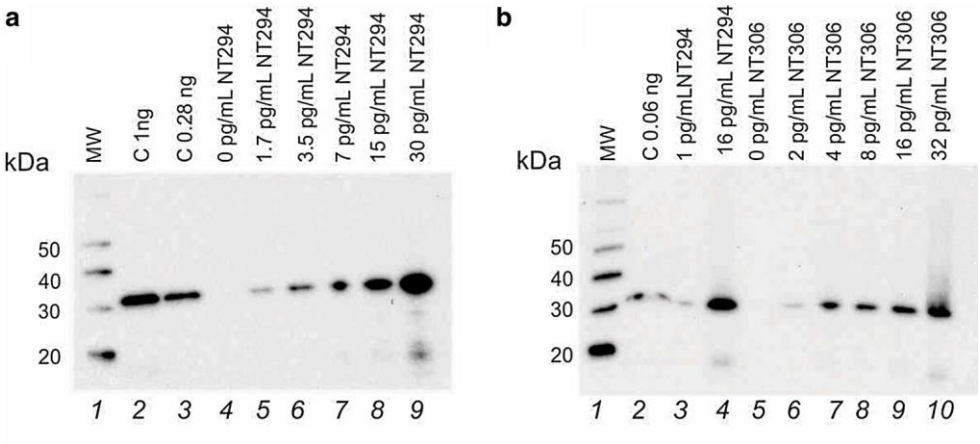

Figure 40. Nanotrap particle batch validation and batch to batch reproducibility. ***a*** *Nanotrap particles are incubated with increasing amount of Bb Lysate spiked in 40 mL of urine; Lane 1: Ladder; Lane 2: Positive control Bb Lyme antigen Grade 2 1 ng; Lane 3: Positive control Bb Lyme antigen Grade 2 0.28 ng; Lanes 4–9: eluate of Nanotrap particles incubated with increasing concentrations of Bb antigen in 40 mL of urine: 0; 1.7; 3.5; 7; 15; 30 pg/mL, respectively* ***b*** *Performance comparison of two batches of Nanotrap particles, NT294 and NT306. Lane 1: Ladder; Lane 2: Positive control Bb Lyme antigen Grade 2 60 pg; Lane 3: eluate of Nanotrap particles batch NT296 incubated with 1 pg/mL Bb antigen urine solution (40 mL); Lane 4: eluate of Nanotrap particles batch NT296 incubated with 16 pg/mL Bb antigen urine solution (40 mL); Lane 5–10: eluate of Nanotrap particles batch NT306 incubated with increasing concentrations of Bb antigen urine solution (40 mL) 0; 2; 4; 8; 16; 32, respectively. (Source: Magni, R. et al., 2015)*

To further prove the reproducibility of the results with different batches three RBB functionalized Nanotraps were spiked with at two different concentration (2pg/ml and 16pg/ml) of Lyme antigen Grade 2, processed and signals were measured by western blot (Figure 41). Densitometric analysis of the bands shows a CV=9%.

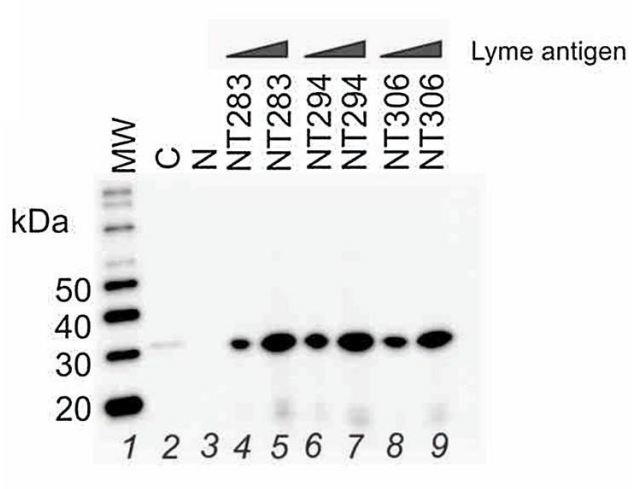

Figure 41. Performance comparison of multiple batches of Nanotrap particles (%CV = 9 % and 5 % at 2 pg/mL and 16 pg/mL Bb antigen in 40 mL of urine, respectively). Lane 1: ladder; lane 2: Positive control Bb Lyme antigen Grade 2 16 pg; lane 3: eluate of Nanotrap particles batch NT283 incubated with 40 mL of urine without Bb Lyme antigen Grade 2; lanes 4–5: eluates of Nanotrap particles batch NT283 incubated with 2 and 16 pg/mL Bb Lyme antigen Grade 2 urine solution (40 mL); lanes 6–7: eluates of Nanotrap particles batch NT294 incubated with 2 and 16 pg/mL Bb Lyme antigen Grade 2 urine solution (40 mL); lanes 8–9: eluates of Nanotrap particles batch NT306 incubated with 2 and 16 pg/mL Bb Lyme antigen Grade 2 urine solution (40 mL). (Source: Magni, R. et al., 2015)

Overall performance of the nanotrap-based western blot was performed. 320pg of spiked-in positive control were compared to the signal produced by a 40 ml solution of urine spiked with 4 pg/ml. Equal intensity of the bands is obtained if the process yields 100% recovery of the antigen after Nanotrap capture and concentration. According to the evaluation of different Nanotrap batches we were able to obtain recovery yield as high as 93% (Figure 42).

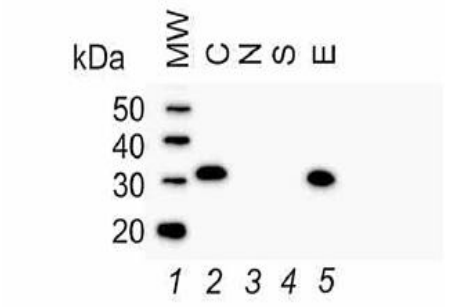

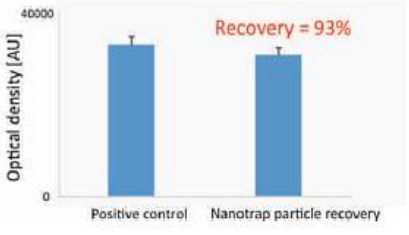

Figure 42. Yield of Nanotrap particle pre-processing. Left panel: Lane 1: ladder; lane 2: Bb antigen 320 pg, lane 3: eluate of Nanotrap particles batch NT283 incubated with 40 mL of urine without Bb Lyme antigen; lane 4: supernatant; lane 5: eluate of Nanotrap particles batch NT283 incubated with 8 pg/mL Bb Lyme antigen Grade 2 urine solution (40 mL). Right panel: densitometric measure of the bands shows an overall yield of 93%.

Overall performance of the nanotrap-based western blot was performed also using sample buffer 2X (5% TCEP) as elution buffer. 320pg of spiked-in positive control were compared to the signal produced by a 40 ml solution of urine spiked with 4 pg/ml. Densitometric analysis shows a yield of 91% thus comparable to the yield previously obtained using the combination of acetonitrile and ammonium hydroxide as elution buffer (Figure 43).

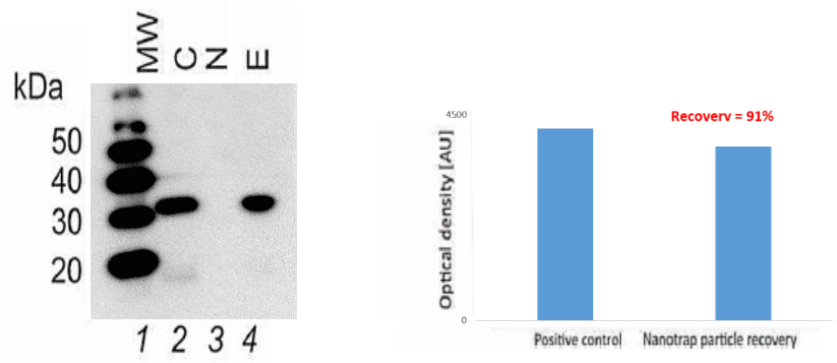

Figure 43. Yield of Nanotrap particle pre-processing using Sample Buffer 2X as elution buffer. Left panel: Lane 1: ladder; lane 2: Bb antigen 320 pg, lane 3: eluate of Nanotrap particles batch NT283 incubated with 40 mL of urine without Bb Lyme antigen; lane 4: eluate of Nanotrap particles batch NT283 incubated with 8 pg/mL Bb Lyme antigen Grade 2 urine solution (40 mL). Right panel: densitometric measure of the bands shows an overall yield of 91%.

4.2.9 Lack of cross-reactivity with relevant non-*Borrelia* infections

Because of the increasing prevalence of other tick-borne infections and the incidence of co-infections in Lyme patients, the most prevalent viral, bacterial, and protozoan antigens were tested with our method in order to exclude the possibility of cross-reactivity. A single band at 31 kDa was detected when 40 mL of human urine were spiked with OspA as well as

increasing amounts viral lysate from *Bartonella henselae* lysate (ATCC 49793), *Babesia microti* (ATCC PRA-399), Epstein-Barr virus (EBV) Cell Extract (Advanced Biotechnologies Inc.; 10-501-001), Herpes Simplex virus-1 (HSV-1) Inactivated Vero Cell Extract (Advanced Biotechnologies Inc; 10-515-001), Cytomegalovirus (CMV) HEK293 Cell Lysate (Sino Biological Inc.; 10202-VCCH1L), Hepatitis C Virus HEK293 Cell Lysate (Sino Biological Inc.; 10202-VCCH1L). No false positives were detected further proving the specificity of our antibody against the OspA epitope (Figure 44).

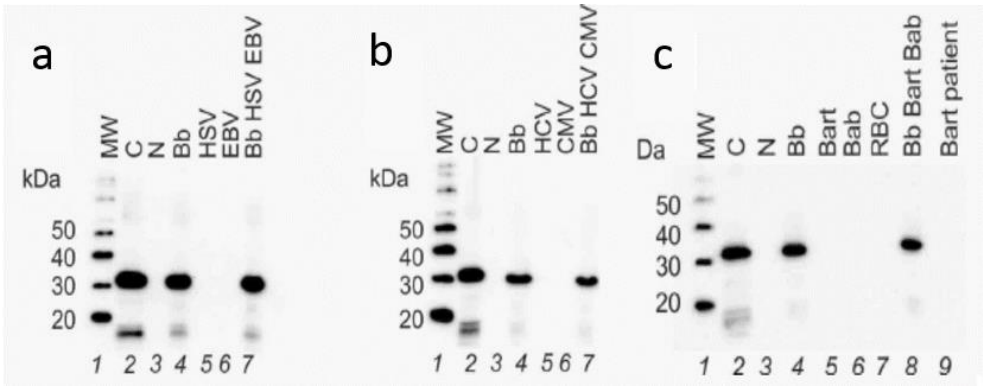

Figure 44. Infection with common non-Lyme pathogens do not generate a false positive for Borrelia in the present Nanotrap test. ***a*** *Herpes simplex 1 and Epstein Barr viral lysates were mixed with urine in presence and absence of Bb antigen. Samples were processed with Nanotrap particles and analyzed with western blot. Lane 1 ladder, lane 2 Bb antigen 1 ng; lanes 3–7 eluates of Nanotrap particles incubated with urine without Bb antigens (lane 3), 25 pg/mL Bb antigen in urine 40 mL (lane 4), HSV-1 lysate (1 µg in 40 mL of urine) (lane 5), EBV lysate (1 µg in 40 mL of urine) (lane 6), HSV-1 lysate (1 µg in 40 mL of urine) plus EBV lysate (1 µg in 40 mL of urine) plus Bb antigen (1 ng in 40 mL of urine) (lane7). (****B****) Hepatitis C and Cytomegalovirus viral lysates were mixed with human urine in presence and absence of Bb antigen. Lane 1: ladder, lane 2 Bb antigen 1 ng; lanes 3–7: eluates of Nanotrap particles incubated with urine without Bb antigen (lane 3), 25 pg/mL Bb antigen in urine 40 mL (lane 4), HCV lysate (1 µg in 40 mL of urine) (lane 5), CMV lysate (1 µg in 40 mL of urine) (lane 6), HCV lysate (1 µg in 40 mL of urine) plus CMV lysate (1 µg in 40 mL of urine) plus Bb antigen (1 ng in 40 mL of urine) (lane 7).* ***c*** *Bartonella henselae and Babesia microti lysates were spiked in human urine in presence and absence of Bb antigen. Lane 1: ladder, lane 2: Bb antigen 1 ng; lanes 3–9: eluates of Nanotrap particles incubated with urine without Bb antigen (lane 3), 25 pg/mL Bb antigen in urine 40 mL (lane 4), Bartonella lysate (1 ng in 40 mL of urine) (lane 5), Babesia lysate (10 ng in 40 mL of urine) (lane 6), red blood cells (10 ng in 40 mL of urine) (lane 7), Bartonella lysate(10 ng in 40 mL of urine) plus Babesia lysate (10 ng in 40 mL of urine) plus Bb antigen (1 ng in 40 mL of urine) (lane 8), 40 mL of urine of a patients with Bartonella positive and Borrelia negative serology at the time of urine collection (lane 9). (Source: Magni, R. et al., 2015)*

4.2.10 Lack of cross-reactivity in the presence of interfering substances

Interfering substances such as Bovine Serum Albumin and blood (hemoglobin) were tested in increasing concentration and showed no cross-reactivity with the mAb. Increasing amounts of bovine serum albumin ranging from 0.31 mg/mL to 20 mg/mL were added to 40 mL of OspA containing human urine; urine samples were processed with Nanotrap particles (Figure 45). Ability of the Nanotrap particles to sequester OspA was not affected by increasing concentration of competing proteins in urine. This suggest that the presence of abnormally high proteins in the urine of patients, as happens in the rare disorder of monoclonal gammopathy (3% incidence in general population >50 yo, decreasing with decreasing age), does not interfere with the Nanotrap OspA test as well.

Because several patients that were affected by late stage Lyme disease are found to have high level of bilirubin we decided to test if high concentration of it in urine could interfere with the results of our test. Bilirubin levels, which were tested in the urine with dipstick prior to analysis, did not cause any interference with the Nanotrap test. Firstly, the Nanotrap particle urine OspA test uses chemiluminescence solid phase based detection whereas bilirubin is known to interfere with absorbance readings at $\lambda \sim 456$ nm[154] in solution-phase homogeneous assays. Secondly, the molecular weight of bilirubin is ~500 Da. This means that bilirubin is too small to be retained in the SDS PAGE system (Tris Gly 4-20%) we use to detect the OspA antigen. Bilirubin would migrate out of the gel during the electrophoretic run necessary to separate the proteins, which have a much higher molecular weight (10,000 – 100,000 Da).

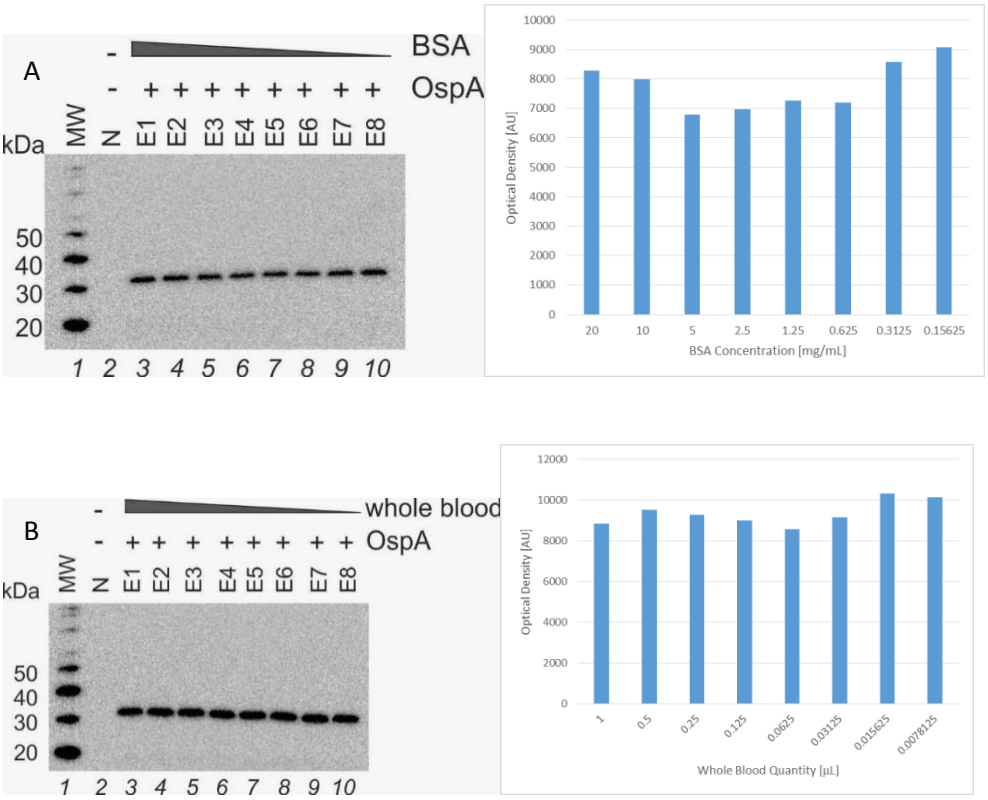

*Figure 45. Interfering substances: the presence of a high amount of protein and blood in the urine does not interfere with Lyme antigen capture and detection. (**A**) 320 pg of Lyme antigen was spiked in samples of 40 mL of human urine. We tested the interference of albumin present in excess up to 10^8 fold. Lanes: 1) ladder; 2) volunteer human urine in absence of OspA antigen (negative control); 3) OspA + BSA 20 mg/mL ; 4) OspA + BSA 10 mg/mL; 5) OspA + BSA 5 mg/mL; 6) OspA + BSA 2.5 mg/mL; 7) OspA + BSA 1.25 mg/mL; 8) OspA + BSA 0.625 mg/mL; 9) OspA + BSA 0.31 mg/mL; 10) OspA + BSA 0.15 mg/mL. (**B**) Lyme antigen 320 pg was spiked in urine samples (40 mL). Increasing amounts of whole blood from 0.015 µL to 1 µL was added to the urine samples; urine samples were processed with Nanotrap particles and analyzed using western blot. Lanes: 1) ladder; 2) volunteer human urine in absence of OspA antigen (negative control); 3) OspA + 1 µL whole blood; 4) OspA + 0.5 µL whole blood; 5) OspA + 0.25 µL whole blood; 6) OspA + 0.125 µL whole blood; 7) OspA + 0.062 µL whole blood; 8) OspA + 0.031 µL whole blood; 9) OspA + 0.015 µL whole blood; 10) OspA + 0.007 µL whole blood. (Source: Magni, R. et al., 2015)*

4.2.11 Precision and sensitivity of Nanotrap-based OspA western blot test

In order to determine the intra-assay precision, replicate of urine spiked-in samples were processed with Nanotrap and western blot was performed. Densitometric analysis of the 31 kDa band showed a very high level of intra-assay precision (n = 4, %CV = 7 %). for the Nanotrap concentration/immunoblotting method achieving a lowest limit of detection (LLD) of 1.7 pg/mL starting from 40 mL of urine (Figure 46). The dynamic range is 1.7–30 pg/mL.

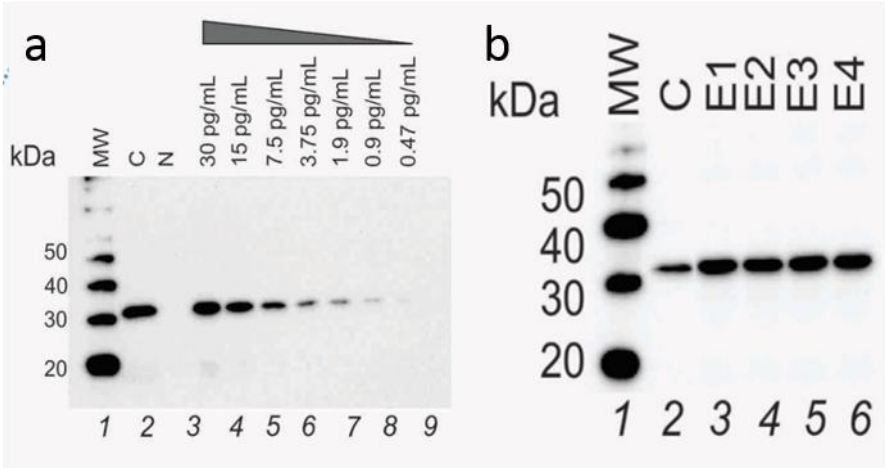

*Figure 46. Lower limit of detection/quantitation and reproducibility of the urinary OspA Lyme test. A): Sensitivity studies on three independent replicates: lower limit of detection (LLD) is 1.7 pg/mL. The lower limit of quantitation (LLQ) is 4.2 pg/mL for a 40 mL urine sample input volume. (Background estimate = 1071 AU, standard deviation (SD) = 323 AU. LLD = background + 2*SD, LLQ = background + 10× SD; polynomial equation y = −19.026x2 + 1160x − 248.76, R2 = 0.9971, was used to estimate the corresponding x value (1.7 pg/mL and 4.2 pg/mL, respectively)). 1 ladder; 2 Bb Lyme antigen control 1000 pg; 3 Eluate from Nanotrap particles incubated with 40 mL of volunteer urine containing no Bb Lyme antigen, negative control; 4–10 Eluate from Nanotrap particles incubated with 40 mL of volunteer urine containing decreasing concentrations of OspA, 30, 15, 7.5, 3.75, 1.9, 0.9, and 0.47 pg/mL, respectively. B): Within run assay %CV is 7 %. Lyme antigen (1200 pg) was spiked in 4 urine aliquots (40 mL) and incubated with 4 mL of Nanotrap particles. Band intensity was measured with Image J. Within run %CV = 7 %. 1 Ladder; 2 OspA Lyme antigen control 200 pg, 3–6 Replicates of Nanotrap particle processed spike-in samples. (Source: Magni, R. et al., 2015)*

4.2.12 Detection of OspA in Ticks

Nanotrap-based western blot test was used to detect OspA in *Ixodes* ticks. According to studies that follow the growth of *Borrelia burgdorferi* in ticks feeding on mice using confocal fluorescence miscroscopy, the bacteria reproduces within the tick gut and by the time that it is transferred to human the number of bacteria is increased from less than 10,000 organisms to more than 150,000[77,155]. Nanotraps have been successfully applied in the past to verify the presence of OspA and OspB in tick vectors[156]. In the previous study by Douglas *et al.* fourteen ticks (females and males collected in Pennsylvania and Virginia) were analyzed. Four out of 14 ticks gave a strong positive signal in the Nanotrap particle system. The exact same band pattern of OspA identified in the extracted tick was also confirmed in this study (Figure 47). Several ticks were frozen and pulverized, resuspended in PBS (1mL) and processed with Remazol Brilliant Blue functionalized Nanotraps. Eluates were analyzed by western blot. Proteins extracted from infected ticks showed the presence of a positive band after pre-processing with Nanotrap demonstrating the ability of our Nanotrap-based immunoassay to capture and detect naturally occurring proteins in single infected ticks.

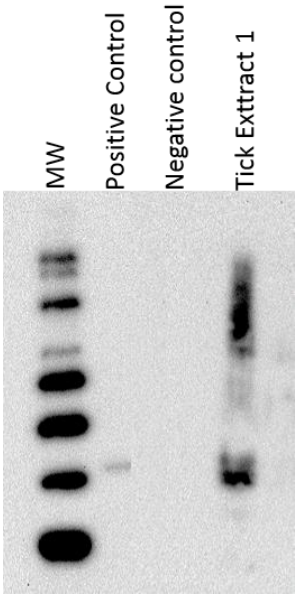

Figure 47. Nanotraps capture OspA in infected ticks. Positive control was made by loading 100pg of B. burgdorferi lysate. The eluate (tick extract) shows a strong band at ~30 kDa indicating that the antibodies reacted with B. burgdorferi protein in the tick, while the eluate from empty Nanotraps (negative control) does not show any cross-reactivity.

4.2.13 Detection of OspA in urine from patients suspected of Lyme disease

In order to assess the ability of the Nanotrap test to capture native OspA in human urine, a urine sample from a patient with clinical symptoms of Lyme disease collected before any antibiotic treatment was processed with Nanotrap and tested by western blot. The initial solution (IS) before Nanotrap processing was loaded on the gel as well as the elution from the Nanotraps. Nanotrap pre-processing results to be necessary for the detection of OspA (Figure 48). No signal was detected when samples from healthy donors were processed through Nanotraps and analyzed by western blot.

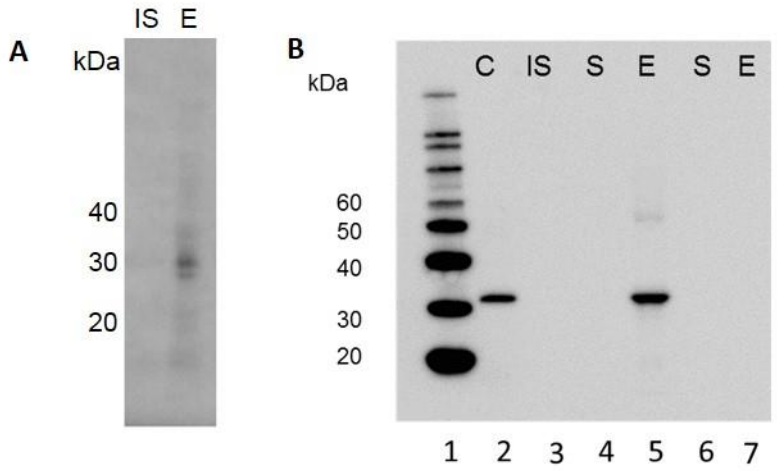

Figure 48. (A) Nanotrap particle preprocessing step is necessary to detect an OspA specific band in the urine of a patient, clinically positive for Lyme disease. Initial solution (IS) before Nanotrap particle processing. Eluate (E) after Nanotrap particle processing. (B) Positive and negative controls run with all Lyme patient samples. Lane 2 contains Borrelia protein lysate (2 ng) in human urine. Lane 5 is a positive control 4 ng spiked in 40 mL of urine sample. Lane 6 and 7 are negative controls of 40 mL of volunteer urine processed through the Nanotrap particles. C=Borrelia lysate control, IS=initial solution, S=supernatant, E=eluate. (Source: Magni, R. et al., 2015)

4.2.14 Detection of OspA in early stage Lyme patients with clinical evidence of Lyme disease before treatment

Patients with suspected of early stage cutaneous LB, manifesting the characteristic EM rash with or without concurrent symptoms such as fever, malaise, or neurologic symptoms (e.g. Bell's Palsy) were tested with our Nanotrap-based immunoassay (Table 3, 4; Supplementary table 2).

Patient characteristics	**Number**
Asymptomatic non-Lyme (healthy volunteers)	117
Symptomatic non-Lyme patients (non-Lyme patients in infectious disease clinic)	3
Untreated, clinical diagnosis of LB (positive diagnosis of Lyme disease with EM rash)	24
Antibiotic treatment for a clinical diagnosis of LB, Arthritis Pos, EM Neg (positive diagnosis of Lyme disease with arthritis symptoms)	6
EM rash present at the time of urine collection during the treatment course	10
Post-treatment with alleviation of symptoms (converted to EM Neg)	8
Patients being worked up for chronic or recurrent LB with negative or inconclusive serology	100

Table 3. Clinical features of patient enrolled in the diagnostic clinical trial. (Source: Magni, R. et al., 2015)

All patients resulted positive for serology using the two tier testing algorithm according to FDA guidelines. 24/24 patients exhibiting a characteristic cutaneous infection (EM rash) at the time of urine collection, were positive for urinary OspA peptides containing the C-terminal domain recognized by the anti-OspA mAb (Figure 49).

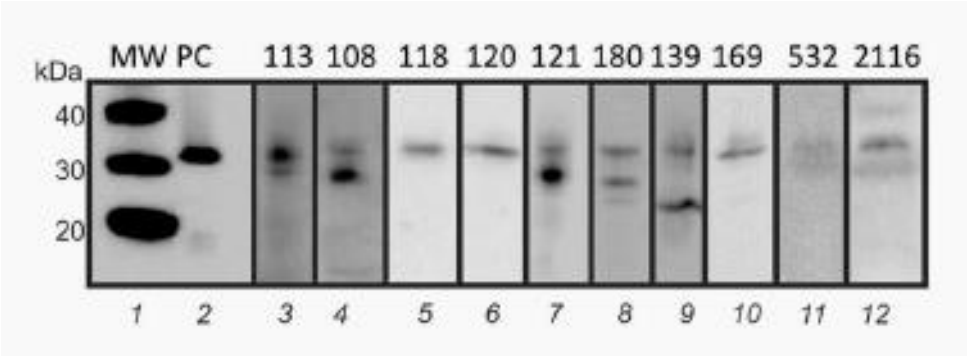

Figure 49. Nanotraps capturing of OspA in patients with clinical diagnosis of Lyme disease. Lane 1 ladder, lane 2 Bb antigen 1 ng; Lanes 3–12: example of patient urine samples demonstrating presence of OspA. Positive OspA bands are normally visible in the 28–30 kDa range although lower molecular bands can be detected and successfully competed suggesting the presence of smaller-than-full-lenght OspA C-terminal domain containing protein fragments in urine. (Source: Magni, R. et al., 2015)

Most of the positive OspA peptide bands were in the range of 28–32 kDa, but in some cases smaller fragments and a higher molecular weight band (that could be competed) in the range of 20–28 and ~60 kDa were noted (Figure 49). Thus the urinary shedding of OspA is likely to include OspA antigen modified by proteases. In contrast, none of 117 untreated, non-symptomatic control patients shed urinary OspA C-terminal antigen (Chi squared p value <2.2e−16; significance = 5 %, power 100 %). Samples classified negative for OspA did not have detectable bands in the 20–32 kDa range (Figure 50).

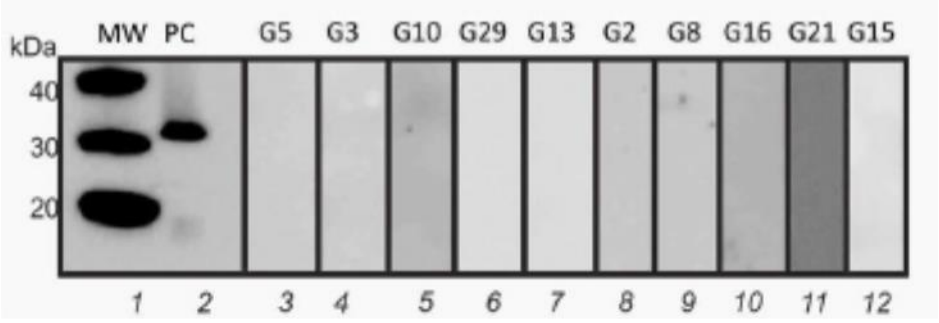

Figure 50. Nanotrap antigen test results on a representative sub-group of the 117 healthy volunteers. Lane 1 ladder, lane 2 Bb antigen 1 ng; Lanes 3–12 example of patient urine samples demonstrating absence of OspA. (Source: Magni, R. et al., 2015)

For the 24 patients that were EM positive and also urinary OspA positive at the time of urine collection, 12 became LB serology positive by CDC criteria for early diagnosis[157], 5 were serology negative[157], 3 were serology equivocal and 4 were not done (ND, Table 4). 3 untreated patients who were LB serology negative, and EM negative, but positive for joint symptoms and fatigue, were negative (0/3) for urinary OspA (Table 4). Specificity of the urinary OspA antigen test for later serology outcome was 87.5 % (21 urinary OspA positive/24 serology positive, Chi squared p = 4.072e−15, Table 5).

Categories	**Patients subcategories (N°)**	**Clinical features**	**OspA Pos**	**OspA Neg**
Non Lyme	Asymptomatic (117)	EM Neg, serology ND	0	117
	Symptomatic, joint pain (3)	EM Neg, serology Neg	0	3
Untreated, clinical diagnosis of LB	EM Pos (24)	Serology: 12 Pos, 5 Neg, 3 Eq. 4 ND	24	0
Antibiotic treatment for a clinical diagnosis of LB	EM rash present at the time of urine collection during the treatment course (10)	Serology: 4 Pos, 6 Neg	10	0
	Arthritis Pos, EM Neg (6)	Serology: 6 Pos	6	0
	Converted to EM Neg (8)	Serology: 4 Pos, 4 Neg, 8/8 urinary OspA Pos prior to therapy	0	8

Table 4. Urinary OspA results compared to serology, clinical diagnosis and treatment status of N = 168 patients suspected of having early stage LB, and healthy controls. OspA pos urinary OspA test positive, OspA neg urinary OspA test negative, EM Erythema Migrans, ND serology not done. (Source: Magni, R. et al., 2015)

	Serology positive*	Serology negative*	Serology Equivocal**	Total
OspA Pos	21	17	3	41
OspA Neg	3	124	0	127
Total	*24*	*141*	*3*	*168*

*Table 5. Correlation of urinary OspA to serology CDC criteria for early stage LB. (Source: Magni, R. et al., 2015); * symptomatic and non-symptomatic,pre and post treatment;** Symptom Positive for clinical diagnosis of LD*

4.2.15 Treated Patients with a clinical diagnosis of Lyme Disease

We evaluated the urinary OspA shedding of patients who presented to a community infectious disease clinic with onset of cutaneous or systemic symptoms and were immediately treated with antibiotics based on a clinical diagnosis of LB (Tables 3, 4; Supplementary table 2). Urinary OspA was scored positive or negative as described above without knowing the clinical outcome, and then compared to the clinical diagnosis based on anonymous coded patient records. Urinary OspA was compared to LB western blot serology for each patient.

A subset of the treated patients donated a urine specimen at a time in the course of antibiotic therapy when the EM rash was still present. 10/10 treated patients with a concurrent EM rash at the time of urine collection were positive for urinary OspA antigen C-terminal containing peptides. Of these 10, four (4/10) post treatment were LB serology positive. Six of six (6/6) patients undergoing antibiotic therapy for a clinical diagnosis of LB who had systemic symptoms such as joint pain or neurologic symptoms, but were EM negative, were also positive for urinary OspA. All of these patients became serology positive by CDC criteria[157]. 8 patients who were initially positive for urinary OspA antigen were clinically diagnosed as symptom free (resolution of EM rash) after a successful course of antibiotic therapy for a clinical diagnosis of LB. None (0/8) asymptomatic post treated patients were positive for urinary OspA (Figure 51) and four (4/8) were subsequently LB serology positive. Thus urinary OspA antigen shedding appears, in this study group, to closely parallel the concurrent presence of symptoms.

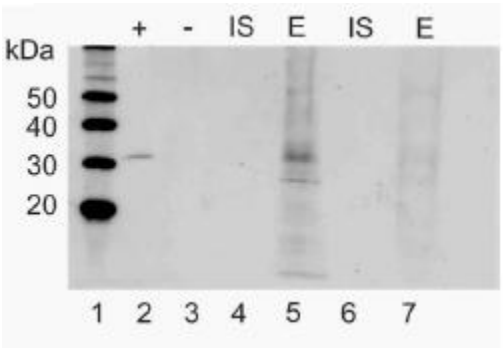

Figure 51. The OspA band is not detectable in the urine of acute stage Lyme patients after successful treatment. Lane 1 ladder; lane 2 Bb Lyme antigen Grade 2 in urine 0.1 ng; lane 3 negative control urine with no OspA; lane 4 Initial solution (=urine without Nanotrap particle pre-processing) of patient 120 before treatment; lane 5 eluate of patient 120 before treatment; lane 6 Initial solution patient 120 after treatment; lane 7 Eluate patient 120 after treatment. (Source: Magni, R. et al., 2015)

4.2.16 Treated patients under clinical evaluation for persistent or recurrent LB

Urinary OspA shedding was further evaluated in a cohort of 100 patients in a Lyme endemic geographic region who were under clinical surveillance for persistent or recurrent LB. All of these patients had been previously treated with antibiotics, and all patients had been followed because of prolonged chronic functional symptoms such as arthralgias, neurocognitive symptoms, and fatigue. All of these patients lacked a CDC criteria defined LB serology positive IgG western blot serum test at the time of urine collection[104]. According to the IDSA (Infectious Diseases Society of America) 2006 and 2010 guidelines[125,158], "To date, there is no convincing biologic evidence for the existence of symptomatic chronic B. burgdorferi infection among patients after receipt of recommended treatment regimens for Lyme disease." In contrast, according to ILADS (The International Lyme and Associated Diseases Society), the diagnosis of persistent Lyme disease is a real phenomenon and often requires clinical judgment to be characterized[159]. Due to the frequent nonspecific nature of complaints and insensitivities of

diagnostic studies, the clinician is forced to weigh the risk profile of any individual presenting with what may be considered Lyme disease. This includes the risk of tick exposure and the presenting symptom complex[109,160–165]. In this study, urinary OspA scoring was performed blinded to the patient diagnosis or clinical findings. After the urine OspA scoring was completed, the clinical data was unblinded. For this special group of previously treated patients under surveillance for persistent or recurrent LB, 41/100 were positive for urinary OspA C-terminal peptides (Figure 32; Supplementary Table 5). This percentage of patients with positive urinary OspA is in keeping with the range of seven previous studies conducted in endemic areas where patients were being evaluated for suspected Lyme disease: 7–31 % active disease and 5–20 % previous Lyme disease in endemic areas[166–168].

4.2.17 Use of HRP-labelled antibodies for Nanotrap-based immunoassays

HRP conjugation of a primary antibody allows for a direct detection of a target antigen without the need of a secondary antibody. As a consequence this would facilitate a quicker workflow as only one antibody is used and it would eliminate the chance of secondary antibody cross-reactivity (background might be reduced). An HRP labeling kit (Lightning-Link®) was used to enable the direct conjugation of Horseradish Peroxidase to the Anti-OspA monoclonal antibody (0551, Virostat). Two concentrations, 5ng and 0.5ng of OspA were loaded in parallel on a gel electrophoresis. The proteins were transferred onto a PVDF membrane. The first half of the membrane was incubated with the HRP-labelled primary antibody, the second half was incubated with the primary and the secondary antibody following standard procedure. Results showed that the signal intensity of the 31 kDa bands for the HRP conjugated antibody were comparable to the ones obtained using both primary and secondary antibody (Figure 52).

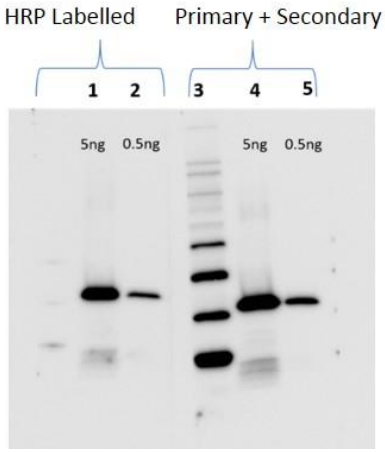

Figure 52. HRP-labelled primary antibody. Left) western blot performed using the HRP-labelled anti-OspA (0551 Virostat) antibody; lane 1, 5ng of Borrelia lysate; Lane 2, 0.5ng of Borrelia lysate. Right) western blot performed using primary and secondary antibody; lane 3, marker; lane 4, 5ng of Borrelia lysate; Lane 2, 0.5ng of Borrelia lysate. (Source: Magni, R. et al., 2015)

Anti-*Borrelia* polyclonal HRP-labelled antibodies, abcam, ab156277, abcam, ab20757, Thermo Scientific. PA1-27289, Virostat 0304against *Borrelia* Lysate were also tested and efficiencies were compared (Figure 53).

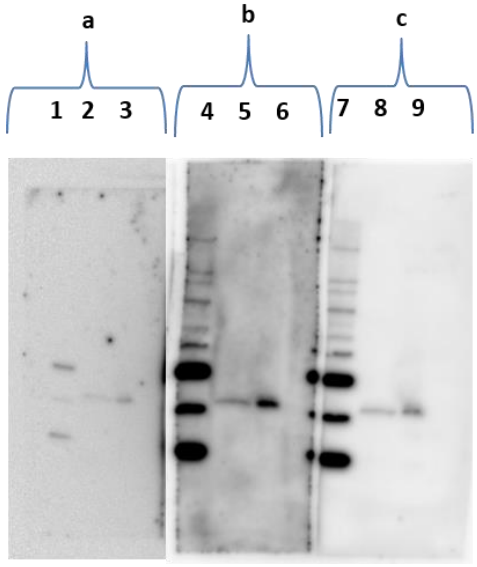

Figure 53. Detection of OspA with commercially available HRP-labelled primary antibodies against Borrelia Lysate compared to monoclonal anti-OspA antibody clone 0551 (s. Cruz). a) S. cruz 0551; lane 1, marker; lane 2, 10pg Borrelia lysate; lane 3, 100pg of Borrelia lysate. b) ; lane 4, marker; lane 5, 10pg Borrelia lysate; lane 6, 100pg of Borrelia lysate. c) Virostat 0304 lane 7, marker; lane 8, 10pg Borrelia lysate; lane 9, 100pg of Borrelia lysate.

Detection of *Borrelia* lysate spike-ins was proven to be successful also with these commercially available antibodies. Further analysis and concentration optimization is required. Also, because these are not monoclonal antibody directed specifically against OspA, more extensive cross-reactivity studies towards other antigens as well as interfering substances need to be performed.

4.3 NANOTRAP-ENHANCED ELISA TEST FOR LYME DISEASE

Western Blot is a labor intensive technique. An ELISA, on the other hand, can be easily scaled-up and results can be quantified, making it more suitable for clinical diagnostics. Nanotrap technology is agnostic to the downstream analytical method but, when transitioning from an immunoassay to another, several steps, including reagent selection need to be evaluated in order to maximize results.

4.3.1 Antibody optimization

We compared Virostat and Santa Cruz suppliers of the monoclonal antibody clone 551 used in our western blot test, which we have previously validated in terms of specificity, affinity, and conservation of antigen epitope across *Borrelia* species. Both Virostat antibody and S. Cruz antibodies were deposited on the ELISA plate in triplicate and incubated with 125pg of *Borrelia* lysate. Although the antibody clone is the same, the antibody commercialized by Virostat showed a far superior result probably because of the absence of gelatin in the preparation. Gelatin and other stabilizer used in commercial antibodies are in fact often found to be incompatible with ELISA (Figure 54).

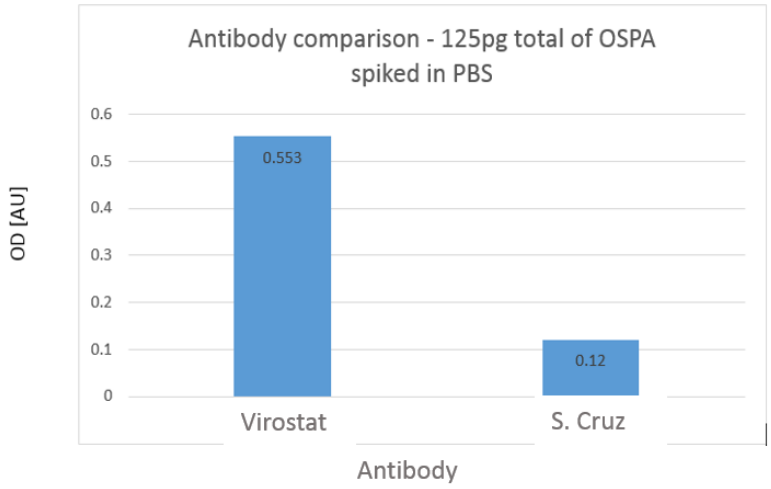

Figure 54. Optical density signal obtained with two different commercial sources of monoclonal antibody clone 0551. Antibody was used at the same dilution and Virostat was superior.

4.3.2 Elution buffers screening

The protocol used for Nanotrap processing of urine samples preceding the ELISA is identical to the one used for the western blot with the exception of the elution step. The elution buffer used for western blot contains SDS which can compete with the antigen for the binding to the antibody[169] and for this reason cannot be used in ELISA. 40 mL of urine were spiked with 100pg of Lyme antigen and processed with Nanotrap. To effectively remove the Lyme antigen from the Nanotrap, without affecting the antibody/antigen interaction, several detergents in different concentration were tested. A combination of 2% n-Octyl-β-D-thioglucopyranoside (OTG) and 0.5% n-Dodecyl β-D-maltoside (DDM) was proven to be the most successful (Figure 55).

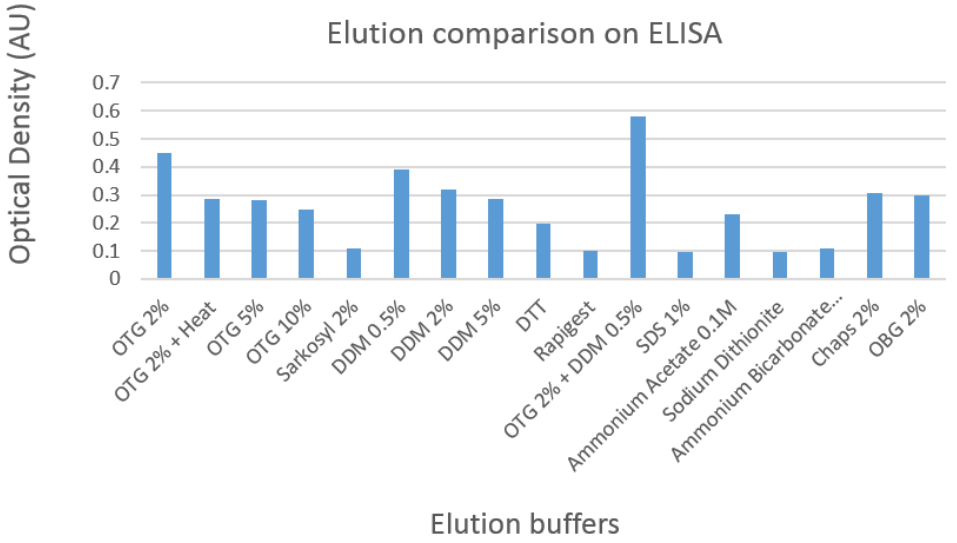

Figure 55. Elution efficiency of several elution buffers. Elution performance of several detergents was evaluated after Nanotrap processing of urine spiked with Lyme antigen. The combination OTG 2% and DDM 0.5% yielded the highest recovery of the antigen.

4.3.3 Linearity of the assay

40 ml urine samples in duplicate, spiked with 5pg/ml (total protein 200pg), 1pg/ml (total protein 40pg), 0.5pg/ml (total protein 20pg). Elution was performed and in parallel a dilution curve of the Bb antigen was produced spiking 2ng/ml, 0.4ng/ml, 0.2ng/ml directly into 100 µL of elution buffer. Lyme ELISA showed linearity in the concentration range 2,000 – 75 pg/mL. Nanotrap particle preprocessing shifts the linearity range of the assay to the concentration range 2 – 0.3 pg/mL, thus improving the effective sensitivity of >250 fold (Figure 56). A yield of 90% was achieved and verified by western blotting. Linearity was R2>0.98.

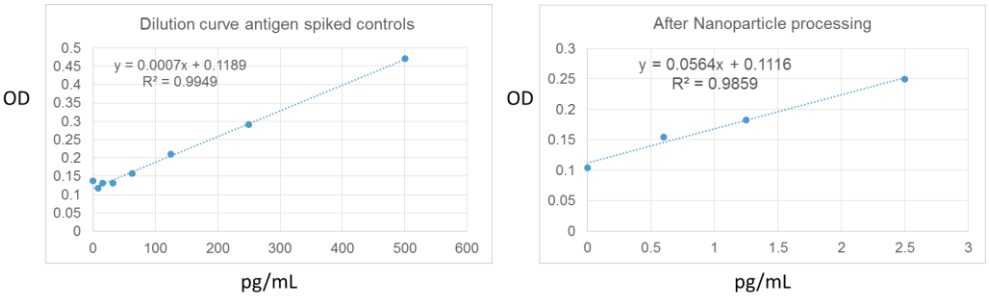

Figure 56. Linearity of the Nanotrap-based ELISA Test. ELISA is linear in the concentration range 2,000 – 75 pg/mL before processing. After Nanotrap processing we obtain a linearity range 2 – 0.3 pg/mL which means an increase in sensitivity of >250 fold.

4.3.4 Reproducibility

The inter assay reproducibility was assessed on three replicates performed by two independent operators in three different days. Lyme antigen was spiked in urine in four different concentrations (2.5 – 1.25 – 0.6 pg/ml – 0pg/ml); samples were processed with Nanotrap particles and analyzed with ELISA (Figure 57). The inter assay %CV was 2%.

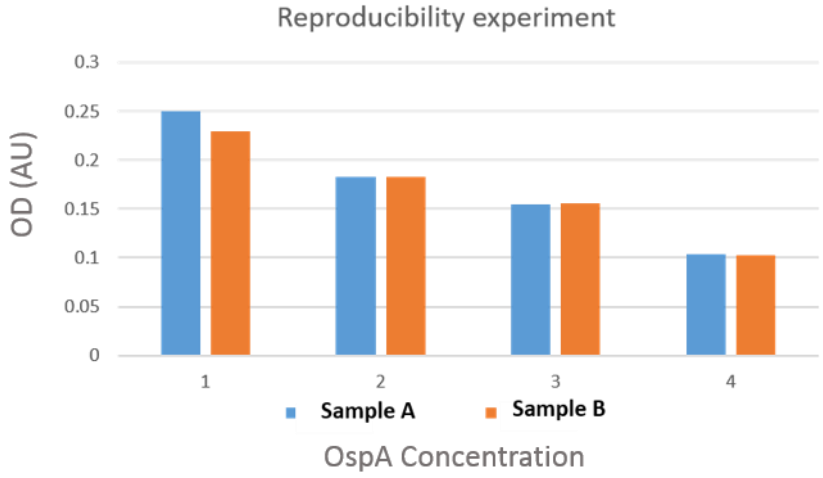

Figure 57. ELISA reproducibility experiment. Samples were spiked in duplicate with 4 different concentrations: 2.5 (1) – 1.25 (2) – 0.6 (3) -0 (4) pg/ml. Samples A and B were processed by two independent operators.

4.3.5 Lower limit of detection

Four concentrations 5-2.5-1.25-0 pg/ml of Lyme antigen were spiked in 40 ml of urine in triplicate, processed with Nanotraps and run on the ELISA. Data obtained were used to estimate the sensitivity of the assay. The lower limit of detection (LLD) was 0.3 pg/mL and the lower limit of quantitation (LLQ) was 2.9 pg/mL for a 40 mL urine sample input volume. (Background estimate = 0.128 AU, standard deviation (SD) = 0.0025 AU. LLD = background + 2*SD, LLQ = background + 10× SD; polynomial equation y = 0.0016x +0.1325, R2 = 0.9984, was used to estimate the corresponding x value (0.3 pg/mL and 2.9 pg/mL, respectively))

4.3.6 Detection of OspA in early stage Lyme patients with clinical evidence of Lyme disease and positive for western blot

In order to evaluate the performance of our ELISA test, a preliminary set of patient samples were selected. All the samples were previously collected, processed and run on the western blot. The set consisted of 10 control samples collected from healthy volunteers, 4 negative patients with high background and non-specific bands, and 3 positive patients. No controls or negative patients resulted positive for the ELISA, while the 3 positive patients according to the western blot were also positive for the ELISA (Figure 58). Positive samples showed an OspA concentration ranging between 0.36 pg/ml and 7.31 pg/ml (Figure 58). A larger number of samples following CAP CLIA regulations will be further analyzed in order to evaluate the possibility to transition from western blot to ELISA.

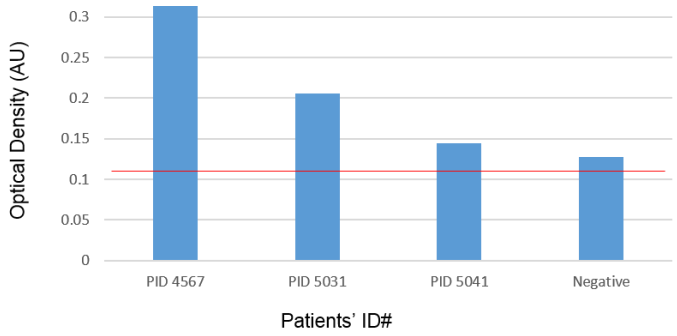

Patients	AU	Estimated Total OspA (pg)	Estimated OspA [pg/ml]
PID 4567	0.336	292.95	7.31
PID 5031	0.2055	91.25	2.28
PID 5041	0.144	14.37	0.36
Negative	0.116	N/A	N/A

Figure 58. ELISA test on patient samples. Optical density measured at λ~450 in patients previously diagnosed as positive (PID 4567, PID 5031, PID 5041) and a healthy volunteer (negative) for the Nanotrap western blot antigen test. While positive samples scored higher than the LLD of the assay, the negative samples scored below the LLD even though the signal rises slightly above the background. Estimated concentration of OspA in the patients resulted to be within the 0.36-7.31pg/mL range.

4.4 NANOTRAP ENHANCED LFA TEST FOR LYME DISEASE

4.4.1 Nanotrap size increases after reducing treatments

In parallel to the development of an ELISA test we are investigating the possibility to develop a novel low-cost and sensitive lateral flow assay (LFA), a format ideal for point of care applications in which the antigen is detected directly on the particles by the biorecognition molecules on the nitrocellulose membrane of the assay. Because of the meshwork-like structure of our Nanotraps the internal surface area vastly exceeds the superficial surface. Because the 3D structure and the pore size of the Nanotraps depend on the amount of cross-linker, incorporating a degradable cross-linker can effectively open up the Nanotrap and display the captured

analyte without the need of an elution buffer. N-isopropylacrylamide (NIPAm) Nanotraps were synthesized via dual cross-linking (degradable N,N'-(1,2-Dihydroxethylene)-bisacrylamide [DHEA] and nondegradable N,N'-methylenebis(acrylamide) [BIS] crosslinkers, and then functionalized with Remazol Brilliant Blue dye. DHEA can be degraded through an oxidizing reagent, $NaIO_4$, causing an increase in the particle pore size that allows the antibody in the LFA to directly access the antigen captured by the particles. Light scattering analysis of degradable Remazol brilliant blue Nanotraps before DHEA degradation show an average diameter of 987 ± 16.01 nm while after degradation the diameter increases to 1119.2 ± 40.87 nm.

4.4.2 Dot-blot for *in-situ* recognition of OspA

100µL of Remazol Brilliant Blue functionalized degradable Nanotraps were used to process 500 µl of urine sample spiked with 10ng of OspA. After antigen capturing the Nanotraps were exposed to $NaIO_4$ centrifuged and resuspended in 20 µl of water. A serial dilution of the Nanotraps containing OspA and empty partially degraded Nanotrap (negative control) as well as OspA (positive control starting from 1ng) were then spotted (5µL) on a nitrocellulose membrane and dot blot was performed. A strong signal in the presence of the partially degraded Nanotraps containing OspA can be visualized on the dot-blot thus showing the ability of the antibody to access the captured Lyme antigen directly on the Nanotrap following crosslinker dissociation; only a faint background signal is visible in the presence of empty Nanotraps (negative control) (Figure 59).

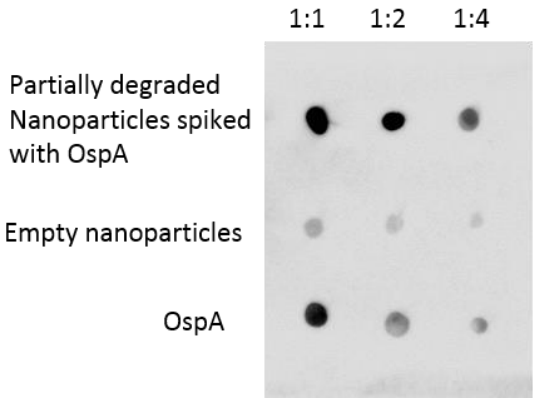

Figure 59. Partially degradable Nanotraps are able to successfully capture and display OspA in solution. The antigen retains the capability to bind to the antibody when it is bound to the affinity probe incorporated in the Nanotrap after oxidation. The negative control of oxidized particles in the absence of antigen shows only a faint background signal.

4.4.3 Assessing recovery and OspA capturing through western blot

OspA spiked urine samples were processed with degradable Nanotrap and capturing performance before and after degradation was assessed with western blot. Complete depletion of the supernatant as well as full recovery of OspA is obtained with DHEA Remazol Nanotraps. Nanotrap oxidation does not affect the antigen and the band intensity relative to OspA is comparable in Nanotraps before and after oxidizing treatment (Figure 60).

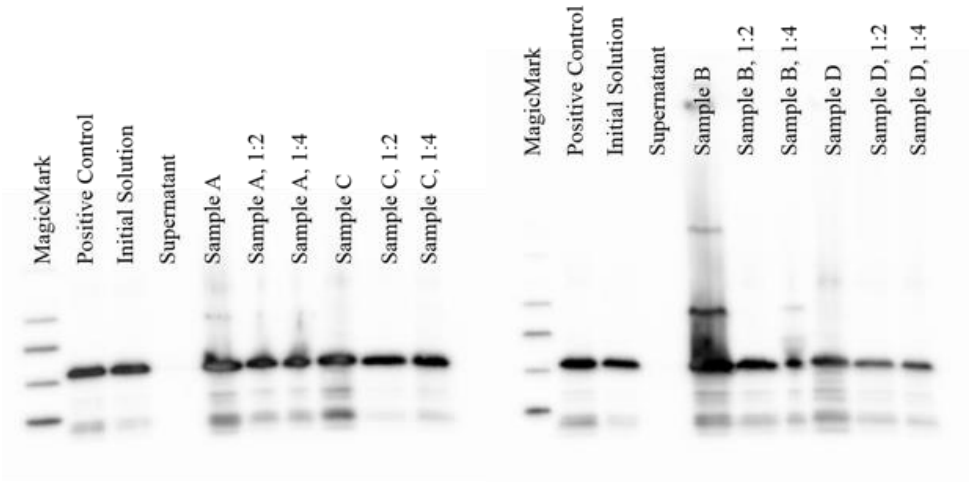

Figure 60. Western blot directed against OspA using degradable Nanotraps. The first gel was loaded left to right as follows: molecular weight maker, positive control, initial solution, supernatant, sample A (non-oxidized particles), sample A diluted 1:2, sample A diluted 1:4, sample C, sample C (oxidized particles), sample C diluted 1:2, and sample C diluted 1:4. The second gel was loaded left to right as follows: molecular weight maker, positive control, initial solution, supernatant, sample B (non-oxidized particles), sample B diluted 1:2, sample B diluted 1:4, sample D, sample D (oxidized particles), sample D diluted 1:2, and sample D diluted 1:4. Supernatant is depleted. Recovery of OspA is obtained before and after oxidation.

4.4.4 Development of NANOTRAP-BASED Lateral Flow Immunoassay

Remazol Brilliant Blue partially degradable Nanotraps were incubated with urine spiked with OspA. After processing the Nanotraps were placed on a lateral flow device previously treated with PEG blocking solution and where an antibody line (anti-OspA) was manually spotted. The membranes were then checked for the presence of an antibody line (Figure 61). The Nanotraps incubated with OspA were shown to quickly flow through nitrocellulose membranes to the adsorbent pad at the end of the strip. The Nanotraps then successfully bound primary OspA antibody spotted directly on the membrane, producing a visible test line on the lateral flow strip.

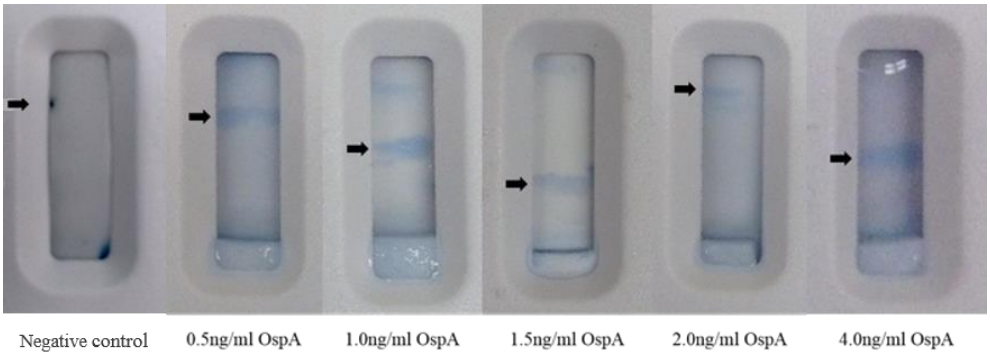

Figure 61. Lateral flow assay with partially degradable Nanotraps. Lateral flow assays conducted with poly(NIPAm-DHEA-Remazol Brilliant Blue R) Nanotraps pre-incubated with varying concentrations of OspA (from left to right: negative control, 0.5ng/ml, 1ng/ml, 1.5ng/ml, 2.0ng/ml, and 4.0ng/ml) and run through nitrocellulose membranes blocked with PEG (500 mg in 10ml water). Arrows indicate test lines where the OspA primary antibody was spotted directly on to the membrane prior to blocking and the antigen sequestered by the Nanotrap bound to it.

In the future, characterization of the test in terms of sensitivity and reproducibility will be performed. Further optimization of the test will include pre-treating the membrane with a surfactant to improve the wicking rate of the nitrocellulose membrane and the overall sensitivity of the assay.

4.5 NANOTRAP-ENHANCED MULTIPLE REACTION MONITORING FOR THE DETECTION OF LYME DISEASE

4.5.1 Selection of new panel of *Borrelia burgdorferi* antigens

In order to further improve the specificity of our antigen test, the detection of a panel of *Borrelia* proteins indicative of an active infection instead of a single protein would be ideal. Mass-spectrometry analysis of *Borrelia burgdorferi* lysate was performed. After label free spectral counting (scaffold analysis) of the LC-MS/MS results, a total of 241 NCBI annotated proteins were identified (Supplementary Table 7). OppA, OspB, OspC, OspA, p66, FlaB, BmpA, FliL,

Rev, DbpA, VISE, BmpB were selected, based on their importance in different stages of the disease, as candidates for a Lyme disease panel for a future Nanotrap-based assay (Table 1).

Name	Symbol	Function	Timing of serology appearance
Oligopeptide permease periplasmic binding protein	**OppA**	*Peptide transport system, (spirochetal chemotaxis, tissue penetration ?)*	Early
Outer surface protein B	**OspB**	*Bb induced immune tolerance, induction of inflammation, host immunologic recognition*	Late (arthritis)
Outer surface protein C	**OspC**	*Transmission and infection of host*	Very early
Outer surface protein A	**OspA**	*Bb induced immune tolerance, induction of inflammation, host immunologic recognition*	Very early and late
integral outer membrane protein p66	**p66**	*Porin, adhesin*	Early
flagellin protein (p41)	**FlaB**	*motility*	Early
membrane lipoprotein BmpA	**BmpA**	*Binding to host extracellular matrix components including Laminin*	Early and Late (arthritis)
flagellar basal body-associated protein	**FliL**	*Motility, chemotaxis*	Early
Borrelia burgdorferi REV protein	**Rev**	*Fibronectin binding protein, adaptation to host physiological stimuli (pH and temperature)*	Early and up to 12 mos
Decorin binding protein	**DbpA**	*Adhesion to host cell*	Early
vmp-like sequence	**VISE**	*colonization, dissemination, adherence, and evasion of host immune systems*	Early and late
membrane lipoprotein BmpB	**BmpB**	*Adhesin*	Late (arthritis)

Table 1. Selection of clinically relevant biomarkers for different stages of Lyme disease from mass-spectrometry analysis of B. burgdorferi lysate.

Current instrumentation allows for the measurement of many proteins in a single sample, making MRM an ideal assay to perform high-throughput measurements on a panel of target proteins[170,171]. Successful application of the MRM assay for detection of *Borrelia* proteins in human skin biopsies has been recently reported[144], however, direct MRM assay in human blood or serum for early detection of Lyme disease poses additional challenges due to the extremely low abundance of total circulating *Borrelia* proteins. Preliminary results obtained separating bacterial membrane vesicles from the blood of individual affected by Lyme disease through high-speed centrifugation suggested the possibility to use MRM detection for *B. burgdorferi* infection[172]. Although MS MRM is a powerful and absolutely specific method for multiplex protein quantification, it has low sensitivity (50

ng/mL)[173]. Our Nanotrap technology, has already proved to be able to enhance sensitivity for MRM that ranges from 100 fold to 1,000 fold depending on the input volume[50]. Because of the versatility of Nanotrap different downstream assays can be coupled with Nanotrap processing with minor modification of the sample processing protocol. In our case, several elution buffers were tested in order to find the optimal condition in compatibility with mass-spectrometry.

4.5.2 Assessing Elution Efficiency with degradable surfactants that are compatible with mass spectrometry analysis

Several surfactants, that have proven to be valuable elution buffers to extract proteins from Nanotraps, are not compatible with mass-spectrometry. For this reason we selected a reversible detergent (RapiGest SF surfactant, Waters) that we have shown to solubilize and liberate the pathogenic protein, but will not interfere with mass spectrometry.

RapiGest SF helps solubilize proteins making them more susceptible to enzymatic cleavage without significantly inhibiting enzyme activity and is heat stable for higher temperature digestions. RapiGest SF is compatible with enzymes such as Trypsin, PNGase F, Lys-C, Arg-C, Asp-N, Glu-C and other enzymes. This reagent is easily removed after use allowing MALDI-TOF MS, LC or LC/MS analyses of digested samples. Rapigest SF can be easily hydrolyzed in acidic solution; its half-life is 8 min. at pH 2 and 60 min. at pH 3 (Figure 62).

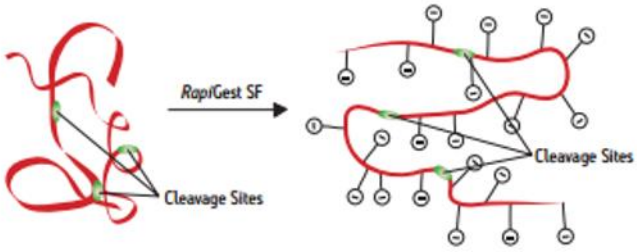

Figure 62. RapiGest SF hydrolyzes in acidic solutions. (Source: Waters, http://www.waters.com/waters/en_US/Home/nav.htm?cid=1000941&locale=en_US#FACETED_NAVIGATION&locale=en_US)

40 mL of urine spiked with 2.5, 5, 10, 25, 50 and 100 pg/mL of *Borrelia* lysate in duplicate. Samples were incubated with the Nanotrap particles, washed according to the patient processing sample (page X). One set was eluted with 20ul of 2 X sample buffer (5% TCEP) and western blot was performed. The other set was eluted 20µl of 1% Rapigest in 50 mM ammonium bicarbonate. Elution were acidified with 0.1% TFA in order to degrade the surfactant. Samples were reduced, alkylated and trypsinized and zip-tip processing was performed before loading them on the mass-spectrometer.
OspA was monitored for peptide GYVLEGTLTAEK using precursor 640.84 $^{2+}$ and transitions 719.40, 848.43, and 961.52 (Figure 63). Another protein. OspB, which is supposed to have an important role in the pathogenesis of the disease was monitored for peptide ATIDQVELK using precursor 508.78 $^{2+}$ and transitions 422.74, 731.40, and 844.48 (Figure 63). Results were analyzed using Skyline (Univ. of Washington) and reported as the area under the curve for transition 961.52 from peptide GYVLEGTLTAEK and transition 844.48 from peptide ATIDQVELK. Peptides GYVLEGTLTAEK (OspA) and ATIDQVELK (OspB) were detectable down to 5pg/mL and 10pg/mL, respectively. In addition, both peptides demonstrated excellent linearity across the entire concentration range up to 100pg/mL, with an R^2 of 0.9941 for peptide GYVLEGTLTAEK, and an R^2 of 0.9883 for peptide ATIDQVELK.

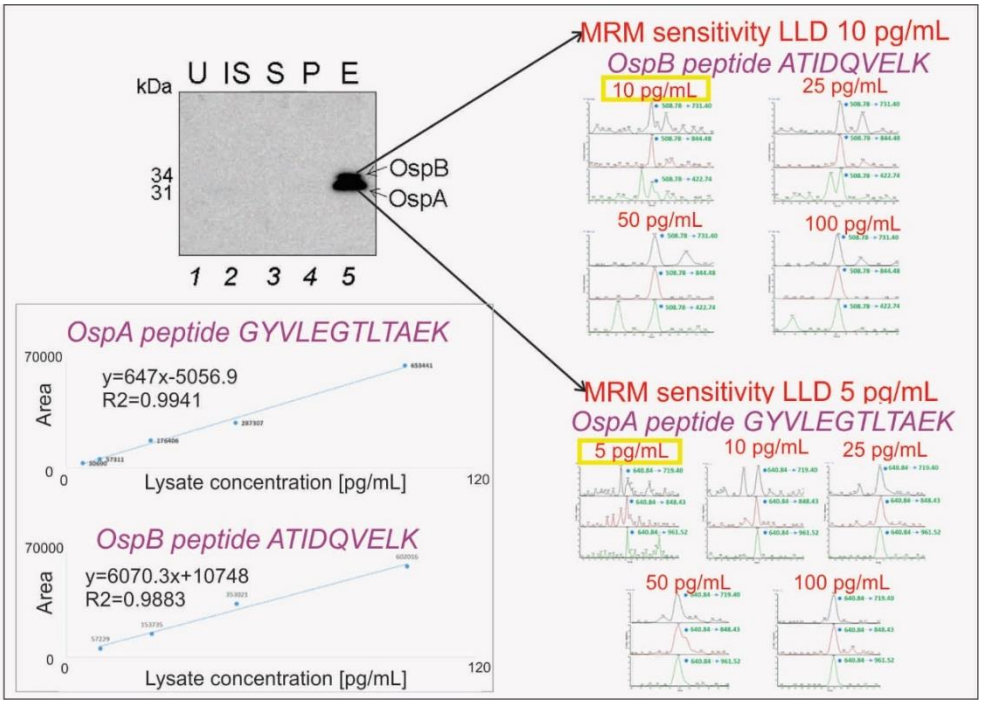

Figure 63: MRM sensitivity and linearity for nanotechnology enhanced MRM bacterial antigen test in urine (Lyme disease). Upper Left: western blot analysis showing OspA and OspB proteins in the bacterial lysate. U=urine negative control, IS=initial solution urine containing OspA and OspB spike ins, S=supernatant after Nanotrap incubation, P=Nanotrap particle pellet after protein elution, E=Nanotrap eluate. Upper and Lower Right: mass analysis of OspB and OspA specific transition ions. Minimum detectable concentration in human urine is 10 and 5 pg/mL, respectively. Lower Left: Linearity of the MRM assay is R^2 = 0.9941 and 0.9883 for OspA and OspB specific transition ions respectively.

In order to expand the panel of *Borrelia* antigens that could be detected in patients' urine, other proteins relevant in the first stage of the disease and previously identified by Mass-spectrometry in the *Borrelia* lysate (supplementary table 7) will be investigated with the MRM. Aminopeptidase will be monitored for peptide GADSNFLSEVLER using precursor 718.85 $^{2+}$ and transitions 1106.58, 992.54, 845.47, 732.38, and 645.35 (Supplementary table 8). P34 will be monitored for peptide

YEDLINPIEPIIPSESPK using precursor 1027.53 $^{2+}$ and transitions 1533.85, 1420.76, and 1306.72. FLiL will be monitored for peptide LALGYAENNVNELGR using precursor 816.92 $^{2+}$ and transitions 1115.54, 1044.50, and 915.46. p66 will be monitored for peptide NTNNAAIGSAFLQFK using precursor 798.41 $^{2+}$ and transitions 1152.64, 1081.60, 1010.56, 897.48, 840.46, 753.42, and 682.39. OppA will be monitored for peptide SWNISEDGIIYTFNLR using precursor 964.48 $^{2+}$ and transitions 1211.64, 1096.61, and 1039.59. BmpA will be monitored for peptide IGFLGGIEGEIVDAFR using precursor 846.95 $^{2+}$ and transitions 1375.72, 1262.63, 1205.61, 1148.59, 1035.51, 906.46, and 849.44. Flagellin will be monitored for peptide NSTEYAIENLK using precursor 641.31 $^{2+}$ and transitions 1080.55, 979.50, 850.46, 687.40, and 503.28.

5. DISCUSSION

5.1 HYDROGEL NANOTRAPS ENHANCE THE DETECTION OF LOW-ABUNDANCE BIOMARKERS

Biological fluid samples are thought to contain low-abundance proteins and peptides which can provide a rich source of information regarding the state of the organism as a whole. Peptidome/LMW proteome is an important source of disease-specific information for the early detection of several diseases, for a better diagnosis and prognosis and for monitoring drug toxicity, and drug abuse. The detection of novel clinically relevant protein biomarkers in body fluids represents a huge challenge because of the complexity of the circulatory proteome, the low concentration and the lability of the candidate biomarkers. Important diagnostic biomarkers may exist in extremely low concentration in blood and other bio-fluids. For example early-stage diseased tissue, such as pre-metastatic cancer lesions, may constitute less than a few cubic millimeters and biomarkers shed into the circulation from such a small tissue volume will become highly diluted in the entire blood volume. Early stage infections may also be difficult to detect because the disease agent may not have reached a sufficient titer in the host and its level will fall below the detection limit of mass spectrometry and conventional immunoassays. Furthermore low abundance biomarkers/proteins are masked by the presence of high abundant proteins such as albumin and immunoglobulin and they are susceptible to degradation by endogenous and exogenous proteinases following venipuncture and sample transport/storage.

Hydrogel Nanotraps represent a powerful tool that can be used to facilitate biomarker research. The novel aspect of dye-functionalized Nanotraps is their ability to perform both an affinity capture and a size exclusion chromatography in one step in solution, allowing to capture and concentrate

low abundance analytes. Depending on the goal of the study, unbiased biomarker discovery or affinity capture of a target analyte, different affinity "baits" - that show preferential affinity with selected classes of proteins - can be easily incorporated into the core of the Nanotraps. The ability of the Nanotraps to capture and concentrate biomarkers from several mL of biofluids while excluding all of the high abundance resident proteins such as albumin and immunoglobulins, provides a concentration step that is equivalent to injecting several mL of sample into a gel electrophoresis or mass-spectrometry at once, thus dramatically increasing the detection sensitivity of the assay and allowing to measure previously invisible proteins. In this study we evaluated the application of hydrogel Nanotraps for the capturing of *Borrelia* antigens in urine with the final goal to create the first highly sensitive urinary antigen test for the detection of Lyme disease. In this study, the Nanotrap pre-processing step was successfully coupled to western blot analysis, ELISA, lateral flow immunoassay and MRM to perform a qualitative screening for the presence of the bacterial antigen in solution, allowing the detection of *Borrelia* antigens present in urine in concentrations as low as 0.3pg/ml.

Optimization of sample processing parameters prior to testing patient specimens is mandatory. An optimum ratio of Nanotraps to sample volume needs to be established. A dose-response curve using recombinant proteins is also necessary to determine the limits of detection of particular analytes. Differently functionalized Nanotraps as well as different elution buffers were thus tested in this study in order to determine the ideal Nanotrap for harvesting of Lyme antigens in the given specimen.

In order to avoid the use of an elution buffer and allow the *in-situ* recognition of the antigen bound to the Nanotraps by an antibody a novel prototype of partially degradable Nanotraps have been successfully synthesized. Cross-linkers such as Dihydroxyethylenebis-acrylamide (DHEA),

bis(acryloyl)cystamine (BAC), 1-(4-Sulfophenyl)-3-methyl-5-pyrazolone and Fast blue 221 allow the formation of hydrogel Nanotraps that could be partially degraded under certain chemical conditions resulting in an increase in the diameter and pore-size of the Nanotrap which allow high molecular weight proteins like immunoglobulins to access the antigen on the Nanotrap itself.

5.2 OSPA MONOCLONAL ANTIBODY SPECIFICITY

In this study, the specificity of the mAb clone 0551 used in the Nanotrap test was verified in three ways: (1) peptide competition and immune affinity depletion, which revealed absolute specificity for a narrow C-terminus sequence of OspA that was conserved in all the *Borrelia burgdorferi sensu latu* species. (2) Viral and bacterial lysates of HSV, EBV, HCV, CMV, *Babesia*, and *Bartonella* tested at the same antigen concentration as the OspA *Borrelia* antigen were devoid of immunoreactivity with the mAb clone 0551 and did not interfere with the recognition of OspA. This was done using the entire Nanotrap concentration system with test antigens spiked in human urine. (3) BLAST sequence analysis of HSV, EBV, HCV, CMV, *Babesia*, *Bartonella*, Rickettsias, human genome database and other non *Borrelia* spirochetes showed no significant similarity with the defined and verified C-terminus OspA epitope domain. It's important to note that the specific domain recognized by the mAb clone 0551 is OspA236-239. This region is quite distant on the OspA molecule from the region that was shown in the past to have sequence similarity with human proteins (OspA154-173 = GSGKAKEVLKGYVLEGTLTA[174]). Based on the conservation of the epitope OspA236-239, the specificity of our test should extend to all the pathogenic *Borrelia* species in the US and Europe (Table 2). In the future, it will be important to verify the sensitivity and specificity obtained in this study to geographically diverse populations. Previously published attempts to

measure Bb proteins and nucleic acids in urine[175,176] may have been compromised by enzymatic degradation and lack of specificity of the diagnostic epitope. The Nanotrap particle technology used in this study has been previously shown to protect the captured analyte from degradation, including nucleic acids[39,177].

5.3 SHEDDING OF OSPA PROTEIN IN THE URINE OF PATIENTS WITH A DIAGNOSIS OF EARLY STAGE LYME BORRELIOSIS

A highly sensitive urine antigen test has potential utility in the management of Lyme disease. A direct antigen test for the bacteria, instead of a serologic test, offers a mean to detect the infection before the immune response is mounted. Because previous immunoassays for the detection of bacterial proteins in the patient's urine have been judged unreliable due to inadequate sensitivity several question remained unanswered.

The goals of the study were to answer the following questions: Is Bb OspA antigen shed in the urine of patients with LB at early stage disease prior to the development of a positive serology? What is the urinary OspA concentration range? Is the OspA antigen containing the C-terminus epitope shed into urine as a full length protein or as fragments? Does the presence of OspA in the urine of a patient with an EM rash suspected of having LB correlate with the concurrent or later development of positive serology (western blot or ELISA)? If urinary OspA is present prior to antibiotic therapy, is it reduced or absent after successful therapy (resolution of symptoms)? What percentage of patients suspected of having persistent or recurrent LB contain urinary OspA C terminal domain antigen?

Borrelia OspA plays a central role in the survival of the spirochete in the tick vector[139]. During the initial phases of a cutaneous infection following a tick bite, OspA is recognized by innate immune cell Toll-like receptor TLR2, and together with TLR8, initiates a cascade of proinflammatory cytokines, such

as interleukin 1 and T-helper derived cytokines that are thought to mediate the initial inflammatory reaction[179]. OspA is upregulated in response to inflammatory cues by host-adapted Bb later in the course of disease[180–182]. In previous studies, specific complexed antibody to whole Bb and recombinant OspA were detected in 10 of 11 of the EM positive patients compared to 0 of 20 endemic area controls[103]. IgM was the predominant isotype recognizing OspA in these EM patients. Free IgM to OspA was found in half the EM cases. IgM to OspA was also detected in 10 of 10 European patients with EM who also had reactive T cells to recombinant OspA[103]. In longitudinal studies of serial serum samples from untreated patients (collected prior to the use of antibiotic therapy for Lyme disease treatment), elevation of IgG reactivity to OspA parallels the rising of the antibody response to Bb proteins[183,184]. Animal models have shown that *Borrelia* antigens are shed into the urine following infection[145]. For example in early studies of *Borrelia* infection of mice in the wild, 76% of 50 mice (white-footed mice *Peromyscus leucopus*) shed *Borrelia* antigens, including OspA, into the urine[145], although the timing of the antigen shedding over time and the relative nanomolar concentration of different *Borrelia* proteins was not determined due to the nature of the assay and its sensitivity limits. In keeping with animal model studies, OspA antigen shedding prior to antibiotic treatment occurred in the urine of 24/24 patients with a positive EM rash and clinical symptoms of LB (Table 4). In contrast, none of 117 untreated patients who were non symptomatic, or were non symptomatic and concurrently serology negative for LB, shed urinary OspA C-terminal antigen.

5.4 OSPA ANTIGEN IS SHED INTO URINE EITHER AS A FULL LENGTH PROTEIN, OR AS A FRAGMENT CONTAINING THE C-TERMINUS DOMAIN

Pepsin fragmentation, followed by mass spectrometry sequencing and

synthetic peptide competition, identified the anti-OspA mAb binding domain to reside in the C-terminus region of OspA (Figure 32, Supplementary Table 3). In previous studies, IgG titers to OspA (and to a lesser extent, OspB) in untreated patients [103] correlate directly with severity of chronic Lyme arthritis, while IgG titers to the C-terminal third of OspA (OspA168–273) correlate with both severity and duration, suggesting the strongest causal link with epitopes contained within this fragment[184]. The C-terminal quarter of OspA (218-273) is also highly conserved among a large number of pathogenic species of *Borrelia* sequenced to date[146,147]. The specific C-terminus peptide sequence (Supplementary Table 3) of the antigenic epitope showed no sequence homology with any human protein and did not have any sequence homology with non-*Borrelia* spirochetes. The size of the OspA antigen shed into the urine in the present study (Figure 48) was close to the expected size of the full length OspA protein (approximately 31kDa) which is small enough to be filtered through the kidney glomeruli. In some cases fragments of OspA containing the C-terminus fragment epitope were detected below the size of 31 kDa. The existence of these fragments may indicate *in vivo* degradation of the antigen, since we have established that Nanotrap particle capture fully stabilizes the captured analyte and prevents enzymatic degradation[29,50,185].

5.5 CORRELATION OF URINARY OSPA PROTEIN WITH POSITIVE LYME BORRELIOSIS SEROLOGY AND PERSISTENCE OF SYMPTOMS

The clinical diagnosis of acute early stage LB is often based on the history of deer tick exposure and clinical evaluation of skin lesions. Unfortunately the skin lesion appearance can be quite variable and the differentiation from arthropod bite reactions, gyrate erythemas and other erythematous skin conditions can be difficult. In 10% of infected patients LB is not considered and many patients are misdiagnosed (in one study 37%[177]). The literature is

mixed in relation to the incidence of Erythema Migrans in acute Lyme disease, ranging from as low as 25%[186] to as high as 80%[127]. This potentially means that a substantial number of individuals presenting with acute Lyme disease will not manifest EM rash but perhaps only nonspecific "flu-like" symptoms. In fact, Feder stated that "patients from Lyme disease endemic areas who have fever and fatigue, especially within a month following a deer tick bite, should be considered for empiric antibiotic therapy for early localized Lyme disease", regardless of whether an EM rash is present[185]. The technology we are presenting may provide additional objective information to assist the clinical diagnosis and to monitor antigen shedding during the course of therapy. A potential value of the urinary assay reported in this study is the evaluation of whether an initial course of therapy is sufficient to eradicate the infection. In 1994 Shadick *et al.*[164] evaluated 38 adult patients diagnosed with Lyme disease, having fulfilled established serologic criteria at the time of the study. Initial antibiotic treatments ranged from 10 to 21 days of a standard regimen. Ten of 38 patients with Lyme disease reported relapses within 1 year of treatment (fatigue, persistent arthritis or arthralgias, headaches, or difficulty with memory and concentration). In 2014, Aucott, *et al*.[187] assessed the clinical response of 77 individuals presenting with an acute EM rash and completing a standard 3 week course of doxycycline. After 6 months, 39 % of this group had persistent functional impairment and/or persistence of new symptoms felt to be related to the acute infection. In 1999 Oksi *et al*. reported the clinical relapses of disseminated LB confirmed by culture and PCR, with various clinical presentations such as arthritis, neuropathy and uveitis[163]. Potential mechanisms contributing to this persistence of *B. burgdorferi* in human[163] and animal models[188–191] have been identified. These include: immune evasion via physical seclusion of Bb within immunologically protected tissue sites such as the CNS, joints and eyes[99,190–192], collagen-rich tissue[191], cells[193], and biofilms[194]; alterations in Osp profiles

through antigenic variation[195–198], phasic variation[183], and alteration in Bb morphology (including cell-wall deficient forms, spherocytes and 'cyst' forms)[132,199–205]; immune modulation via alterations in complement[206–208], neutrophil and dendritic cell functioning[209,210], and changes in cytokine and chemokine levels[211–213] and innate antibiotic tolerance of some *B. burgdorferi* populations[214]. Theoretically, Nanotrap technology would have the capacity to determine which, if any of these individuals had perpetuation of their symptoms due to ongoing infection. Antibodies specific to *B. burgdorferi* proteins can take[61] three to four weeks to develop, and early stage Lyme disease, prior to the appearance of a serologic titer, is extremely difficult to diagnose due to the low sensitivity of current diagnostic tests for *B. burgdorferi* antigen. For this reason, treating physicians worry that Lyme serology is unreliable for early stage disease because the development of antibodies differs widely, especially in the early stages of the infection[126,215]. In prior studies[177], only 43 % had a positive serology at the time of cutaneous EM positive LB diagnosis. Thus, the inflammatory reaction manifest in the border of the LB EM rash contains proliferating spirochetes and the inflammatory infiltrate is the result of innate immune recognition of OspA. By definition it would be expected that OspA protein antigen would be shed into the circulation and be concentrated in the urine for a significant time period prior to the development of a positive serology with 5 IgG bands as specified under CDC guidelines[126]. Prior to antibiotic treatment, in this study, 24/24 patients with an EM rash contained OspA protein in the urine, verified by peptide competition. Our analysis was blinded to outcome. Based on the sensitivity and dose response of the assay, the concentration range was between 1.7 and 30 pg/mL. 5 of these 24 early stage patients were serology negative and 3 had an equivocal serology at the time of urine collection and clinical diagnosis. Following antibiotic therapy of patients with a clinical diagnosis of LB, 10/14 patients with a positive serology were found to be

positive for urinary OspA in this study. Following antibiotic therapy for a clinical diagnosis of LB, 10 patients in this study were serology negative. 4/10 of these post-treatment patients were negative for urinary OspA. Importantly, for 10 patients who exhibited persistence of the EM rash during the course of antibiotic therapy, 10/10 were positive for urinary OspA. In contrast 4/10 of these same patients who had the EM rash during antibiotic therapy ultimately became serology positive. Urinary OspA measurement of 8 patients for whom the therapeutic response was judged complete (absence of EM rash and absence of symptoms) following antibiotic therapy revealed that all 8 patients switched from being urinary OspA positive to urinary OspA negative (Table 4). 4 of these 8 patients were subsequently found to be serology positive for Bb infection. These data are in keeping with the correlation of urinary shed of OspA and the presence of concurrent objective symptoms (EM rash). When CDC criteria serology, and in accord with the Infectious Diseases Society of America (IDSA), was compared to urinary OspA regardless of pre or post treatment status of early stage LB, 87.5 % of serology positive were also urinary OspA positive and 88 % of serology negative were also urinary OspA negative (Chi squared p value = 4.072e−15; significance level = 5 %, power = 99.99 %, Table 5). The remaining 12 % of patients who were urinary OspA positive who were serology negative demonstrated positive symptoms qualifying for clinical diagnosis of LB and may not have yet mounted an antibody response. In this study, 100 % of pre and post treatment samples that had active symptoms were found to be positive for detectable urinary OspA (40/40, Table 4). Urinary OspA outcome (positive) was significantly associated with presence of clinical symptoms (EM rash, Chi squared p value <2.2e−16; significance level = 5 %, power = 100 %). Of these 40 patients, 22 were serology positive by CDC standards for early stage disease[144]. This is in keeping with prior studies showing positive serology in approximately 50 % of early stage cutaneous LB

patients[177]. Early prompt treatment of LB is known to blunt the serology response because the infection and immune response is being interrupted at an early stage[216,217].

5.6 URINARY OSPA IN PATIENTS SUSPECTED OF HAVING "CHRONIC" LB

Lyme disease is too often diagnosed after the infection is well established and the patient has raised an antibody titer against the bacteria B. burgdorferi[218]. Persistent LB, treatment resistant, recurrent, or a new LB is also extremely difficult to diagnose when the serologic titer is equivocal or if the patient has persistent symptoms (e.g. neurologic, arthritic, or dermatologic) in the face of therapy. Unfortunately patients with clinical history of LB (serology positive or serology inconclusive) can present with articular and neuromuscolar symptoms. Lack of response to treatment can theoretically be due to persistence of infection via one or more mechanims already discussed, such as sequestration in tissue or biofilm. Given the polymicrobial nature of tick borne illnesses, infection with one or more different pathogens is a consideration[139,219–222]. On the other hand, persistence of symptoms has been postulated to be the result of a new LB infection, or perhaps to improper diagnosis of LB and unrelated co-existing musculoskeletal morbidity or to persistence of infection in a sequestered tissue such as joint cartilage[223], or biofilm[224]. In this study, we evaluated the level of urinary OspA protein in 100 previously or currently treated patients with joint, neurologic, and other objective symptoms (Supplementary table 2). This group of patients were being evaluated for the potential of recurrent or persistent infection with *Borrelia*. Our analysis was blinded to outcome. 41 of 100 (41 %) patients were positive for urinary OspA protein. This percentage of positive urinary OspA, assuming that it reflects a specific

infection by Bb that is shedding OspA C-terminal fragments, is in keeping with prior studies. Patients evaluated in endemic LB regions who presented with arthritis and neurologic symptoms were estimated to have active and prior LB (7–31 % active disease and 5–20 % previous Lyme disease in endemic areas[166–168]). IDSA and ILADS differ in their recommendations for the clinical assessment and treatment of persistent LB. A highly specific antigen test for *Borrelia* proteins might provide new class of evidence to refine the guidelines for diagnosis and treatment of LB. It is widely acknowledged that patients suspected of having chronic Lyme borreliosis based neurologic or joint symptomatology may not truly have Lyme borreliosis, or may have other tick borne diseases. Therefore in patients who are suspected of having chronic Lyme disease, as evaluated in the present study, there has not been a means to assess the true positive patients. Most, if not all, of these patients have a negative Lyme serology by the 2 tier criteria. Although we feel confident that a positive outcome of our test reflect the presence of an active *Borrelia* infection, our findings that 41 % of these "chronic patients" are positive cannot be defined as a level of sensitivity and specificity, since there is not an alternative mean beyond our test to assess that these patients could actually have had an active *Borrelia* infection. Importantly, our data provides the first antigenic evidence that at least 41 % of these patients may have an active Bb infection. Therefore these data contribute significant new information to the debate about chronic Lyme disease.

5.7 ALTERNATIVE FORMATS FOR THE DETECTION OF LYME ANTIGEN IN URINE: ELISA, LATERAL FLOW IMMUNOASSAY, AND MRM

Successful results have been obtained coupling Nanotrap processing with an ELISA assay, which permitted the detection of OspA at concentrations as

low as 0.3pg/ml starting from 40 ml of urine. 3/3 samples with clinical symptoms and positive on our western blot also resulted positive with ELISA. Clinical samples are currently received at George Mason University and are processed with Nanotraps and analyzed through western blot. A larger number of samples will be tested in parallel with western blot and ELISA, following CAP CLIA guidelines, in order to transition from a western blot to an ELISA format of the test with the goal of eventually outsource it to independent clinical laboratories. MRM coupled with Nanotrap processing of urine samples has also shown very promising results, allowing the detection of OspA in urine sample (40 ml) at a concentration as low as 5pg/mL. Although according to our data this would be sufficient to detect OspA in many infected patients, further optimization of the protocol will be necessary to lower the detection limit and reduce the number of potential false negatives. The development of a novel partially degradable type of Nanotrap allowed us to engineer a Lateral Flow Immunoassay that would serve the need of a point of care test. These Nanotraps after partial degradation are able to flow through a nitrocellulose membrane and expose the OspA cargo for the direct recognition by an antibody. Because of the intrinsic color of the functionalized Nanotraps, their immobilization due to the antibody recognition of the antigen will result in the formation of a colored line on the lateral flow immunoassay within seconds from the deposition of the Nanotrap on the device.

5.8 SELECTION OF NOVEL BIOMARKERS

Measurement of a panel of Lyme antigens in the urine of patients with different stage of Lyme disease, as opposed to a single antigen, is an important clinical goal for surveillance and monitoring of Lyme disease. Mass-spectrometry analysis of *B. burgdorferi* lysate allowed us to select a panel proteins that are well represented in the bacterial lysate and are

thought to benrelevant for human pathogenesis. According to different studies only few antigens are expressed by *B. burgdorferi* in very early infection such as FlaB, p66, RevA, oligopeptide permease A1 (OppA1), OppA2, and OppA4 [215,225,225–227], while OspC (25 kDa), VlsE, BBK32, FlaA (37 kDa), BmpA (39 kDa), FliL, BBG33, LA7, and DbpA proteins still appear in the early stage of infection although slightly later[125,127,228–233]. These antigens will be evaluated as potential candidate for our Nanotrap based immunoassay and MRM test.

6. CONCLUSIONS

Hydrogel Nanotraps covalently functionalized with combinations of molecular dye baits offer a one-step technology for biomarker harvesting, concentration, and preservation from degradation, with simultaneous exclusion of unwanted abundant molecules such as albumin and immunoglobulins. Nanotraps can be used to dramatically increase the chance of identifying and measuring proteins and peptides from complex biofluids such as blood, urine, CSF, sweat, saliva, vitreus and any biologic solution-phase sample. Our hydrogel Nanotraps have been used for biomarker discovery as well as for the development of new diagnostic tests. The results from this study indicate that bait loaded hydrogel Nanotraps are suitable to sequester bacterial proteins, such as Lyme disease *B. burgdorferi* antigen in urine and concentrate them in a small volume that can be analyzed by immunoassays or mass-spectrometry. Once captured and concentrated in the Nanotraps, the Bacterial antigen can be detected using immunoassays or MRM with an enhanced sensitivity, more than 400 fold starting from an initial volume of 40 mL of urine. Because of the significance of OspA in the pathogenesis of Lyme disease we focused on the synthesis and functionalization of Nanotraps that could capture this protein with high affinity and developed a western blot test that could target a particularly conserved C-terminal region of this protein. Our data support the hypothesis that urinary OspA protein fragments containing the C-terminal domain occur prior to the development of a full IgG serology response, and urinary OspA strongly correlates with a clinical diagnosis and active clinical symptoms (e.g. EM rash positive) of early stage LB. Because the C-terminal domain is conserved among most of the pathogenic species of *Borrelia*, our Nanotrap-based test can potentially be employed for the detection of Lyme disease in the Americas, Europe and Asia with a greater chance of success compared to

current serological tests that are mostly targeted towards US strains[129,130]. Thus, this technology has the potential to provide clarity in the settings of individuals at risk of tick exposure and acutely presenting with either an atypical EM rash or without a rash at all, but consistent with the nonspecific findings of acute Lyme. Moreover, persistence of objective clinical manifestations in these patients was accompanied by continued shedding of urinary OspA even during the course of treatment. In contrast, after successful resolution of symptoms in promptly treated early stage LB, urinary OspA protein became undetectable (Table 4).

Antigenuria in the setting of chronic persistent symptoms may be due to new, acute infectious exposures. Alternatively, antigenuria detected in individuals with consistent, persistent symptoms would warrant consideration of an ongoing active infection, supportive of the concept of LB in the chronic active state.

PCR analysis of urinary *Borrelia*, or urinary *Borrelia* culture was not done, because of the very low MRM sensitivity of these tests in human urine[149]. Consequently, a weakness of this study is that a true positive diagnosis of LB could only be based on the CDC clinical criteria (e.g. EM rash and other objective symptoms), and the development of a later positive serology in patients who underwent therapy at the time of the clinical diagnosis of LB. Despite this weakness, the strong correlation of urinary OspA with treatment response may offer a new class of information to assist the treating physician to determine whether a first round of therapy is successful in primary cutaneous early stage LB. In a population of patients being under surveillance for persistent or recurrent LB, the percentage of positive urinary OspA patients is in keeping with previous studies on patients estimated to actually have LB in endemic areas. It is impossible to know if urinary OspA, assuming that is indicative of Bb infection, is caused by a recurrent or new infection. Urinary OspA measurements may provide additional information to

assist the clinical workup of patients under investigation of disseminated later stages of LB. Considering the interest for the test by independent clinical laboratories we are currently transitioning from a western blot test to an ELISA. Even though the materials used to synthesize the Nanotraps are relatively inexpensive, a western blot format is time consuming and cannot be easily scaled-up. An ELISA on the other end could be easily employed by diagnostic laboratories, automatized for the processing of a larger number of samples thus reducing the cost per patient. In parallel a highly sensitive nanotrap MRM test is under development and provided very promising preliminary results. A lateral flow immunoassay employing antigen-displaying Nanotraps that can be used as a point of care test has also been successfully tested using model solutions. For the next generation of this technology we plan to extend our analyte panel to other *Borrelia* antigens such as OspC, DbpE, DbpA, DbpB, ViSE, flagellin and host inflammatory markers, as well as other members of Lyme disease co-infection pathogens.

REFERENCES

1. Petricoin, E. F. & Liotta, L. A. Clinical applications of proteomics. *J. Nutr.* **133,** 2476S–2484S (2003).
2. Ahn, S.-M. & Simpson, R. J. Body fluid proteomics: Prospects for biomarker discovery. *Proteomics Clin. Appl.* **1,** 1004–1015 (2007).
3. Petricoin, E. F., Belluco, C., Araujo, R. P. & Liotta, L. A. The blood peptidome: a higher dimension of information content for cancer biomarker discovery. *Nat. Rev. Cancer* **6,** 961–967 (2006).
4. Fredolini, C. *et al.* Investigation of the Ovarian and Prostate Cancer Peptidome for Candidate Early Detection Markers Using a Novel Nanoparticle Biomarker Capture Technology. *AAPS J.* **12,** 504–518 (2010).
5. Textbook of medical physiology / Arthur C. Guyton, John E. Hall - Details. *Trove* Available at: http://trove.nla.gov.au/work/6130114. (Accessed: 6th April 2016)
6. Anderson, N. L. & Anderson, N. G. The human plasma proteome: history, character, and diagnostic prospects. *Mol. Cell. Proteomics MCP* **1,** 845–867 (2002).
7. Tirumalai, R. S. *et al.* Characterization of the low molecular weight human serum proteome. *Mol. Cell. Proteomics MCP* **2,** 1096–1103 (2003).
8. Veenstra, T. D. *et al.* Biomarkers: mining the biofluid proteome. *Mol. Cell. Proteomics MCP* **4,** 409–418 (2005).
9. *Proteomics of Human Body Fluids*. (Humana Press, 2007).
10. Sedlaczek, P. *et al.* Comparative analysis of CA125, tissue polypeptide specific antigen, and soluble interleukin-2 receptor alpha levels in sera, cyst, and ascitic fluids from patients with ovarian carcinoma. *Cancer* **95,** 1886–1893 (2002).
11. Jacobs, I. J. *et al.* Screening for ovarian cancer: a pilot randomised controlled trial. *Lancet Lond. Engl.* **353,** 1207–1210 (1999).
12. Chang, P., Aronson, D. L., Borenstein, D. G. & Kessler, C. M. Coagulant proteins and thrombin generation in synovial fluid: a model for extravascular coagulation. *Am. J. Hematol.* **50,** 79–83 (1995).

13. Andersen, J. D. *et al.* Identification of candidate biomarkers in ovarian cancer serum by depletion of highly abundant proteins and differential in-gel electrophoresis. *Electrophoresis* **31,** 599–610 (2010).
14. Mahn, A. & Ismail, M. Depletion of highly abundant proteins in blood plasma by ammonium sulfate precipitation for 2D-PAGE analysis. *J. Chromatogr. B Analyt. Technol. Biomed. Life. Sci.* **879,** 3645–3648 (2011).
15. Righetti, P. G., Castagna, A., Antonioli, P. & Boschetti, E. Prefractionation techniques in proteome analysis: the mining tools of the third millennium. *Electrophoresis* **26,** 297–319 (2005).
16. Zhang, H., Li, X.-J., Martin, D. B. & Aebersold, R. Identification and quantification of N-linked glycoproteins using hydrazide chemistry, stable isotope labeling and mass spectrometry. *Nat. Biotechnol.* **21,** 660–666 (2003).
17. Huang, L. *et al.* Overexpression of long noncoding RNA HOTAIR predicts a poor prognosis in patients with cervical cancer. *Arch. Gynecol. Obstet.* **290,** 717–723 (2014).
18. Pierobon, M., Wulfkuhle, J., Liotta, L. & Petricoin, E. Application of molecular technologies for phosphoproteomic analysis of clinical samples. *Oncogene* **34,** 805–814 (2015).
19. Popova, T. G. *et al.* Reverse-Phase Phosphoproteome Analysis of Signaling Pathways Induced by Rift Valley Fever Virus in Human Small Airway Epithelial Cells. *PLOS ONE* **5,** e13805 (2010).
20. Zhou, W. *et al.* An initial characterization of the serum phosphoproteome. *J. Proteome Res.* **8,** 5523–5531 (2009).
21. Dunn, J. D., Reid, G. E. & Bruening, M. L. Techniques for phosphopeptide enrichment prior to analysis by mass spectrometry. *Mass Spectrom. Rev.* **29,** 29–54 (2010).
22. Adam, G. C., Cravatt, B. F. & Sorensen, E. J. Profiling the specific reactivity of the proteome with non-directed activity-based probes. *Chem. Biol.* **8,** 81–95 (2001).
23. Van den Bergh, G. & Arckens, L. Fluorescent two-dimensional difference gel electrophoresis unveils the potential of gel-based proteomics. *Curr. Opin. Biotechnol.* **15,** 38–43 (2004).

24. Wolters, D. A., Washburn, M. P. & Yates, J. R. An automated multidimensional protein identification technology for shotgun proteomics. *Anal. Chem.* **73,** 5683–5690 (2001).

25. Washburn, M. P., Wolters, D. & Yates, J. R. Large-scale analysis of the yeast proteome by multidimensional protein identification technology. *Nat. Biotechnol.* **19,** 242–247 (2001).

26. Mann, M., Hendrickson, R. C. & Pandey, A. Analysis of proteins and proteomes by mass spectrometry. *Annu. Rev. Biochem.* **70,** 437–473 (2001).

27. Aebersold, R. & Mann, M. Mass spectrometry-based proteomics. *Nature* **422,** 198–207 (2003).

28. Poste, G. Bring on the biomarkers. *Nature* **469,** 156–157 (2011).

29. Tamburro, D. *et al.* Multifunctional core-shell nanoparticles: discovery of previously invisible biomarkers. *J. Am. Chem. Soc.* **133,** 19178–19188 (2011).

30. Merrell, K. *et al.* Analysis of low-abundance, low-molecular-weight serum proteins using mass spectrometry. *J. Biomol. Tech. JBT* **15,** 238–248 (2004).

31. Marshall, J. *et al.* Processing of serum proteins underlies the mass spectral fingerprinting of myocardial infarction. *J. Proteome Res.* **2,** 361–372 (2003).

32. Longo, C. *et al.* A novel biomarker harvesting nanotechnology identifies Bak as a candidate melanoma biomarker in serum. *Exp. Dermatol.* **20,** 29–34 (2011).

33. Luchini, A., Longo, C., Espina, V., Petricoin, E. F. & Liotta, L. A. Nanoparticle technology: Addressing the fundamental roadblocks to protein biomarker discovery. *J. Mater. Chem.* **19,** 5071–5077 (2009).

34. Magni, R. *et al.* Application of Nanotrap technology for high sensitivity measurement of urinary outer surface protein A carboxyl-terminus domain in early stage Lyme borreliosis. *J. Transl. Med.* **13,** 346 (2015).

35. Lv, S., Liu, L. & Yang, W. Preparation of soft hydrogel nanoparticles with PNIPAm hair and characterization of their temperature-induced aggregation. *Langmuir ACS J. Surf. Colloids* **26,** 2076–2082 (2010).

36. Hu, Y. *et al.* Cytosolic delivery mediated via electrostatic surface binding of protein, virus, or siRNA cargos to pH-responsive core-shell gel particles. *Biomacromolecules* **10,** 756–765 (2009).

37. Petros, R. A. & DeSimone, J. M. Strategies in the design of nanoparticles for therapeutic applications. *Nat. Rev. Drug Discov.* **9,** 615–627 (2010).

38. Choudhury, R. P., Fuster, V. & Fayad, Z. A. Molecular, cellular and functional imaging of atherothrombosis. *Nat. Rev. Drug Discov.* **3,** 913–925 (2004).

39. Castro-Sesquen, Y. E. *et al.* Use of a novel chagas urine nanoparticle test (chunap) for diagnosis of congenital chagas disease. *PLoS Negl. Trop. Dis.* **8,** e3211 (2014).

40. Luchini, A. *et al.* Application of Analyte Harvesting Nanoparticle Technology to the Measurement of Urinary HGH in Healthy Individuals. *J. Sports Med. Doping Stud.* **2,** (2012).

41. Shafagati, N. *et al.* The use of NanoTrap particles as a sample enrichment method to enhance the detection of Rift Valley Fever Virus. *PLoS Negl. Trop. Dis.* **7,** e2296 (2013).

42. Fredolini, C. *et al.* Investigation of the ovarian and prostate cancer peptidome for candidate early detection markers using a novel nanoparticle biomarker capture technology. *AAPS J.* **12,** 504–518 (2010).

43. Hu, Z. Nanostructured polymer gels. *Macromol. Symp.* **207,** 47–56 (2004).

44. Sahoo, S. K., De, T. K., Ghosh, P. K. & Maitra, A. pH- and Thermo-sensitive Hydrogel Nanoparticles. *J. Colloid Interface Sci.* **206,** 361–368 (1998).

45. Buchwald, P., Margolles-Clark, E., Kenyon, N. S. & Ricordi, C. Organic dyes as small molecule protein-protein interaction inhibitors for the CD40-CD154 costimulatory interaction. *J. Mol. Recognit. JMR* **23,** 65–73 (2010).

46. Böhme, H.-J., Kopperschläger, G., Schulz, J. & Hofmann, E. Affinity chromatography of phosphofructokinase using Cibacron blue F3G-A. *J. Chromatogr. A* **69,** 209–214 (1972).

47. Röschlau, P. & Hess, B. Affinity chromatography of yeast pyruvate kinase with Cibacronblau bound to Sephadex G-200. *Hoppe-Seylers Z. Für Physiol. Chem.* **353,** 441–443 (1972).

48. Gianazza, E. & Arnaud, P. Chromatography of plasma proteins on immobilized Cibacron Blue F3-GA. Mechanism of the molecular interaction. *Biochem. J.* **203,** 637–641 (1982).

49. Thompson, S. T. & Stellwagen, E. Binding of Cibacron blue F3GA to proteins containing the dinucleotide fold. *Proc. Natl. Acad. Sci. U. S. A.* **73,** 361–365 (1976).

50. Luchini, A. *et al.* Smart hydrogel particles: biomarker harvesting: one-step affinity purification, size exclusion, and protection against degradation. *Nano Lett.* **8,** 350–361 (2008).

51. Denizli, A. & Pişkin, E. Dye-ligand affinity systems. *J. Biochem. Biophys. Methods* **49,** 391–416 (2001).

52. Thompson, S. T., Cass, K. H. & Stellwagen, E. Blue dextran-sepharose: an affinity column for the dinucleotide fold in proteins. *Proc. Natl. Acad. Sci. U. S. A.* **72,** 669–672 (1975).

53. Subramanian, S. & Kaufman, B. T. Dihydrofolate reductases from chicken liver and Lactobacillus casei bind Cibacron blue F3GA in different modes and at different sites. *J. Biol. Chem.* **255,** 10587–10590 (1980).

54. Fredolini, C. *et al.* Concentration and Preservation of Very Low Abundance Biomarkers in Urine, such as Human Growth Hormone (hGH), by Cibacron Blue F3G-A Loaded Hydrogel Particles. *Nano Res.* **1,** 502–518 (2008).

55. Nayak, S. & Lyon, L. A. Soft nanotechnology with soft nanoparticles. *Angew. Chem. Int. Ed Engl.* **44,** 7686–7708 (2005).

56. Lee, J. H., Oh, S. H. & Kim, W. G. MMA/MPEOMA/VSA copolymer as a novel blood-compatible material: ex vivo platelet adhesion study. *J. Mater. Sci. Mater. Med.* **15,** 155–159 (2004).

57. Gaulding, J. C., Smith, M. H., Hyatt, J. S., Fernandez-Nieves, A. & Lyon, L. A. Reversible Inter- and Intra-Microgel Cross-Linking using Disulfides. *Macromolecules* **45,** 39–45 (2012).

58. Aliyar, H. A., Hamilton, P. D. & Ravi, N. Refilling of ocular lens capsule with copolymeric hydrogel containing reversible disulfide. *Biomacromolecules* **6,** 204–211 (2005).

59. Hiratani, H. *et al.* Effect of Reversible Cross-linker, N,N‘-Bis(acryloyl)cystamine, on Calcium Ion Adsorption by Imprinted Gels. *Langmuir* **17,** 4431–4436 (2001).

60. Conti, A. *et al.* Identification of novel candidate circulating biomarkers for malignant soft tissue sarcomas: Correlation with metastatic progression. *Proteomics* **16,** 689–697 (2016).
61. Nageswara Rao, A. A., Scafidi, J., Wells, E. M. & Packer, R. J. Biologically targeted therapeutics in pediatric brain tumors. *Pediatr. Neurol.* **46,** 203–211 (2012).
62. Khatua, S., Sadighi, Z. S., Pearlman, M. L., Bochare, S. & Vats, T. S. Brain tumors in children--current therapies and newer directions. *Indian J. Pediatr.* **79,** 922–927 (2012).
63. Pisitkun, T., Johnstone, R. & Knepper, M. A. Discovery of urinary biomarkers. *Mol. Cell. Proteomics MCP* **5,** 1760–1771 (2006).
64. Lakshmanachetty, S. & Koster, M. I. Emerging roles for collagen XV and XVIII in cancer progression. *Exp. Dermatol.* **25,** 346–347 (2016).
65. Newman, A. C., Nakatsu, M. N., Chou, W., Gershon, P. D. & Hughes, C. C. W. The requirement for fibroblasts in angiogenesis: fibroblast-derived matrix proteins are essential for endothelial cell lumen formation. *Mol. Biol. Cell* **22,** 3791–3800 (2011).
66. Wu, Z.-S. *et al.* Prognostic significance of the expression of GFRα1, GFRα3 and syndecan-3, proteins binding ARTEMIN, in mammary carcinoma. *BMC Cancer* **13,** 34 (2013).
67. Das, D. S. *et al.* Dickkopf homolog 3 (DKK3) plays a crucial role upstream of WNT/β-CATENIN signaling for Sertoli cell mediated regulation of spermatogenesis. *PloS One* **8,** e63603 (2013).
68. Wu, Y. *et al.* Prosaposin, a regulator of estrogen receptor alpha, promotes breast cancer growth. *Cancer Sci.* **103,** 1820–1825 (2012).
69. Barratt, J. & Topham, P. Urine proteomics: the present and future of measuring urinary protein components in disease. *CMAJ Can. Med. Assoc. J. J. Assoc. Medicale Can.* **177,** 361–368 (2007).
70. Chomel, B. Lyme disease. *Rev. Sci. Tech. Int. Off. Epizoot.* **34,** 569–576 (2015).
71. Rizzoli, A. *et al.* Lyme borreliosis in Europe. *Euro Surveill. Bull. Eur. Sur Mal. Transm. Eur. Commun. Dis. Bull.* **16,** (2011).
72. Strle, F. & Stanek, G. Clinical manifestations and diagnosis of lyme borreliosis. *Curr. Probl. Dermatol.* **37,** 51–110 (2009).

73. Fraser, C. M. *et al.* Genomic sequence of a Lyme disease spirochaete, Borrelia burgdorferi. *Nature* **390,** 580–586 (1997).

74. Preac-Mursic, V., Wilske, B. & Schierz, G. European Borrelia burgdorferi isolated from humans and ticks culture conditions and antibiotic susceptibility. *Zentralbl. Bakteriol. Mikrobiol. Hyg. [A]* **263,** 112–118 (1986).

75. Barbour, A. G. Isolation and cultivation of Lyme disease spirochetes. *Yale J. Biol. Med.* **57,** 521–525 (1984).

76. Gray, J. S. Review The ecology of ticks transmitting Lyme borreliosis. *Exp. Appl. Acarol.* **22,** 249–258

77. Piesman, J., Mather, T. N., Sinsky, R. J. & Spielman, A. Duration of tick attachment and Borrelia burgdorferi transmission. *J. Clin. Microbiol.* **25,** 557–558 (1987).

78. des Vignes, F. *et al.* Effect of tick removal on transmission of Borrelia burgdorferi and Ehrlichia phagocytophila by Ixodes scapularis nymphs. *J. Infect. Dis.* **183,** 773–778 (2001).

79. Peavey, C. A. & Lane, R. S. Transmission of Borrelia burgdorferi by Ixodes pacificus nymphs and reservoir competence of deer mice (Peromyscus maniculatus) infected by tick-bite. *J. Parasitol.* **81,** 175–178 (1995).

80. Piesman, J. in *Lyme borreliosis: biology, epidemiology and control* (eds. Gray, J., Kahl, O., Lane, R. S. & Stanek, G.) 223–249 (CABI, 2002).

81. Hubálek, Z. Epidemiology of lyme borreliosis. *Curr. Probl. Dermatol.* **37,** 31–50 (2009).

82. Jasik, K. P. *et al.* Congenital Tick Borne Diseases: Is This An Alternative Route of Transmission of Tick-Borne Pathogens In Mammals? *Vector Borne Zoonotic Dis. Larchmt. N* **15,** 637–644 (2015).

83. Lyme disease transmission. Available at: https://www.cdc.gov/lyme/transmission/. (Accessed: 10th January 2017)

84. Moore, A., Nelson, C., Molins, C., Mead, P. & Schriefer, M. Current Guidelines, Common Clinical Pitfalls, and Future Directions for Laboratory Diagnosis of Lyme Disease, United States. *Emerg. Infect. Dis.* **22,** (2016).

85. WPRO | Climate change and vectorborne diseases. *WPRO* Available at: http://www.wpro.who.int/mvp/climate_change/en/. (Accessed: 7th October 2016)

86. Kugeler, K. J., Farley, G. M., Forrester, J. D. & Mead, P. S. Geographic Distribution and Expansion of Human Lyme Disease, United States. *Emerg. Infect. Dis.* **21,** 1455–1457 (2015).

87. Pepin, K. M. *et al.* Geographic variation in the relationship between human Lyme disease incidence and density of infected host-seeking Ixodes scapularis nymphs in the Eastern United States. *Am. J. Trop. Med. Hyg.* **86,** 1062–1071 (2012).

88. Surveillance for Lyme Disease --- United States, 1992--2006</FONT>. Available at: https://www.cdc.gov/mmwr/preview/mmwrhtml/ss5710a1.htm. (Accessed: 16th June 2016)

89. Government of Canada, H. C. and the P. H. A. of C. National Lyme Disease Surveillance in Canada 2009-2012. (2015). Available at: http://healthycanadians.gc.ca/publications/diseases-conditions-maladies-affections/2009-2012-lyme/index-eng.php. (Accessed: 7th October 2016)

90. Lyme borreliosis in Europe. Influences of climate and climate change, epidemiology, ecology and adaptation measures. (2014). Available at: http://www.euro.who.int/en/publications/abstracts/lyme-borreliosis-in-europe.-influences-of-climate-and-climate-change,-epidemiology,-ecology-and-adaptation-measures. (Accessed: 22nd October 2016)

91. Wilking, H. & Stark, K. Trends in surveillance data of human Lyme borreliosis from six federal states in eastern Germany, 2009-2012. *Ticks Tick-Borne Dis.* **5,** 219–224 (2014).

92. Steere, A. C. & Angelis, S. M. Therapy for Lyme arthritis: strategies for the treatment of antibiotic-refractory arthritis. *Arthritis Rheum.* **54,** 3079–3086 (2006).

93. Lyme Disease | Lyme Disease | CDC. Available at: http://www.cdc.gov/lyme/. (Accessed: 7th October 2016)

94. Pistone, D. *et al.* Lyme borreliosis, Po River Valley, Italy. *Emerg. Infect. Dis.* **16,** 1289–1291 (2010).

95. Steere, A. C., Coburn, J. & Glickstein, L. The emergence of Lyme disease. *J. Clin. Invest.* **113,** 1093–1101 (2004).

96. Rosa, P. Lyme disease agent borrows a practical coat. *Nat. Med.* **11,** 831–832 (2005).

97. Baranton, G. & De Martino, S. J. Borrelia burgdorferi sensu lato diversity and its influence on pathogenicity in humans. *Curr. Probl. Dermatol.* **37,** 1–17 (2009).

98. Steere, A. C. *et al.* Antibiotic-refractory Lyme arthritis is associated with HLA-DR molecules that bind a Borrelia burgdorferi peptide. *J. Exp. Med.* **203,** 961–971 (2006).

99. Cabello, F. C., Godfrey, H. P. & Newman, S. A. Hidden in plain sight: Borrelia burgdorferi and the extracellular matrix. *Trends Microbiol.* **15,** 350–354 (2007).

100. Strle, K. *et al.* Borrelia burgdorferi stimulates macrophages to secrete higher levels of cytokines and chemokines than Borrelia afzelii or Borrelia garinii. *J. Infect. Dis.* **200,** 1936–1943 (2009).

101. Diterich, I., Rauter, C., Kirschning, C. J. & Hartung, T. Borrelia burgdorferi-Induced Tolerance as a Model of Persistence via Immunosuppression. *Infect. Immun.* **71,** 3979–3987 (2003).

102. Battisti, J. M. *et al.* Outer surface protein A protects Lyme disease spirochetes from acquired host immunity in the tick vector. *Infect. Immun.* **76,** 5228–5237 (2008).

103. Schutzer, S. E., Coyle, P. K., Dunn, J. J., Luft, B. J. & Brunner, M. Early and specific antibody response to OspA in Lyme Disease. *J. Clin. Invest.* **94,** 454–457 (1994).

104. Cameron, D. J. An appraisal of 'chronic Lyme disease'. *N. Engl. J. Med.* **358,** 429-430-431 (2008).

105. Fallon, B. A. *et al.* Regional cerebral blood flow and metabolic rate in persistent Lyme encephalopathy. *Arch. Gen. Psychiatry* **66,** 554–563 (2009).

106. Heckler, A. K. & Shmorhun, D. Asymptomatic, transient complete heart block in a pediatric patient with Lyme disease. *Clin. Pediatr. (Phila.)* **49,** 82–85 (2010).

107. Barr, W. B., Rastogi, R., Ravdin, L. & Hilton, E. Relations among indexes of memory disturbance and depression in patients with Lyme borreliosis. *Appl. Neuropsychol.* **6,** 12–18 (1999).

108. Steere, A. C. Lyme disease. *N. Engl. J. Med.* **345,** 115–125 (2001).

109. Halperin, J. J. Nervous system Lyme disease. *Infect. Dis. Clin. North Am.* **29,** 241–253 (2015).

110. Forrester, J. D. *et al.* Notes from the field: update on Lyme carditis, groups at high risk, and frequency of associated sudden cardiac death--United States. *MMWR Morb. Mortal. Wkly. Rep.* **63,** 982–983 (2014).

111. Sanchez E, Vannier E, Wormser GP & Hu LT. Diagnosis, treatment, and prevention of lyme disease, human granulocytic anaplasmosis, and babesiosis: A review. *JAMA* **315,** 1767–1777 (2016).

112. Arvikar, S. L. & Steere, A. C. Diagnosis and treatment of Lyme arthritis. *Infect. Dis. Clin. North Am.* **29,** 269–280 (2015).

113. Wormser, G. P. *et al.* The clinical assessment, treatment, and prevention of lyme disease, human granulocytic anaplasmosis, and babesiosis: clinical practice guidelines by the Infectious Diseases Society of America. *Clin. Infect. Dis. Off. Publ. Infect. Dis. Soc. Am.* **43,** 1089–1134 (2006).

114. Hunfeld, K.-P., Ruzic-Sabljic, E., Norris, D. E., Kraiczy, P. & Strle, F. In vitro susceptibility testing of Borrelia burgdorferi sensu lato isolates cultured from patients with erythema migrans before and after antimicrobial chemotherapy. *Antimicrob. Agents Chemother.* **49,** 1294–1301 (2005).

115. Morgenstern, K. *et al.* In vitro susceptibility of Borrelia spielmanii to antimicrobial agents commonly used for treatment of Lyme disease. *Antimicrob. Agents Chemother.* **53,** 1281–1284 (2009).

116. Wormser, G. P. *et al.* Duration of antibiotic therapy for early Lyme disease. A randomized, double-blind, placebo-controlled trial. *Ann. Intern. Med.* **138,** 697–704 (2003).

117. Ljøstad, U. *et al.* Oral doxycycline versus intravenous ceftriaxone for European Lyme neuroborreliosis: a multicentre, non-inferiority, double-blind, randomised trial. *Lancet Neurol.* **7,** 690–695 (2008).

118. Mygland, A. *et al.* EFNS guidelines on the diagnosis and management of European Lyme neuroborreliosis. *Eur. J. Neurol.* **17,** 8–16, e1-4 (2010).

119. Steere, A. C., Schoen, R. T. & Taylor, E. The clinical evolution of Lyme arthritis. *Ann. Intern. Med.* **107,** 725–731 (1987).

120. Singh, S. K. & Girschick, H. J. Molecular survival strategies of the Lyme disease spirochete Borrelia burgdorferi. *Lancet Infect. Dis.* **4,** 575–583 (2004).

121. Livengood, J. A. & Gilmore, R. D. Invasion of human neuronal and glial cells by an infectious strain of Borrelia burgdorferi. *Microbes Infect.* **8,** 2832–2840 (2006).

122. Ma, Y., Sturrock, A. & Weis, J. J. Intracellular localization of Borrelia burgdorferi within human endothelial cells. *Infect. Immun.* **59,** 671–678 (1991).

123. Aguero-Rosenfeld, M. E., Wang, G., Schwartz, I. & Wormser, G. P. Diagnosis of Lyme Borreliosis. *Clin. Microbiol. Rev.* **18,** 484–509 (2005).

124. Rauter, C. *et al.* Critical Evaluation of Urine-Based PCR Assay for Diagnosis of Lyme Borreliosis. *Clin. Diagn. Lab. Immunol.* **12,** 910–917 (2005).

125. Wormser, G. P. *et al.* The Clinical Assessment, Treatment, and Prevention of Lyme Disease, Human Granulocytic Anaplasmosis, and Babesiosis: Clinical Practice Guidelines by the Infectious Diseases Society of America. *Clin. Infect. Dis.* **43,** 1089–1134 (2006).

126. Centers for Disease Control and Prevention (CDC). Recommendations for test performance and interpretation from the Second National Conference on Serologic Diagnosis of Lyme Disease. *MMWR Morb. Mortal. Wkly. Rep.* **44,** 590–591 (1995).

127. Bacon, R. M. *et al.* Serodiagnosis of Lyme disease by kinetic enzyme-linked immunosorbent assay using recombinant VlsE1 or peptide antigens of Borrelia burgdorferi compared with 2-tiered testing using whole-cell lysates. *J. Infect. Dis.* **187,** 1187–1199 (2003).

128. Wormser, G. P. *et al.* Single-tier testing with the C6 peptide ELISA kit compared with two-tier testing for Lyme disease. *Diagn. Microbiol. Infect. Dis.* **75,** 9–15 (2013).

129. Branda, J. A. *et al.* Performance of United States serologic assays in the diagnosis of Lyme borreliosis acquired in Europe. *Clin. Infect. Dis. Off. Publ. Infect. Dis. Soc. Am.* **57,** 333–340 (2013).

130. Wormser, G. P. *et al.* Utility of serodiagnostics designed for use in the United States for detection of Lyme borreliosis acquired in Europe and vice versa. *Med. Microbiol. Immunol. (Berl.)* **203,** 65–71 (2014).

131. Mathiesen, M. J. *et al.* Peptide-based OspC enzyme-linked immunosorbent assay for serodiagnosis of Lyme borreliosis. *J. Clin. Microbiol.* **36,** 3474–3479 (1998).

132. Alby, K. & Capraro, G. A. Alternatives to Serologic Testing for Diagnosis of Lyme Disease. *Clin. Lab. Med.* **35,** 815–825 (2015).

133. Coulter, P. *et al.* Two-Year Evaluation of Borrelia burgdorferi Culture and Supplemental Tests for Definitive Diagnosis of Lyme Disease. *J. Clin. Microbiol.* **43,** 5080–5084 (2005).

134. Avery, R. A., Frank, G. & Eppes, S. C. Diagnostic utility of Borrelia burgdorferi cerebrospinal fluid polymerase chain reaction in children with Lyme meningitis. *Pediatr. Infect. Dis. J.* **24,** 705–708 (2005).

135. Steere, A. C., Berardi, V. P., Weeks, K. E., Logigian, E. L. & Ackermann, R. Evaluation of the intrathecal antibody response to Borrelia burgdorferi as a diagnostic test for Lyme neuroborreliosis. *J. Infect. Dis.* **161,** 1203–1209 (1990).

136. Hytönen, J. *et al.* CXCL13 and neopterin concentrations in cerebrospinal fluid of patients with Lyme neuroborreliosis and other diseases that cause neuroinflammation. *J. Neuroinflammation* **11,** 103 (2014).

137. Sillanpää, H., Skogman, B. H., Sarvas, H., Seppälä, I. J. T. & Lahdenne, P. Cerebrospinal fluid chemokine CXCL13 in the diagnosis of neuroborreliosis in children. *Scand. J. Infect. Dis.* **45,** 526–530 (2013).

138. Tjernberg, I., Henningsson, A. J., Eliasson, I., Forsberg, P. & Ernerudh, J. Diagnostic performance of cerebrospinal fluid chemokine CXCL13 and antibodies to the C6-peptide in Lyme neuroborreliosis. *J. Infect.* **62,** 149–158 (2011).

139. Stanek, G., Wormser, G. P., Gray, J. & Strle, F. Lyme borreliosis. *Lancet Lond. Engl.* **379,** 461–473 (2012).

140. Nelson, C., Elmendorf, S. & Mead, P. Neoplasms misdiagnosed as 'chronic lyme disease'. *JAMA Intern. Med.* **175,** 132–133 (2015).

141. Halpern, M. D., Molins, C. R., Schriefer, M. & Jewett, M. W. Simple Objective Detection of Human Lyme Disease Infection Using Immuno-PCR and a Single Recombinant Hybrid Antigen. *Clin. Vaccine Immunol. CVI* **21,** 1094–1105 (2014).

142. Babady, N. E., Sloan, L. M., Vetter, E. A., Patel, R. & Binnicker, M. J. Percent positive rate of Lyme real-time polymerase chain reaction in blood, cerebrospinal fluid, synovial fluid, and tissue. *Diagn. Microbiol. Infect. Dis.* **62,** 464–466 (2008).

143. Molins, C. R. *et al.* Development of a metabolic biosignature for detection of early Lyme disease. *Clin. Infect. Dis. Off. Publ. Infect. Dis. Soc. Am.* **60,** 1767–1775 (2015).

144. Schnell, G. *et al.* Discovery and targeted proteomics on cutaneous biopsies infected by borrelia to investigate lyme disease. *Mol. Cell. Proteomics MCP* **14,** 1254–1264 (2015).

145. Magnarelli, L. A., Anderson, J. F. & Stafford, K. C. Detection of Borrelia burgdorferi in urine of Peromyscus leucopus by inhibition enzyme-linked immunosorbent assay. *J. Clin. Microbiol.* **32,** 777–782 (1994).

146. Zumstein, G. *et al.* Genetic polymorphism of the gene encoding the outer surface protein A (OspA) of Borrelia burgdorferi. *Med. Microbiol. Immunol. (Berl.)* **181,** 57–70 (1992).

147. Luft, B. J., Dunn, J. J. & Lawson, C. L. Approaches toward the Directed Design of a Vaccine against Borrelia burgdorferi. *J. Infect. Dis.* **185,** S46–S51 (2002).

148. Dorward, D. W., Schwan, T. G. & Garon, C. F. Immune capture and detection of Borrelia burgdorferi antigens in urine, blood, or tissues from infected ticks, mice, dogs, and humans. *J. Clin. Microbiol.* **29,** 1162–1170 (1991).

149. Brettschneider, S., Bruckbauer, H., Klugbauer, N. & Hofmann, H. Diagnostic value of PCR for detection of Borrelia burgdorferi in skin biopsy and urine samples from patients with skin borreliosis. *J. Clin. Microbiol.* **36,** 2658–2665 (1998).

150. Bockenstedt, L. K., Gonzalez, D. G., Haberman, A. M. & Belperron, A. A. Spirochete antigens persist near cartilage after murine Lyme borreliosis therapy. *J. Clin. Invest.* **122,** 2652–2660 (2012).

151. Jones, C. D. & Lyon, L. A. Synthesis and Characterization of Multiresponsive Core−Shell Microgels. *Macromolecules* **33,** 8301–8306 (2000).

152. Dorfmüller, T. R. Pecora (Ed.): Dynamic light scattering — applications of photon correlation spectroscopy, Plenum Press, New York and London 1985. 420 Seiten, Preis: $ 59.90. *Berichte Bunsenges. Für Phys. Chem.* **91,** 498–499 (1987).

153. Altschul, S. F. *et al.* Gapped BLAST and PSI-BLAST: a new generation of protein database search programs. *Nucleic Acids Res.* **25,** 3389–3402 (1997).

154. Dimeski, G. Interference Testing. *Clin. Biochem. Rev.* **29,** S43–S48 (2008).

155. De Silva, A. M. & Fikrig, E. Growth and migration of Borrelia burgdorferi in Ixodes ticks during blood feeding. *Am. J. Trop. Med. Hyg.* **53,** 397–404 (1995).

156. Douglas, T. A. *et al.* The use of hydrogel microparticles to sequester and concentrate bacterial antigens in a urine test for Lyme disease. *Biomaterials* **32,** 1157–1166 (2011).

157. halperin_2012_chap4_johnsonb.pdf.

158. IDSALymeDiseaseFinalReport.pdf.

159. Cameron, D. J., Johnson, L. B. & Maloney, E. L. Evidence assessments and guideline recommendations in Lyme disease: the clinical management of known tick bites, erythema migrans rashes and persistent disease. *Expert Rev. Anti Infect. Ther.* **12,** 1103–1135 (2014).

160. Donta, S. T. Issues in the diagnosis and treatment of lyme disease. *Open Neurol. J.* **6,** 140–145 (2012).

161. Halperin, J. J., Little, B. W., Coyle, P. K. & Dattwyler, R. J. Lyme disease: cause of a treatable peripheral neuropathy. *Neurology* **37,** 1700–1706 (1987).

162. Halperin, J. J., Volkman, D. J. & Wu, P. Central nervous system abnormalities in Lyme neuroborreliosis. *Neurology* **41,** 1571–1582 (1991).

163. Oksi, J., Marjamäki, M., Nikoskelainen, J. & Viljanen, M. K. Borrelia burgdorferi detected by culture and PCR in clinical relapse of disseminated Lyme borreliosis. *Ann. Med.* **31,** 225–232 (1999).

164. Shadick, N. A. *et al.* The long-term clinical outcomes of Lyme disease. A population-based retrospective cohort study. *Ann. Intern. Med.* **121,** 560–567 (1994).

165. lymes.pdf.

166. Sigal, L. H. Summary of the first 100 patients seen at a Lyme disease referral center. *Am. J. Med.* **88,** 577–581 (1990).

167. Steere, A. C., Taylor, E., McHugh, G. L. & Logigian, E. L. The overdiagnosis of Lyme disease. *JAMA* **269,** 1812–1816 (1993).

168. Hassett, A. L., Radvanski, D. C., Buyske, S., Savage, S. V. & Sigal, L. H. Psychiatric comorbidity and other psychological factors in patients with 'chronic Lyme disease'. *Am. J. Med.* **122,** 843–850 (2009).

169. McCabe, J. P., Fletcher, S. M. & Jones, M. N. The effects of detergent on the enzyme-linked immunosorbent assay (ELISA) of blood group substances. *J. Immunol. Methods* **108,** 129–135 (1988).

170. Liebler, D. C. & Zimmerman, L. J. Targeted quantitation of proteins by mass spectrometry. *Biochemistry (Mosc.)* **52,** 3797–3806 (2013).

171. Gillette, M. A. & Carr, S. A. Quantitative analysis of peptides and proteins in biomedicine by targeted mass spectrometry. *Nat. Methods* **10,** 28–34 (2013).

172. Cheung, C. S. F. *et al.* Quantification of Borrelia burgdorferi Membrane Proteins in Human Serum: A New Concept for Detection of Bacterial Infection. *Anal. Chem.* **87,** 11383–11388 (2015).

173. Kuhn, E. *et al.* Developing multiplexed assays for troponin I and interleukin-33 in plasma by peptide immunoaffinity enrichment and targeted mass spectrometry. *Clin. Chem.* **55,** 1108–1117 (2009).

174. Gross, D. M. *et al.* Identification of LFA-1 as a candidate autoantigen in treatment-resistant Lyme arthritis. *Science* **281,** 703–706 (1998).

175. Klempner, M. S. *et al.* Intralaboratory reliability of serologic and urine testing for Lyme disease. *Am. J. Med.* **110,** 217–219 (2001).

176. Akin, E., McHugh, G. L., Flavell, R. A., Fikrig, E. & Steere, A. C. The immunoglobulin (IgG) antibody response to OspA and OspB correlates with severe and prolonged Lyme arthritis and the IgG response to P35 correlates with mild and brief arthritis. *Infect. Immun.* **67,** 173–181 (1999).

177. Brandt, F. C., Ertas, B., Falk, T. M., Metze, D. & Böer-Auer, A. Genotyping of Borrelia from formalin-fixed paraffin-embedded skin biopsies of cutaneous borreliosis and tick bite reactions by assays targeting the intergenic spacer region, ospA and ospC genes. *Br. J. Dermatol.* **171,** 528–543 (2014).

178. Weis, J. J., Ma, Y. & Erdile, L. F. Biological activities of native and recombinant Borrelia burgdorferi outer surface protein A: dependence on lipid modification. *Infect. Immun.* **62,** 4632–4636 (1994).

179. Gross, D. M. & Huber, B. T. Cellular and molecular aspects of Lyme arthritis. *Cell. Mol. Life Sci. CMLS* **57,** 1562–1569 (2000).

180. Yang, X. F., Pal, U., Alani, S. M., Fikrig, E. & Norgard, M. V. Essential role for OspA/B in the life cycle of the Lyme disease spirochete. *J. Exp. Med.* **199,** 641–648 (2004).

181. Oosting, M., Buffen, K., van der Meer, J. W. M., Netea, M. G. & Joosten, L. A. B. Innate immunity networks during infection with Borrelia burgdorferi. *Crit. Rev. Microbiol.* **42,** 233–244 (2016).

182. de Silva, A. M., Telford, S. R., Brunet, L. R., Barthold, S. W. & Fikrig, E. Borrelia burgdorferi OspA is an arthropod-specific transmission-blocking Lyme disease vaccine. *J. Exp. Med.* **183,** 271–275 (1996).

183. Schwan, T. G. & Piesman, J. Temporal changes in outer surface proteins A and C of the lyme disease-associated spirochete, Borrelia burgdorferi, during the chain of infection in ticks and mice. *J. Clin. Microbiol.* **38,** 382–388 (2000).

184. Crowley, H. & Huber, B. T. Host-adapted Borrelia burgdorferi in mice expresses OspA during inflammation. *Infect. Immun.* **71,** 4003–4010 (2003).

185. Feder, H. M., Gerber, M. A., Krause, P. J., Ryan, R. & Shapiro, E. D. Early Lyme disease: a flu-like illness without erythema migrans. *Pediatrics* **91,** 456–459 (1993).

186. Nadelman, R. B. *et al.* The clinical spectrum of early lyme borreliosis in patients with culture-confirmed erythema migrans. *Am. J. Med.* **100,** 502–508 (1996).

187. Aucott, J. N., Crowder, L. A. & Kortte, K. B. Development of a foundation for a case definition of post-treatment Lyme disease syndrome. *Int. J. Infect. Dis. IJID Off. Publ. Int. Soc. Infect. Dis.* **17,** e443-449 (2013).

188. Barthold, S. W. *et al.* Ineffectiveness of Tigecycline against Persistent Borrelia burgdorferi. *Antimicrob. Agents Chemother.* **54,** 643–651 (2010).

189. Embers, M. E. *et al.* Persistence of Borrelia burgdorferi in Rhesus Macaques following Antibiotic Treatment of Disseminated Infection. *PLoS ONE* **7,** (2012).

190. Embers, M. E., Ramamoorthy, R. & Philipp, M. T. Survival strategies of Borrelia burgdorferi, the etiologic agent of Lyme disease. *Microbes Infect. Inst. Pasteur* **6,** 312–318 (2004).

191. Hodzic, E., Feng, S., Holden, K., Freet, K. J. & Barthold, S. W. Persistence of Borrelia burgdorferi following antibiotic treatment in mice. *Antimicrob. Agents Chemother.* **52,** 1728–1736 (2008).

192. Szczepanski, A. & Benach, J. L. Lyme borreliosis: host responses to Borrelia burgdorferi. *Microbiol. Rev.* **55,** 21–34 (1991).

193. Mahmoud, A. A. The challenge of intracellular pathogens. *N. Engl. J. Med.* **326,** 761–762 (1992).

194. Sapi, E. *et al.* Characterization of biofilm formation by Borrelia burgdorferi in vitro. *PloS One* **7,** e48277 (2012).

195. Zhang, J. R., Hardham, J. M., Barbour, A. G. & Norris, S. J. Antigenic variation in Lyme disease borreliae by promiscuous recombination of VMP-like sequence cassettes. *Cell* **89,** 275–285 (1997).

196. Coutte, L., Botkin, D. J., Gao, L. & Norris, S. J. Detailed analysis of sequence changes occurring during vlsE antigenic variation in the mouse model of Borrelia burgdorferi infection. *PLoS Pathog.* **5,** e1000293 (2009).

197. Liang, F. T., Jacobs, M. B., Bowers, L. C. & Philipp, M. T. An immune evasion mechanism for spirochetal persistence in Lyme borreliosis. *J. Exp. Med.* **195,** 415–422 (2002).

198. Barbour, A. G. & Restrepo, B. I. Antigenic variation in vector-borne pathogens. *Emerg. Infect. Dis.* **6,** 449–457 (2000).

199. Brorson, O. & Brorson, S. H. Transformation of cystic forms of Borrelia burgdorferi to normal, mobile spirochetes. *Infection* **25,** 240–246 (1997).

200. Brorson, O. & Brorson, S. H. In vitro conversion of Borrelia burgdorferi to cystic forms in spinal fluid, and transformation to mobile spirochetes by incubation in BSK-H medium. *Infection* **26,** 144–150 (1998).

201. Mursic, V. P. *et al.* Formation and cultivation of Borrelia burgdorferi spheroplast-L-form variants. *Infection* **24,** 218–226 (1996).

202. Duray, P. H. *et al.* Invasion of human tissue ex vivo by Borrelia burgdorferi. *J. Infect. Dis.* **191,** 1747–1754 (2005).

203. Kersten, A., Poitschek, C., Rauch, S. & Aberer, E. Effects of penicillin, ceftriaxone, and doxycycline on morphology of Borrelia burgdorferi. *Antimicrob. Agents Chemother.* **39,** 1127–1133 (1995).

204. Miklossy, J. *et al.* Persisting atypical and cystic forms of Borrelia burgdorferiand local inflammation in Lyme neuroborreliosis. *J. Neuroinflammation* **5,** 40 (2008).

205. Alban, P. S., Johnson, P. W. & Nelson, D. R. Serum-starvation-induced changes in protein synthesis and morphology of Borrelia burgdorferi. *Microbiol. Read. Engl.* **146 (Pt 1),** 119–127 (2000).

206. Kraiczy, P. *et al.* Complement resistance of Borrelia burgdorferi correlates with the expression of BbCRASP-1, a novel linear plasmid-encoded surface protein that interacts with human factor H and FHL-1 and is unrelated to Erp proteins. *J. Biol. Chem.* **279,** 2421–2429 (2004).

207. Kraiczy, P., Skerka, C., Kirschfink, M., Zipfel, P. F. & Brade, V. Immune evasion of Borrelia burgdorferi: insufficient killing of the pathogens by complement and antibody. *Int. J. Med. Microbiol. IJMM* **291 Suppl 33,** 141–146 (2002).

208. Pausa, M. *et al.* Serum-resistant strains of Borrelia burgdorferi evade complement-mediated killing by expressing a CD59-like complement inhibitory molecule. *J. Immunol. Baltim. Md 1950* **170,** 3214–3222 (2003).

209. Hartiala, P. *et al.* Transcriptional response of human dendritic cells to Borrelia garinii--defective CD38 and CCR7 expression detected. *J. Leukoc. Biol.* **82,** 33–43 (2007).

210. Hartiala, P. *et al.* Borrelia burgdorferi inhibits human neutrophil functions. *Microbes Infect. Inst. Pasteur* **10,** 60–68 (2008).

211. Fallon, B. A., Levin, E. S., Schweitzer, P. J. & Hardesty, D. Inflammation and central nervous system Lyme disease. *Neurobiol. Dis.* **37,** 534–541 (2010).

212. Lazarus, J. J., Kay, M. A., McCarter, A. L. & Wooten, R. M. Viable Borrelia burgdorferi enhances interleukin-10 production and suppresses activation of murine macrophages. *Infect. Immun.* **76,** 1153–1162 (2008).

213. Giambartolomei, G. H., Dennis, V. A. & Philipp, M. T. Borrelia burgdorferi stimulates the production of interleukin-10 in peripheral blood mononuclear

cells from uninfected humans and rhesus monkeys. *Infect. Immun.* **66,** 2691–2697 (1998).

214. Sartakova, M. L. *et al.* Novel antibiotic-resistance markers in pGK12-derived vectors for Borrelia burgdorferi. *Gene* **303,** 131–137 (2003).

215. Engstrom, S. M., Shoop, E. & Johnson, R. C. Immunoblot interpretation criteria for serodiagnosis of early Lyme disease. *J. Clin. Microbiol.* **33,** 419–427 (1995).

216. Aguero-Rosenfeld, M. E. *et al.* Evolution of the serologic response to Borrelia burgdorferi in treated patients with culture-confirmed erythema migrans. *J. Clin. Microbiol.* **34,** 1–9 (1996).

217. Nowakowski, J., Nadelman, R. B., Forseter, G., McKenna, D. & Wormser, G. P. Doxycycline versus tetracycline therapy for Lyme disease associated with erythema migrans. *J. Am. Acad. Dermatol.* **32,** 223–227 (1995).

218. Wormser, G. P. Clinical practice. Early Lyme disease. *N. Engl. J. Med.* **354,** 2794–2801 (2006).

219. Hunfeld, K.-P., Hildebrandt, A. & Gray, J. S. Babesiosis: recent insights into an ancient disease. *Int. J. Parasitol.* **38,** 1219–1237 (2008).

220. dos Santos, C. C. & Kain, K. C. Two tick-borne diseases in one: a case report of concurrent babesiosis and Lyme disease in Ontario. *CMAJ Can. Med. Assoc. J.* **160,** 1851–1853 (1999).

221. Coinfecting Deer-Associated Zoonoses: Lyme Disease, Babesiosis, and Ehrlichiosis. Available at: http://cid.oxfordjournals.org/content/33/5/676.long. (Accessed: 23rd August 2016)

222. Aguero-Rosenfeld, M. E. Laboratory aspects of tick-borne diseases: lyme, human granulocytic ehrlichiosis and babesiosis. *Mt. Sinai J. Med. N. Y.* **70,** 197–206 (2003).

223. Seidel, M. F., Domene, A. B. & Vetter, H. Differential diagnoses of suspected Lyme borreliosis or post-Lyme-disease syndrome. *Eur. J. Clin. Microbiol. Infect. Dis.* **26,** 611–617 (2007).

224. Berndtson, K. Review of evidence for immune evasion and persistent infection in Lyme disease. *Int. J. Gen. Med.* **6,** 291–306 (2013).

225. Brissette, C. A. *et al.* The Borrelial Fibronectin-Binding Protein RevA Is an Early Antigen of Human Lyme Disease. *Clin. Vaccine Immunol. CVI* **17,** 274–280 (2010).

226. Nowalk, A. J., Gilmore, R. D. & Carroll, J. A. Serologic proteome analysis of Borrelia burgdorferi membrane-associated proteins. *Infect. Immun.* **74,** 3864–3873 (2006).

227. Magnarelli, L. A., Ijdo, J. W., Padula, S. J., Flavell, R. A. & Fikrig, E. Serologic Diagnosis of Lyme Borreliosis by Using Enzyme-Linked Immunosorbent Assays with Recombinant Antigens. *J. Clin. Microbiol.* **38,** 1735–1739 (2000).

228. Nowakowski, J. *et al.* Laboratory diagnostic techniques for patients with early Lyme disease associated with erythema migrans: a comparison of different techniques. *Clin. Infect. Dis. Off. Publ. Infect. Dis. Soc. Am.* **33,** 2023–2027 (2001).

229. Gomes-Solecki, M. J. C. *et al.* Recombinant assay for serodiagnosis of Lyme disease regardless of OspA vaccination status. *J. Clin. Microbiol.* **40,** 193–197 (2002).

230. Coleman, A. S. *et al.* BBK07 Immunodominant Peptides as Serodiagnostic Markers of Lyme Disease. *Clin. Vaccine Immunol. CVI* **18,** 406–413 (2011).

231. Gomes-Solecki, M. J. C., Meirelles, L., Glass, J. & Dattwyler, R. J. Epitope Length, Genospecies Dependency, and Serum Panel Effect in the IR6 Enzyme-Linked Immunosorbent Assay for Detection of Antibodies to Borrelia burgdorferi. *Clin. Vaccine Immunol. CVI* **14,** 875–879 (2007).

232. Wormser, G. P., Aguero-Rosenfeld, M. E. & Nadelman, R. B. Lyme disease serology: problems and opportunities. *JAMA* **282,** 79–80 (1999).

233. Halperin, J. J. Nervous system lyme disease: diagnosis and treatment. *Rev. Neurol. Dis.* **6,** 4–12 (2009).

APPENDICES

LIST OF ABBREVIATIONS

AA	Allylamine
AAc	acrylic acid
AU	arbitrary units
BAC	bis(acryloyl)cystamine
Bb	*Borrelia* burgdorferi
BIS	N, N′-methylenebisacrylamide
CDC	centers for disease control
CV	coefficient of variation
DHEA	Dihydroxyethylenebis-acrylamide
EIA	enzyme immunoassay
EM	erythema migrans
IRB	internal review board
LB	Lyme Borreliosis
LD	Lyme Disease
LFA	Lateral Flow Assay
LLD	lower limit of detection
LLQ	lower limit of quantification
mAb	monoclonal antibody
NIPAm	N-isopropylacrylamide
OspA	outer surface protein A
PCR	polymerase chain reaction
PDB	protein data bank
SD	standard deviation
TLR2	toll like receptor 2
TLR8	toll like receptor 8
WB	western blot

SUPPLEMENTARY FIGURES

Supplementary table 1. List of 27 candidate relevant proteins statistically significant (raw p-value) and/or with a biological relevance in at least one of the following comparisons: cases vs controls, metastatic vs controls, non-metastatic vs controls, metastatic vs non–metastatic cases.

protein	27 cases vs 13 controls (486 considered proteins)		10 metastatic vs 13 controls (335 considered proteins)		17 non-metastatic vs 13 controls (389 considered proteins)		10 metastatic vs 17 non-metastatic (437 considered proteins)	
	p-value logistic model	p-value fisher	p-value logistic model	p-value fisher	p-value logistic model	p-value fisher	p-value logistic model	p-value fisher
fibrinogen alpha polypeptide isoform alpha-E preprotein	0.01	0.01	0.00	0.00	0.05	0.06	0.073	0.091
pancreatic ribonuclease precursor	0.28	0.39	0.09	0.13	0.71	1.00	0.105	0.153
fibrinogen, gamma chain isoform gamma-A	0.03	0.03	0.94	0.01	0.18	0.26	0.954	0.124
inter-alpha (globulin) inhibitor H4	0.08	0.07	0.02	0.02	0.27	0.35	0.066	0.101
alpha 1 type XVIII collagen isoform 1 precursor	0.10	0.12	0.95	0.05	0.38	0.44	0.959	0.264
latent transforming growth factor beta binding protein 2	0.85	1.00	0.71	1.00	0.98	1.00	0.712	1.000
insulin-like growth factor binding protein 4	0.96	0.04	0.95	0.01	0.96	0.24	0.086	0.102
insulin-like growth factor binding protein 6	0.28	0.39	0.09	0.13	0.71	1.00	0.105	0.153
histidine-rich glycoprotein precursor	0.96	0.04	0.95	0.01	0.96	0.24	0.086	0.102
procollagen C-endopeptidase enhancer	0.96	0.02	0.96	0.07	0.95	0.02	0.778	1.000
alpha 1 type I collagen preprotein	0.95	0.00	0.94	0.00	0.95	0.02	0.218	0.257
melanoma inhibitory activity	0.15	0.23	0.09	0.13	0.27	0.35	0.370	0.415
plasma kallikrein B1	0.96	0.28	0.96	0.07	0.98	1.00	0.121	0.128
neural proliferation, differentiation and control, 1	0.81	1.00	0.41	0.62	0.77	1.00	0.253	0.326
alpha 2 type I collagen	0.95	0.00	0.94	0.00	0.95	0.02	0.218	0.257
complement factor D	0.96	0.15	0.96	0.07	0.97	0.49	0.253	0.326
elastin isoform a precursor	0.96	0.15	0.96	0.07	0.97	0.49	0.253	0.326
seleroprotein P isoform 1	0.38	0.64	0.09	0.13	0.84	1.00	0.052	0.047
matrix Gla protein	0.28	0.39	0.09	0.13	0.71	1.00	0.105	0.153
GDNF family receptor alpha 2 preproprotein	0.81	1.00	0.20	0.34	0.41	0.56	0.052	0.047
immunoglobulin superfamily, member 8	0.33	0.37	0.71	1.00	0.96	0.07	0.962	0.041
matrix metalloproteinase 14 preproprotein	0.97	0.54	0.97	0.18	0.98	1.00	0.286	0.535
complement factor H-related 3	0.97	1.00	0.97	0.18	.	.	0.969	0.128
ST6 beta-galactosamide alpha-2,6-sialyltranferase 2	0.96	0.28	0.96	0.07	0.98	1.00	0.121	0.128
mannosyl (alpha-1,3-) glycoprotein beta-1,2-N-acetylglucosaminyltransferase	0.97	1.00	0.97	0.18	.	.	0.969	0.128
somatostatin preproprotein	0.97	0.54	0.97	0.18	0.98	1.00	0.286	0.535
significance level of 0.05;								
significance level of 0.10								

Supplementary table 2. Clinical and diagnostic information of patients suspected of having

early stage Lyme disease N=51 (N= 117 healthy volunteers were recruited under informed consent and included in the study). Treatment: Dx = doxycycline, Pd = prednisone, RC = rocepherin, sv = synovectomy, st = steroids, Am = amoxil, Zm = Zithromax. Urine collection timing and presence of symptoms: B = before treatment, PT = during or after treatment, symptoms present at the time urine was collected.

Supplementary table 2. Clinical and diagnostic information of patients suspected of having

Pt ID#	Clinical manifestation	Treatment	Serology results* (ELISA, IgG, IgM)	Urine collection timing	OspA urine test **
1	joint pain, malaise, neck pain, headache, nausea, dizziness	Dx	N, ND, ND	PT	N
3	EM, bell's palsy, myalgia	Dx, Pd	P, N, N	PT	P
8	myalgia, fever, joint pain	Dx, Rc, Sv	P, P, N	PT	P
11	EM, Bell's palsy, joint pain	Dx, Rc	N, ND, ND	PT	P
13	EM, fever, joint pain, neck pain, fatigue	Dx	P, N, P	PT	P
14	joint pain	St, Dx	P, P, ND	PT	P
15	EM, myalgia, fever, joint pain, malaise, fatigue	Rc, Pc	P, N, P	PT	P
17	joint pain	Dx, Rc	P, P, N	PT	P
18	EM, fever, joint pain	Dx	P, P, P	PT	P
21	Headaches	Dx	N, N, N	PT	P
23	EM, fever, anthralgiatis	Am	P, P, P	B	P
24	EM, fever, anthralgias	Zm	P, N, P	PT	P
25	EM, fever, neck pain, fatigue	Dx	P, N, P	B	P
26	EM, anthralgiatis	Dx, Rc, Am	N, N, N	PT	P
27	EM, fatigues, anthralgiatis	Dx, Zm	ND, ND, ND	PT	P
102	EM		N, ND, ND	PT	P
103	fatigue, joint pain, pos for Lyme on lumber puncture	Dx	P, P, N	PT	P
103.1	No symptoms	Rc	P, P, N	-	N
105	joint pain, arthritis	Dx	P, N, N	PT	P
108	EM, fever, joint pain	Dx	P, N, P	B	P
108.1	no symptoms	Dx	P, N, P	-	N
113	EM, fever, neck pain, fatigue		P, N, P	PT	P
116	joint paint, fatigue		N, ND, ND	-	N
117	Tick bite		N, NA	B	P
118	EM fatigue		P, P, P	B	P
119	joint pain, arthritis, fatigue, neurologic	Dx	P, N, P	PT	P
120	EM, fever, malaise	Dx	P, N, P	B	P
120.1	No symptoms	Dx	P, N, P	-	N
121	EM	Dx	N, NA, NA	B	P

early stage Lyme disease N=51 (N= 117 healthy volunteers were recruited under informed consent and included in the study) (continued).

133	joint pain, fever, fatigue		N, N, N	-	N
139	joint pain, fatigue	Dx	P, N, P	B	P
139.1	No symptoms		P, N, P	-	P
142	rash joint pain		P, N, P	B	P
148	joint pain, fatigue		P, P, P	B	P
151	fatigue	Dx	P, N, N	PT	P
169	EM, neck stiffness, migraine		Equivocal	B	P
180	EM, tick bite	Dx	N, N, N	B	P
180.1	no symptoms	Dx	P, N, P	-	N
601	EM	Az	Equiv	B	P
601.1	no symptoms	Az	Equiv	-	N
602	EM	Dx	N, ND, ND	B	P
603	EM	Dx	P, P, P	B	P
604	EM	Dx	ND	B	P
605	EM	Dx	ND	B	P
606	EM	Dx	ND	B	P
607	EM	Dx	Equiv	B	P
608	EM	Dx	ND	B	P
623	EM	Dx	N, ND, ND	B	P
623.1	EM	Dx	N, ND, ND	-	P
623.2	EM	Dx	N, ND, ND	-	N
623.3	EM	Dx	N, ND, ND	-	N
623.4	EM	Dx	N, ND, ND	-	N
623.5	EM	Dx	N, ND, ND	-	N

N=negative, P=positive, ND=not done

**N=negative; P=positive confirmed by competition

Supplementary Table 3. Sequences of peptides tested for antibody binding.

Peptide ID	*Sequence*	*Reactivity with mAb 0551*
OspA peptide 1	KQNVSSLDEKNSASVDLPGE	Negative
OspA peptide 2	VLKNFTLEGKVANDKTLEV	Negative
OspA peptide 3	EVKEGTVTLSKEIAKSGEVT	Negative
OspA peptide 4	VALNDTNTTQATKKTGAWDS	Negative
OspA peptide 5	KTSTLTISVNSKKTTQL**VFTK**	Positive
OspA peptide 6	QL**VFTK**QDTITVQKYDSAGT	Positive
OspA peptide 7	NLEGTAVEIKTLDELKNALK	Negative
OspA219-253	KTSTLTISVNSKKTTQL**VFTK**QDTITVQKYDSAGT	Positive
OspA219-235	KTSTLTISVNSKKTTQL	Negative
OspA240-253	QDTITVQKYDSAGT	Negative

Supplementary Table 4. The mAb epitope used herein (red rectangle) is conserved in common pathogenic species of Borrelia. BAA22342.1 in Borrelia garinii Taxonomy ID 29519, ADD14639.1 in Borrelia burgdorferi taxonomy ID 139, WP_012665647.1 in Borrelia valaisiana taxonomy ID 62088, WP_012665647.1 in Borrelia sp. SV1 taxonomy ID 498741[114], YP_003110622.1 in Borrelia burgdorferi 297 taxonomy ID 521009, NP_045688.1 in Borrelia burgdorferi B31 taxonomy ID 224326, WP_014023199.1 in Borrelia bissettii taxonomy ID 64897, ADG02035.1 in Borrelia afzelii taxonomy ID 29518, AAN65460.1 in Borrelia spielmanii taxonomy ID 88916 [115]. BLAST analysis was performed on the sequence KTSTLTISVNSKTTQLVFTKQDTITVQKYDSAGT (combination of peptide 5 and 6) with the following organisms: Treponema pertenue (taxonomy ID 168), Leptospiraceae (taxonomy ID 170), Treponema (taxonomy ID 157), Spirochaetes (taxonomy ID 203691) excluding Borrelia (taxonomy ID 138), Homo sapiens (taxonomy ID 9606), Epstein-Barr virus EBV (taxid:10376), Human cytomegalovirus (taxid:10359), herpes simplex virus 1 HSV-1 (taxid:10298), hepatitis C virus HCV (taxid:11103), Babesia txid5864, Anaplasma txid768, Ehrlichieae txid942,Bartonella txid773, Rickettsias txid766. No significant similarity found. No homology was identified.

```
BAA22342.1        1     -----LGIGLILALIACKQNVSSLDEKNSVSVDLPGEMKVLVSKEKDKDGKYSLMA
ADD14639.1        1     ----------ILALIACKQNVSSLDEKNSVSVDLPGEMKVLVSKEKNKDGKYDLIA
WP_012672372.1    1     MKKYLLGIGLILALIACKQNVSSLDEKNSVSVDLPGEIKVLVSKEKNKDGKYSLMA
WP_012665647.1    1     MKKYLLGIGLILALIACKQNVSSLDEKNSASVDLPGEMKVLVSKEKDKDGKYSLVA
YP_003110622.1    1     MKKYLLGIGLILALIACKQNVSSLDEKNSVSVDLPGEMKVLVSKEKNKDGKYDLIA
NP_045688.1       1     MKKYLLGIGLILALIACKQNVSSLDEKNSVSVDLPGEMKVLVSKEKNKDGKYDLIA
WP_014023199.1    1     MKKYLLGIGLILALIACKQNVSGLDEKNSVSVDLPGEMKVLVSKEKDKDGKYSLMA
ADG02035.1        1     ------------ALIACKQNVSSLDEKNSASVDLPGEMKVLVSKEKDKDGKYSLKA
AAN65460.1        1     ----------ILALIACKQNVSGLDEKNSTSVDVPGELKVLVSKEKDKDGKYSLMA

BAA22342.1        52    TVDKLELKGTSDKSNGSGILEGVKTDKSKAKLTISDDLSKTTFEVFKEDGKTLVSR
ADD14639.1        47    TVDKLELKGTSDKNNGSGVLEGVKADKSKVKLTISDDLGQTTLEVFKEDGKTLVSK
WP_012672372.1    57    TVDKLELKGTSDKNNGSGVLEGVKADKSKVKLTVSDDLGQTTLEVLKEDGKTLVSR
WP_012665647.1    57    TVDKVELKGTSDKNNGSGTLEGVKDDKSKVKLTISDDLGETKLETFKEDG-TLVSR
YP_003110622.1    57    TVDKLELKGTSDKNNGSGVLEGVKADKSKVKLTISDDLGQTTLEVFKEDGKTLVSK
NP_045688.1       57    TVDKLELKGTSDKNNGSGVLEGVKADKSKVKLTISDDLGQTTLEVFKEDGKTLVSK
WP_014023199.1    57    TVDKLELKGTSDKNNGSGILEGVKADKSKVKLTVSEDLSTTTLEVLKEDGKTLVSK
ADG02035.1        45    TVDKIELKGTSDKDNGSGVLEGTKDDKSKAKLTIADDLSKTTFELFKEDGKTLVSR
AAN65460.1        47    TVDKLELKGTSDKNDGSGVLEGVKADKSKVKLTISDHLSKTTFEVFKEDGKTLVSR

BAA22342.1        108   KVNSKDKSSTEEKFNAKGELSEKVVTRANGNRLEYTEI-KSDGSGKAKEVLKDFTL
ADD14639.1        103   KVTSKDKSSTEEKFNEKGEVSEKIITRADGTRLEYTEI-KSDGSGKAKEVLKG-YV
WP_012672372.1    113   KVTSKDKSSTEEKFNEKGELAEKIMTRANGTRLEYTEI-KSDGSGKAKEVLKD-YV
WP_012665647.1    112   KVNFKDKSFTEEKFNEKGEVSEKILTRSNGTTLEYSQMtDAENATKAVETLKNgIK
YP_003110622.1    113   KVTSKDKSSTEEKFNEKGEVSEKIITRADGTRLEYTEI-KSDGSGKAKEVLKG-YV
NP_045688.1       113   KVTSKDKSSTEEKFNEKGEVSEKIITRADGTRLEYTGI-KSDGSGKAKEVLKG-YV
WP_014023199.1    113   KTTSKDKSSTEEKFNDKGELAEKTIVRANGTRLEYTEV-KSDGSGKAKETLKD-YA
ADG02035.1        101   KVSSKDKTSTDEMFNEKGELSAKTMTRENGTKLEYTEM-KSDGTGKAKEVLKN-FT
AAN65460.1        103   NVNSKDKSSTKEKFNEKGELSEKTLVRANGTKLEYTEI-KSDGTGKAKEVLKD-FT

BAA22342.1        163   LEGTLTADKTTLTIQEGSVTLSKNIAKSGEITVELNDTDSS-GDKKSGQWNSSTST
ADD14639.1        157   LEGTLTAEKTTLVVKEGTVTLSKNISKSGEVSVELNDTDSSAATKKTAAWNSGTST
WP_012672372.1    167   LEGTLTAEKTTLVVKEGTVTLSKHISKSGEVTAELNDTESSSATKKTAAWNSGTST
WP_012665647.1    168   LPGNLVGGKTTLKITEGTVTLSKHIAKSGEVTVEINDTSSTPNTKKTGKWDARNST
YP_003110622.1    167   LEGTLTAEKTTLVVKEGTVTLSKNISKSGEVSVELNDTDSSAATKKTAAWNSGTST
NP_045688.1       167   LEGTLTAEKTTLVVKEGTVTLSKNISKSGEVSVELNDTDSSAATKKTAAWNSGTST
WP_014023199.1    167   LEGTLTAEKATLVVKEGTVTLSKHISKSGEVTAELNDTDSAQATKKTGKWDAGTST
ADG02035.1        155   LEGKVANDKVTLEVKEGTVTLSKEIAKSGEVTVALNDTNTTQATKKTGAWDSKTST
AAN65460.1        157   LEGTLANEKATLTVKEGTVTLSKNIDKSGEVTVALNDTDSTAATKKTGAWDSKTST

BAA22342.1        218   LTISAKSKKTKDIVFTKQDTITVQKYDSAGTNLEGSAVEIKTLDELKNALK
ADD14639.1        213   LTITVNSKKTKDIVFTKENTITVQQYDSNGTKLEGSAVEITKLDEIKNALR
WP_012672372.1    223   LTITVNSKKTKDIVFTKENTITVQKYDTAGTNLEGSAVEIKKLDELKNALK
WP_012665647.1    224   LTIIVDSKNKTKIVFTKQDTITVQSYNPAGNKLEGTAVEIKTLQELKNALK
YP_003110622.1    223   LTITVNSKKTKDIVFTKENTITVQQYDSNGTKLEGSAVEITKLDEIKNALK
NP_045688.1       223   LTITVNSKKTKDIVFTKENTITVQQYDSNGTKLEGSAVEITKLDEIKNALK
WP_014023199.1    223   LTISVNSKKTKNIVFTKQDTITVQKYDSAGTNLEGTAVEIKTLDELKNALK
ADG02035.1        211   LTISVNSKKTTQIVFTKQDTITVQKYDSAGTNLEGTAVEIKTLDELKNA--
AAN65460.1        213   LTITVNSKKTKDIVFTKQDTITVQKYDSAGTNLEGSAVEIK----------
```

*Supplementary table 5: Post treatment patients being evaluated for recurrent or persistent disseminated Lyme disease derived from a Lyme endemic geographic region. **(N=negative; P=positive confirmed by competition)*

PtID#	Clinical Manifestation	Serology results (IgG, IgM)	OspA urine test**
300	Neurocognitive	ND	N
306	Neurologic	ND	N
309	Neurologic	ND	N
310	Joint pain	ND	N
315	Joint pain	ND	P
318	Joint pain	ND	N
319	Bladder pain	ND	N
320	Neurologic	ND	N
323		ND	P
324	asymptomatic	ND	N
327	Bladder pain	ND	N
328	Bladder pain	ND	P
329	Joint pain	ND	N
331	neurologic	ND	N
333	Bladder pain	ND	N
334	Joint pain	ND	P
336	Fatigue	ND	N
337	Joint pain	ND	P
339	neurologic	ND	P
340	Neurologic	ND	P
341	Joint pain	ND	P
343	Myalgia	ND	N
344	Neurolocognitive	ND	N
346	EM	N,P	P
347	Neurologic	ND	P
348	Neurologic	ND	N
349	Neurocognitive	ND	P
350	Neurologic	ND	P
353	Neurologic	ND	N
355	Neurologic	ND	N
356	Neurologic	ND	P
360	Joint pain	ND	P
361	fatigue	ND	N
363	Joint pain	ND	N
364	Joint pain	ND	N
377	Joint pain	ND	N
378	Neurologic	ND	N
379	Neurologic	ND	P
380	Fatigue	ND	P
381	Joint pain	ND	P
382	Joint pain	ND	P
383	Neurologic	ND	P
384	Joint pain	N,N	P

*Supplementary table 5: Post treatment patients being evaluated for recurrent or persistent disseminated Lyme disease derived from a Lyme endemic geographic region. **(N=negative; P=positive confirmed by competition) (continued).*

386	Joint pain	ND	N
388	Joint pain, fatigue	ND	P
389	Joint pain	ND	P
390	Joint pain	N,N	P
391	Joint pain	N, P	N
392	Joint pain	N, N	N
393	Joint pain	ND	P
394	Joint pain	N, N	N
397		ND	N
400	EM	N, N	N
401		ND	N
402		ND	N
403		ND	N
404		ND	N
406	Neurocognitive	ND	N
407	Joint pain	N,N	P
410		N,N	P
413		ND	N
414	Joint pain	ND	N
416		ND	N
417		ND	N
419		ND	P
421		ND	N
424	Neurologic	N,N	N
425		N,N	P
426		ND	N
427	EM, joint pain	N,N	P
429	Neurologic	ND	N
430	Neurocognitive	ND	N
431	Neurologic	ND	N
433	Joint pain	ND	N
435	Neurocognitive	ND	N
437		ND	P
438	Joint pain	ND	P
439	Joint pain	ND	P
443	Myocarditis	ND	P
446	Neurocognitive	ND	N
452	Myalgia	ND	N
458	Joint pain	ND	N
459		ND	N
465		ND	N
466	Joint pain	ND	N

*Supplementary table 5: Post treatment patients being evaluated for recurrent or persistent disseminated Lyme disease derived from a Lyme endemic geographic region. **(N=negative; P=positive confirmed by competition) (continued).*

469			P
470			N
478		ND	N
487	Neurocognitive, Fatigue	ND	N
488	Neurocognitive, Neurological	ND	P
489	Joint pain, Fatigue	ND	P
490		ND	P
491		ND	N
492	Fatigue	ND	P
493	Neurocognitive	ND	N
495	Neurocognitive	ND	P
497		ND	P
498	Neurocognitive	ND	N
499		ND	N
500		ND	N
501	Joint pain	ND	P

Supplementary table 6. Quantification of the amount of remazol brilliant blue (RBB) dye covalently bound to the Nanotrap particles and percentage of reacted acrylic acid (AAc) moles. This information is obtained and recorded for every batch of produced Nanotrap particles (example batch # RM37B4 is reported here).

Parameter	**Numerical value**	**Unit of Measure**
Weight of 20 mL of freezed dried poly(NIPAm-co-AAc) Nanotrap*	110	Mg
Weight of 20 mL of freeze dried poly(NIPAm/RBB) Nanotrap	153	Mg
Δ weight	43	Mg
Molar quantity of RBB covalently bound to the Nanotrap	0.0686	Mmol
Molar quantity of AAc in the poly(NIPAm-co-AAc) Nanotrap	0.2430	Mmol
Percentage of mol RBB bound to AAc / tot mol AAc	28	%

*Note: The weight is relative to the poly(NIPAm-co-AAc) Nanotrap before RBB covalently binding.

Supplementary table 7. List of proteins identified by Mass-spec analysis performed on Lyme antigen Grade 2.

Proteins	P (pro)	MW	Peptide Hits
outer surface protein A	2.22E-15	29421.7	47
60 kDa heat shock protein	2.66E-14	58915.0	29
elongation factor Tu	6.66E-15	43371.5	29
glyceraldehyde 3-phosphate dehydrogenase, partial	1.00E-30	34582.3	29
integral outer membrane protein p66	2.22E-16	68129.8	28
outer surface protein B (plasmid)	1.00E-30	31713.6	25
heat-shock protein	8.88E-15	69232.8	24
chaperonin GroS	8.16E-11	9899.5	23
PTS system transporter subunit IIBC (plasmid)	1.00E-30	58899.2	22
DNA-directed RNA polymerase subunit beta'	2.66E-14	154560.7	21
enolase	1.00E-30	47260.4	19
A Chain A, The Crystal Structure Of Aminopeptidase I From Borrelia Burgdorferi B31	1.41E-13	51341.9	17
DNA gyrase subunit A	1.34E-13	91322.5	17
oligopeptide permease periplasmic binding protein	3.33E-16	62315.8	17
phosphoglycerate kinase	1.00E-30	42319.2	15
borrelia P83/P100 antigen	3.37E-11	79910.6	14
membrane lipoprotein BmpA	8.22E-13	36885.3	14
ospB	2.06E-05	31755.7	12
aminoacyl-histidine dipeptidase	3.92E-11	53542.7	10
DNA-directed RNA polymerase subunit beta	6.66E-15	129543.5	10
hypothetical protein BB_0238	1.13E-11	29643.5	10
L-lactate dehydrogenase	1.92E-09	34879.3	10
periplasmic serine protease DO	9.87E-09	52039.5	10
B Chain B, X-Ray Crystal Structure Of A Periplasmic Oligopeptide-Binding ProteinOLIGOPEPTIDE ABC TRANSPORTER(OPPAIV) FROM BORRELIA Burgdorferi	7.92E-12	60505.8	9
flagellar filament outer layer protein	3.60E-12	38416.8	9
glycerol kinase	1.00E-30	55570.8	9
oligopeptide permease periplasmic binding protein	5.55E-15	59876.1	9

Supplementary table 7. List of proteins identified by Mass-spec analysis performed on Lyme antigen Grade 2 (continued).

phosphoglycerate kinase	1.00E-30	42319.2	15
borrelia P83/P100 antigen	3.37E-11	79910.6	14
membrane lipoprotein BmpA	8.22E-13	36885.3	14
ospB	2.06E-05	31755.7	12
aminoacyl-histidine dipeptidase	3.92E-11	53542.7	10
DNA-directed RNA polymerase subunit beta	6.66E-15	129543.5	10
hypothetical protein BB_0238	1.13E-11	29643.5	10
L-lactate dehydrogenase	1.92E-09	34879.3	10
periplasmic serine protease DO	9.87E-09	52039.5	10
B Chain B, X-Ray Crystal Structure Of A Periplasmic Oligopeptide-Binding ProteinOLIGOPEPTIDE ABC TRANSPORTER(OPPAIV) FROM BORRELIA Burgdorferi	7.92E-12	60505.8	9
flagellar filament outer layer protein	3.60E-12	38416.8	9
glycerol kinase	1.00E-30	55570.8	9
oligopeptide permease periplasmic binding protein	5.55E-15	59876.1	9
P22	1.83E-09	21809.0	9
fructose-bisphosphate aldolase	2.55E-14	39955.3	8
glycerol-3-phosphate dehydrogenase, partial	6.77E-14	54933.2	8
hypothetical protein BB_0323	1.45E-12	44123.4	8
hypothetical protein (plasmid)	1.33E-14	34535.2	7
phosphoenolpyruvate-protein phosphatase	5.39E-12	64554.9	7
elongation factor G	4.03E-10	77523.8	6
Fla, partial	1.16E-05	15751.8	6
long-chain-fatty-acid CoA ligase	2.92E-12	72841.3	6
outer membrane protein (plasmid)	2.78E-14	19210.1	6
outer surface protein A	1.73E-07	29375.7	6
phosphotransferase enzyme II	5.78E-12	20768.0	6
protein GrpE	1.24E-10	21925.3	6
30S ribosomal protein S1	4.00E-11	63209.0	5
30S ribosomal protein S4	2.41E-13	23938.3	5
AF288609_1 BmpD	1.83E-09	37068.1	5
B Chain B, Structure Of A Pyrophosphate-dependent Phosphofructokinase From The Lyme Disease Spirochete Borrelia Burgdorferi	8.88E-15	62437.5	5

Supplementary table 7. List of proteins identified by Mass-spec analysis performed on Lyme antigen Grade 2 (continued).

D Chain D, Crystal Structure Of A Phosphoglycerate Mutase Gpma From Borrelia Burgdorferi B31	2.72E-10	31099.4	5
DNA-directed RNA polymerase subunit alpha	4.69E-09	38530.1	5
hypothetical protein BB_0752	1.60E-08	57398.6	5
peptidase	1.77E-11	67584.6	5
polyribonucleotide nucleotidyltransferase	4.81E-09	79261.1	5
ribosomal protein L25, partial	4.00E-07	21177.4	5
transcription elongation factor GreA	6.25E-09	105248.4	5
triosephosphate isomerase	3.86E-08	27741.5	5
30S ribosomal protein S2	4.04E-07	29657.8	4
30S ribosomal protein S6	1.49E-10	16426.8	4
30S ribosomal protein S7	1.65E-13	18240.6	4
30S ribosomal protein S9	2.05E-10	15407.2	4
50S ribosomal protein L13	9.21E-08	16683.2	4
50S ribosomal protein L15	3.97E-13	16029.0	4
50S ribosomal protein L4	1.08E-09	23477.9	4
A Chain A, Crystal Structure Of A Putative 5'-methylthioadenosine/s-Adenosylhomocysteine Nucleosidase From Borrelia Burgdorferi B31 Bound To Adenine (target Nysgrc-029268)	2.45E-06	29030.7	4
arginine--tRNA ligase	1.96E-08	66809.9	4
ATP-dependent zinc metalloprotease FtsH	2.22E-15	70758.3	4
bifunctional methylenetetrahydrofolate dehydrogenase/methenyltetrahydrofolate cyclohydrolase	1.21E-11	34010.5	4
D Chain D, Napa Protein From Borrelia Burgdorferi	3.69E-07	17740.0	4
DNA polymerase III subunit beta	1.87E-09	44586.0	4
elongation factor Ts	2.95E-13	31284.7	4
F Chain F, Transition State Mimic Of Nucleoside-Diphosphate Kinase From Borrelia Burgdorferi With Bound Vanadate And Adp	1.56E-04	21646.9	4
flagellin	2.13E-13	35742.9	4

Supplementary table 7. List of proteins identified by Mass-spec analysis performed on Lyme antigen Grade 2 (continued).

hypothetical protein BB_K13 (plasmid)	4.50E-10	26517.8	4
peptidase S41	6.07E-11	53508.1	4
superoxide dismutase	2.89E-14	23507.9	4
transcription termination/antitermination protein NusA	3.76E-08	54782.5	4
50S ribosomal protein L18	7.34E-06	13713.7	3
50S ribosomal protein L7/L12	1.77E-07	12895.9	3
50S ribosomal protein L9	4.93E-10	19946.8	3
aminopeptidase	3.39E-10	47354.8	3
basic membrane protein	1.52E-07	37972.0	3
chaperone protein DnaJ	5.49E-09	40472.8	3
flagellar hook protein FlgE	6.06E-10	47359.9	3
hypothetical protein BB_0713	9.40E-06	29688.6	3
hypothetical protein BB_0751	4.28E-06	39518.5	3
methionine aminopeptidase	3.23E-08	27693.7	3
protein HflC	4.57E-05	33282.1	3
UDP-N-acetylglucosamine 1-carboxyvinyltransferase	8.28E-11	46579.9	3
unknown, partial	1.35E-09	8117.2	3
30S ribosomal protein S11	7.46E-09	13870.4	2
30S ribosomal protein S13	1.16E-07	14068.8	2
30S ribosomal protein S3	4.11E-05	33122.2	2
30S ribosomal protein S5	2.63E-07	17767.7	2
30S ribosomal protein S8	6.08E-09	14805.0	2
3-hydroxy-3-methylglutaryl-CoA synthase	2.01E-04	46000.3	2
50S ribosomal protein L1	2.23E-06	25651.6	2
50S ribosomal protein L11	3.62E-07	15158.3	2
50S ribosomal protein L2	6.19E-07	30572.6	2
50S ribosomal protein L20	1.32E-08	13460.7	2
50S ribosomal protein L22	3.84E-05	13657.4	2
50S ribosomal protein L5	8.13E-08	20403.1	2
50S ribosomal protein L6	2.55E-06	19926.0	2
acetyl-CoA C-acetyltransferase	4.87E-06	42913.6	2
AF305611_1 LMP1	1.26E-07	97373.1	2
aminopeptidase II	1.18E-07	46769.2	2

Supplementary table 7. List of proteins identified by Mass-spec analysis performed on Lyme antigen Grade 2 (continued).

ATP synthase subunit A	5.07E-06	63992.9	2
ATP-dependent Clp protease proteolytic subunit	7.24E-08	22201.9	2
ATP-dependent protease La	3.55E-08	90653.2	2
ATP-dependent protease subunit HslV	1.43E-06	19624.5	2
B Chain B, 2.4 A Resolution Crystal Structure Of Borrelia Burgdorferi Inosine 5'- Monphosphate Dehydrogenase In Complex With A Sulfate Ion	8.71E-06	43740.0	2
B Chain B, Erpc, A Member Of The Complement Regulator Acquiring Family Of Surface Proteins From Borrelia Burgdorfei, Possesses An Architecture Previously Unseen In This Protein Family.	9.36E-12	18287.3	2
cell division protein FtsZ	7.77E-15	42371.8	2
cysteine desulfurase	1.49E-11	48094.4	2
family 5 extracellular solute-binding protein	2.25E-08	59864.0	2
flagellar assembly protein FliH	5.61E-10	35168.8	2
flagellar basal body-associated protein FliL	4.44E-14	20047.7	2
GroEL, partial	3.42E-08	9830.2	2
hypothetical protein BB_0195	2.06E-10	44095.8	2
hypothetical protein BB_0405	2.23E-09	22237.7	2
hypothetical protein BB_0749	1.00E+00	48642.2	2
hypothetical protein BBA69, partial (plasmid)	3.20E-07	30402.3	2
lipoprotein	5.55E-06	21852.1	2
long-chain-fatty-acid CoA ligase	6.55E-09	70717.7	2
lysine--tRNA ligase	4.05E-11	60900.4	2
membrane fusion protein	7.03E-09	35021.2	2
methionine--tRNA ligase	8.21E-11	85160.6	2
methyl-accepting chemotaxis protein	2.66E-10	84517.5	2
outer membrane protein	7.62E-09	94508.4	2
P34 protein	1.25E-13	34114.0	2
PF-49 protein (plasmid)	2.74E-10	21934.0	2
protein RepU (plasmid)	4.56E-12	25824.0	2

Supplementary table 7. List of proteins identified by Mass-spec analysis performed on Lyme antigen Grade 2 (continued).

RepU (plasmid)	2.76E-08	18734.8	2
spermidine/putrescine ABC transporter substrate-binding protein	2.05E-08	40655.1	2
1-phosphofructokinase	3.55E-04	33573.5	1
30S ribosomal protein S10	1.00E+00	11758.6	1
30S ribosomal protein S15	5.19E-05	10210.8	1
30S ribosomal protein S16	4.05E-06	10030.4	1
30S ribosomal protein S17	1.15E-04	9845.6	1
30S ribosomal protein S19	9.47E-09	10403.7	1
30S ribosomal protein S20	1.42E-04	9940.9	1
4-methyl-5(b-hydroxyethyl)-thiazole monophosphate biosynthesis protein	1.00E+00	19871.4	1
50S ribosomal protein L10	6.57E-05	18047.9	1
50S ribosomal protein L14	1.39E-05	13435.3	1
50S ribosomal protein L16	4.85E-05	15558.4	1
50S ribosomal protein L19	3.10E-07	14001.9	1
50S ribosomal protein L23	2.50E-05	11136.1	1
50S ribosomal protein L25/general stress protein Ctc	5.32E-07	20437.0	1
50S ribosomal protein L3	2.09E-10	22198.0	1
A Chain A, Crystal Structure Of Complement Factors H And Fhl-1 Binding Protein Bbh06 Or Crasp-2 From Borrelia Burgdorferi (native)	4.82E-09	25001.9	1
A Chain A, Crystal Structure Of Psts (bb_0215) From Borrelia Burgdorferi	9.65E-07	29292.2	1
ABC transporter ATP-binding protein	8.71E-09	35161.4	1
acetate kinase, partial	1.11E-15	45307.3	1
acylphosphatase (plasmid)	2.26E-11	11035.7	1
AF410891_1 putative partitioning protein (plasmid)	1.80E-07	29505.7	1
aminopeptidaseI-like	1.73E-05	51467.6	1
arginine deiminase	4.03E-06	46814.2	1
asparagine--tRNA ligase	9.65E-04	53080.5	1
aspartyl/glutamyl-tRNA(Asn/Gln) amidotransferase subunit B	2.29E-13	54486.5	1

Supplementary table 7. List of proteins identified by Mass-spec analysis performed on Lyme antigen Grade 2 (continued).

ATP-dependent DNA helicase RecG	7.44E-06	78993.6	1
ATP-dependent protease ATP-binding subunit ClpX	3.62E-04	47571.5	1
B Chain B, Bbcrasp-1 From Borrelia Burgdorferi	1.00E+00	21433.4	1
B Chain B, Crystal Structure Of A Glutamyl-Trna Synthetase Glurs From Borrelia Burgdorferi Bound To Glutamic Acid And Zinc	3.85E-08	59110.8	1
B Chain B, Crystal Structure Of Borrelia Burgdorferi Pur-alpha	9.02E-08	11299.7	1
B Chain B, Crystal Structure Of The Chex-Chey-Bef3-Mg+2 Complex From Borrelia Burgdorferi	1.66E-05	18762.0	1
Borrelia burgdorferi REV protein (plasmid)	4.19E-04	17879.4	1
carboxypeptidase	4.22E-08	30656.4	1
cell division protein FtsA	1.97E-06	38216.4	1
chemoreceptor glutamine deamidase CheD	6.60E-06	18129.5	1
D Chain D, Crystal Structure Of Glycine Betaine, L-Proline Abc Transporter, GlycineBETAINEL-Proline-Binding Protein (Prox) From Borrelia Burgdorferi	4.79E-06	31730.0	1
D Chain D, Outer Surface Protein C (ospc) Of Borrelia Burgdorferi Strain B31	6.82E-07	18555.0	1
deoxyguanosine/deoxyadenosine kinase	5.24E-05	23645.3	1
DNA gyrase subunit B	9.02E-09	71406.4	1
DNA polymerase III subunit alpha	2.79E-04	132283.7	1
DNA-directed RNA polymerase subunit omega	5.05E-09	7573.9	1
dnaK suppressor	1.19E-07	14537.6	1
elongation factor P	7.64E-04	21399.6	1
ErpA8 protein (plasmid)	1.54E-09	19557.9	1
excinuclease ABC subunit A	4.13E-04	105729.7	1

F Chain F, Crystal Structure Of Glucosamine-6-phosphate Deaminase From Borrelia Burgdorferi	1.30E-08	32620.6	1
flagellar distal rod protein	4.87E-08	39950.2	1
flagellar motor switch protein FliG	1.92E-11	38982.7	1

Supplementary table 7. List of proteins identified by Mass-spec analysis performed on Lyme antigen Grade 2 (continued).

flagellar MS-ring protein FliF	8.84E-04	65093.2	1
flagellin	6.23E-05	35767.0	1
flagellin, partial	2.61E-05	17275.5	1
glucose-6-phosphate isomerase	3.87E-06	60083.2	1
glucose-6-phosphate isomerase	5.94E-06	60153.3	1
glycerol uptake facilitator	3.13E-05	27177.4	1
glycerol-3-phosphate dehydrogenase	9.26E-10	39442.8	1
glycine--tRNA ligase	1.91E-05	52176.2	1
glycosyl transferase	9.65E-07	42078.8	1
haloacid dehalogenase-like hydrolase	3.63E-09	33257.8	1
hypothetical protein BB_0227	1.47E-04	27473.4	1
hypothetical protein BB_0267	2.88E-06	70708.5	1
hypothetical protein BB_0345	6.57E-04	46427.4	1
hypothetical protein BB_0351	3.50E-07	60696.8	1
hypothetical protein BB_0429	3.54E-10	14687.0	1
hypothetical protein BB_0449	4.21E-10	11583.4	1
hypothetical protein BB_0458	3.52E-12	58175.1	1
hypothetical protein BB_0543	1.98E-09	24078.5	1
hypothetical protein BB_0563	1.46E-07	18806.0	1
hypothetical protein BB_0646	3.06E-06	37572.1	1
hypothetical protein BB_0650	9.80E-07	11434.8	1
hypothetical protein BB_0696	1.61E-05	9247.1	1
hypothetical protein BB_0739	1.02E-04	23087.2	1
hypothetical protein BB_A40 (plasmid)	5.24E-05	22348.6	1
hypothetical protein BB_A46 (plasmid)	1.43E-07	40334.1	1
hypothetical protein BB_A59 (plasmid)	1.19E-06	8989.4	1
hypothetical protein BB_B28 (plasmid)	7.99E-05	49348.9	1
hypothetical protein BB_D21 (plasmid)	2.70E-05	28750.1	1
hypothetical protein BBA69, partial (plasmid)	3.04E-06	30293.3	1
hypothetical protein L144_02645	2.88E-13	7775.1	1
immunogenic protein P37 (plasmid)	2.86E-04	34269.5	1
leucine--tRNA ligase	3.70E-10	98096.6	1
lipoprotein (plasmid)	1.06E-09	22690.8	1
lipoprotein (plasmid)	1.40E-08	22690.8	1

mannose-6-phosphate isomerase	5.54E-13	42812.3	1
membrane fusion protein	1.17E-04	35021.2	1

Supplementary table 7. List of proteins identified by Mass-spec analysis performed on Lyme antigen Grade 2 (continued).

membrane lipoprotein BmpB	1.00E+00	37525.5	1
membrane protein insertase YidC	4.52E-04	63961.2	1
methionyl-tRNA formyltransferase	7.78E-10	35084.8	1
N-acetylglucosamine-6-phosphate deacetylase	4.99E-05	44174.7	1
nucleotide sugar epimerase	9.80E-10	40157.2	1
oligoendopeptidase F	5.44E-10	69678.9	1
outer membrane efflux protein	8.28E-04	49307.9	1
outer membrane porin OMS28 (plasmid)	2.35E-06	27930.6	1
outer membrane protein P13	4.29E-06	19081.0	1
p41, partial	1.56E-12	35729.9	1
peptide ABC transporter ATP-binding protein	7.64E-05	37076.8	1
PF-32 protein (plasmid)	4.00E-14	29341.5	1
phenylalanine--tRNA ligase subunit alpha	2.91E-04	59915.0	1
phosphocarrier protein HPr	3.91E-07	9380.0	1
phosphoribosylpyrophosphate synthetase	9.41E-06	45720.2	1
proline--tRNA ligase	1.28E-06	56275.2	1
protein HflK	4.57E-05	35803.3	1
protein-export membrane protein SecG	2.15E-05	13363.0	1
RIP metalloprotease RseP	3.28E-12	49206.8	1
S-adenosylmethionine synthetase	8.80E-04	43043.7	1
septation protein SpoVG	1.35E-04	11189.0	1
serine--tRNA ligase	4.89E-04	48756.4	1
sugar ABC transporter ATP-binding protein	1.78E-06	60352.0	1
telomere resolvase ResT (plasmid)	1.12E-04	54260.2	1
transcriptional regulator	2.62E-07	27017.2	1
transglycosylase SLT domain-containing protein	1.42E-08	83813.3	1
translation initiation factor IF-3	3.72E-05	21520.7	1
xylose operon regulatory protein	1.05E-10	46051.9	1

Supplementary table 8. Protein candidates for an expanded panel of Borrelia antigen. Peptides and respective transitions are listed.

Precursor	Product M/Z	Collision Energy	Peptide	Subunits	Fragment Ion
718.854437	1106.584	24.5	GADSNFLSEVLER	aminopeptidase	y9
718.854437	992.5411	24.5			y8
718.854437	845.4727	24.5			y7
718.854437	732.3886	24.5			y6
718.854437	645.3566	24.5			y5
1027.538245	1533.852	33.7	YEDLINPIEPIIPSESPK	P34	y14
1027.538245	1420.768	33.7			y13
1027.538245	1306.725	33.7			y12
1027.538245	1209.673	33.7			y11
1027.538245	1096.588	33.7			y10
1027.538245	967.5459	33.7			y9
1027.538245	644.325	33.7			y6
816.920643	1115.544	27.4	LALGYAENNVNELGR	FLiL	y10
816.920643	1044.507	27.4			y9
816.920643	915.4643	27.4			y8
798.412454	1152.641	26.9	NTNNAAIGSAFLQFK	p66	y11
798.412454	1081.604	26.9			y10
798.412454	1010.567	26.9			y9
798.412454	897.4829	26.9			y8
798.412454	840.4614	26.9			y7
798.412454	753.4294	26.9			y6
798.412454	682.3923	26.9			y5
964.481065	1211.642	31.8	SWNISEDGIIYTFNLR	OppA	y10
964.481065	1096.615	31.8			y9
964.481065	1039.593	31.8			y8
846.951412	1375.722	28.3	IGFLGGIEGEIVDAFR	BmpA	y13
846.951412	1262.638	28.3			y12
846.951412	1205.616	28.3			y11
846.951412	1148.595	28.3			y10
846.951412	1035.511	28.3			y9
846.951412	906.468	28.3			y8
846.951412	849.4465	28.3			y7

Supplementary table 8. Protein candidates for an expanded panel of Borrelia antigen. Peptides and respective transitions are listed.

1150.076255	1485.722	37.4	LTVSADLNTVYLEAFDASNQK	OspB	y13
1150.076255	1384.674	37.4			y12
1150.076255	1285.606	37.4			y11
641.319699	1080.557	22.1	NSTEYAIENLK	Flagellin	y9
641.319699	979.5095	22.1			y8
641.319699	850.4669	22.1			y7
641.319699	687.4036	22.1			y6
641.319699	503.2824	23.1			y5

LIST OF SCIENTIFIC PRODUCTS

Articles

a) Magni R, Espina BH, Shah K, Lepene B, Mayuga C, Douglas TA, Espina V, Rucker S, Dunlap R, Petricoin EF, Kilavos MF, Poretz DM, Irwin GR, Shor SM, Liotta LA, Luchini A. Application of Nanotrap technology for high sensitivity measurement of urinary outer surface protein A carboxyl-terminus domain in early stage Lyme borreliosis. J Transl Med. 2015 Nov 4;13:346.

b) Popova TG, Teunis A, Magni R, Luchini A, Espina V, Liotta LA, Popov SG. Chemokine-Releasing Nanoparticles for Manipulation of Lymph Node Microenvironment. Nanomaterials (Basel). 2015 Mar;5(1):298-320.

c) Magni R, Espina BH, Liotta LA, Luchini A, Espina V. Hydrogel nanoparticle harvesting of plasma or urine for detecting low abundance proteins. J Vis Exp. 2014 Aug;(90):e51789

Posters

a) Ruben Magni, Angela Dailing, Alessandra Luchini, Virginia Espina, Lance A Liotta. Exposing Hidden Drug Targets Within Binding Interfaces of Protein-Protein Interactions Using "Protein Painting".Presented as a Poster and Oral Presentation at Discovery on Target 12th Annual Conference, 9-10 October 2014, Boston, US.

b) Ruben Magni, Paolo Verderio, Lance Liotta, Filippo Spreafico, Maura Massimino, Alessandra Luchini, Italia Bongarzone. ‘Investigation of the cerebrospinal fluid proteome from Central Nervous System pediatric tumors using bait loaded hydrogel nanoparticles and mass spectrometry’. Presented at AACR Annual Meeting, 5-9 April 2014, San Diego, US.

GRANTS AND FUNDING

GMU Grant # 222801 (Liotta, Lance A) 11/15/2015 - 5/15/2017
Virginia Biosciences Health Research Corporation (N/A) $466,494
Role: Faculty Associate
Nanotrap Tick-Panel Test Development
Goals: Mason will identify and validate reagents for the detection of Lyme disease co-infection pathogens in human urine. In order to achieve this goal, Mason will perform the following tasks: 1) procure lysates of Bartonella henselae and Babesia microti, 2) perform mass spectrometry analysiis in order to identify major protein components, 3) source antibodies against Babesia and Bartonella, 4) test antibody specificity, 5) map the antibody binding domain with pepsin digestion and mass spectrometry analysis, 6) custom order new antibodies against Bartonella and Babesia antigens identified in point 1).

Istituto Superiore di Sanita' 10/1/2005 – 5/31/2015
Role: Faculty Associate $2,496,295
MOU between GMU and Istituto Superiore Di Sanita
This project applies mass spectrometry and protein array technologies to serum and tissue samples supplied by collaborators from Italy. The goal is to discover protein biomarkers which correlate with cancer stage for several types of cancer.

Italian Health Ministry PE-2011-02346849 05/30/2014-05/29/2017
Role: Faculty Associate € 369,109.16
Nanotechnology for the multiplex diagnosis of infectious diseases

Ceres Nanosciences, Inc 02/21/2011 – 31/12/2016
Role: Faculty Associate $ 173,933
Development of Urine Lyme Disease Assay Using Nanotrap Capture
This project applies hydrogel nanoparticles to the capture and concentration of Lyme disease antigens in urine of patients. Quantitative immunoassays are developed against bacterial antigens. Nanoparticle-enhanced immunoassay results are correlated to standard of care predicate devices.

GMU Grant # 222836 (Petricoin, Emanuel F) 7/1/2015 - 1/31/2017
Medstar Research Institute (N/A) $25,987
Role: Faculty Associate
Proteomics, Genomics, and MicroRNA Analysis of Pancreatic Cancer
Goals: CAPMM will perform the Laser Capture Microdissection on 28 frozen pancreatic tissue specimens and perform RPPA pathway analysis on ~150 analytes and share all data with MedStar Health Research Institute. CAPMM will perform nanoparticle capture and high resolution mass spectrometry analysis of 54 serum blood samples (including 13 healthy controls). CAPMM will share data with MedStar Health Research Institute and jointly analyze the data. Specimens shall be provided by MedStar Health Research Institute.

NIH 1R33CA173359-01 09/20/2012 – 08/31/2015
Role: Faculty Associate $1,386,472
Nanotrap Technology for One Step Preservation and Amplification of Cancer Biomarkers
This project is advanced development and validation of capturing nanoparticles that will maximize the quality and utility of biologic fluid specimens, and permit the measurement of previously invisible low abundance biomarkers emanating from small (<2 mm) early stage cancers with high precision and accuracy.

This thesis interpolates material previously published by the Author[34] with new scientific discoveries. Author and Publisher agree that in addition to any rights under copyright retained by Author in the Publication Agreement, Author retains: the rights to reproduce, to distribute, to publicly perform, and to publicly display the Article in any way, subject only to proper attribution.

ACKNOWLEDGEMENTS

Desidero ringraziare inanzitutto gli organizzatori e coordinatori del corso di Dottorato in Medicina Molecolare e Traslazionale e in particolar modo il mio tutore Prof.ssa Cristina Battaglia e il direttore Prof. Mario Clerici. Nutro verso di loro un enorme debito di gratitudine che mi auguro, perlomeno in parte, di riuscire a ripagare promouvendo nuove e fruttuose opportunita' di ricerca all'interno del connubio tra la George Mason University e l'Universita' di Milano. Io saro' qui, per ogni futura idea di collaborazione, ad una semplice mail di distanza.

Un grazie enorme va ad Alessandra di cui ammiro la genialita', la passione e curiosita' scientifica, ma anche la sua positivita' e filosofia di vita che rende ancora piu' facile e piacevole lavorare insieme. Averla come mentore mi ha immensamente aiutato a crescere dal punto di vista professionale; averla come vicina d'ufficio e confidente mi ha fatto sentire come in una piccola oasi italiana in mezzo ai boschi della Virginia.

I truly thank all the members at GMU and in particular Prof. Lance Liotta, a wonderful person, a great boss, and mentor. I can't be more proud to work under his tutelage, to be able to pick his sparkling brain, and to learn from his advice day in and day out.

I'm so thankful to Meaghan, my love, my partner, my best friend. She motivates and supports me everyday, without her help, without her love, I know would be such a different person today. It amazes me every time how she is able to bring the best out of me, and I'm so proud to call her my wife. Loving somebody is wonderful but probably not so uncommon - truly admiring the person you love is a rare gift, and I couldn't feel luckier.

Grazie alla mia famiglia, ai miei genitori per tutto l'amore che mi avete dato e ogni giorno mi date. Grazie per tutti i sacrifici che avete fatto e siete sempre disposti a fare. Non penso risuciro' mai a ripagarvi per tutto quanto, ma vi prometto che faro' del mio meglio per far fruttare cio' che mi avete insegnato e rendervi fieri, questo ve lo devo.
Grazie alle mie sorelle Veronica e Eleonora, lo so che fate sempre il tifo per me, vi sento sempre vicine e vi voglio un mondo di bene. Mi fa quasi specie pensare che entrambe siate ormai delle giovani professioniste e mi dispiace di poter seguire solo a distanza le scelte di vita che state facendo, anche perche' da buon fratello maggiore avrei sempre un'opinione pronta, oltreche' stramaledettamente intelligente.

Grazie a tutti i miei parenti, ai nonni, gli zii, ai cugini, ogni volta che torno a casa (e non solo) sento il vostro calore. Sono fortunato ad avervi.

Un grazie agli amici, Marco in particolare, sempre presente nella mia vita da quasi trent'anni. Siamo cresciuti insieme, ne abbiamo fatte di cose (stupide e non) e non ci siamo mai persi di vista; e' proprio vero che le grandi amicizie non son schiave ne' del tempo ne' dello spazio. Ora con qualche anno in piu' (entrambi), qualche tatuaggio in piu' (certo non io), ma sempre gli stessi: vecchia scuola. Grazie per esserci sempre, che sia per un consiglio, per una risata, o semplicemente per truffare con una chiacchierata la malinconia. Grazie ad Alfonso di cui ammiro la forza e la tenacia oltre che la sua prospettiva cinica ottimista che ti mostra il mondo per quello che e', e nonostante cio' te lo fa piacere. Nella vita alle volte si perde (qualcosa o qualcuno) e qualche medicina dell'anima fa comodo, ma altre volte si vince, magari anche di cavallo o di pieno. Grazie dei consigli e delle scorribande sui tappeti verdi.

A questo punto, dopo piu' di duecento pagine penso di essermi perso ciascuno dei cinque lettori di questa terza (e si spera ultima) tesi; un grazie di cuore a tutti quanti - that's all folks!